UNIVERSIDADE FEDERAL DE SANTA MARIA
CENTRO DE CIÊNCIAS NATURAIS E EXATAS
PROGRAMA DE PÓS-GRADUAÇÃO EM BIODIVERSIDADE ANIMAL

Ane Elise Branco Pavanatto

ANATOMIA, TAXONOMIA E FILOGENIA DE *Siriusgnathus niemeyerorum* (EUCYNODONTIA, TRAVERSODONTIDAE) DO TRIÁSSICO SUPERIOR SUL-BRASILEIRO

Santa Maria, RS
2019

Ane Elise Branco Pavanatto

ANATOMIA, TAXONOMIA E FILOGENIA DE *Siriusgnathus niemeyerorum* (EUCYNODONTIA, TRAVERSODONTIDAE) DO TRIÁSSICO SUPERIOR SUL-BRASILEIRO

Tese apresentada ao Programa de Pós-Graduação em Biodiversidade Animal, Área de Concentração em Sistemática e Biologia Evolutiva, da Universidade Federal de Santa Maria (UFSM, RS), como requisito parcial para obtenção do grau de **Doutora em Ciências Biológicas - Área Biodiversidade Animal**

Orientador: Prof. Dr. Sérgio Dias da Silva

Santa Maria, RS
2019

Pavanatto, Ane Elise Branco
ANATOMIA, TAXONOMIA E FILOGENIA DE Siriusgnathus niemeyerorum (EUCYNODONTIA, TRAVERSODONTIDAE) DO TRIÁSSICO SUPERIOR SUL-BRASILEIRO / Ane Elise Branco Pavanatto.- 2019.
134 p.; 30 cm

Orientador: Sérgio Dias da Silva
Tese (doutorado) - Universidade Federal de Santa Maria, Centro de Ciências Naturais e Exatas, Programa de Pós-Graduação em Biodiversidade Animal, RS, 2019

1. Siriusgnathus 2. Exaeretodon 3. Traversodontidae 4. Gomphodontia 5. Supersequência Santa Maria I. , Sérgio Dias da Silva II. Título.

Sistema de geração automática de ficha catalográfica da UFSM. Dados fornecidos pelo autor(a). Sob supervisão da Direção da Divisão de Processos Técnicos da Biblioteca Central. Bibliotecária responsável Paula Schoenfeldt Patta CRB 10/1728.

Ane Elise Branco Pavanatto

ANATOMIA, TAXONOMIA E FILOGENIA DE *Siriusgnathus niemeyerorum* (EUCYNODONTIA, TRAVERSODONTIDAE) DO TRIÁSSICO SUPERIOR SUL-BRASILEIRO

Tese apresentada ao Programa de Pós-Graduação em Biodiversidade Animal, Área de Concentração em Sistemática e Biologia Evolutiva, da Universidade Federal de Santa Maria (UFSM, RS), como requisito parcial para obtenção do grau de **Doutora em Ciências Biológicas - Área Biodiversidade Animal**

Aprovada em 30 de abril de 2019:

Sérgio Dias da Silva, Dr. (UFSM)
(Presidente/Orientador)

Ana Maria Ribeiro, Dra. (FZB)

Felipe Lima Pinheiro, Dr. (UNIPAMPA)

Marina Bento Soares, Dra. (UFRGS)

Téo Veiga de Oliveira, Dr. (UEFS)

Santa Maria, RS
2019

DEDICATÓRIA

Dedico esta tese aos meus pais, Marinês e Alcedir.

AGRADECIMENTOS

Em primeiro lugar eu gostaria de fazer um agradecimento para a Universidade Federal de Santa Maria (UFSM), onde eu ingressei em 2007 e permaneci por 12 anos, que me proporcionou a oportunidade de conquistar os títulos de Bacharel e Licenciada em Ciências Biológicas, Mestre e por fim hoje o tão sonhado título de Doutora.

Ao meu orientador Dr. Sérgio Dias da Silva, por ter aceitado me orientar, pela orientação recebida ao longo desses seis anos entre o mestrado e o doutorado.

Ao Prof. Dr. Átila Augusto Stock da Rosa por ter aberto as portas do mundo da paleontologia para mim, por ter proporcionado as minha primeiras experiências e oportunidades no fantástico mundo dos fósseis.

Ao pessoal do Centro de Apoio à Paleontologia da Quarta Colônia - CAPPA (não vou nomear todo mundo para não correr o risco de esquecer alguém!), pelas conversas e (muitas!) risadas, por toda a ajuda, principalmente na preparação dos materiais. Gostaria de agradecer em especial os paleontólogos do CAPPA, Dr. Flávio Pretto e Dr. Leonardo Kerber, por toda a ajuda de vocês ao longo do doutorado, na preparação e coleta dos materiais, com ideias, sugestões e discussões sobre o mundo dos cinodontes.

Ao Programa de Pós-Graduação em Biodiversidade Animal (PPGBA) pelo suporte ao longo do mestrado e do doutorado.

E em especial à minha família, em particular meu pai Marinês e Alcedir, que me criaram com todo amor e carinho apesar das dificuldades. Agradeço por todo o incentivo e apoio ao longo dessa jornada. Se hoje eu consegui alcançar o título de doutora, o mérito não é só meu, pois esse título não foi alcançado só com o meu esforço, foi graças ao esforço de vocês também. Devo tudo a vocês!

Aos meus avós Julieta, Roque (*in memorian*), Albino (*in memorian*) e Catharina (*in memorian*).

Ao secretário do PPGBA, Sidnei Cruz, pela disponibilidade em sempre responder as minhas dúvidas. À Coordenação de Aperfeiçoamento de Pessoal de Nível Superior (CAPES) pela bolsa de doutorado concedida. Aos funcionários do Consórcio de Desenvolvimento Sustentável da Quarta Colônia (CONDESUS) por toda a ajuda, caronas, etc... quando eu cheguei no CAPPA.

Aos colegas, professores, amigos... enfim, a todos que de alguma forma contribuíram ao longo dessa jornada, o meu muito obrigada!

"Há uma teoria que diz que se um dia alguém descobrir exatamente qual é o propósito do Universo e por que ele está aqui, ele desaparecerá instantaneamente e será substituído por algo ainda mais bizarro e inexplicável.

Há uma outra teoria que diz que isso já aconteceu..."

Douglas Adams – O Restaurante no Fim do Universo

RESUMO

ANATOMIA, TAXONOMIA E FILOGENIA DE *Siriusgnathus niemeyerorum* (EUCYNODONTIA, TRAVERSODONTIDAE) DO TRIÁSSICO SUPERIOR SUL-BRASILEIRO

AUTORA: Ane Elise Branco Pavanatto
ORIENTADOR: Sérgio Dias da Silva

A presente tese apresenta a descrição de um novo táxon de cinodonte traversodontídeo, filogeneticamente relacionado com *Exaeretodon*, mas que possui uma combinação única de características não presentes em outros cinodontes, o que justificou a nomeação do novo táxon, *Siriusgnathus niemeyerorum*: presença de dois incisivos superiores; cúspide labial acessória distal dos pós-caninos superiores posicionada mais labialmente, em comparação com *Exaeretodon*; dois a três incisivos inferiores; rostro curto e amplo, com aproximadamente o mesmo comprimento da região temporal; processo descendente do jugal incipiente; barra pós-orbital posicionada mais anteriormente do que em *Exaeretodon*; borda posterior do processo zigomático do esquamosal curto e arredondado; crista lambdoidal não forma uma concavidade, como em *Exaeretodon*; e basicrânio curto anteroposteriomente. *S. niemeyerorum* provêm de uma nova localidade fossilífera do Triássico Superior (Supersequência Santa Maria) do sul do Brasil, aqui também apresentada, nomeada Sítio Niemeyer, cuja litologia se assemelha a da Sequência Candelária. Essa nova localidade apresenta uma grande prevalência de registros de cinodontes traversodontídeos. A maioria de seus fósseis é constituída de ossos isolados e fragmentados, com alguns poucos exemplares de crânios e mandíbulas mais completos e com boa preservação. Espécimes de cinodontes probainognátios e de arcossauromorfos também foram encontrados, mas são significativamente menos frequentes em comparação com os registros de traversodontídeos. Os espécimes coletados até este momento foram classificados de acordo com os Grupos de Voorhies, sendo o Grupo 3 o mais abundante e o Grupo 2 o menos representado (Grupo III > Grupo I > Grupo II). Foi observado em alguns espécimes evidências de icnofósseis resultantes da ação de invertebrados. Quanto à possível geocronologia dessa nova localidade, foi sugerida uma idade Carniana, já que, até o momento, não há registros confirmados de traversodontídeos nas porções superiores da Sequência Candelária.O holótipo de *S. niemeyerorum* (CAPPA/UFSM 0032) assim como dos espécimes de *Exaeretodon riograndensis* (CAPPA/UFSM 0030 e 0227), foram tomografados em um tomógrafo médico, na intenção de acessar as suas estruturas internas, objetivando o estudo da morfologia endocraniana desses táxons. Após a segmentação das cavidades endocranianas e geração dos modelos 3D, observou-se que ambos apresentam molde da cavidade endocraniana (*endocast*) alongado e tubular, sem uma clara separação entre as regiões do cérebro. Em ambos, um sulco longitudinal dividindo os bulbos olfatórios e os hemisférios cerebrais está ausente. Apresentam a zona não ossificada bem desenvolvida e o tubo pineal ausente. *S. niemeyerorum* apresenta a fossa hipofiseal bem delimitada, enquanto que, em *E. riograndensis*, esta não está bem marcada. Foram calculados os Quocientes de Encefalização para cada espécime, os quais resultaram em valores mais altos do que observado em outros traversodontídeos, provavelmente devido a diferenças na técnica para obtenção do volume dos *endocast*. De formal geral a morfologia de endocast de *S. niemeyerorum* e *E. riograndensis* é semelhante àquela descrita para outros cinodontes. Este estudo fornece os primeiros dados sobre a morfologia endocraniana de cinodontes traversodontídeos acessada através de técnicas tomográficas.

Palavras-chave: *Siriusgnathus. Exaeretodon*. Gomphodontia. Supersequência Santa Maria.

ABSTRACT

ANATOMY, TAXOMY AND PHYLOGENY OF *Siriusgnathus niemeyerorum* (EUCYNODONTIA, TRAVERSODONTIDAE) FROM THE UPPER TRIASSIC OF SOUTHERN BRAZIL

AUTHOR: Ane Elise Branco Pavanatto
ADVISOR: Sérgio Dias da Silva

This thesis provides information of new traversodontid cynodont taxon, *Siriusgnathus niemeyerorum*, which is closely related to *Exaeretodon*, although the new taxonomic unit shows a unique combination of features not present in other cynodonts: two upper incisors; distal accessory labial cusp of upper postcanines more labially placed in comparison with *Exaeretodon*; two/three lower incisors; rostrum short, broad with almost the same length of the temporal region; postorbital bar more anteriorly positioned than in *Exaeretodon*; descending process of the jugal incipient; posteriormost border of zygomatic process of squamosal, short and rounded; lambdoidal crest not forming a concavity such as that present in *Exaeretodon*; and an anteroposteriorly short basicranium. *S. niemeyerorum* was found in a new Upper Triassic fossiliferous outcrop (Santa Maria Supersequence) of Southern Brazil, the Niemeyer Site, which lithology is consistent with that of the Candelária Sequence. This new locality presents a high prevalence of traversodontid cynodonts. The majority of the collected specimens are mostly composed of isolated bones and fragmentary specimens, but also including well-preserved skulls and lower jaws. Probainognathian cynodonts and archosauromorphs are also present, but they are rare in comparison with the records of traversodontids. The specimens collected so far were grouped into Voorhies Groups. There is a predominance of Voorhies Group III and the Group II the less represented (Group III > Group I > Group II). Some specimens display evidence of ichnological activity of invertebrate scavengers. Given that so far no confirmed traversodontids recorded in the uppermost levels of the Candelária Sequence, we suggest a Carnian age for the new outcrop. The holotype of *S. niemeyerorum* (CAPPA/UFSM 0032) as well as two specimens of *Exaeretodon riograndensis* (CAPPA/UFSM 0030 e 0227), were scanned in a medical tomograph, in order to access its internal structures, to investigate the endocranial morphology of both taxa. After the segmentation of endocranial cavities and generation of the 3D models, it was observed that the endocasts were elongated and tubular, without a clearly division between the cerebral regions. In both taxa, a longitudinal sulcus dividing, the olfactory bulbs and the cerebral hemispheres are absent. The unossified zone is well developed and the pineal tube is absent. *S. niemeyerorum* has a well delimited hypophyseal fossa, whereas in *E. riograndensis* it is not well delimited. Encephalization Quotients was calculated to each specimen, resulting in higher values than the observed in other traversodontids, probably because technic differences employed to obtain the endocast volume. Overall, the endocast morphology of *S. niemeyerorum* and *E. riograndensis* is similar to described to others cynodonts. This study provide the first data about the endocranial morphology of traversodontids through tomography.

Key words: *Siriusgnathus*. *Exaeretodon*. Gomphodontia. Santa Maria Supersequence.

LISTA DE FIGURAS

TEXTO INTEGRADOR

ARTIGO 1 - A new Upper Triassic cynodont-bearing fossiliferous site from southern Brazil, with taphonomic remarks and description of a new traversodontid taxon

ARTIGO 2 - Virtual reconstruction of cranial endocasts of traversodontid cynodonts (Eucynodontia: Gomphodontia) from the Upper Triassic of southern Brazil

SUMÁRIO

APRESENTAÇÃO

A presente tese está estruturada de acordo com o Manual de Dissertações e Teses da UFSM (MDT). Atendendo as exigências do Programa de Pós-Graduação em Biodiversidade Animal, a tese é composta por um texto integrador, seguido de dois artigos (publicados e/ou a serem submetidos em periódicos dos quatro estratos superiores do Qualis Capes – A1, A2, B1 e B2 – na área de Biodiversidade), discussão geral e conclusões.

O texto integrador apresenta uma breve contextualização dos Synapsida, Therapsida e Cynodontia, partindo-se então diretamente para os Traversodontidae, onde os objetos de estudos da presente tese estão incluídos. Em seguida, é apresentado um breve histórico acerca dos estudos envolvendo paleoneurologia de cinodontes.

O Artigo 1 trata da apresentação de uma nova localidade fossilífera para o Triássico Superior do sul do Brasil, com uma incomum acumulação e predomínio de um novo táxon da família Traversodontidae em comparação com o registro de outros grupos de Cynodontia, como o clado Probainognathia e de Archosauromorpha. São apresentados os aspectos geológicos e tafonômicos da nova localidade, bem como o seu conteúdo fossilífero e descrição do novo táxon, *Siriusgnathus niemeyerorum*. O artigo foi publicado no periódico *Journal of South American Earth Sciences* (Qualis B1 na área de Biodiversidade, na avaliação do quadriênio 2013-2016).

O Artigo 2 apresenta a descrição da cavidade endocraniana de duas espécies de cinodontes da família Traversodontidae, *Siriusgnathus niemeyerorum* e *Exaeretodon riograndensis*, bem como sua comparação com outros cinodontes cuja cavidade endocraniana é conhecida. O artigo está formatado de acordo com as normas do periódico *Journal of Morphology* (Qualis B1 na área de Biodiversidade, na avaliação do quadriênio 2013-2016), para o qual foi submetido e aceito para publicação.

1 INTRODUÇÃO

Cynodontia Owen, 1861, juntamente com Biarmosuchia Sigogneau-Russell, 1989; Dinocephalia Seeley, 1894; Anomodontia Owen, 1859; Gorgonopsia Seeley, 1894; e Therocephalia Broom, 1903 é um dos seis clados que compõem Therapsida Broom, 1905, o qual, por sua vez, se inclui no grande clado Synapsida Osborn, 1903 (ver próximo subitem). Cynodontia surgiu no final do Período Permiano e se constituiu em um importante componente em ecossistemas terrestres durante todo o Triássico e Jurássico, estendendo-se até o início do Cretáceo (aproximadamente de 258 a 130 milhões de anos atrás - Ma; BOTHA; ABDALA; SMITH, 2007; KAMMERER, 2016; MATSUOKA; KUSUHASHI; CORFE, 2016). Atualmente, é representado pelos mamíferos.

No Sul do Brasil, Cynodontia é encontrado em rochas da Supersequência Santa Maria (Triássico Médio e Superior). Ao longo do Período Triássico, Cynodontia atingiu grande diversificação, tendo sofrido inúmeras e importantes modificações anatômicas como, por exemplo, a especialização da dentição, do padrão de oclusão dentária e, consequentemente, de seus hábitos alimentares. Ao final do Triássico, sofrem drástica diminuição no tamanho corporal. Os brasilodontes, pequenas formas não-mamaliaformes provenientes do Triássico sul brasileiro, são apontados como o provável grupo-irmão dos mamíferos, devido à presença de várias características em seu crânio (e.g. articulação da mandíbula formada pelo dentário e o esquamosal, ossos pós-dentários bastante reduzidos, opistótico e proótico fusionados formando o petrosal; presença de promontório no petrosal, pré-frontal e pós-orbital ausentes, arco zigomático delgado, entre outras) e dentição "triconodonte" (ABDALA, 2007; BONAPARTE et al., 2003; BONAPARTE; MARTINELLI; SCHULTZ, 2005; LIU; OLSEN, 2010; LUO, 2007).

1.1 SYNAPSIDA OSBORN, 1903

Synapsida é o clado que inclui todos os taxa extintos e atuais mais proximamente relacionados à Mammalia do que à Sauropsida (RUBIDGE; SIDOR, 2001). Seus primeiros registros são provenientes de Joggins, Nova Escócia, Pensilvaniano (Carbonífero da América do Norte), entre 311-314 Ma (REISZ, 2014). Até o início do Permiano, formas basais de Synapsida, (Synapsida não-Therapsida - "pelicossauros"), foram as mais diversificadas e dominantes nas paleofaunas terrestres, ocupando uma ampla variedade de nichos ecológicos (RUBIDGE; SIDOR, 2001). A grande maioria das espécies de "pelicossauros" conhecidas é

oriunda principalmente da América do Norte e da Europa, sendo o registro desse grupo pouco frequente no Hemisfério Sul (BOTHA-BRINK; MODESTO, 2007). Os "pelicossauros" estão divididos em seis clados distintos que apresentam uma grande variedade de tamanhos e de estratégias alimentares (REISZ, 2014).

O clado Eothyrididae Romer; Price, 1940 é conhecido atualmente apenas por dois gêneros, *Oedaleops* Langston, 1965 (Firgura 1A) e *Eothyris* Romer; Price, 1940 (Figura 1B), são formas predadoras pequenas, com um par de dentes caniniformes superiores muito grandes, possivelmente insetívoras (REISZ, 2014; REISZ; GODFREY; SCOTT, 2009).

O clado Caseidae Williston, 1911, (Figura 1C) é composto por grandes formas herbívoras, cujo o crânio é muito pequeno em relação ao corpo, apresentam dentes em forma de "folha", que lembram a morfologia dos dentes das iguanas atuais (REISZ, 2014; SUES; REISZ, 1998).

O clado Varanopidae Romer; Price, 1940 inclui formas predadoras, carnívoras, de tamanho pequeno a médio, com membros mais alongados (em comparação com outros "pelicossauros") e com dentição comprimida labiolingualmente e bastante recurvada (Figura 1D). Entre os demais clados de "pelicossauros", Varanopidae foi o mais longevo (com registro desde o final do Carbonífero, estendendo-se até o final do Permiano) e amplamente distribuído (KEMP, 2005; REISZ, 2014).

O clado Ophiacodontidae Nopsca, 1923, também de formas carnívoras, é caracterizado pelo crânio ser bastante alto e estreito e de grande proporção, em relação ao corpo, com membros curtos e largos (Figura 1E). Apresentam numerosos dentes, o quais são levemente recurvados (REISZ, 2014).

O clado Edaphosauridae Cope, 1882 é composto por formas herbívoras especializadas que apresentam um grande alongamento do processo espinhoso das vértebras formando uma estrutura dorsal ("vela"; Figura 1F). Além da dentição marginal isodonte, o clado apresenta placas com numerosos dentes na região palatal e na face interna da mandíbula (KEMP, 2005; MODESTO, 1995).

Os membros do clado Sphenacodontia Marsh, 1878 são considerados grandes predadores (atingindo até 4 metros de comprimento), cujos membros são relativamente alongados. O crânio apresenta grandes proporções e os dentes incisiformes e caniniformes são robustos e bem desenvolvidos (Figura 1G). Além disso, também apresentam alongamento do processo espinhoso das vértebras, formando a já mencionada "vela", a qual estaria relacionada ao processo de termorregulação (KEMP, 2005; REISZ, 2014). O clado Sphenacodontia é apontado como o provável grupo irmão de Therapsida (RUBIDGE; SIDOR, 2001).

Figura 1 – Diversidade de Synapsida basais

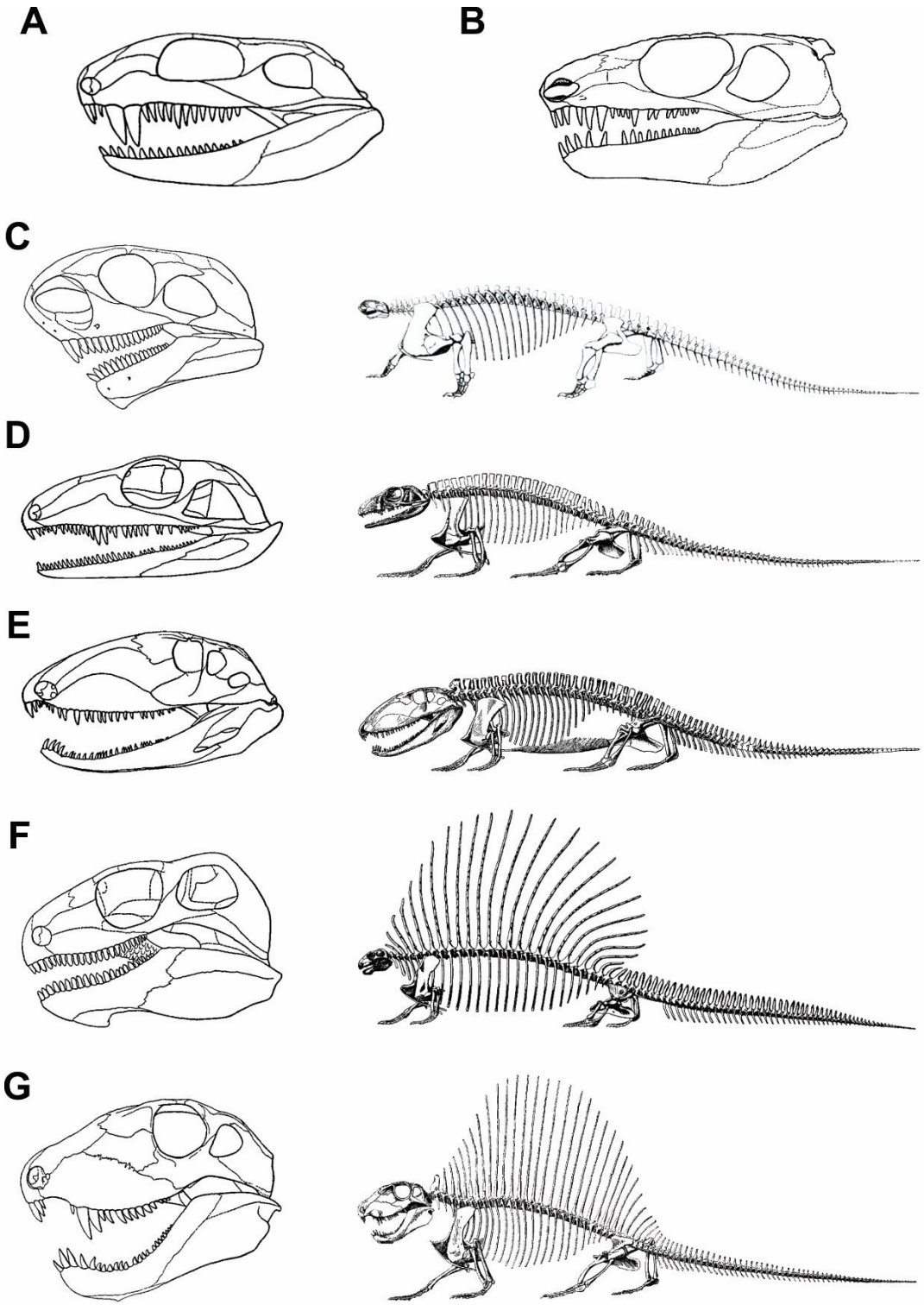

Legenda: Eothyrididae A, *Eothyris*; B, *Oedaleops*; C, Caseidae – *Cotylorhynchus romeri* Stovall, 1937; D, Varanopidae – *Varanops brevirostris* Williston, 1911; E, Ophiacodontidae – *Ophiacodon retroversus* Cope, 1878; F, Edaphosauridae – *Edaphosaurus boanerges* Romer; Price, 1940; G, Sphenacodontia – *Dimetrodon milleri* Romer, 1937. Fonte: A, C-G modificado de Romer; Price (1940); B modificado de Langston (1965). As imagens não estão em escala.

1.2 THERAPSIDA

Durante o Guadalupiano (Mesopermiano) e Lopinguiano (Neopermiano), época de grandes mudanças climáticas, houve uma grande troca faunística marcada pelo declínio dos "pelicossauros" e ascensão dos Therapsida (BENTON, 2012; MODESTO et al., 2011). Therapsida, é definido como todos os Synapsida filogeneticamente mais derivados do que os Sphenacodontidae Marsh, 1878 (LAURIN; REISZ, 1996). Os primeiros registros desse grupo são provenientes da Rússia e da África do Sul (KEMP, 1982; RUBIDGE; SIDOR, 2001). O Clado Therapsida sofreu uma grande radiação, atingindo grande diversidade taxonômica, e vindo a formar o maior subclado de Synapsida (BENTON, 2012). Assim, no final do Permiano Therapsida já estava completamente estabelecido e amplamente distribuído, compondo seis diferentes clados menos inclusivos: Biarmosuchia, Dinocephalia, Anomodontia, Gorgonopsia, Therocephalia e Cynodontia (KEMP, 2005; RUBIDGE; SIDOR, 2001; Figura 2).

Figura 2 – Filogenia de Therapsida

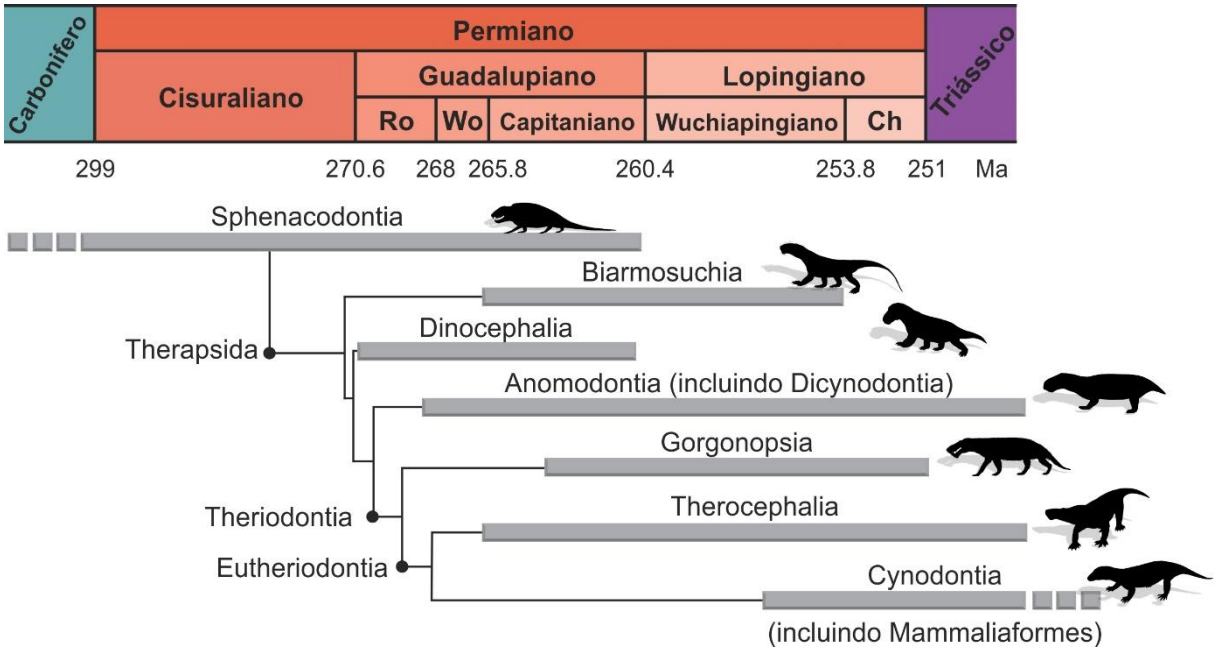

Legenda: Ch, Changhsingiano; Ro, Roadiano; Wo, Wordiano. Fonte: Relações filogenéticas baseado em Rubidge; Sidor (2001), datação baseada em Day et al. (2015). Modificado de Benoit et al. (2017).

O clado Biarmosuchia é apontado como o mais basal de Therapsida e reúne uma série de características ainda consideradas plesiomórficas, principalmente em relação ao crânio, que lembram o crânio dos esfenacodontídeos, como a margem dorsal do crânio convexa, região intertemporal curta e ampla e rostro alongado, contudo apresentam a fenestra temporal mais desenvolvida (KEMP, 2005, 2012; SIGOGNEAU-RUSSEL, 1989). São formas carnívoras de pequeno a médio porte. Alguns membros do clado apresentam paquiostose nos ossos cranianos, além de protuberâncias ósseas na região orbital e no esquamosal (KEMP, 2012; RUBIDGE; SIDOR, 2001, 2002; Figura 3A).

O clado Dinocephalia é composto por formas carnívoras e herbívoras de grande tamanho e robustas. Apresentam incisivos com uma espécie de "salto" ("*heel*") na face lingual, aumento do tamanho da fenestra temporal e paquiostose nos ossos cranianos. É divido em dois subgrupos os anteossáurios, carnívoros basais (Figura 3B) e os tapinocefalídeos (Figura 3C, D) as formas mais derivadas herbívoras (KAMMERER, 2011; KEMP, 2012; RUBIDGE; SIDOR, 2001).

Anomodontia é o único clado de Therapsida com registros em todos os continentes, além de ser o clado mais longevo. A grande maioria dos taxa estão agrupados no subclado Dicynodontia Owen, 1859, o qual inclui formas herbívoras especializadas que apresentam uma redução no número de dentes, sendo a maioria ou todos substituídos por um bico córneo, e um par de caniniformes alongados, formando presas (característica que dá nome ao grupo; KEMP, 2005, 2012; Figura 3 E, F).

Gorgonopsia é um clado de formas de médio a grande porte, que compunham os predadores terrestres dominantes do final do Permiano (Figura 3G, H). São caracterizados pela presença de caninos superiores e inferiores grandes e desenvolvidos, muitas vezes referidos com "dente de sabre"; incisivos, tanto superiores quanto inferiores, bem desenvolvidos, enquanto que os pós-caninos eram pequenos e reduzidos (KEMP, 1982, 2005).

O clado Therocephalia é composto, em sua maioria, de formas de pequeno porte carnívoras, com caninos grandes e pós-caninos reduzidos (Figura 3I). Apresentam a fenestra temporal grande e a região intertemporal do teto craniano bastante reduzida. Bauriidae é um clado derivado de Therocephalia, possivelmente herbívoro. Apresenta, assim como os cinodontes (de forma convergente) dentes pós-caninos expandidos, oclusão entre os dentes superiores e inferiores e palato secundário completo (KEMP, 2005, 2012).

Gorgonopsia, Therocephalia e Cynodontia (Figura 3J) compõem o Clado Theriodontia Owen, 1881, constituído de formas primariamente carnívoras e caracterizado pela aquisição de características "mamalianas" (KAMMERER, 2014; KEMP, 2005; RUBIDGE; SIDOR, 2001).

Figura 3 – Diversidade de Therapsida

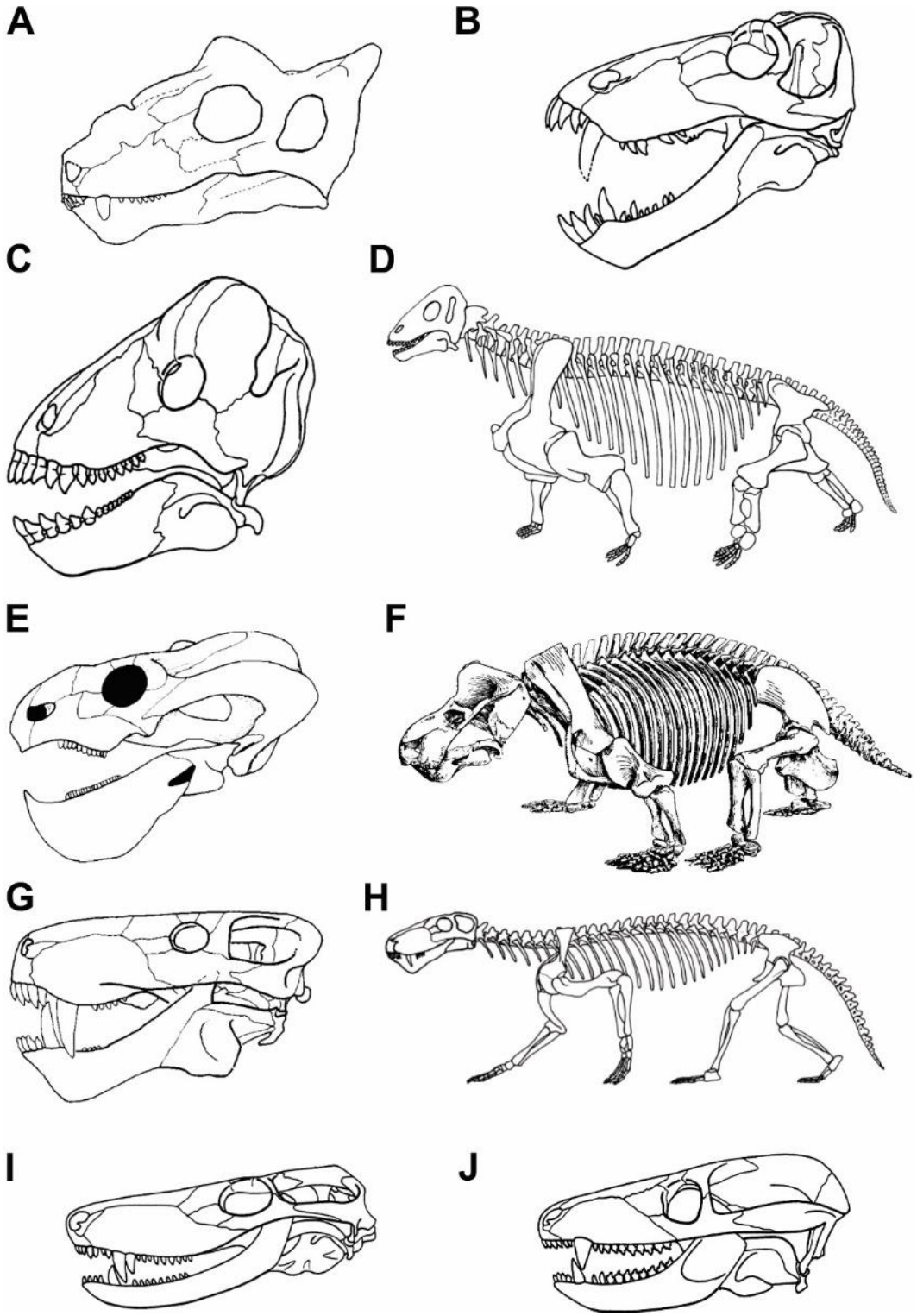

Legenda: A, Biarmosuchia – *Proburnetia viatkensis* Tatarinov, 1968; Dinocephalia B, anteossaurio *Titanophoneus* Efremov, 1940*;* tapinocefalideos C, *Ulemosaurus* Riabinin, 1938; D, *Moschops* Broom, 1911; Anomodontia (Dicynodontia) E, *Endothiodon* Owen, 1876; F, *Kannemeyeria* Seeley,1908; Gorgonopsia G, *Aelurognathus* Haughton, 1924; H, *Lycaenops* Broom, 1925; I, Therocephalia – *Ictidosuchoides* Broom 1931; J, Cynodontia – *Procynosuchus* Broom, 1937. Fonte: A modificado de Rubidge; Sidor (2002); B, C, G, I, J modificado de Hopson (1994); D, F, H modificado de Kemp (2005); E modificado de Kemp (1982). As imagens não estão em escala.

1.3 CYNODONTIA

O clado Cynodontia é definido como o mais inclusivo contendo Mammalia Linnaeus, 1758 e excluindo *Bauria* Broom, 1909 (HOPSON; KITCHING, 2001). Apresenta as seguintes sinapomorfias: contato entre o nasal e o lacrimal; frontal excluído da margem da órbita; côndilo occipital duplo; ângulo do dentário no mesmo nível ou posterior à barra pós-orbital; lâmina refletida do angular lisa com pequenas depressões e entalhe na base do processo coronoide do dentário (BOTHA; ABDALA; SMITH, 2007).

Cynodontia é o clado mais diversificado de Therapsida, no qual os mamíferos estão incluídos e no qual surgiram várias características anatômicas como: heterodontia, desenvolvimento de oclusão dentária, fenestra temporal grande margeada pela crista sagital e pelos arcos zigomáticos, redução dos ossos pós-dentários na mandíbula e aumento de tamanho do dentário, presença de um palato ósseo secundário e postura mais verticalizada dos membros (KEMP, 2005, 2012). Até recentemente, *Procynosuchus* era considerado o mais antigo cinodonte conhecido. Atualmente, os cinodontes da família Charassognathidae Kammerer, 2016, *Charassognathus gracilis* Botha et al., 2007 e *Abdalodon diastematicus* Kammerer, 2016, da Zona de Associação (ZA) de *Tropidostoma*, base do Permiano Superior da Bacia de Karoo, África do Sul são apontados como os mais antigos cinodontes, representando sua primeira radiação e indicando uma possível origem sul-africana para o grupo (BOTHA; ABDALA; SMITH, 2007; KAMMERER, 2016).

Dentro de Cynodontia, destaca-se o clado Eucynodontia, proposto por Kemp (1982) que o definiu como todos os cinodontes mais próximos aos mamíferos atuais do que de *Thrinaxodon* Seeley, 1894 (KEMP, 1982). Hopson; Kitching (2001) definem Eucynodontia como o clado menos inclusivo incluindo Mammalia e *Exaeretodon* Cabrera, 1943. É caracterizado pelas seguintes feições anatômicas: processo descendente do jugal lateral ao quadradojugal contatando o suprangular; processo para o quadrado ausente no pterigoide; sínfise mandibular fusionada; contato dorsal do dentário com o suprangular mais próximo da articulação mandibular do que da barra pós-orbital; altura dos pós-dentários inferior à metade do comprimento; lâmina refletida do angular com menos da metade da distância do processo angular do dentário à articulação mandibular; lâmina refletida do angular com formato de gancho; padrão de substituição dos dentes pós-caninos espaçado; escápula com processo acrômio e dígitos manuais III e IV com três falanges (HOPSON; KITCHING, 2001).

Figura 4 – Relações filogenéticas de Cynodontia

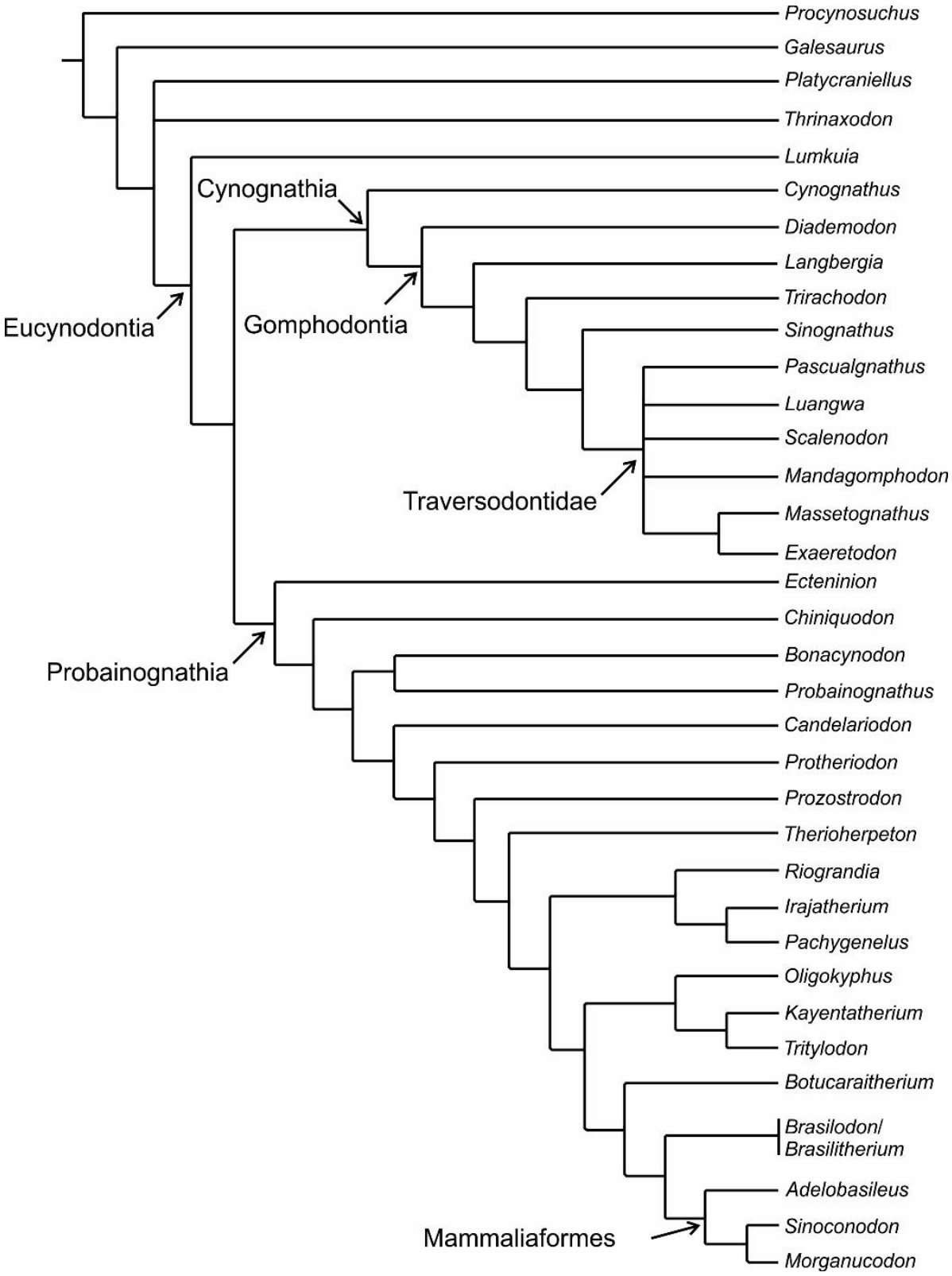

Fonte: Modificado de Guignard; Martinelli; Soares (2019).

Eucynodontia subdivide-se em dois clados menos inclusivos, Probainognathia Hopson, 1990 e Cynognathia Hopson & Barghusen, 1986 (ABDALA, 2007; HOPSON; KITCHING, 2001; Figura 4):

Probainognathia é definido como o clado menos inclusivo contendo *Probainognathus* Romer, 1970 e excluindo *Exaeretodon* (HOPSON; KITCHING, 2001). De forma geral, é composto por cinodontes carnívoros e/ou onívoros e inclui o clado dos Mammaliaformes Rowe, 1988 (HOPSON; KITCHING, 2001; KEMP, 2012; LIU; OLSEN, 2010). É caracterizado pela ausência do forâmen parietal; ectopterigoide ausente; margem posterior do palato secundário situada no nível da borda anterior da órbita; crista lambdoidal separada do arco zigomático por um entalhe com formato de "V"; costelas sem expansão lateral e pró-coracoide participando pouco ou não participando da cavidade glenoide (HOPSON; KITCHING, 2001; Figura 5A, B).

Cynognathia é definido como o clado menos inclusivo contendo *Exaeretodon* e excluindo *Probainognathus* (HOPSON; KITCHING, 2001). As formas mais basais, e.g. *Cynognathus* Seeley, 1895, eram carnívoras e apresentavam dentes pós-caninos setoriais, comprimidos labiolingualmente (Figura 5C). Os demais membros do clado Cynognathia apresentam dentição predominantemente gonfodonte, ou seja, os dentes são transversamente alargados, típicos de formas herbívoras e/ou onívoras, os Gomphodontia Seeley, 1895, definido como o clado menos inclusivo contendo *Exaeretodon* e excluindo *Cynognathus* (HOPSON; KITCHING, 2001). Cynognathia apresenta as seguintes sinapomorfias: arco zigomático alto, estendendo-se acima do nível da órbita, com a sua largura máxima na porção final; processo suborbital no jugal; sulco para o meato auditivo externo muito profundo; basisfenoide sem forâmen para as carótidas internas; caninos com dentículos; expansão das costelas lombares sobrepondo-se à costela precedente (HOPSON; KITCHING, 2001). Gomphodontia, por sua vez, é caracterizado por: profundidade do jugal no arco zigomático maior do que o dobro da parte exposta do esquamosal; saída do nervo Trigeminal por dois foramens; entalhe em formato de "V" separando a crista lambdoidal do arco zigomático; cíngulo interno dos pós-caninos superiores expandido lingualmente; pós-caninos superiores com três cúspides na crista transversa; pós-caninos com duas cúspides na crista transversa; perfil dorsal do ílio plano a côncavo (HOPSON; KITCHING, 2001). Gomphodontia compreende as famílias Diademodontidae Haughton, 1925; Trirachodontidae Crompton, 1955 e Traversodontidae Huene, 1936 (ABDALA; NEVELING; WELMAN, 2006; KEMP, 2005).

Para a família Diademodontidae, *Diademodon* (Figura 5D) é o táxon mais conhecido, caracterizado por apresentar pós-caninos com três tipos morfológicos distintos: os mais anteriores cônicos, na porção média da série dentes gonfodontes (transversamente largos e

multicuspidados) e na porção final da série, dentes setoriais, semelhantes aos de *Cynognathus* (KEMP, 2005; MARTINELLI; FUENTE; ABDALA, 2009). Foram membros abundantes da ZA de *Cynognathus* do Grupo Beaufort da África do Sul (final do Olenekiano ao final do Anisiano), há também registro para o Anisiano da Argentina e um possível registro para o nível inferior da Formação Elliot do Noriano (ABDALA et al., 2007; MARTINELLI; FUENTE; ABDALA, 2009).

Figura 5 – Diversidade de Eucynodontia

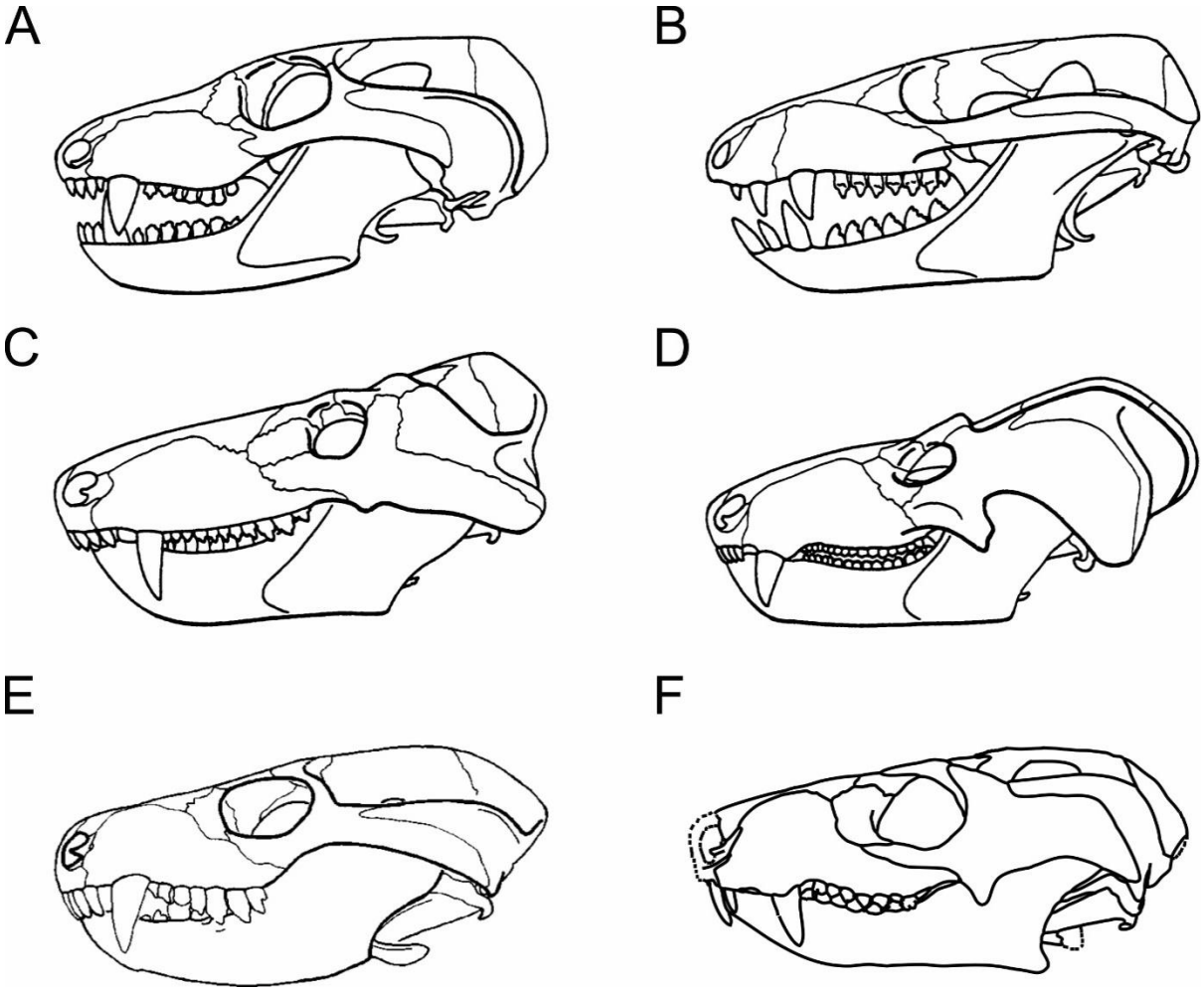

Legenda: Probainognathia A, *Probainognathus*; B, *Pachygenelus* Watson 1913; Cynognathia C, *Cynognathus*; D, *Diademodon* Seeley 1895; Trirachodontidae E, *Trirachodon* Seeley 1895; F, *Cricodon* Crompton, 1955. Fonte: A-D modificado de Hopson (1994); E modificado de Rubidge; Sidor (2001); F modificado de Sidor; Hopson (2017). As imagens não estão em escala.

A família Trirachodontidae é caracterizada por apresentar pós-caninos transversalmente expandidos com três cúspides principais dispostas em uma fileira transversal central, e com os cíngulos mesial e distal com pequenas cúspides (ABDALA; NEVELING; WELMAN, 2006; CROMPTON, 1955). Estão incluídas em Trirachodontidae as espécies *Trirachodon berryi* Seeley, 1895 (Figura 5E), *Cricodon metabolus* Crompton, 1955 (Figura 5F), *Langbergia modisei* Abdala; Neveling; Welman, 2006 da ZA de *Cynognathus*, e *Sinognathus gracilis* Young, 1959 e *Beishanodon youngi* Gao et al., 2010 da China (ABDALA; NEVELING; WELMAN, 2006; GAO et al., 2010). Contudo a análise filogenética realizada por Sidor; Hopson (2017), exclui *Sinognathus* e *Beishanodon* de Trirachodontidae, que são recuperadas dentro de Traversodontidae. Além disso, algumas características dessas duas espécies, como ausência do forâmen parietal e processo do jugal ausente, arco zigomático amplamente curvado, compartilhadas com Probainognathia, mas não compartilhadas com formas basais de Cynognathia (i.e., *Cynognathus*, Trirachodontidae e Traverdodontidae basais), poderiam posicionar essas espécies dentro de Probainognathia, ao invés de Gomphodontia.

1.4 TRAVERSODONTIDAE

A família Traversodontidae foi estabelecida por Huene (1936) para agrupar os cinodontes do Triássico brasileiro que possuíam pós-caninos transversalmente expandidos: *Traversodon stahleckeri* Huene, 1936, ?*Traversodon major* Huene, 1936 e *Gomphodontosuchus brasiliensis* Huene, 1928 (LIU; ABDALA, 2014). Representa o mais inclusivo clado contendo *Traversodon stahleckeri* mas não *Trirachodon kannemeyeri* Seeley, 1895 ou *Diademodon tetragonus* Seeley, 1894 (KAMMERER et al., 2008; LIU; ABDALA, 2014). Segundo a diagnose mais recente da família, a mesma é caracterizada pela ausência do ectopterigoide; presença do contato epipterigoide-quadrado; plataforma maxilar lateral à série de pós-caninos; pós-caninos superiores expandidos labiolingualmente com uma profunda bacia oclusal; dentes gonfodontes superiores maiores do que os inferiores com contorno variando de elipsoide a retangular; dentes gonfodontes inferiores com formato quadrangular, com a crista transversa posicionada anteriormente (KAMMERER et al., 2008; LIU; ABDALA, 2014).

Traversodontidae é a família mais diversificada, cosmopolita e bem sucedida de cinodontes possivelmente herbívoros e/ou onívoros, desde o Anisiano da África (BRINK, 1963; CROMPTON, 1955) e Argentina (BONAPARTE, 1966a, 1969; mas veja OTTONE et al., 2014) e mantendo-se como um grupo importante até o Carniano (ABDALA; RIBEIRO, 2010). Atualmente, a família é composta por 25 espécies consideradas válidas, divididas em 19

gêneros. Exemplares da família já foram encontrados na África (seis gêneros), América do Norte (dois gêneros), América do Sul (doze gêneros), Índia (dois gêneros) e Europa (um gênero) (LIU; ABDALA, 2014; MELO; MARTINELLI; SOARES, 2017; PAVANATTO et al., 2018; RAY, 2015).

Na África são registradas do final do Anisiano e início do Ladiniano as espécies *Luangwa drysdalli* Brink, 1963 (Porção superior da Formação Ntawere, Zâmbia; Figura 6A-B), *Mandagomphodon attridgei* Crompton, 1972, *Mandagomphodon hirschsoni* Crompton, 1972 e *Scalenodon angustifrons* Parrington, 1946 (Formação Manda, Tanzânia); e *Luangwa* sp. (Porção superior da Formação Omingonde, Namíbia). No Carniano, *Menadon besairiei* Flynn et al., 2000 e *Dadadon isaloi* Flynn et al., 2000 (Formação Isalo II = Formação Makay; Madagascar; Figura 6C); e para o Noriano *Scalenodontoides macrodontes* Crompton; Ellenberger, 1957 (Porção inferior da Formação Elliot, África do Sul e Lesoto)(ABDALA; RIBEIRO, 2010; LIU; ABDALA, 2014).

Nos EUA há registro de três espécies *Arctotraversodon plemmyridon* Sues; Hopson; Shubin, 1992 (Formação Wolfville) e *Boreogomphodon jeffersoni* Sues; Olsen, 1990 (Formação Turkey Branch) do Carniano e *Boreogomphodon herpetairus* Sues; Hopson; Shubin, 1992 (Supergrupo Newark) possivelmente do Noriano (LIU; ABDALA, 2014). Na Europa há apenas uma espécie conhecida *Nanogomphodon wildi* Hopson; Sues, 2006 do Ladiniano (Formação Erfurt, Alemanha). Na Índia há registro de duas espécies: *Exaeretodon statisticae* Chatterjee, 1982, considerada como *Exaeretodon* sp. por Liu; Abdala (2014), para o início do Noriano (Porção inferior da Formação Maleri; Figura 6D) e *Ruberodon roychowdhurii* Ray, 2015 (Formação Tiki) do Carniano (ABDALA; RIBEIRO, 2010; LIU; ABDALA, 2014; RAY, 2015).

Na América do Sul, na Triássico da Argentina são registradas do final do Anisiano e início do Ladiniano as espécies *Andescynodon mendozensis* Bonaparte, 1967 (Formação Cerro de Las Cabras; Figura 6E-F) e *Pascualgnathus polanskii* Bonaparte, 1965 (Formação Río Seco de la Quebrada; Figura 6G-H). No início do Carniano *Massetognathus pascuali* Romer, 1967 (Formação Chañares; Figura 6I-J). E por fim *Exaeretodon argentinus* Cabrera, 1943 (Formação Ischigualasto; Figura 6K-L) do fim do Carniano e início do Noriano (ABDALA; RIBEIRO, 2010; LIU; ABDALA, 2014; MARSICANO et al., 2016; MARTINEZ et al., 2011).

Figura 6 – Seleção de algumas espécies da Família Traversodontidae

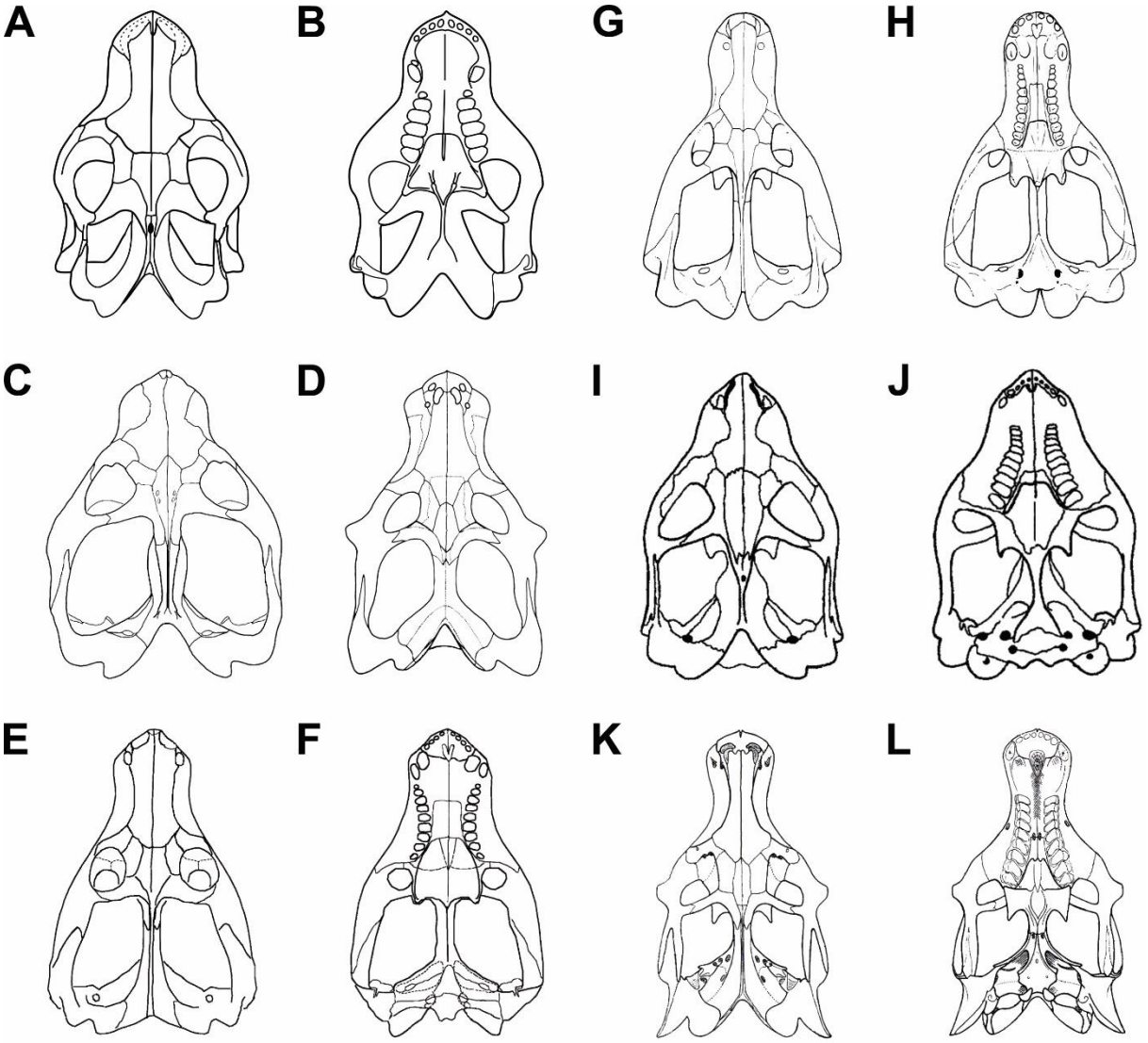

Legenda: África: *Luangwa drysdalli*, dorsal (A) e ventral (B); *Dadadon isaloi*, dorsal (C); India: *Exaeretodon* sp. (*Exaeretodon statisticae*), dorsal (D). Argentina: *Andescynodon mendozensis*, dorsal (E) e ventral (F); *Pascualgnathus polaskii*, dorsal (G) e ventral (H); *Massetognathus pascuali*, dorsal (I) e ventral (J); *Exaeretodon argentinus* dorsal (K) e ventral (L); Fonte: A-B modificado de Brink (1963); C modificado de Kammerer et al. (2012); D modificado de Chatterjee (1982); E-F modificado de Liu; Powell (2009); G-H modificado de Martinelli (2010); I-J modificado de Abdala; Giannini (2000); K-L modificado de Bonaparte (1962). As imagens não estão em escala.

No Triássico do sul do Brasil são registradas as espécies *Luangwa sudamericana* Abdala & Teixeira, 2004; *Massetognathus ochagaviae* Barberena 1981 (Figura 7A-B); *Massetognathus pascuali*; *Protuberum cabralense* Reichel et al., 2009 (Figura 7C-D), *Scalenodon ribeiroae* Melo et al., 2017; *Traversodon stahleckeri* Huene, 1936 (Figura 7E-F), para a ZA de *Dinodontosaurus*. *Menadon besairiei* (Figura 7G-H) e *Santacruzodon hopsoni* Abdala & Ribeiro, 2003 para a ZA de *Santacruzodon*. *Exaeretodon riograndensis* Abdala et

al., 2002 (Figura 7I-J) e *Gomphodontosuchus brasiliensis* Huene, 1928 para a ZA de *Hyperodapedon*; e *Siriusgnathus niemeyerorum* Pavanatto et al., 2018 (Figura 7K-L), ainda sem uma ZA apropriadamente definida (LIU; ABDALA, 2014; LIU; SOARES; REICHEL, 2008; MELO; MARTINELLI; SOARES, 2017; PAVANATTO et al., 2018). Além disso Ribeiro; Abdala; Bertoni (2011) reportam preliminarmente a possível presença de Traversodontidae para a ZA de *Riograndia* (ver seções 1.5 e 5.1).

1.4.1 Traversodontídeos do Triássico do sul do Brasil

Como mencionado acima, no Triássico sul-brasileiro, são registradas onze espécies (dez gêneros). Abaixo, cada uma das espécies está listada, bem como suas características diagnósticas:

A espécie *Luangwa sudamericana* é caracterizada pelo rostro curto, órbitas grandes, processo angular do dentário levemente projetado posteriormente; pós-caninos superiores com formato oval e com cíngulo anterolabial; cíngulo posterior com pequenas cúspules localizado posteriormente à crista transversa, estendendo-se ao longo de parte da borda posterior; cúspide posterior acessória da crista labial bem definida, presença de três cúspides na crista transversa. Os pós-caninos inferiores não apresentam cíngulo labial e o cíngulo posterior é composto por duas pequenas cúspules na frente da crista transversa (ABDALA; SA-TEIXEIRA, 2004; LIU; ABDALA, 2014).

A espécie *Scalenodon ribeiroae* é caracterizada pelos pós-caninos superiores com a face lingual côncava, com uma crista transversa formada por três cúspides, localizada no meio da coroa dentária, e com cíngulo anterior e cúspide anterolabial acessória ausentes; fossa paracanina localizada medialmente em relação aos caninos superiores; e processo descendente do jugal ausente (LIU; ABDALA, 2014; MELO; MARTINELLI; SOARES, 2017).

A espécie *Traversodon stahleckeri* (Figura 7 E-F) apresenta rostro curto e moderadamente largo, com constrição após a área de implantação dos caninos; processo angular do dentário agudo e bem desenvolvido; nove a dez pós-caninos superiores com formato oval e com as cúspides labial e lingual conectadas por uma crista transversal e cíngulo posterior bem desenvolvido; oito pós-caninos inferiores com a cúspide labial inferior em relação ao nível da cúspide lingual e sem cíngulo anterior à crista transversa (BARBERENA, 1981a; LIU; ABDALA, 2014).

O gênero *Massetognathus* Romer, 1967 apresenta incisivos alargados mesiodistalmente e denticulados; incisivos superiores próximos aos caninos; caninos pequenos, sendo os

superiores posicionados lateralmente à fossa paracanina; pós-caninos superiores aproximadamente retangulares com "*shouldering*" incipiente e com duas cúspides mesiolabiais acessórias; pós-caninos inferiores com a crista transversa alta e aguda e com a cúspide mesiolabial mais alta do que a mesiolingual; palato secundário estende-se posteriormente além do nível da margem anterior da órbita plataforma maxilar lateral aos pós-caninos e bem desenvolvida; ausência do processo descendente do jugal (LIU; ABDALA, 2014).

Figura 7 – Seleção de algumas espécies da Família Traversodontidae do Triássico do Sul do Brasil

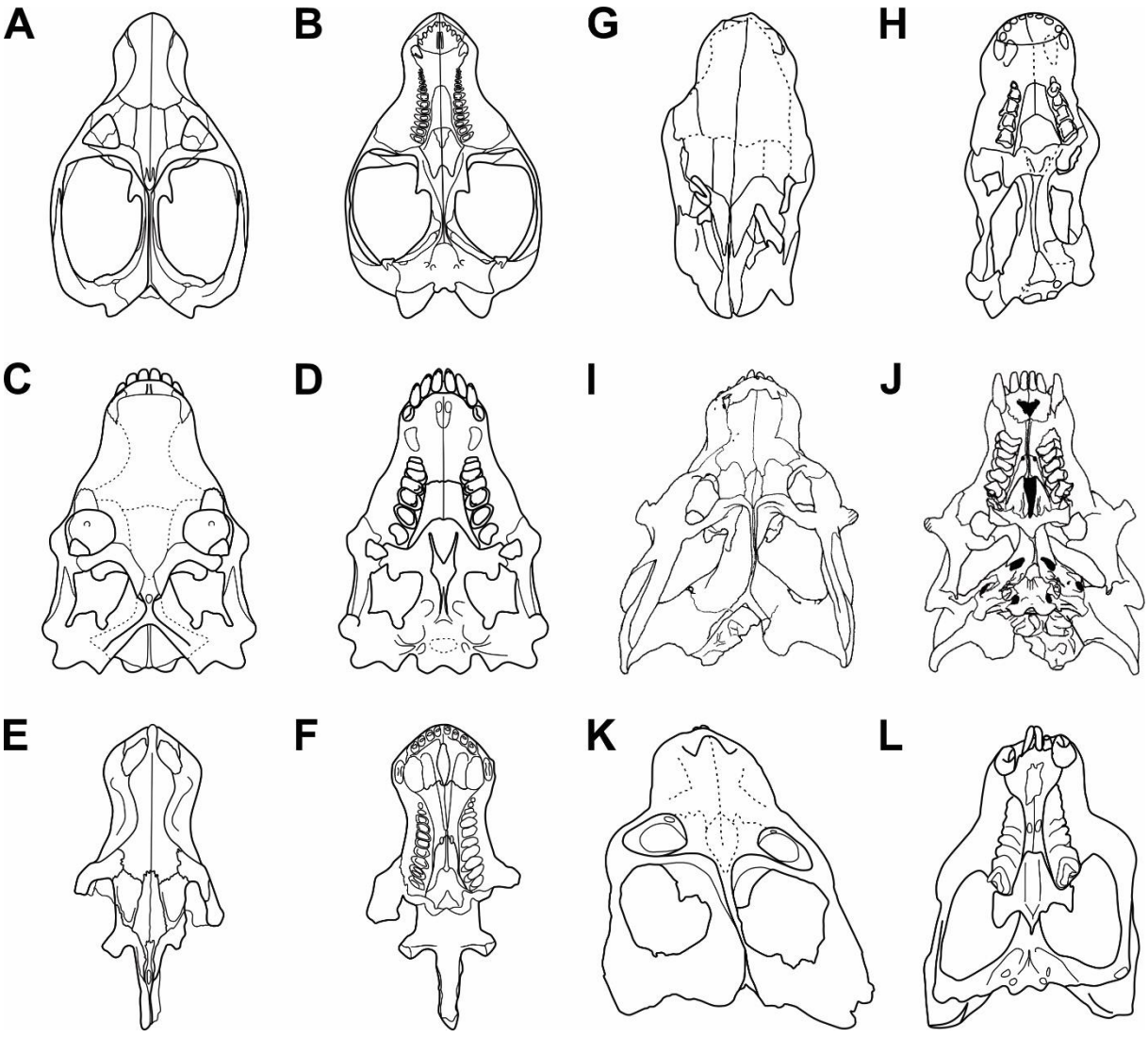

Legenda: *Massetognathus ochagaviae*, dorsal (A) e ventral (B); *Protuberum cabralense*, dorsal (C) e ventral (D); *Traversodon stahleckeri*, dorsal (E) e ventral (F); *Menadon besairiei*, dorsal (G) e ventral (H); dorsal (K); *Exaeretodon riograndensis* dorsal (I) e ventral (J); *Siriusgnathus niemeyerorum*, dorsal (K) e ventral (L). Fonte: A-B modificado de Liu; Soares; Reichel (2008); C-D modificado de Reichel et al. (2009); E-F modificado de Barberena (1981a); G-H modificado de Melo; Abdala; Soares (2015); I-J modificado de Abdala; Barberena; Dornelles (2002); K-L modificado de Pavanatto et al. (2018). As imagens não estão em escala.

A espécie *Massetognathus pascuali* (Figura 6I-J) apresenta caninos pequenos; pós-caninos superiores com cíngulo anterior ausente; pós-caninos com cíngulo posterior presente; rostro e região temporal com aproximadamente o mesmo comprimento; margem dorsal do coracoide e do procoracoide no mesmo nível, em vista medial; costelas lombares com formato de "T", com contato restrito com a costela sucessiva (LIU; ABDALA, 2014).

A espécie *Massetognathus ochagaviae* (Figura 7A-B) é diagnosticada pelo número de pós-caninos menos variável do que em que *M. pascuali*; projeção lateral da base labial dos pós-caninos superiores, formando um triângulo isósceles em vista oclusal; bacia oclusal dos pós-caninos superiores quase triangular, devido à crista lingual curta; caninos inferiores robustos; pós-caninos inferiores com formato sub-retangular, rostro mais curto do que a região temporal; crânio e mandíbula mais altos do que em *M. pascuali* (BARBERENA, 1981b; LIU; ABDALA, 2014; LIU; SOARES; REICHEL, 2008).

A espécie *Protuberum cabralense* (Figura 7C-D) apresenta pós-caninos superiores com duas cúspides principais, conectadas por uma crista transversa e ausência de "*shouldering*"; fossa paracanina alongada anteroposteriormente e localizada posteriormente aos caninos superiores; crista parietal curta; processo descendente do jugal bem desenvolvido; processo paraoccipital bifurcado; forâmen incisivo totalmente incluso na maxila; espessamento ósseo formando uma crista ampla na superfície dorsal do crânio; costelas com processos bastante pronunciados e serie de rugosidades ao longo da borda dorsal da lâmina ilíaca (LIU; ABDALA, 2014; REICHEL; SCHULTZ; SOARES, 2009).

A espécie *Menadon besairiei* (Figura 7G-H) apresenta quatro incisivos superiores (incisivos 1 e 2, procumbentes; incisivos 3 e 4, caniniformes, sendo o incisivo 4 fortemente recurvado e com margens denticuladas), incisivos inferiores procumbentes, caninos superiores pequenos, com tamanho semelhante ao dos incisivos; diastema entre os incisivos e os caninos superiores ausente; pós-caninos com formato quadrangular a trapezoidal, oito superiores e de seis a sete inferiores; processo descendente do jugal ausente; processo ventral do esquamosal no arco zigomático cobrindo lateralmente o complexo quadrato-quadradojugal (KAMMERER et al., 2008; MELO; ABDALA; SOARES, 2015).

A espécie *Santacruzodon hopsoni* é caracterizada pela presença do processo descendente do jugal em formato esférico; incisivos achatados labiolingualmente, apresentando uma série de 7-9 cúspules na margem; pós-caninos superiores com uma pequena crista anterior formada por uma série de cúspules cingulares e com três cúspides labiais, sendo a posterior bem desenvolvida, compondo mais da metade do comprimento da crista labial; pós-caninos

inferiores com a cúspide anterolingual fortemente inclinada posteriormente (ABDALA; RIBEIRO, 2003; LIU; ABDALA, 2014).

A espécie *Exaeretodon riograndensis* (Figura 7I-J) possui três incisivos superiores; caninos superiores grandes e inferiores de tamanho reduzido; pós-caninos superiores com uma cúspide póstero-labial acessória bem desenvolvida e com "*shouldering*" bem desenvolvido, resultando da separação dos lobos labial e lingual; cúspide anterolingual dos pós-caninos inferiores fortemente inclinada posteriormente; barra internarial ausente; processo descendente do jugal bem desenvolvido; aba lateral do proótico com uma série de cristas anteriores a *fenestra ovalis* e costelas sem placas costais (ABDALA; BARBERENA; DORNELLES, 2002; LIU; ABDALA, 2014).

A espécie *Gomphodontosuchus brasiliensis* é caracterizada pelo rostro curto e alto; palato secundário curto e amplo, com a margem posterior localizada anteriormente em relação à órbita; cinco a seis pós-caninos superiores e inferiores; pós-caninos superiores com formato variando de triangular (nos dentes mais anteriores) a quadrangular (nos dentes mais posteriores); fossa paracanina localizada medialmente em relação aos caninos superiores; sínfise do dentário robusta; borda anterior do processo coronoide do dentário localizada no nível do quarto pós-canino inferior (LIU; ABDALA, 2014).

Siriusgnathus niemeyerorum (ver Seção 3 – Artigo 1; Figura 7K-L) apresenta dois incisivos superiores; cúspide labial acessória distal dos pós-caninos superiores posicionada mais labialmente, em comparação com *Exaeretodon*; dois a três incisivos inferiores; rostro curto e amplo, com aproximadamente o mesmo comprimento da região temporal; processo descendente do jugal incipiente; barra pós-orbital posicionada mais anteriormente do que em *Exaeretodon*; borda posterior do processo zigomático do esquamosal curto e arredondado; crista lambdoidal não forma uma concavidade, como em *Exaeretodon*; e basicrânio curto anteroposteriomente (PAVANATTO et al., 2018).

1.4.2 As relações filogenéticas de Traversodontidae

A monofilia da família Traversodontidae vem sendo debatida em vários estudos. Alguns autores posicionavam a família Tritylodontidae Cope, 1884 em Gomphodontia como um subgrupo derivado da família Traversodontidae, então considerada parafilética (e.g., CROMPTON, 1972; CROMPTON; ELLENBERGER, 1957; HOPSON; KITCHING, 2001; SUES, 1985; Figura 8A). Contudo estudos mais recentes, baseados em análises filogenéticas, posicionam a família Tritylodontidae em Probainognathia, proximamente relacionada aos

mamaliaformes, e nesse caso Traversodontidae se manteria monofilética (ABDALA, 2007; ABDALA; RIBEIRO, 2003; LIU; ABDALA, 2014; LIU; OLSEN, 2010; LUO, 2007; RUTA et al., 2013; Figura 8B). Segundo Liu; Olsen (2010), os caracteres que suportam Tritylodontidae dentro de Cynognathia, a maioria delas ligadas a características do arco zigomático e dos dentes pós-caninos, pode ser resultado de adaptações convergentes para o hábito herbívoro, compartilhado por tritilodontídeos e traversodontídeos. Porém, Sidor et al. (2016), descrevem brevemente um novo cinodonte com dentição gonfodonte, proveniente dos níveis superiores da Formação Ntawere, Zâmbia, o qual é recuperado como filogeneticamente próximo de Tritylodontidae, o que sugeriria que os Tritylodontidae seriam Gomphodontia derivados.

Dentre as relações filogenéticas entre os membros da família Traversodontidae, com a relação a base do grupo, a relação entre os membros basais é bastante variável, geralmente recuperado uma grande politomia nas análises filogenéticas realizadas (e.g., ABDALA; NEVELING; WELMAN, 2006; ABDALA; RIBEIRO, 2003; LIU, 2007; Figura 8C). Nas análises filogenéticas mais recentes, *Nanogomphodon wildi* é recuperado como o traversodontídeo mais basal (LIU; ABDALA, 2014; MELO; ABDALA; SOARES, 2015; MELO; MARTINELLI; SOARES, 2017; PAVANATTO et al., 2018; SCHMITT et al., 2019; Figura 8D-F). Contudo, esse posicionamente pode estar sendo influenciado pela incompletude do táxon, conhecido apenas por um pós-canino inferior isolado (HOPSON; SUES, 2006; LIU; ABDALA, 2014). Em outras abordagens *Luangwa* Brink, 1963 e *Scalenodon angustifrons* são recuperados como os mais basais, em adição a *Andescynodon mendozensis* e *Pascualgnathus polanskii* (ABDALA; NEVELING; WELMAN, 2006; ABDALA; RIBEIRO, 2003; KAMMERER et al., 2008; LIU; OLSEN, 2010; Figura 8C-F). Um dos clados mais comumente recuperados dentro de Traversodontidae é o formado por *Exaeretodon*, *Gomphodontosuchus brasiliensis*, *Menadon besairiei*, *Protuberum cabralense* e *Scalenodontoides macrodontes* (ABDALA; RIBEIRO, 2003; FLYNN et al., 2000; KAMMERER et al., 2008; LIU; ABDALA, 2014; REICHEL; SCHULTZ; SOARES, 2009; Figura 8C-F). Kammerer et al. (2008) nomeou esse clado de Gomphodontosuchinae Watson; Romer, 1956 definindo-o como o clado mais inclusivo contendo *Gomphodontosuchus brasiliensis*, mas não *Massetognathus pascuali*. As relações entre alguns taxa dentro de Gomphodontosuchinae ainda são incertas. Na análise filogenética realizada por Liu; Abdala (2014) e em trabalhos subsequentes (MELO; ABDALA; SOARES, 2015; MELO; MARTINELLI; SOARES, 2017), as duas espécies de *Exaeretodon*, *E. argentinus* e *E. riograndensis*, juntamente com *Scalenodontoides macrodontes*, formam uma politomia. *Siriusgnathus niemeyerorum*, recentemente descrito, também é recuperado dentro desta politomia (PAVANATTO et al., 2018; Figura 8D).

Figura 8 – Relações filogenéticas de Traversodontidae

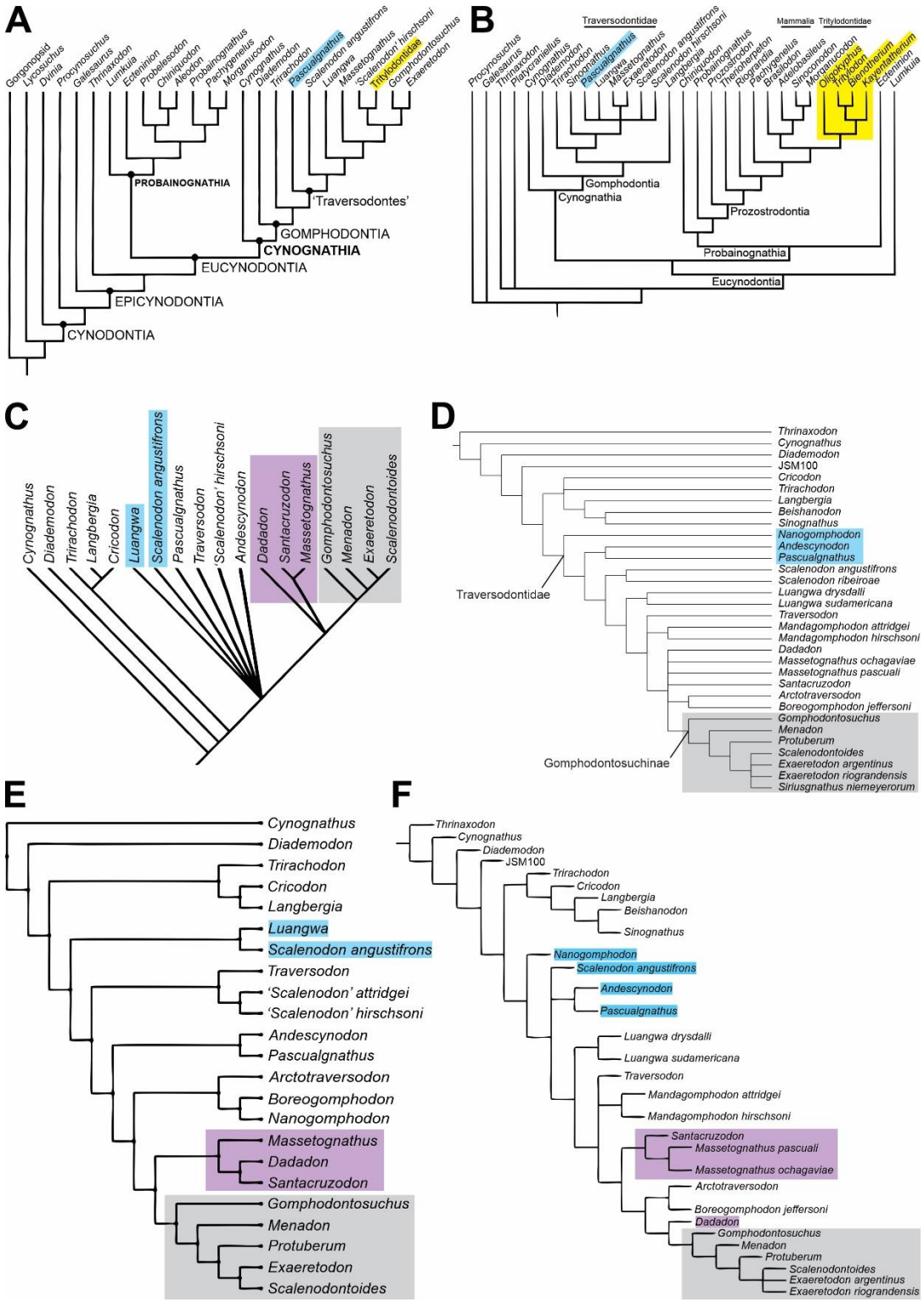

Legenda: A, Árvore filogenética ilustrando a hipótese Tritylodontidae-Cynognathia; B, Árvore filogenética ilustrando a hipótese Tritylodontidae-Probainognathia; C-E, Hipóteses filogenéticas para Traversodontidae. Amarelo: Tritylodontidae; Azul: traversodontídeos basais; Cinza: Gomphodontosuchinae; Lilás: Massetognathinae. Fonte: A modificado de Hopson; Kitching (2001); B modificado de Liu; Olsen (2010); C modificado de Kammerer et al. (2008); D modificado de Pavanatto et al. (2018); E modificado de (Kammerer et al. (2012); E, modificado de Liu; Abdala (2014).

Em algumas hipóteses filogenéticas os gêneros *Dadadon*, *Massetognathus* e *Santacruzodon* formam um clado (GAO et al., 2010; KAMMERER et al., 2008, 2012; RANIVOHARIMANANA et al., 2011). Kammerer et al. (2012) nomeou esse clado de Massetognathinae, definindo-o como o clado contendo todos os traversodontídeos mais proximamente relacionados a *Massetognathus pascuali* do que *Gomphodontosuchus brasiliensis* (Figura 8C, E-F). Na hipótese filogenética de Liu; Abdala (2014), *Santacruzodon* é recuperado como grupo irmão do clado formado pelas duas espécies de *Massetognathus* (*M. pascuali* e *M. ochagaviae*), enquanto que *Dadadon*, por sua vez, é recuperado como grupo irmão de Gomphodontusuchinae (Figura 8F).

1.5 CONTEXTO BIOESTRATIGRÁFICO DOS CINODONTES DO TRIÁSSICO SUL BRASILEIRO

Tradicionalmente, o conjunto litológico do pacote Triássico Médio a Superior, é composto pelas Formações Santa Maria (Triássico Médio/Superior) e Caturrita (Triássico Superior) as quais apresentam uma grande diversidade de vertebrados fósseis, sendo os cinodontes membros abundantes nessas unidades litológicas (ZERFASS et al., 2003), as quais são agrupadas na Supersequência Santa Maria e subdivididas em três sequências estratigráficas, denominadas, da base para o topo, Sequências Santa Maria 1, 2 e 3 (ZERFASS et al., 2003). Recentemente, Horn et al. (2014) propuseram uma quarta sequência entre as Sequências 1 e 2 originais, denominada Sequência Santa Cruz. Novos nomes também foram propostos para as demais sequências da base para o topo: Sequência Pinheiros-Chiniquá, Sequência Santa Cruz, Sequência Candelária e Sequência Mata (Figura 9). As quatro ZAs reconhecidas para o Triássico do Rio Grande do Sul, *Dinodontosaurus*, *Santacruzodon*, *Hyperodapedon* e *Riograndia*, estão incluídas, da base para o topo, nas Sequências Pinheiros-Chiniquá, Santa Cruz e Candelária (HORN et al., 2014).

A ZA de Dinodontosaurus é caracterizada pela predominância do dicinodonte *Dinodontosaurus* Romer, 1943 e do cinodonte traversodontídeo *Massetognathus* Romer, 1967. Tradicionalmente a ZA de *Dinodontosaurus* é correlacionada com a fauna da Formação Chañares da Argentina, devido a presença compartilhada dos taxa mencionados acima, além da presença de arcossauros similares às formas brasileiras, e datada para o início do Carniano (236-234 Ma; EZCURRA et al., 2017; MARSICANO et al., 2016). Contudo, foi realizada datação radiométrica para a Sequência Santa Cruz, datando a idade máxima da sequência em 236 Ma (PHILIPP et al., 2013, 2018). Como essa sequência inclui a ZA de *Santacruzodon*, considerada

mais recente do que a ZA de *Dinodontosaurus*, levantou a possibilidade de que talvez a ZA de *Dinodontosaurus* tenha sido depositada durante o Ladiniano e início do Carniano. Porém, alguns taxa da ZA de *Dinodontosaurus*, i.e., os cinodontes *Aleodon cromptoni* Martinelli et al., 2017, *Luangwa sudamericana* e *Scalenodon ribeiroae*; e o rincossauro *Brasinorhynchus mariantensis* Schultz et al., 2016, apresentam um padrão de distribuição ao longo da coluna estratigráfica, que levou alguns autores a considerar que a ZA de *Dinodontosaurus* poderia estar subdivida em duas subzonas: uma mais antiga representada pelos taxa citados acima e outra mais recente representada pela fauna associada a *Massetognathus*/*Dinodontosaurus* (EZCURRA et al., 2017; MARTINELLI et al., 2017b; MELO; MARTINELLI; SOARES, 2017).

Figura 9 – Unidades crono-, bioestratigráficas e ZAs, com as respectivas ocorrências de cinodontes para o Triássico sul-brasileiro

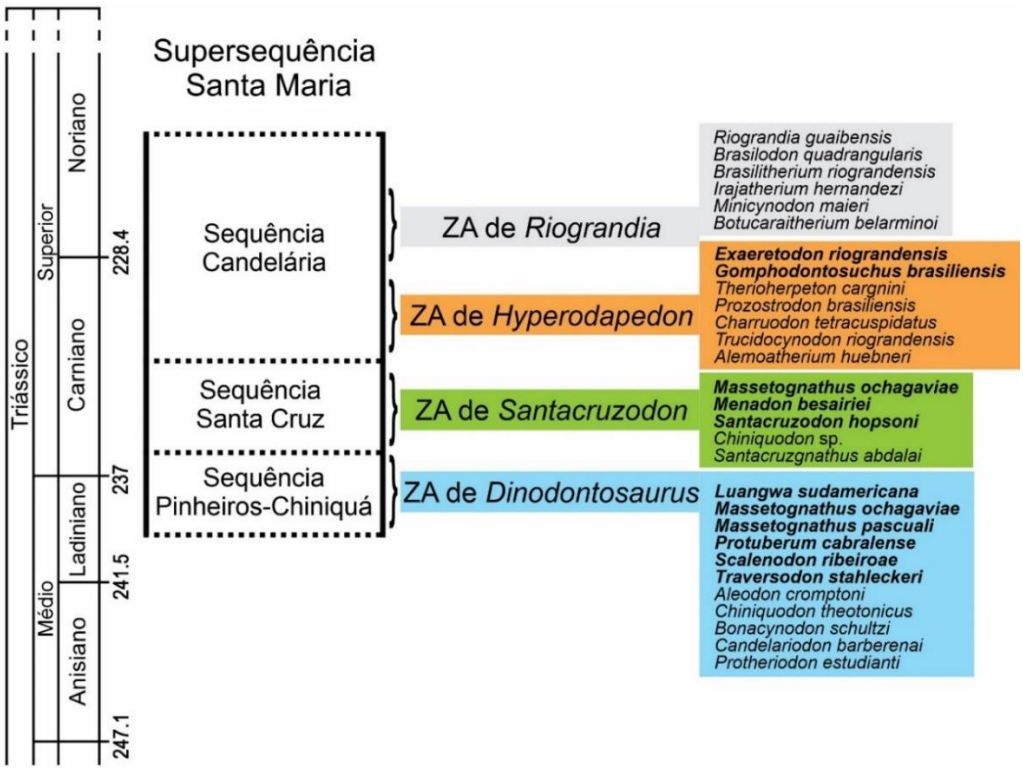

Legenda: Em negrito estão destacados os registros de cinodontes na família Traversodontidae. Fonte: Modificado de Martinelli et al. (2017b).

A ZA de *Santacruzodon* é quase exclusivamente dominada por cinodontes traversodontídeos, i.e., *Santacruzodon*, *Menadon* e *Massetognathus* (ABDALA et al., 2009; ABDALA; RIBEIRO, 2003; ABDALA; RIBEIRO; SCHULTZ, 2001; MELO; ABDALA; SOARES, 2015; SCHMITT et al., 2019; SOARES; SCHULTZ; HORN, 2011). A fauna da ZA

de *Santacruzodon* apresenta semelhanças com fauna da Formação Isalo II de Madagascar pela presença compartilhada de *Menadon besairiei* (MELO; ABDALA; SOARES, 2015), além de similaridades entre as espécies de cinodontes encontradas em ambas as faunas, e.g. *Santacruzodon* e *Dadadon* (ABDALA et al., 2009; ABDALA; RIBEIRO, 2003; ABDALA; RIBEIRO; SCHULTZ, 2001; MELO; ABDALA; SOARES, 2015; SOARES; SCHULTZ; HORN, 2011). Como mencionado acima, Philipp et al. (2013; 2018) obteve uma idade máxima de 236 Ma para a Sequência Santa Cruz, o que posiciona a ZA de *Santacruzodon* no Carniano (MARTINELLI; SOARES; SCHWANKE, 2016; SCHULTZ; LANGER; MONTEFELTRO, 2016).

Na ZA de *Hyperodapedon*, há prevalência do rincossauro *Hyperodapedon* Huxley, 1859 e do cinodonte traversodontídeo *Exaeretodon riograndensis* (LANGER et al., 2007; SCHULTZ; SCHERER; BARBERENA, 2000). Para AZ são registrados também dinossauros sauropodomorfos: *Bagualosaurus agudoensis* Pretto; Langer; Schultz, 2018; *Buriolestes schultzi* Cabreira et al., 2016; *Pampadromaeus barberenai* Cabreira et al., 2011 e *Saturnalia tupiniquim* Langer et al., 1999 (CABREIRA et al., 2011, 2016; LANGER et al., 1999; PRETTO; LANGER; SCHULTZ, 2018). A ZA de *Hyperodapedon* pode ser correlacionada com a Formação Ischigualasto, na qual também há a predominância do rincossauro *Hyperodapedon* e de cinodontes do gênero *Exaeretodon* (ROGERS et al., 1993). Essa correlação posiciona a ZA de *Hyperodapedon* no final do Carniano, início do Noriano (LANGER et al., 2007; MARTINEZ et al., 2011). Recentemente, a localidade tipo de *S. tupiniquim* foi datada através de radioisotopia, obtendo uma idade de 233,23 ± 0,73 Ma (Carniano; LANGER; RAMEZANI; DA-ROSA, 2018).

E por fim a ZA de *Riograndia* é dominada por pequenos cinodontes probainognátios, como *Riograndia guaibensis*, *Brasilodon quadrangulares* Bonaparte et al., 2003 e *Irajatherium hernandezi* Martinelli et al., 2005 (BONAPARTE et al., 2003, 2010; BONAPARTE; FERIGOLO; RIBEIRO, 2001; BONAPARTE; MARTINELLI; SCHULTZ, 2005; BONAPARTE; SOARES; MARTINELLI, 2013; MARTINELLI et al., 2005; SOARES; SCHULTZ; HORN, 2011). A ZA de *Riograndia* pode ser correlacionada com a fauna dos níveis inferiores da Formação Los Colorados e com os níveis superiores da Formação Ischigualasto devido à presença do dicinodonte *Jachaleria* Bonaparte, 1971, datadas como Noriano (BONAPARTE et al., 2010; KENT et al., 2014; LANGER et al., 2007; LANGER; RAMEZANI; DA-ROSA, 2018; MARTINEZ et al., 2011; MARTÍNEZ et al., 2012; MÜLLER; LANGER; DIAS-DA-SILVA, 2017; SOARES; SCHULTZ; HORN, 2011). O Sítio Linha São

Luiz foi datado recentemente, através de radioisotopia, obtendo uma idade de 225,42 ± 0,37 Ma, corroborando a idade noriana dessa AZ (LANGER; RAMEZANI; DA-ROSA, 2018).

Ribeiro; Abdala; Bertoni (2011), reportam preliminarmente a presença de cinodontes traversodontídeos para a ZA de *Riograndia*, por registros fragmentários (cf. *Exaeretodon*), associados a materiais de formas típicas dessa ZA (i.e. o silesaurídeo *Sacisaurus agudoensis* Ferigolo; Langer, 2006, *Riograndia guaibensis* e *Brasilitherium riograndesis* Bonaparte et al., 2003). Essa descoberta levanta a possibilidade de que *Exaeretodon* poderia ter sobrevivido até o Noriano ou pelo menos até a transição Carniano/Noriano. Poderia ainda ter sido preservado em estratos depositados no final do Carniano (no topo da ZA de *Hyperodapedon*) e posteriormente retrabalhado e finalmente redepositado na ZA posterior (ZA de *Riograndia*).

1.6 BREVE HISTÓRICO DO ESTUDO DA PALEONEUROLOGIA EM CINODONTES

Os primeiros estudos sobre a paleoneurologia de cinodontes foram publicados por Watson (1913), onde são descritos os moldes endocranianos naturais de *Diademodon* e de *Nythosaurus larvatus* Owen, 1876 (= *Thrinaxodon liorhinus* Seeley, 1894). Posteriormente, o endocrânio de *N. larvatus* foi redescrito por Simpson (1927) e por Hopson (1969). Bonaparte (1966b), descreveu a morfologia das cavidades nasal e cerebral de *Exaeretodon argentinus* e Jerison (1973) descreveu a cavidade endocraniana de *Thrinaxodon*. Um pouco depois, Kemp (1979) apresentou a morfologia craniana do *Procynosuchus delaharpeae* Broom, 1937, bem como de seu endocrânio. Hopson (1979), faz um revisão dos estudos até então publicados sobre paleoneurologia de repteis fósseis, e descreve a morfologia endocraniana de *Trirachodon kannemeyeri* (Figura 10A). Quiroga (1979a, 1979b) descreveu a morfologia endocraniana e da orelha interna de *Massetognathus* sp. (Figura 10B) e cf. *Probelesodon* Romer, 1969. Posteriormente Quiroga (1980), apresentou a morfologia endocraniana de outros espécimes de *Massetognathus* (*Massetognathus pascuali*), além de *Andescynodon mendozensis* e de *Probelesodon* sp. No mesmo ano, Quiroga (1980b) apresentou a morfologia endocraniana de *Probainognathus jenseni* Romer, 1970 (Figura 10C). Posteriormente, Quiroga (1984) descreveu o endocrânio de *Therioherpeton cargnini* Bonaparte & Barberena, 1975. Kielan-Jaworowska (1986) reinterpretou o endocrânio de *Probainognathus* e *Therioherpeton*. Mais recentemente, Kemp (2009), descreveu a cavidade endocraniana de *Chiniquodon theotonicus* von Huene, 1936.

Todos os estudos acima foram realizados em base em moldes endocranianos naturais, i.e., a cavidade endocraniana é preenchida por sedimento, preservando o formato da mesma, o

que geralmente requeria a destruição ou remoção de parte do fóssil para acessar o molde endocraniano. Com o avanço de tecnologias de aquisição de imagens internas para fins médicos, vários trabalhos sobre paleoneurologia começaram a ser realizados empregando técnicas de tomografia computadorizada, cuja a vantagem é ser uma técnica não destrutiva. Rowe; Macrini; Luo (2011) descreveram o molde endocraniano digital dos mammaliaformes *Morganucodon* Kuehne, 1949 e *Hadrocodium* Luo; Crompton; Sun, 2001. Rodrigues; Ruf; Schultz (2014), apresentaram o molde endocraniano digital de *Brasilitherium riograndensis* (= *Brasilodon quadrangularis*) (Figura 10D) e mais recentemente de *Riograndia guaibensis* (RODRIGUES et al., 2018; Figura 10E). Hoffmann (2018), descreveu moldes endocranianos digitais de *Massetognathus ochagaviae* e *Probelesodon kitching* Sá-Teixeira, 1982. E por fim Pusch; Kammerer; Fröbisch (2019), apresentaram o molde endocraniano digital de *Galesaurus planiceps* Owen, 1859. Além disso vários estudos sobre a paleoneurologia de membros do clado Therapsida foram publicados (e.g., ARAÚJO et al., 2017; BENDEL et al., 2018; BENOIT et al., 2017b, 2017a, 2017c; BENOIT; MANGER; RUBIDGE, 2016; LAASS, 2015; LAASS; SCHILLINGER; KAESTNER, 2017).

Figura 10 – Moldes endocranianos de alguns cinodontes

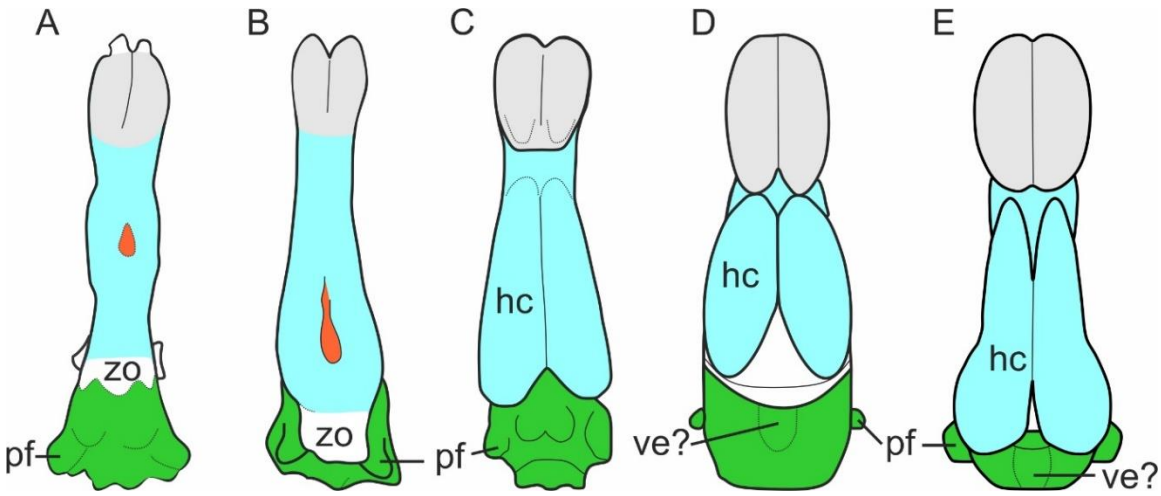

Legenda: A, *Trirachodon*; B, *Massetognathus*; C, *Probainognathus*; D, *Riograndia*; E, *Brasilitherium*. Cinza: bulbos olfatórios; azul: telencéfalo e mesencéfalo; verde: rombencéfalo; laranja: tubo pineal; branco: vascularizações. Abreviações: hc, hemisférios cerebrais; pf, *paraflocculus*; ve, *vermis* do cerebelo; zo, zona não ossificada. Fonte: A modificado de Hopson (1979); B modificado de Quiroga (1979b); C modificado de Quiroga (1980b); D modificado de Rodrigues et al. (2018); E modificado de Rodrigues et al. (2014). As imagens não estão em escala.

De forma geral, o endocrânio the *Galesaurus*, *Thrinaxodon*, *Trirachodon*, *Andescynodon*, *Massetognathus* e *Exaeretodon* é estreito, tubular e alongado, apresentando

pouca diferenciação entre as estruturas do encéfalo, destacando-se a apresenta da zona não-ossificada e dos paraflóculos bem desenvolvidos (BONAPARTE, 1966b; HOPSON, 1979; PUSCH; KAMMERER; FRÖBISCH, 2019; QUIROGA, 1979a, 1980a). Apesar do fato de que em *Galesaurus, Thrinaxodon, Trirachodon* e *Massetognathus* os bulbos olfatórios serem levemente diferenciados entre si, devido à presença de um sulco longitudinal, uma maior diferenciação das estruturas do cérebro é observada em Probainognathia, e.g. *Probainognathus*, nos Prozostrodontia Liu; Olsen, 2010 *Therioherpeton*, *Riograndia* e *Brasilitherium* e nos Mammaliaformes (HOPSON, 1969, 1979; PUSCH; KAMMERER; FRÖBISCH, 2019; QUIROGA, 1979a, 1980b, 1984; RODRIGUES et al., 2018; RODRIGUES; RUF; SCHULTZ, 2014; ROWE; MACRINI; LUO, 2011). *Probainognathus* apresenta os bulbos olfatórios bem diferenciados entre si e dos pedúnculos olfatórios, os hemisférios cerebrais são separados por um sulco longitudinal e uma exposição parcial na superfície dorsal endocrânio do mesencéfalo, devido a presença de uma estrutura interpretada como o colículo anterior. Segundo Quirora (1980b), *Probainognathus* apresentaria evidências da presença de um neocórtex, devido a um sulco na região posterior aos hemisférios cerebrais que marcaria a extensão posterior do neocórtex. Contudo Kielan-Jaworowska (1986) interpreta esse sulco como a impressão de um vaso sanguíneo o colículo anterior como o molde do seio transverso. *Therioherpeton* apresenta os hemisférios cerebrais bem diferenciados, com os polos posteriores amplos e divergentes e, segundo Quiroga (1984) com o mesencéfalo exposto na superfície dorsal do endocrânio. Contudo a região posterior do endocrânio de *Therioherpeton* não está bem preservada, e a exposição do mesencéfalo é incerta (KIELAN-JAWOROWSKA, 1986). O mesencéfalo geralmente não é exposto na superfície dorsal porque ele é coberto por seios vasculares e pelas meninges associadas ou devido à expansão posterior do telencéfalo ou expansão anterior do cerebelo, ou mesmo por uma combinação dessas estruturas (EDINGER, 1964; MACRINI; ROUGIER; ROWE, 2007; RODRIGUES et al., 2018). Segundo Macrini; Rougier; Rowe (2007) a condição plesiomórfica do grupo coronal dos mamíferos é a não exposição do mesencéfalo. *Riograndia* apresenta os bulbos olfatórios e hemisférios cerebrais bem delimitados e muito mais amplos, além disso, apresentam uma pequena protuberância na região cerebelar que pode ser interpretada como o *vermis* do cerebelo (RODRIGUES et al., 2018). *Brasilitherium*, apresenta os bulbos olfatórios bem diferenciados entre si e anteroposteriormente expandidos, ocupando uma grande proporção da cavidade endocraniana. Os hemisférios cerebrais também são bem diferenciados, e assim como em *Riograndia* apresentam uma pequena protuberância na região cerebelar que pode ser interpretada como o *vermis* do cerebelo. Em *Brasilitherium* é observado, além do aumento dos bulbos olfatórios,

um alargamento dos hemisférios cerebrais e do cerebelo, em comparação com o observado para outros cinodontes (RODRIGUES; RUF; SCHULTZ, 2014). Os Mammaliaformes *Morganucodon* e *Hadrocodium* apresentam uma grande expansão do endocrânio, principalmente da região dos bulbos olfatórios e dos hemisférios cerebrais. Para esses taxa o morfologia geral do endocrânio lembra mais o padrão mamíferos atuais do que o observado nos cinodontes não-mamaliaformes. Provavelmente ambos os taxa apresentavam o desenvolvimento do neocórtex, devido o alargamento da região dos hemisférios cerebrais (ROWE; MACRINI; LUO, 2011). O grande cérebro dos mamíferos, em comparação ao cérebro de outros vertebrados, está relacionado com o desenvolvimento do neocórtex (KIELAN-JAWOROWSKA; CIFELLI; LUO, 2004). A aquisição do neocórtex está ligada ao desenvolvimento de um sistema sensorial mais acurado, funções cognitivas e controle motor mais elaborados (KIELAN-JAWOROWSKA; CIFELLI; LUO, 2004; LAASS; KAESTNER, 2017; ROWE; MACRINI; LUO, 2011). Jerison (1973), atribuiu o aumento da encefalização nos mamíferos ao hábito de vida noturno dos primeiros mamíferos, o que teria impulsionado um aperfeiçoamento dos sistemas auditivo e olfativo. Por outro lado, a aquisição da endotermia e aumento das taxas metabólicas nos mamíferos também pode estar ligada com aumento de cérebro nesse grupo, uma vez que um cérebro grande requer uma taxa metabólica mais alta para sua manutenção (ALLMAN, 1990; KEMP, 2006; QUIROGA, 1980b; ROWE; MACRINI; LUO, 2011). Rowe et al. (2011), reconheceram dois pulsos de encefalização pré-mamalianos. O primeiro pulso foi impulsionado pelos sistemas olfatório e táctil mais sensíveis e por uma melhora na coordenação neuromuscular. O mamaliforme basal *Morganucodon*, apresenta uma expansão dos bulbos olfatórios e do córtex olfatório, representaria o primeiro pulso. O segundo pulso foi provavelmente também foi impulsionado principalmente pela olfação. O mamaliforme *Hadrocodium*, representa esse segundo pulso, apresenta uma grande expansão dos bulbos olfatórios e do córtex olfatório, levando a um aumento do cérebro, cujo tamanho é comparável ao cérebro mamaliano. O grupo coronal de Mammalia, representa um terceiro pulso de aprimoramento da olfação, apresentando etmoturbinais e placa cribiforme ossificados sustentando o epitélio olfatório dentro da cavidade nasal (ROWE; MACRINI; LUO, 2011). Segundo Rodrigues et al. (2014; 2018), o aumento da encefalização impulsionada pela melhora do sistema de recepcção sensorial, ligado a adaptações da cavidade nasal e aumento dos bulbos olfatórios, relacionados com a endotermia, poderia estar ocorrendo antes da origem dos Mammaliaformes (e.g., *Brasilitherium*). Da mesma forma, essas mudanças também teriam ocorrido antes do aumento do volume cerebral, relacionado com um maior desenvolvimento dos hemisférios cerebrais, ocorrido nos Mammaliaformes.

2 OBJETIVOS

A presente tese tem por objetivo principal descrever a morfologia craniana de um novo morfotipo atribuído à família Traversodontidae, para o Neotriássico do sul do Brasil, e verificar a sua posição e relações filogenéticas dentro do grupo.

2.1 OBJETIVOS ESPECÍFICOS

1- Apresentar e caracterizar um novo sítio fossilífero para o Triássico Superior do Sul do Brasil, o qual apresenta uma grande acumulação de um novo morfotipo de cinodonte traversodontídeo;

2- Analisar e descrever a morfologia externa desse novo morfotipo para a família Traversodontidae;

3- Verificar a posição filogenética do novo morfotipo dentro da família Traversodontidae;

4- Analisar e descrever e a morfologia das cavidades cerebrais, do novo morfotipo (CAPPA/UFSM 0032) e de dois espécimes de *Exaeretodon riograndensis* (CAPPA-UFSM 0030 e 0227), acessadas através de tomografia computadorizada;

5- Comparar a morfologia das cavidades cerebrais entre o novo morfotipo e *E. riograndensis*, com outros traversodontídeos, bem como os demais cinodontes não-mamaliarformes cuja morfologia endocraniana é conhecida;

6- Calcular os coeficientes de encefalização de CAPPA/UFSM 0030, 0032 e 0227 e compará-los com o de outros cinodontes, descritos na literatura.

3 ARTIGO 1

O Artigo 1 intitulado: "*A new Upper Triassic cynodont-bearing fossiliferous site from southern Brazil, with taphonomic remarks and description of a new traversodontid taxon*", foi publicado no periódico *Journal of South American Earth Sciences*, doi: 10.1016/j.jsames.2018.08.016.

Journal of South American Earth Sciences 88 (2018) 179–196

Contents lists available at ScienceDirect

Journal of South American Earth Sciences

journal homepage: www.elsevier.com/locate/jsames

A new Upper Triassic cynodont-bearing fossiliferous site from southern Brazil, with taphonomic remarks and description of a new traversodontid taxon

Ane Elise Branco Pavanatto[a,*], Flávio Augusto Pretto[a,b], Leonardo Kerber[a,b], Rodrigo Temp Müller[a,b], Átila Augusto Stock Da-Rosa[a,b,c], Sérgio Dias-da-Silva[a,b]

[a] Programa de Pós-Graduação em Biodiversidade Animal, Universidade Federal de Santa Maria, Avenida Roraima 1000, 97105-900, Santa Maria, RS, Brazil
[b] Centro de Apoio à Pesquisa Paleontológica, Universidade Federal de Santa Maria, São João do Polêsine, Rua Maximiliano Vizzotto 598, CEP 97230-000, RS, Brazil
[c] Laboratório de Estratigrafia e Paleobiologia, Departamento de Geociências, Universidade Federal de Santa Maria, Avenida Roraima 1000, 97105-900, Santa Maria, RS, Brazil

ARTICLE INFO

Keywords:
Traversodontidae
Gomphodontosuchinae
Santa maria supersequence
Late triassic
Biostratigraphy

ABSTRACT

A new Upper Triassic fossiliferous outcrop, the Niemeyer Site, from the Santa Maria Supersequence (Paraná Basin, Southern Brazil) is reported. The lithology found in this locality is consistent with that found in the Candelária Sequence. The high prevalence of traversodontid cynodonts in this site is particularly notable, with collected specimens mostly composed of isolated bones and fragmentary specimens, but also including well-preserved skulls and mandibles. Probainognathian cynodonts and archosauromorphs are also present, but they are rare in comparison. There is a predominance of Voorhies Group III (Group III > Group I > Group II) for the specimens so far collected. These data, as well as the sedimentary data of the outcrop, indicate a mostly autochthonous fossiliferous assemblage. Some specimens display evidence of ichnological activity of invertebrate scavengers (bone alteration comprising small tubules, channels and isolated boreholes). A remarkable aspect of this site is the presence of a new traversodontid cynodont closely related to *Exaeretodon*. Although similar to the former taxon, the new taxonomic unit shows a unique combination of several craniodental features not present in other cynodonts. Given that no traversodontids are recorded in the uppermost levels of the Candelária Sequence, this site is likely placed in the lower levels of this unit, with the fauna suggesting a Carnian age.

1. Introduction

The Triassic sedimentary rocks from southern Brazil (central portion of Rio Grande do Sul State) were deposited into two second-order sequences – the Sanga do Cabral Supersequence (Lower Triassic) and Santa Maria Supersequence (?Middle-Upper Triassic, Zerfass et al., 2003, see also Marsicano et al., 2016). Conspicuous faunal associations are recognized in these units, and their Assemblage Zones (AZs) provide a biostratigraphic framework for comparison with other Triassic localities worldwide. These Brazilian biostratigraphic schemes have been reviewed and improved in resolution throughout time. According to Soares et al. (2011) and Horn et al. (2014), the most recent reviews on this topic, the Santa Maria Supersequence comprises from bottom to the top four third-order sequences, three of them with four distinct AZs: (1) Pinheiros-Chiniquá Sequence (*Dinodontosaurus* AZ), (2) Santa Cruz Sequence (*Santacruzodon* AZ), (3) Candelária Sequence (with two distinct faunas: *Hyperodapedon* AZ, at the bottom, and *Riograndia* AZ, at the top). The fourth and overlying unit, the Mata Sequence, is devoid of fossil vertebrates and contains silicified logs of gimnospermales.

The *Dinodontosaurus* AZ (Pinheiros-Chiniquá Sequence, Ladinian-early Carnian) is dominated by the dicynodont *Dinodontosaurus* Romer, 1943 and the traversodontid cynodont *Massetognathus* Romer, 1967 (Table S1). The *Dinodontosaurus* AZ is conventionally considered coeval to the classic Chañares fauna (Chañares Formation, Argentina) by the shared presence of the above-mentioned taxa, and considered early Carnian (236-234 Ma; Marsicano et al., 2016; Ezcurra et al., 2017). Recent study on radiometric dating for the Santa Cruz Sequence (maximum age 236 Ma, encompassing the *Santacruzodon* AZ, which is considered younger than *Dinodontosaurus* AZ; Philipp et al., 2013), raise the possibility that *Dinodontosaurus* AZ might have been deposited

* Corresponding author.
E-mail addresses: anepavanatto@hotmail.com (A.E.B. Pavanatto), flavio.pretto@ufsm.br (F.A. Pretto), leonardokerber@gmail.com (L. Kerber), rodrigotmuller@hotmail.com (R.T. Müller), atila@smail.ufsm.br (Á.A.S. Da-Rosa), paleosp@gmail.com (S. Dias-da-Silva).

https://doi.org/10.1016/j.jsames.2018.08.016
Received 2 May 2018; Received in revised form 20 August 2018; Accepted 20 August 2018
Available online 24 August 2018
0895-9811/

during Ladinian to early Carnian. However, the pattern of distribution along the stratigraphic column of several taxa recently included into the *Dinodontosaurus* AZ (the cynodonts *Aleodon cromptoni* Martinelli et al., 2017 and *Scalenodon ribeiroae* Melo et al., 2017; the rhynchosaur *Brasinorhynchus mariantensis* Schultz et al., 2016) and also *Luangwa sudamericana* Abdala and Sá-Teixeira, 2004 led some authors to suggest that the *Dinodontosaurus* AZ should be subdivided into two subzones (see Ezcurra et al., 2017; Martinelli et al., 2017; Melo et al., 2017).

The *Santacruzodon* AZ (Santa Cruz Sequence, early Carnian) is almost exclusively dominated by traversodontid cynodonts (*Massetognathus* sp., *Menadon besairei* Flynn et al., 2000, and *Santacruzodon hopsoni* Abdala and Ribeiro, 2003; Abdala et al., 2001, 2009; Abdala and Ribeiro, 2003; Soares et al., 2011; Melo et al., 2015; Table S1). This AZ was correlated to the fauna of the Isalo II Formation from Madagascar, based upon anatomic similarities between traversodontid cynodonts from both units (e.g. *Santacruzodon* and *Dadadon* Flynn et al., 2000) and the shared presence of the traversodontid *Menadon besairei* (Abdala et al., 2001, 2009; Abdala and Ribeiro, 2003; Soares et al., 2011; Melo et al., 2015). These similarities allow a late Ladinian/early Carnian age estimation for the *Santacruzodon* AZ. Indeed, Philipp et al. (2013) obtained for the middle portion of the Santa Cruz Sequence, a radioisotopic dating of detrital zircons, with a maximum age of 236 Ma, placing this AZ within the Carnian (Martinelli et al., 2016; Schultz et al., 2016).

The *Hyperodapedon* AZ (lower portion of the Candelária Sequence, late Carnian) is characterized by the predominance of the rhynchosaur *Hyperodapedon* Huxley, 1859, as well as the traversodontid *Exaeretodon* Cabrera, 1943 (Schultz et al., 2000; Langer et al., 2007). Notable records in this AZ include sauropodomorph dinosaurs (Langer et al., 1999; Cabreira et al., 2011, 2016; Table S1). The presence of both *Hyperodapedon* and *Exaeretodon* in this AZ allows a correlation with the Ischigualasto Formation from Argentina, indicating a late Carnian to early Norian age for the *Hyperodapedon* AZ (Langer et al., 2007; Martínez et al., 2011). The type stratum of the basal sauropodomorph *Saturnalia tupiniquim* Langer et al., 1999 was recently radioisotopically dated as 233.23 ± 0.73 Ma (Langer et al., 2018).

The *Riograndia* AZ (Upper portion of the Candelária Sequence, Norian) is dominated by small probainognathian mammaliaform cynodonts (Bonaparte et al., 2003, 2005, 2010, 2013; Soares et al., 2011; Table S1). The presence of the dicynodont *Jachaleria* Bonaparte, 1971 allows a direct correlation of the *Riograndia* AZ to the Argentinean lower fauna from the Los Colorados Formation and uppermost Ischigualasto Formation, dated as Norian (Langer et al., 2007; Bonaparte et al., 2010; Soares et al., 2011; Martínez et al., 2011, 2013; Kent et al., 2014; Müller et al., 2017). The Linha São Luiz site was recently radioisotopically dated as 225.42 ± 0.37 Ma (Langer et al., 2018), corroborating a Norian age for this AZ.

Newly discovered Triassic outcrops from southern Brazil are generally easily included within any of the above mentioned AZs, based on their fossiliferous content. However, the new site here presented (Niemeyer Site, discovered in 2014), shows a peculiar fossil content, with most of the discovered fossils comprising a new species of traversodontid cynodont and the presence of rare probainognathian cynodonts and archosauromorphs. There is so far no index fossils collected from this site, which prevents a robust biostratigraphical assessment.

Traversodontidae is the most diverse clade of Triassic cynodonts (Abdala and Ribeiro, 2010), characterized by the presence of labiolingual expanded upper postcanine teeth with a deep occlusal basin (Kammerer et al., 2008; Liu and Abdala, 2014). The oldest records of traversodontids are from the Anisian of Africa (Crompton, 1955; Brink, 1963) and South America (Bonaparte, 1966, 1969; but see Ottone et al., 2014, for another interpretation of age to the Argentinean Puesto Viejo fauna, traditionally considered Anisian), becoming more abundant and cosmopolite from Ladinian to Carnian (Abdala and Ribeiro, 2010; Liu and Abdala, 2014). In south Brazilian Triassic, traversodontids are present in the four AZs. In the *Riograndia* AZ, traversodontids are scarce, but fragmented specimens similar to *Exaeretodon* were collected associated with taxa typical of that AZ (Ribeiro et al., 2011). The predominance of traversodontids in other Triassic faunas is frequent: *Scalenodon angustifrons* Parrington, 1946 in mid-Lifua Member of the Manda Beds (Tanzania, Anisian, Smith et al., 2018); *Andescynodon* Bonaparte, 1969 in the Cerro de Las Cabras Formation (Argentina, late Anisian/early Ladinian, Liu and Abdala, 2014); *Massetognathus pascuali* Romer, 1967 in the Chañares Formation (Argentina, early Carnian; Rogers et al., 2001; Marsicano et al., 2016); *Santacruzodon* in the Santa Cruz Sequence (Brazil, *Santacruzodon* AZ, early Carnian; Philipp et al., 2013), Santa Maria Supersequence (Abdala et al., 2001, 2009; Abdala and Ribeiro, 2010); *Exaeretodon* in the upper portion of the Candelária Sequence (Brazil, *Hyperodapedon* AZ, late Carnian) and in the Ischigualasto Formation (Argentina, late Carnian; Langer et al., 2007; Oliveira et al., 2007; Martínez et al., 2013; Pretto et al., 2015).

In this contribution, we present the first data concerning the geological and taphonomic context of the Niemeyer Site, as well as the description of the best-preserved specimens, including the description of a new traversodontid cynodont.

1.1. Institutional abbreviations

CAPPA/UFSM, Centro de Apoio à Pesquisa Paleontológica, Universidade Federal de Santa Maria, São João do Polêsine, Brazil. **MCP**, Museu de Ciências e Tecnologia, Pontifícia Universidade Católica do Rio Grande do Sul, Porto Alegre, Brazil. **MCZ**, Museum of Comparative Zoology, Harvard University, Cambridge, USA.

2. Materials and methods

2.1. Collecting and comparisons

The specimens, collected at the Niemeyer site, municipality of Agudo, Rio Grande do Sul, are housed at the Centro de Apoio à Pesquisa Paleontológica da Quarta Colônia – Universidade Federal de Santa Maria (CAPPA/UFSM). The specimens assigned to the new traversodontid taxon were compared first-hand to the type-series of *Exaeretodon riograndensis* Abdala et al., 2002 (MCP 1522 PV, MCP 2361 PV, and MCP 3843 PV) housed at the Museu de Ciências e Tecnologia da Pontifícia Universidade Católica do Rio Grande do Sul and with other specimens from the Janner site (Municipality of Agudo, CAPPA/UFSM 0030 and 0033) housed at CAPPA/UFSM. Comparisons with other taxa were conducted based on the literature.

2.2. Taphonomy

Geographic coordinates for each accumulation of bones were taken during fieldwork, and the specimens were analyzed under a taphonomic approach: degree of disarticulation, fragmentation, weathering, presence of ichnological trace fossils on bone surface (Dodson, 1971; Behrensmeyer, 1975, 1978, 1982, 1991), and grouped into Voorhies Groups (Voorhies, 1969; Behrensmeyer, 1975). The number of individuals per taxon was estimated in order to determine the taxonomic abundance within the fossiliferous assemblage. This estimation was performed employing two methods: the Number of Identified Specimens per taxon (NISP) and the Minimum Number of Individuals per taxon (MNI; Badgley, 1986). For the NISP Index, an isolated bone or tooth was considered as an individual. MNI was based upon the number of unpaired elements (e.g., skull) and the more abundant elements from a single side of paired bones as well (e.g., right femur, left humerus; Badgley, 1986).

2.3. Phylogenetic analysis of the new species of Traversodontidae

The phylogenetic affinities of the new taxon were tested based on

the dataset of Liu and Abdala (2014), with modifications from Melo et al. (2015, 2017). This dataset comprises 78 morphological characters and 31 operational taxonomic units (OTUs), currently being the most comprehensive dataset of traversodontid cynodonts. The coding for the new species was taken from specimens CAPPA/UFSM 0032 and CAPPA/UFSM 0109. Some previous scores of *E. riograndensis* were modified based on personal observation of new specimens, and modifications were performed on the coding of *Arctotraversodon* Sues et al., 1992 (S2).

The software TNT v1.1 (Goloboff et al., 2008) was employed to conduct the phylogenetic analysis. All characters received the same weight and were treated as unordered. *Thrinaxodon* Seeley, 1894 was adopted to root the most parsimonious trees (MPTs), which were recovered via 'Traditional search' (random addition sequence + tree bisection reconnection) with 1000 replicates of Wagner trees (with random seed = 1), tree bisection and reconnection and branch swapping (holding 20 trees save per replicate). Decay indices (Bremer support values), as well as bootstrap values (1000 replicates), were also obtained.

2.4. Computed tomography

CAPPA/UFSM 0032 was scanned in a medical clinic (DIX – Diagnóstico por Imagem do Hospital de Caridade) in Santa Maria, Rio Grande do Sul, using a Philips Brilliance 16-Slice CT Scanner, with a voltage of 140 kV and amperage of 280 mA. 687 slices were generated with a slice thickness of 0.8 mm and interslice of 0.4 mm. The image resolution is 512 × 512 pixels, and the pixel size is 0.447 mm. The raw scan data were exported from the scanner computer in DICOM format. 3D Slicer 4.8 (Fedorov et al., 2012) was employed to generate 3D models of this specimens. Design Spark Mechanical 2.0 was used to generate PDF file of the model (S6).

3. Geological settings

The Niemeyer Site is located on the outskirts of the municipality of Agudo (29°40′25″ S; 53°14′4.20″ W), southern Brazil (Fig. 1A–C). The main fossiliferous sectors are exposed around an artificial dam (labeled as 2, 3 and 4 in Fig. 1D and E), with an additional isolated section (labeled as 1 in Fig. 1D and E). The stratigraphic column comprises a 23 m thick lithology of reddish mudstones, sandstones, and intraformational conglomerates, with carbonatic concretions and hydromorphic levels (Fig. 1E).

The first three-four meters of exposure (Sector 1; Fig. 1D–E, Figure S3) are mostly composed of reddish (7.5R 4/6) mudstones and very fine sandstones, with vertical fractures and levels of carbonatic concretions and crusts. Fossils are scarce, only consisting of indeterminate fragments with severe signs of abrasion. A nine meters thick deposit of reddish mudstones and very fine sandstones (Sector 2 and 3, Fig. 1D–E, Figure S3) overlays the exposure of sector 1. It includes carbonatic concretions and thin, isolated lenses of fine orange (10R 5/6) sandstones. Fossil specimens from this sector include CAPPA/UFSM 0100 and 0157 (within reddish mudstones) and CAPPA/UFSM 0109, as well as small skulls (CAPPA/UFSM 0191 and 0192) and a lower jaw (CAPPA/UFSM 0190) from the carbonatic mudstones on top (Sector 3). The topmost Sector 4 (Fig. 1D–E, Figure S3), with nine meters of mudstones and very fine sandstones, yielded the following specimens: CAPPA/UFSM 0032, 0125, 0132 and 0133. This sector includes hydromorphism levels (discoloration), lenses of fine sandstones and intraformational conglomerates, with clay and carbonatic intraclasts. These lithologies present channel and overbank facies that correspond to part of the Candelária Sequence (Horn et al., 2014) in the Agudo structural block (Da-Rosa and Faccini, 2005; Da-Rosa, 2015).

4. Taphonomic remarks

A sample of 1032 specimens was recovered between 2014 and 2016, and taphonomical aspects of this fossiliferous concentration (in which an exhaustive effort of collecting was carried out) were considered during fieldwork. Isolated materials (including unidentifiable fragments) were surface-picked, whereas more complete specimens were mostly gathered through excavation. Anatomically identifiable bone elements comprise 189 specimens, 85 of which were mapped on the outcrop (Table S4). There are no complete skeletons, and semi-articulated specimens comprise a very small sample (0.48%), mostly represented by skulls and mandibles in occlusion. At least one specimen (CAPPA/UFSM 0109) preserved associated cranial and postcranial bones. Conversely, isolated elements and unidentifiable fragments (17.83% and 81.69%, respectively) comprise the majority of the sample.

The specimens were separated into Voorhies Groups (Voorhies, 1969; Behrensmeyer, 1975), according to the degree of susceptibility to transport of each bone element. Group I is composed of those more easily transportable elements (i.e., phalanges, ribs, vertebrae); Group II includes those elements removed gradually and transported by saltation and traction (i.e., femora, humeri); and Group III includes elements of resisted transport, such as skulls and lower jaws. We observed the following order of predominance: Group III (53.8%) > Group I (31.46%) > Group II (15.73%) (Table 1). According to these parameters, we hypothesize that this assemblage was winnowed and specimens included in Group III may represent a "residual lag" with some degree of autochthony (see Behrensmeyer, 1975), whereas, prior to the burial, most elements of groups I and II were transported away.

Several specimens present bone alterations. For instance, some long bones show a severe degree of bone loss in both proximal and distal surfaces, where cancellous bone is prevalent. This is also the condition in a few scattered vertebral centra. These cases are interpreted as resulting from pre-burial weathering (Behrensmeyer, 1978). The same elements also display a cracked and flaked texture along the external surface of the shafts, which are composed of compact bone tissue, characterizing weathering stages 3 and 4 of Behrensmeyer (1978). Some elements show deeper cracks and bone loss, consistent with weathering stage 5. Notwithstanding, the sample also includes elements with less severe degrees of weathering stages 1 and 2 (Behrensmeyer, 1978).

Data on disarticulation and weathering suggest some degree of transport and exposition (see Dodson, 1971; Behrensmeyer, 1975, 1978, 1982, 1991). Semi-articulated specimens with weathering stages 1 and 2 suffered more rapid burial than those scattered, fragmented and abraded elements (weathering stages 3, 4 and 5) which reflects more time of exposure before burial, but there is no clear association among elements of each weathering stage. The extreme condition observed in fragmentary specimens characterizes weathering stage 5.

The presence of invertebrate traces is observed in four specimens. The mandibular ramus CAPPA/UFSM 0054 (Fig. 2A) presents small tubules of detritus close to the level of tooth row (Fig. 2B) and a perforation on the ventral border of its lateral surface (Fig. 2D) with a tubular extrusion of detritus over its medial surface (Fig. 2C). Similar tubules are encountered in the rostrum of the skull CAPPA/UFSM 0125 (Fig. 2E–F) and also on the medial surface of the left ilium CAPPA/UFSM 0188 (Fig. 2J). All these tubules were found underneath the specimen, facing the substrate, and may represent tunnels usually produced by burrowing invertebrate scavengers (Kirkland and Bader, 2010; Xing et al., 2013; Pirrone et al., 2014; Paes Neto et al., 2016). The humerus CAPPA/UFSM 0077 (Fig. 2G) shows isolated perforations on its proximal portion (Fig. 2H) and a shallow, isolated perforation on its distal portion (Fig. 2I). These marks can be interpreted as either feeding traces or pupation chamber traces (Pirrone et al., 2014; Paes Neto et al., 2016; Vallon et al., 2016; Xing et al., 2016).

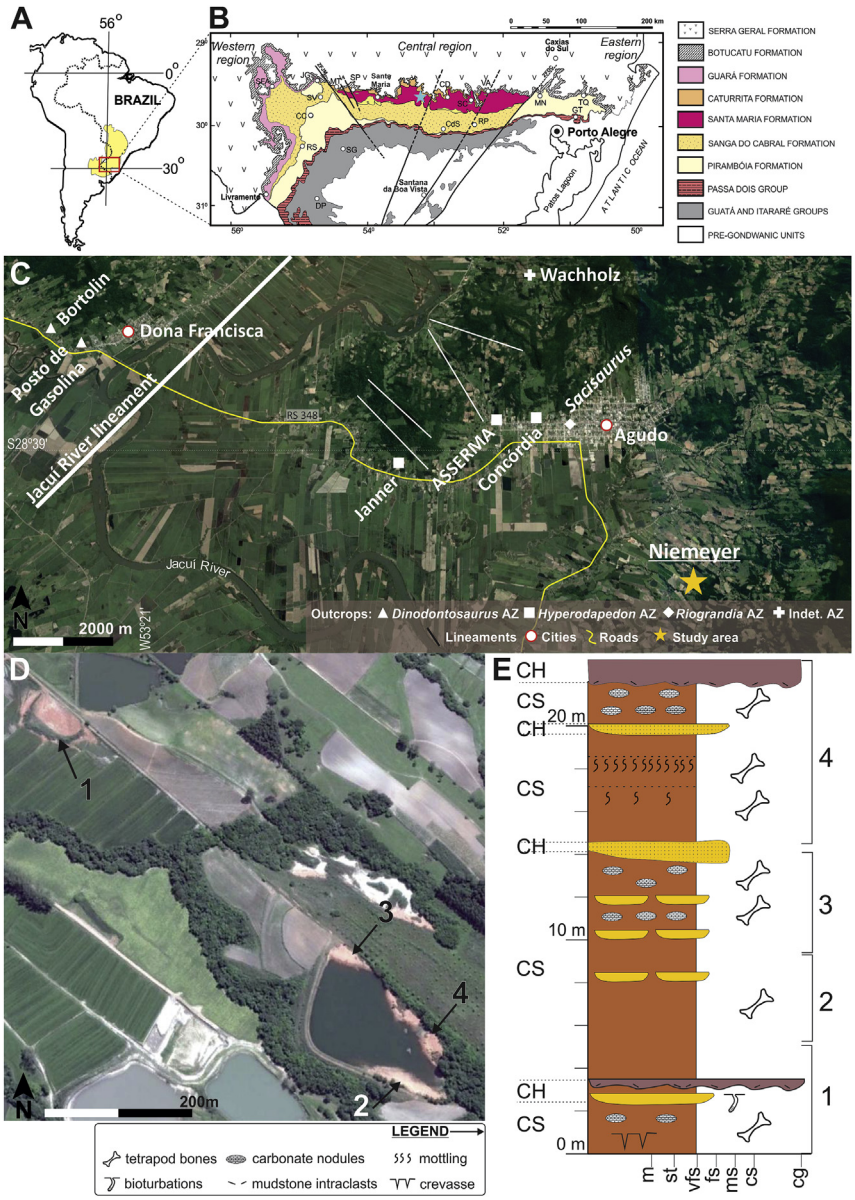

Fig. 1. Location and geological context of the Niemeyer site. **A**, Location map of the Paraná Basin in South America; **B**, Sedimentary units in Southern Brazil (modified from Da-Rosa and Faccini, 2005); **C**, Satellite image showing the location of the new site, Niemeyer (yellow star at the lower right); **D**, Outcropping sectors of the Niemeyer site; **E**, Columnar geological profile. Abbreviations: **CC**, Cacequi; **CD**, Candelária; **cg**, conglomerate; **CH**, channel; **CS**, crevasse deposits; **cs**, coarse sandstone; **CdS**, Cachoeira do Sul; **DP**, Dom Pedrito; **fs**, fine sandstone; **GT**, Gravataí; **JG**, Jaguari; **m**, mudstone; **MN**, Monte Negro; **ms**, medium sandstone; **MT**, Mata; **RP**, Rio Pardo; **RS**, Rosário do Sul; **SC**, Santa Cruz do Sul; **SFA**, São Francisco de Assis; **SG**, São Gabriel; **SP**, São Pedro do Sul; **st**, siltstone; **SV**, São Vicente do Sul; **TQ**, Taquara; **VA**, Venâncio Aires; **vfs**, very fine sandstone. (Source C–D: Google Earth*).

5. Characterization of the fossiliferous assemblage

As a result of the NISP and MNI methods, most specimens were assigned to Cynodontia (mainly traversodontids), about 97.3% of the sample (Fig. 3) and, so far, only two specimens were otherwise assigned to Probainognathia. Non-cynodont tetrapods comprise three specimens of Archosauromorpha indet. Among Traversodontidae, four specimens possess a unique combination of features, allowing the erection of a new genus and species described below. The other traversodontid specimens probably might be assigned to this new taxon, but as of yet, no distinctive features were recognized in those elements to allow a less inclusive taxonomic assignation.

6. Systematic paleontology of the new taxon

THERAPSIDA Broom, 1905
CYNODONTIA Owen 1861
EUCYNODONTIA Kemp 1982
TRAVERSODONTIDAE von Huene, 1936 (*sensu* Kammerer et al., 2008)
Siriusgnathus gen. nov.

the registration in the Zoobank of the new taxon: **LSID urn:lsid:zoobank.org:act:C62F7E7C-07B7-4315-ADCD-93F69F3CCA30**

6.1. Etymology

Sirius, the brightest star of the *Canis Majoris* constellation, also known as “dog star” in reference to *cyno* (from Greek, dog); *gnathus* (from Greek, mandible), a common suffix denoting cynodonts.

6.2. Diagnosis

Thus far, no autaphomorfies are proposed for *Siriusgnathus*. Notwithstanding, the taxon posssesses a combination of features that is unique and, combined, allow for the diagnosis. Therefore, *Siriusgnathus* possesses two upper incisors; eight upper postcanines; triangular first upper postcanines; distal accessory labial cusp of upper postcanines more labially placed in comparison with *Exaeretodon*; two/three lower incisors; rostrum short and broad with almost the same length of the temporal region; interorbital depression poorly developed; postorbital bar more anteriorly positioned than in *Exaeretodon*; descending process

Table 1
Number and relative abundance of skeletal elements per Voorhies Groups from the Niemeyer site.

Skeletal Elements	Number of Elements	Relative Abundance (%)
Group I		
Phalanges	6	3.37
Vertebrae	14	7.86
Scapula	1	0.56
Ribs	35[a]	19.66
Subtotal	56	31.46
Group II		
Humeri	9	5.05
Ulnae	4	2.24
Femora	11	6.18
Tibiae	2	1.12
Ilium	2	1.12
Subtotal	28	15.73
Group III		
Skull	7	3.93
Maxilla[b]	8	4.49
Lower jaw	9	5.06
Mandibular ramus	28	15.73
Skull + postcranium	1	0.56
Isolated teeth	41	23.03
Subtotal	94	53.80
Total	**178**	**100**

[a] Complete or fragmentary ribs.
[b] Maxilla = fragments of the maxilla and premaxilla which contained teeth.

of the jugal incipient (less developed than in *Exaeretodon*, though not as reduced as in *Massetognathus*); ventral part of the posteriormost region of the jugal dorsoventrally short and tapering posteriorly; zygomatic process of the squamosal not reaching anteriorly the level of postorbital bar; very tenuous dorsoventral crest at middle point of zygomatic process of the squamosal; contact of the zygomatic process of the squamosal and jugal almost flat and smooth (not forming a depressed area); posteriormost border of zygomatic process of squamosal, short and rounded; lambdoidal crest not forming a concavity such as that present in *Exaeretodon*; and an anteroposteriorly short basicranium.

Siriusgnathus niemeyerorum gen. et sp. nov.
the registration in the Zoobank of the new taxon: **LSID urn:lsid:zoobank.org:act:C7552927-EA4D-4DE0-839B-4B31602AE561**
Figs. 4–7 and S6

6.3. Etymology

Type species *niemeyerorum*, in honor of the Family Niemeyer, the owners of the propriety were the Niemeyer site is located.

6.4. Diagnosis

As for the genus.

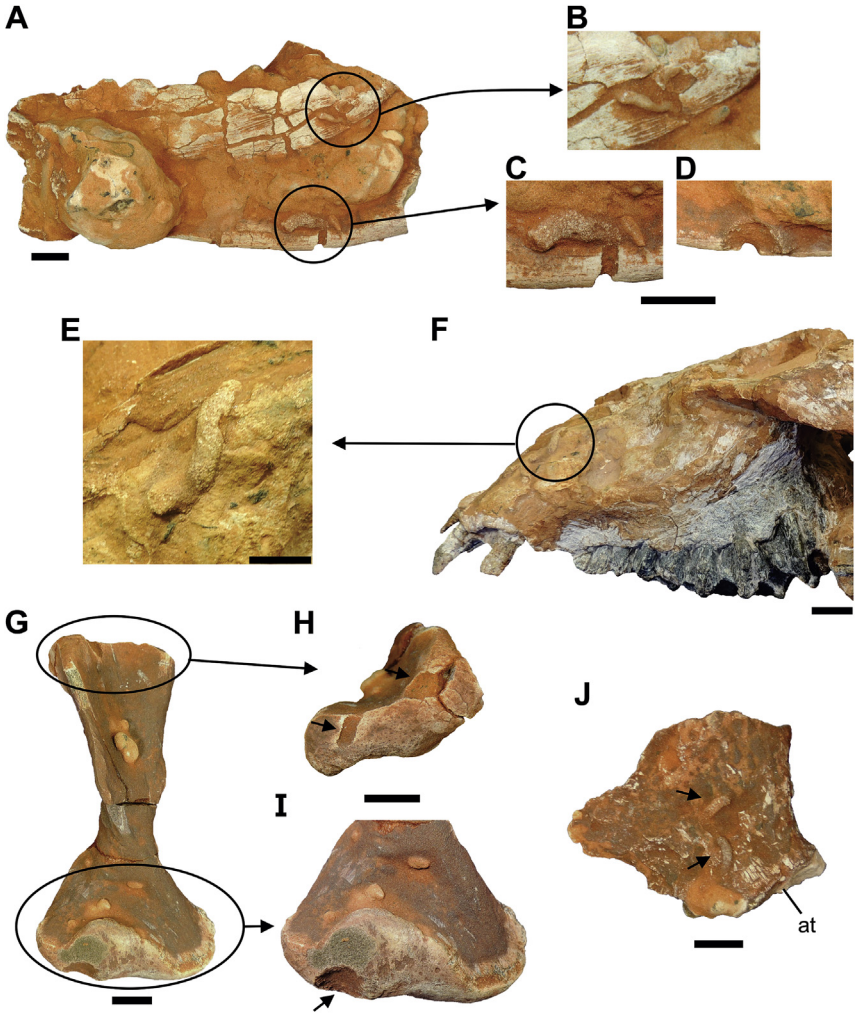

Fig. 2. Ichnological samples from the Niemeyer site. CAPPA/UFSM 0054, a right mandibular ramus: **A**, in medial view, **B**, small tubules near the level of the teeth, **C**, extrusion tubule, in medial view, **D**, isolated hole, in lateral view. CAPPA/UFSM 0125, skull: **E**, detail of detritus-filled tubule on the surface of the rostrum, **F**, rostrum in left lateral view. CAPPA/UFSM 0077, right humerus in **G**, ventral view, **H**, proximal portion with arrows indicating the burrows, **I**, distal portion with the arrow indicating the isolated borehole. **J**, CAPPA/UFSM 0188, fragment of left ilium, in medial view, the arrows point small detritus-filled tubules. Abbreviations: at, acetabulum. Scale bar: 10 mm.

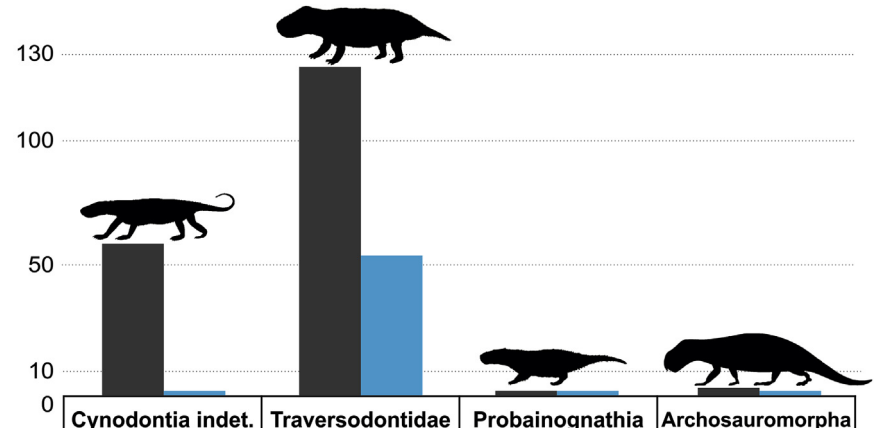

	Cynodontia indet.	Traversodontidae	Probainognathia	Archosauromorpha
NISP	57	126	2	3
MNI	2	54	2	2
Percent values	~30.3%	~67%	~1%	~1.6%
	~97.3%			

Fig. 3. Chart and table with the Number of Identified Specimens per taxon (NISP) and the Minimum Number of Individuals per taxon (MNI) and percent values for the four main groups found at Niemeyer site.

6.5. Holotype

CAPPA/UFSM 0032, skull with the associated lower jaw.

6.6. Paratypes

CAPPA/UFSM 0109, partial skull with articulated lower jaw and associated postcranial material; CAPPA/UFSM 0124, partial skull and CAPPA/UFSM 0125, skull and associated lower jaw.

6.7. Horizon and locality

Santa Maria Supersequence, Candelária Sequence, Niemeyer Site, municipality of Agudo, Rio Grande do Sul, Brazil.

6.8. Characterization of the specimens

Although many specimens collected at the Niemeyer site might belong to *Siriusgnathus niemeyerorum*, this study focuses on four better-preserved specimens of distinct ontogenetic stages to characterize the new taxon. Among the specimens, CAPPA/UFSM 0032, the holotype (Figs. 4–7), is the most complete and better-preserved specimen. Hence, the description is mostly based upon this specimen, which comprises a complete skull, slightly distorted, associated to its lower jaws (the right ramus has several fractures, and the left element is severely damaged). The specimen has two left upper incisors (I) and one right upper incisor, plus an empty right alveolus (Fig. 4E; 7B-D); both upper canines (C); the last upper postcanine teeth (PC), plus a single one in eruption and seven empty alveoli, on each side (Fig. 4B–C). The right ramus of the lower jaw does not preserve lower incisors (i), or canine teeth (c) and only part of the alveolus of the canine are preserved (Fig. 6A–B). There are six lower postcanines (pc) plus an empty alveolus for the first one, and an eighth postcanine is in process of eruption (Fig. 6A–C). Additional information is unavailable for the severely damaged left ramus.

CAPPA/UFSM 0109 (Fig. 8) is the largest specimen (see Table S5): a skull preserving the postorbital region, lacking the right orbit and rostrum. Additionally, some postcranial elements (i.e., several vertebrae and ribs, left scapula, left humerus, an ulna, and several indeterminate fragments) were associated with the skull. Five left, and two right upper postcanines are preserved (Fig. 8B). The specimen preserves a lower jaw, with part of the left mandibular ramus and the coronoid process of the right dentary associated with the skull (Fig. 8C–E). In the lower jaw, there are three right and two left incisors, plus the right canine, all broken (Fig. 8D–E). Eight right postcanine teeth are preserved (six in the alveoli, being the 1–3 PC covered by a hard matrix, plus two elements out of place (Fig. 8D–E).

CAPPA/UFSM 0125 (Fig. 9A–G) comprises a laterally compressed skull with its associated lower jaw, in which part of the right zygomatic arch is missing (Fig. 9A and B). It preserves the two left upper incisors, the alveolus to right I1, and the right I2 (broken at its apical part). Both upper canines are broken, the left at its base and right at its apex (Fig. 9D). Eight functional upper postcanines, plus one in eruption, are present on each sides (Fig. 9C–D). The coronoid processes of both dentaries are broken, as well as the angular process of the right ramus (Fig. 9E). Two right and one left incisors are preserved, the alveolus for the second left lower incisor being broken (Fig. 9G). The base of the right lower canine and the alveolus for the left one are present (Fig. 9G). There are six lower postcanines on each mandible, but the right pc1 is broken at its base, and left pc2 is damaged. In addition, a seventh postcanine is in process of eruption (Fig. 9F).

CAPPA/UFSM 0124 (Fig. 9H–I) is the smallest described specimen (see Table S5), corresponding to an immature individual. It comprises a partial skull lacking the postorbital part of the zygomatic arches (Fig. 9H). The specimen bears two left and two right upper incisors. The first right incisor is broken at the base, whereas the others are broken at their apical portions; two canines, broken at the apices; eight right upper postcanines; six empty alveoli from the left side, plus the seventh and eighth postcanines, and a ninth in process of eruption (Fig. 9I).

6.9. Anatomical description

General Morphology. *Siriusgnathus niemeyerorum* is a large traversodontid with a skull that displays a short and broad rostrum, lacking an internarial bar. The temporal region is widely expanded, with diverging zygomatic arches. The poorly developed descending process of the jugal is slightly convex. The basicranial region is anteroposteriorly short. In CAPPA/UFSM 0032, CAPPA/UFSM 0124, and CAPPA/UFSM 0125 there are two large, procumbent upper incisors, well-developed upper canines and eight functional upper postcanine teeth, plus one in process of eruption. The postcanines show well-developed shouldering, a robust main labial cusp, a well-developed distal labial accessory cusp, and a smaller mesial labial accessory cusp. The crown of the first upper

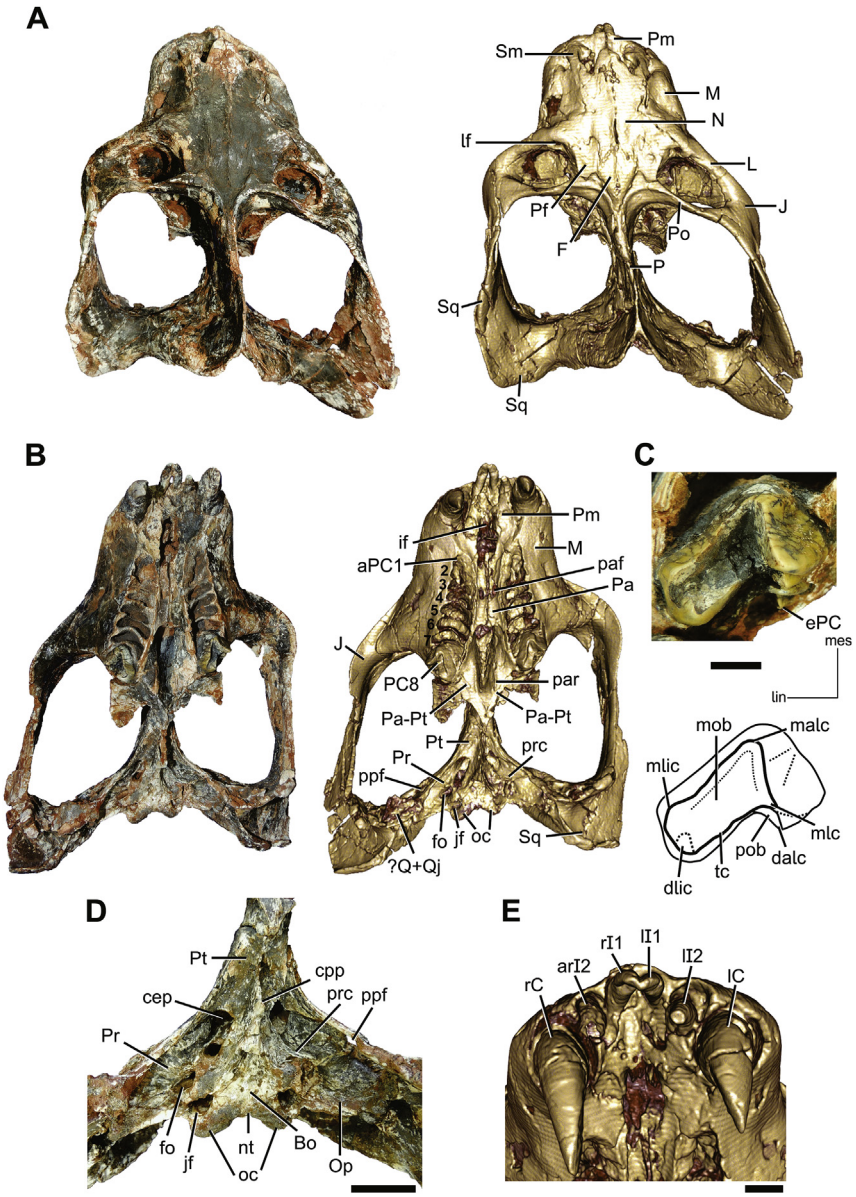

Fig. 4. *Siriusgnathus niemeyerorum* gen. et sp. nov., holotype (CAPPA/UFSM 0032). **A,** skull in dorsal view, photograph (left) and 3D model (right); **B**, skull in ventral view, photograph (left) and 3D model (right); **C**, eighth left upper postcanine (top) and interpretive drawing (bottom); **D**, basicranium; **E**, detail of the rostrum, showing the upper incisors and canines in occlusal view. Abbreviations: **aPC**, upper postcanine alveolus; **arI**, upper incisor alveolus; **Bo**, basioccipital; **cpp**, cultriform process of parasphenoid; **cep**, cavum epiptericum; **dalc**, distal accessory labial cusp; **dlic**, distal lingual cusp; **ePC**, upper postcanine in eruption; **F**, frontal; **fo**, fenestra ovalis; **if**, incisive foramen; **J**, jugal; **jf**, jugular foramen; **L**, lacrimal; **lC**, left upper canine; **lf**, lacrimal foramen; **lI**, left upper incisor; **lin**, lingual; **M**, maxilla; **malc**, mesial accessory labial cusp; **mes**, mesial; **mlc**, main labial cusp; **mlic**, mesial lingual cusp; **mob**, main occlusal basin; **N**, nasal; **nt**, notch; **oc**, occipital condyles; **Op**, opisthotic; **P**, parietal; **Pa**, palatine; **paf**, palatine foramen; **par**, palatine ridge; **Pa-Pt**, palatine-pterygoid suture; **PC**, upper postcanine; **Pf**, prefrontal; **Pm**, premaxilla; **Po**, postorbital; **pob**, posterior occlusal basin; **ppf**, pterygoparoccipital foramen; **Pr**, prootic; **prc**, prootic crest; **Pt**, pterygoid; **Q** + **Qj**, quadrate plus quadratojugal; **rC**, right upper canine; **rI**, right upper incisor; **Sm**, septomaxilla; **Sq**, squamosal; **tc**, transverse crest. Scale bar 50 mm (A–B) and 10 mm (C–E).

postcanine is triangular in occlusal view, the remaining ones rectangular. In the lower jaw, the masseteric fossa is shallow and extended longitudinally. The angular process is strongly-built and markedly projected posteriorly. The coronoid process of the dentary is tall and robust, covering the last lower postcanine in labial view. There are two to three lower incisors and the lower canines are reduced in size, compared to the upper ones, having almost the same size of the incisors. In occlusal view, the eight lower postcanines are quadrangular, with the mesial labial cusp distally inclined. Based on the four specimens here recognized, the dental formula for *Siriusgnathus niemeyerorum* is 2I/2-3i, 1C/1c, 8 + 1PC/6 + 1–7 + 1pc.

Rostrum. The rostrum is short (28.5% of the basal length of the skull in CAPPA/UFSM 0032) and broad (Fig. 4A). The premaxillary internarial process is absent, and the external naris is wide (Fig. 5A). The maxillary process of the premaxilla is poorly developed. The septomaxilla is more developed at its base than in its dorsomedial part. The septomaxillary foramen is well developed and placed lateral to the naris (Fig. 5A). Its medial margin is bounded by the septomaxilla, and the premaxilla contributes to its ventral border.

In lateral view, the maxilla contacts the premaxilla at the level of the mesial margin of the canine (Fig. 5C). Two maxillary foramina can be observed, a larger anterior dorsal to the base of the canine, and the smaller one, higher on the rostrum, is located posterodorsal to the first (Fig. 5C). The naso-maxillary fossa is shallow, possibly due to taphonomic deformation. The maxillary platform is well developed laterally, forming a roof lateral to the postcanine teeth (Fig. 4B). The nasal is elongated anteroposteriorly, with a lateral constriction at its midpoint. In the left nasal, this portion bears a small foramen (Fig. 4A).

Orbit and Zygomatic Arch. In dorsal view, the lacrimal mostly contributes to the anterior margin of the orbit. Inside the orbital margin, in the lacrimal, a sizeable lacrimal foramen is present near to the contact with the prefrontal, though this bone does not contribute to the margin of the foramen (Fig. 4A). The prefrontal contributes to the medial border of the orbit, and the postorbital extends to the middle point of its posterior margin. Its contacts the ascendant process of the jugal, which encloses the posterior margin of the orbit. The anterior process of the jugal contacts the lacrimal anteriorly (Fig. 4A). In ventral view, the postorbital is not visible through the temporal fenestra, given the anterior position of the orbit (Fig. 4B). The zygomatic arch is dorsoventrally high in lateral view, with its dorsal margin surpassing the level of the dorsal margin of the orbit. The descending process of the jugal is gently rounded ventrally, posterior to the orbit and slightly

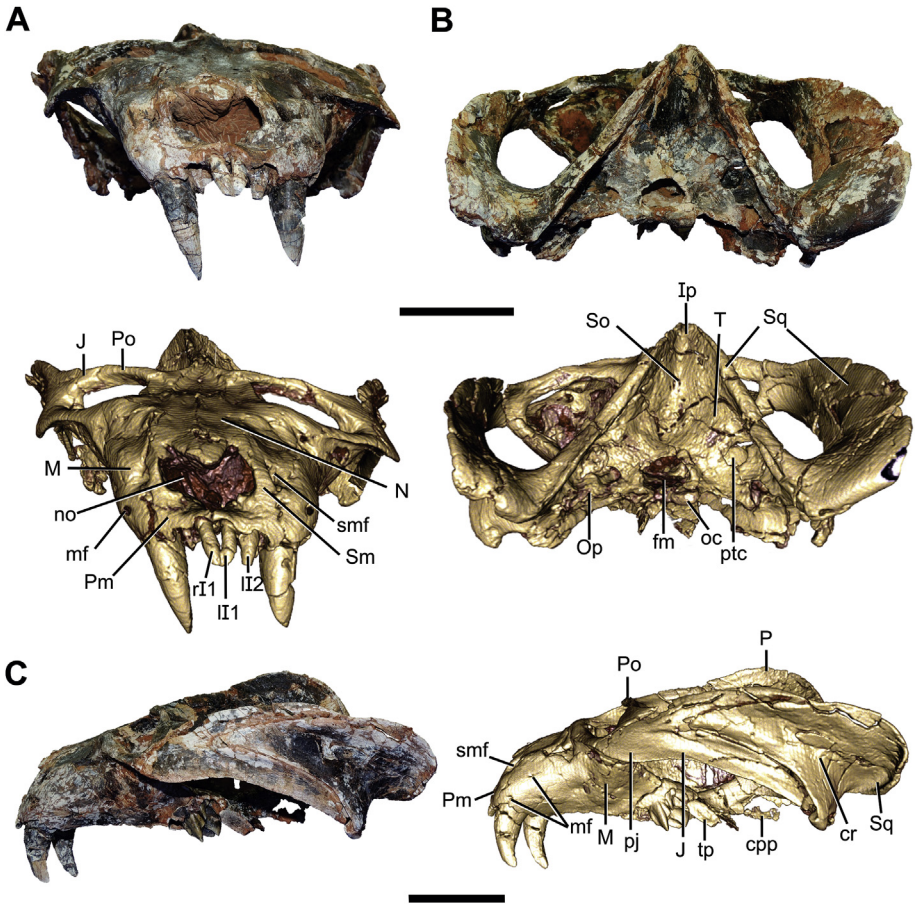

Fig. 5. Holotype (CAPPA/UFSM 0032) of *Siriusgnathus niemeyerorum* gen. et sp. nov. **A**, skull in anterior view, photograph (top) and tridimensional model (bottom); **B**, skull in occipital view, photograph (top) and 3D model (bottom); **C**, skull in left lateral view, photograph (left) and 3D model (right). Abbreviations: **cr**, dorsoventral crest; **cpp**, cultriform process of parasphenoid; **fm**, foramen magnum; **Ip**, interparietal; **J**, jugal; **lI**, left upper incisor; **M**, maxilla; **mf**, maxillary foramen; **N**, nasal; **no**, nasal opening; **oc**, occipital condyles; **Op**, opisthotic; **P**, parietal; **pj**, descending process of jugal; **Pm**, premaxilla; **Po**, postorbital; **ptc**, posttemporal canal; **rI**, right upper incisor; **Sm**, septomaxilla; **smf**, septomaxillary foramen; **So**, supraoccipital; **Sq**, squamosal; **T**, tabular; **tp**, transverse process of pterygoid. Scale bar 50 mm.

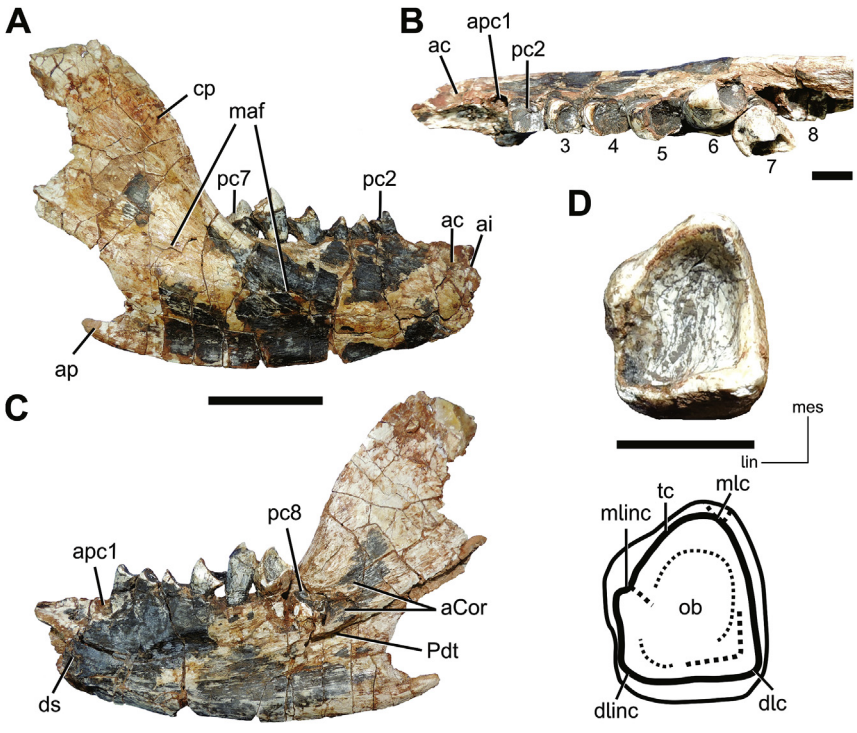

Fig. 6. Holotype (CAPPA/UFSM 0032) of *Siriusgnathus niemeyerorum* gen. et sp. nov. Lower jaw (A, B, C) and lower postcanine (D). Right ramus of the lower jaw in **A**, lateral view; **B**, occlusal view; **C**, medial view; **D**, seventh right lower postcanine (top) and interpretive drawing (bottom). Abbreviations: **ac**, lower canine alveolus; **aCor**; articulation area for coronoid bone; **ai**, lower incisor alveolus; **ap**, angular process of dentary; **apc**, lower postcanine alveolus; **cp**, coronoid process of dentary; **dlc**, distal labial cusp; **dlinc**, distal lingual cusp; **ds**, dentary symphysis; **lin**, lingual; **maf**, masseteric fossa; **mes**, mesial; **mlc**, mesial labial cusp; **mlinc**, mesial lingual cusp; **ob**, occlusal basin; **pc**, lower postcanine; **Pdt**, postdentary bones trough; **tc**, transverse crest. Scale bar 50 mm (A–B) and 10 mm (C–D).

projected ventrolaterally, without any form of protuberance (Fig. 5C). The posteriormost region of jugal is overlapped by the anterior (zygomatic) process of the squamosal, slitting the visible portions of the jugal in a dorsal and a ventral projection. The dorsal part is dorsoventrally lower than the ventral, extending until the posterior margin of the temporal fenestra. The ventral portion, in contrast, is comparatively deeper and tapering posteriorly, but extends posteriorly to a similar level (Fig. 5C). In lateral view, the zygomatic process of the squamosal

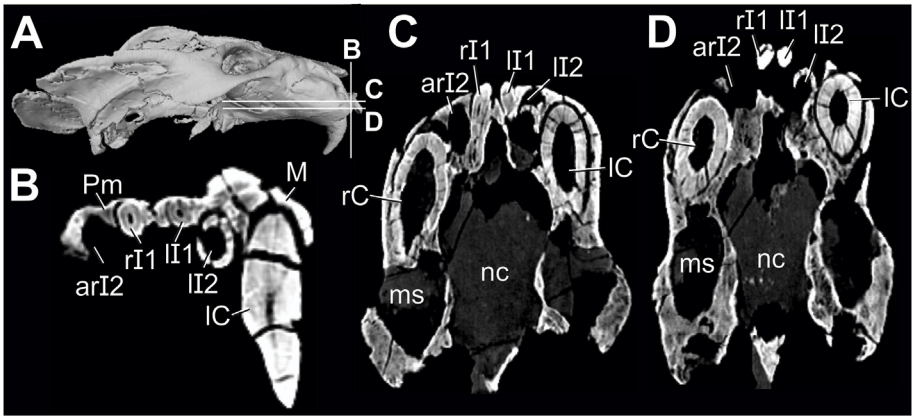

Fig. 7. Computed Tomography sections of the rostral region of the skull of *Siriusgnathus niemeyerorum* gen. et sp. nov. (CAPPA/UFSM 0032). **A**, tridimensional model of the skull in right lateral view showing the three slices (B–D); **B**, coronal section; **C** and **D**, axial sections. Abbreviations: **arI**, right upper incisor alveolus; **lC**, left upper canine; **lI**, left upper incisor; **M**, maxilla; **ms**, maxillary sinus; **nc**, nasal cavity; **Pm**, premaxilla; **rC**, right upper canine; **rI**, right upper incisor.

extends anteriorly to the level of the midpoint of the zygomatic process of the jugal not reaching the level of the postorbital. The posterior margin of the zygomatic process of the squamosal is rounded. On the lateral view of the anterior process of the squamosal, at the middle point, there is a tenuous dorsoventral crest (Fig. 5C).

Skull roof. The frontal is smaller than the prefrontal. Its anterior margin reaches the level of the anterior orbital margin in dorsal view, whereas the posterior margin is located anteriorly to the parietals, extending beyond the posterior margin of the orbit (Fig. 4A). The overlapping of the postorbital on the prefrontal is weak, resulting in a poorly developed interorbital depression. The sagittal crest is slightly higher than the main profile of the skull at the level of the parietal-frontal suture, and it increases in height towards the lambdoid crest (Fig. 5C).

Palate. In ventral view of the holotype, the premaxillae are damaged posteriorly to the incisors. The preserved portions of these bones bear small foramina and form the anterior margin of the incisive foramen, of which the posterior margin is broken (Fig. 4B). The suture between the premaxilla and maxilla lies in the posterior margin of the shallow paracanine fossa, located posteromedially to the upper canine. The maxillary-palatine suture is badly preserved in all the specimens. A well-developed palatine foramen is located at the level of the third postcanine. The palatal lamina of the palatine extends posteriorly until the level of the sixth postcanine (Fig. 4B). A longitudinal crest, formed by the maxilla anteriorly and the palatine posteriorly, initiates at the level of the first postcanine and extends posteriorly up to the end of the palate. The ectopterygoid is absent. The palatine ridges run at the lateral margin of the posterior portion of the internal choanae and do not reach the pterygoid (Fig. 4B). In the holotype, the posterior part of the pterygoids is broken, including part of the left transverse process. The transverse processes are located lateral to the palatine ridges and have a prominent posteroventral orientation (Fig. 5C).

Lateral wall of the braincase. In CAPPA/UFSM 0032, this region is damaged, showing several fractures. The anterior and dorsal limits of

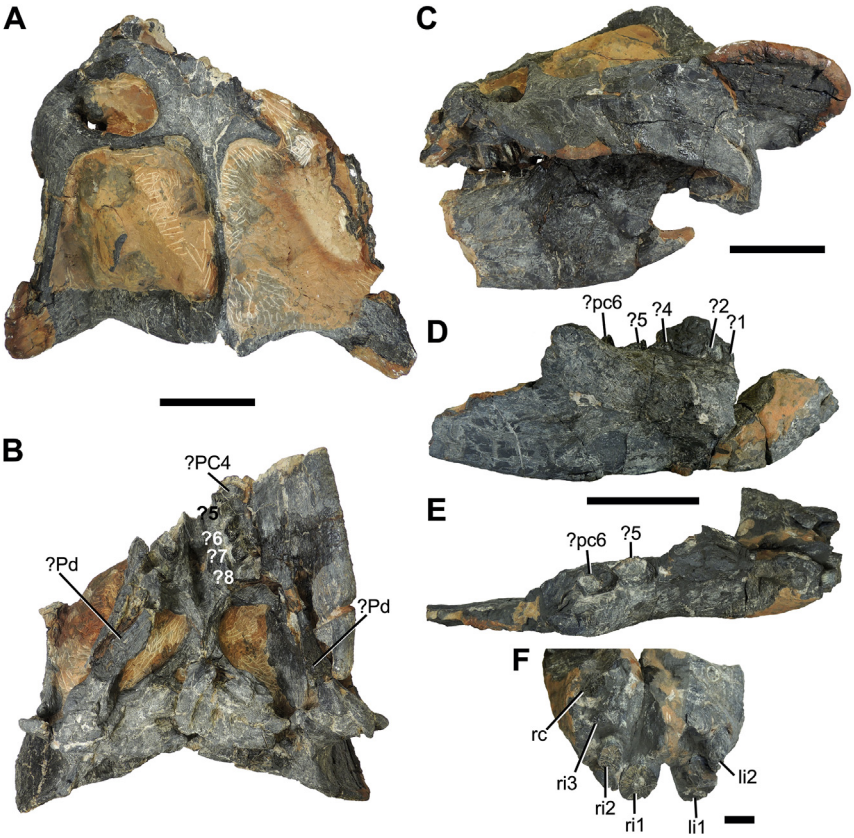

Fig. 8. Skull and lower jaw of *Siriusgnathus niemeyerorum* gen. et sp. nov. CAPPA/UFSM 0109: **A**, dorsal view; **B**, ventral view; **C**, left lateral view; Right ramus of lower jaw and associated rostral tip of left dentary in **D**, right lateral view; **E**, occlusal view; **F**, rostral tip of the dentaries, showing the lower incisor and canines in occlusal view. Abbreviations: **li**, left lower incisor; **PC**, upper postcanine; **pc**, lower postcanine; **Pd**, postdentary bones; **rc**, right lower canine; **ri**, right lower incisor. Scale bar: 50 mm (A–E), and 10 mm (F).

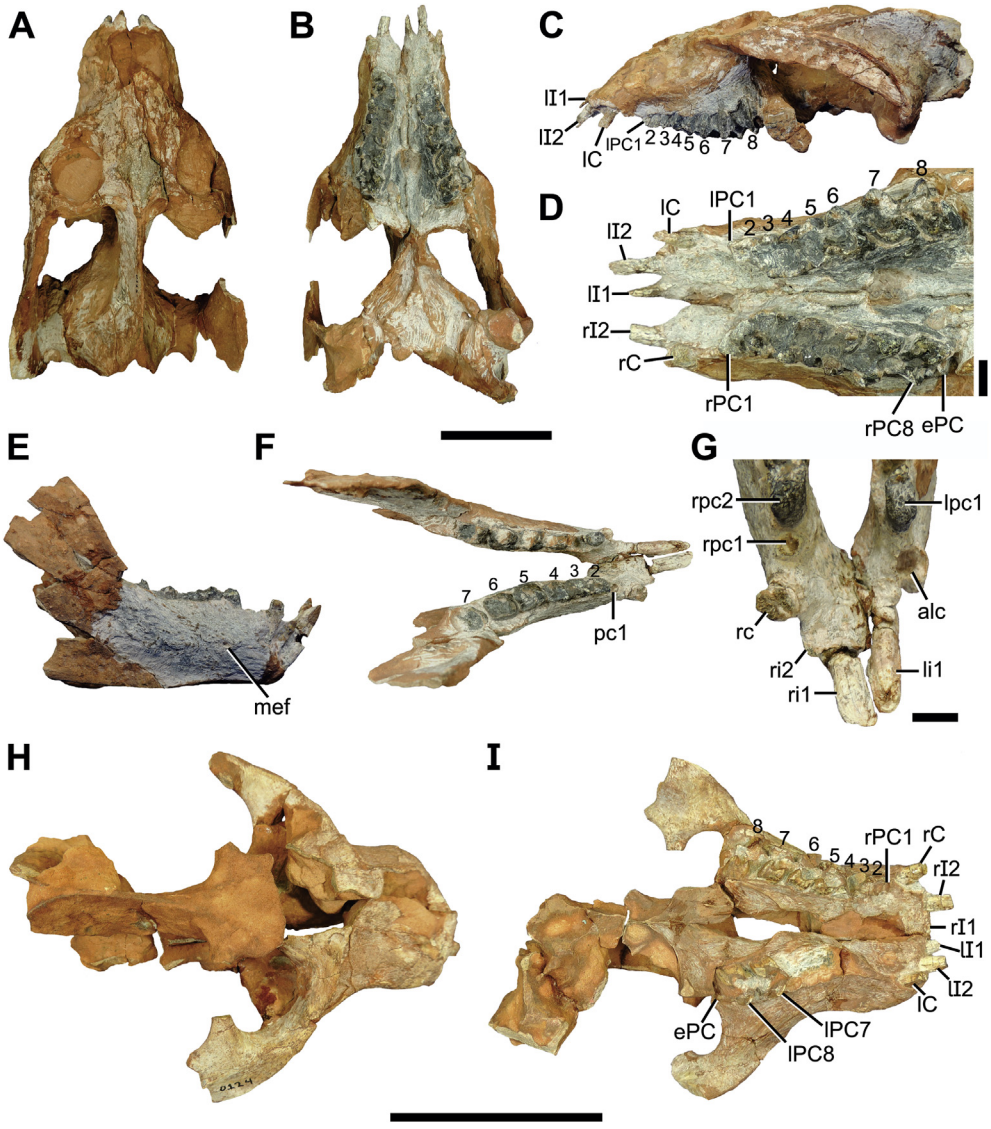

Fig. 9. Skull and lower jaw of *Siriusgnathus niemeyerorum* gen. et sp. nov. CAPPA/UFSM 0125, skull with associated lower jaw: **A**, dorsal view of the skull; **B**, ventral view of the skull; **C**, skull in left lateral view; **D**, upper dentition in occlusal view; **E**, lower jaw in lateral view; **F**, lower jaw in occlusal view; **G**, rostral tip of the dentaries, showing lower incisors and canines in occlusal view. CAPPA/UFSM 0124, incomplete skull of a juvenile individual: **H**, dorsal view; **I**, ventral view. Abbreviations: **alc**, left lower canine alveolus; **ePC**, upper postcanine in eruption; **lC**, left upper canine; **lI**, left upper incisor; **li**, left lower incisor; **lpc**, left lower postcanine; **mef**, mental foramen; **lPC**, left upper postcanine; **pc**, lower postcanine; **rC**, right upper canine; **rc**, right lower canine; **rI**, right upper incisor; **ri**, right lower incisor; **rPC**, right upper postcanine; **rpc**, right lower postcanine. Scale bar: 50 mm (A-C, E-F, H-I), and 10 mm (D and G).

epipterygoid are unclear, and only the suture with the prootic is visible. At the posterior portion of the prootic, the posttemporal canal is located. A large pterygoparoccipital foramen opens laterally. Dorsal to this foramen, an opening communicates with the posttemporal fossa.

Basicranium. The basicranium is short and wide. In ventral view of CAPPA/UFSM 0032, a notch in the squamosal, which acts as a point of attachment to the quadrate is preserved, although this area is damaged on both sides. The anterior projection of the squamosal meets the quadrate ramus of the epipterygoid and forms the ventral margin of pterygoparoccipital foramen (Fig. 4B). On the right side, a damaged structure probably corresponds to both the quadrate and the quadratojugal. The paraoccipital process of the opisthotic contacts the squamosal laterally, and its posterior border is posteroventrally projected. The suture between the basioccipital and basisphenoid is unclear. The basisphenoid wings extent towards the margin of the fenestra ovalis, but do not contribute to it. The fenestra ovalis is located anterolaterally to the jugular foramen and is posteriorly formed by the opisthotic and anteriorly by the prootic. The jugular foramen is slightly larger than the fenestra ovalis (Fig. 4D). The prootic forms the floor of a broad cavum epiptericum. The lateral flange of the prootic forms the dorsal margin of pterygoparoccipital foramen and, in the holotype, there is a crest anterior to the fenestra ovalis that runs lateroanteriorly towards the cavum epiptericum (Fig. 4D). The cultriform process of parasphenoid is well developed.

Occiput. Several fractures obscure most sutural contacts of the occipital plate of CAPPA/UFSM 0032. The lambdoid crest is well developed, lateroventrally projected, with the cranial process of the squamosal contributing to its lateral margin. The cranial and zygomatic processes of the squamosal meet at the base of the lambdoid crest forming a well pronounced V-shaped angle (Fig. 5B). The interparietal contributes to the dorsal margin of the lambdoid crest (Fig. 5B) and, ventrally contacts the supraoccipital. The supraoccipital is elongated dorsoventrally, occupying most of the area of the occipital plate. The tabular does not contribute to the lambdoid crest, being laterally overlapped by the squamosal. The foramen magnum is large and ellipsoid. A marked thickening on its lateroventral margins probably acts as an articular facet for the proatlas. The occipital condyles are separated by a notch (Fig. 4B, D). The paroccipital processes of the opisthotic are damaged on both sides. The rounded post-temporal canal is large, about half the size of the foramen magnum.

Lower Jaw. The dentary symphysis is damaged in the holotype. However, its preserved portion indicates that it is robust, as is also observed in CAPPA/UFSM 0109 and CAPPA/UFSM 0125 (Figs. 6C, Fig. 8D–E, and Fig. 9F). The dentary body is deep and thin. On the lateral surface, a broad and shallow masseteric fossa extends anteriorly until the level of the fifth or sixth postcanine, and posteriorly across the tall, and posterodorsally projected coronoid process (Fig. 6A). The dorsal and posterior margins of the coronoid process are not preserved.

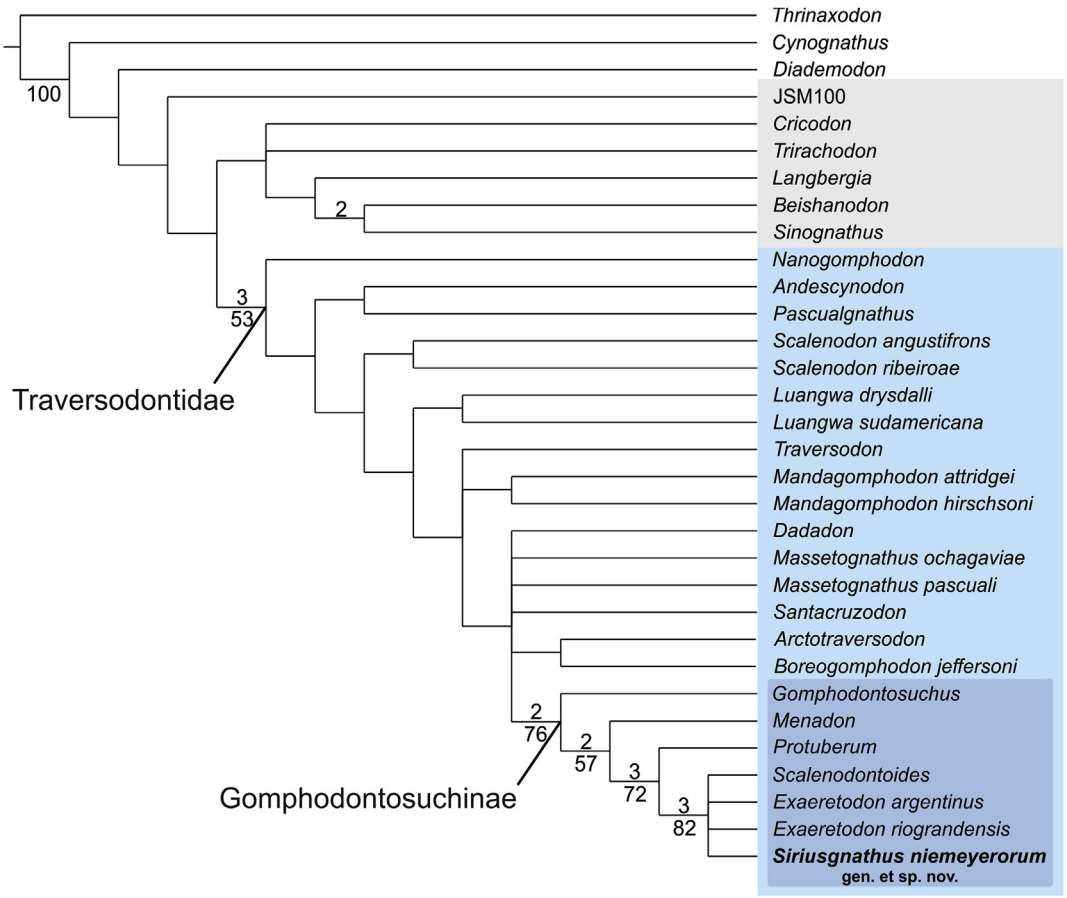

Fig. 10. Strict consensus of 6 most parsimonious trees resulting from the phylogenetic analysis. Notes: Bremer supports greater than 1 are listed above nodes, and Bootstrap values higher than 50% are listed below nodes. Gray: taxa traditionally assigned to Trirachodontidae; light blue: Traversodontidae; and dark blue: Gomphodontosuchinae.

The base of the coronoid process covers the labial surface of the last lower postcanine (Fig. 6C). The angular process of the dentary is well pronounced, acute, and posteriorly projected (Fig. 6A, C). The mental foramen is located at the level of the contact between the second and the third postcanines (Fig. 9E). In medial view, at the base of the coronoid process, on the level of the seventh postcanine, there is the area for the attachment of the coronoid bone. Below this area, there is a sulcus for the attachment of the postdentary bones (Fig. 6C). CAPPA/UFSM 0109 preserves some fragments interpreted as postdentary elements but the poor preservation precludes a secure morphological assessment (Fig. 8B).

Upper dentition. There are two large and procumbent upper incisors (Fig. 7A–D). The first incisors of the holotype are spatulated, with a wear facet on their lingual face, but the second right incisor is conical (Fig. 4E). In the smaller CAPPA/UFSM 0125, the left I1 does not present this lingual wear facet (Fig. 9D). There is no diastema between the incisor and the canine. The upper canine of the holotype is large, distally curved, with wear facets on their lingual edges (Fig. 4B, E and Fig. 5C). A diastema with a length similar to the mesiodistal length of the canine is present between the canine and the first postcanine (Fig. 4B). The maxillary postcanine rows are anteriorly parallel to each other, becoming slightly divergent posteriorly, at the level of the palatine foramina (Fig. 4B). The first upper postcanine is triangular in occlusal view and smaller than the subsequent ones that gradually increase in size towards the distal end of the row. The postcanines two to the eighth are subrectangular, with extensive shouldering (Fig. 4B). The main labial cusp is well-developed, connected by a continuous descendent crest to the mesial accessory labial cusp, which is less developed and, overall, poorly distinguishable from the crest (Fig. 4C). The distal accessory labial cusp is discontinuous of the distal descendent crest from the main labial cusp and separated from it by a distinct sulcus. The distal accessory labial cusp is located at a lower level than the mesial accessory labial cusp. The mesial lingual cusp is connected to the mesial accessory labial cusp by an elongated anterior transverse crest. The distal lingual cusp is more robust and higher than the anterior lingual one. It is connected to the main labial cusp by a distal, slightly concave transverse crest that divides the occlusal basin into two portions. The distal portion is much smaller and shallower than the anterior. It is formed by the distal accessory labial cusp and a small labial extremity of the posterior transverse crest. The main occlusal basin is much broader and deeper, formed labially by the mesial accessory and the main labial cusp, and lingually by the mesial and the distal lingual cusp (Fig. 4C). In CAPPA/UFSM 0032, a ninth postcanine shows a small portion of the main labial cusp, the distal accessory labial cusp, and the distal lingual cusp erupted.

Lower dentition. CAPPA/UFSM 0125 has two preserved incisors in the right dentary: the i1 has a long, procumbent and spatulated crown, whereas the i2 does not preserve a complete crown, but its cross section is comparatively smaller (Fig. 9G). In CAPPA/UFSM 0109, all the lower incisors are broken at the bases of their crowns. The preserved portion of i1 presents the most extensive transverse section, with a comparatively smaller i2. There is also a tiny vestigial i3 on the right side, with about 1/4 of the transverse area of the right i1 (Fig. 8F). In CAPPA/UFSM 0109 and 0125, diastemas are absent between the incisors and the canines. The lower canines are smaller in comparison to the upper ones, with almost the same size as the lower incisors. There is a small diastema between the canine and the first postcanine (Fig. 9G). CAPPA/UFSM 0032 has seven postcanines plus one in process of eruption

(Fig. 6B) whereas the smaller CAPPA/UFSM 0125 has six postcanines plus one in process of eruption (Fig. 9F). All postcanines are quadrangular in occlusal view (Fig. 6B, D), with a high mesial transverse crest formed by the mesial, labial and lingual cusps. The mesial labial cusp is larger and higher in comparison to the lingual one (Fig. 6D). It also shows a conspicuous distal curvature (Fig. 6A, D). The distal labial and lingual cusps are less developed than their mesial counterparts. These four cusps delimit a deep central occlusal basin (Fig. 6D). The lower postcanines gradually increase in size posteriorly. Similarly, the mesial transverse crest becomes progressively higher and recurved, and the occlusal basin increases in depth (Fig. 6A, C).

6.10. Phylogenetic position of Siriusgnathus niemeyerorum gen. et sp. nov

The phylogenetic analysis recovered six MPTs of 221 steps each (Consistency Index: 0.434; Retention Index: 0.729; Rescaled Consistency Index: 0.316). The new traversodontid consistently nests within Gomphodontosuchinae, in all generated cladograms. However, in the strict consensus tree (Fig. 10), the new taxon lies within a polytomy with *Exaeretodon argentinus* Cabrera, 1943, *E. riograndensis*, and *Scalenodontoides* Crompton and Ellenberger, 1957. The node is supported by the following synapomorphies: (1) a skull greater than 25 cm (character 1, state 0), (2) two sides of the temporal fenestra diverging posteriorly (character 3, state 0); (3) large upper canines (character 41, state 0); (4) well developed shouldering in the posterior margin of the upper postcanines (character 48, state 2); and (5) presence of a posterolabial accessory cusp on the upper postcanines (character 53, state 0). The relationships of members of this clade are unsolved as, among the MPTs, the new species either lies as the sister-taxon to *E. argentinus* or the sister-taxon of a clade including *E. riograndensis* plus *Scalenodontoides*.

6.11. Anatomical and taxonomic remarks

We erected *Siriusgnathus niemeyerorum* based on CAPPA/UFSM 0032, CAPPA/UFSM 0109, CAPPA/UFSM 0125, and CAPPA/UFSM 0124, the best-preserved specimens, but additional specimens present similar traits. Although the strict consensus tree of the phylogenetic analysis nests this new taxon with *E. riograndensis*, *E. argentinus,* and *Scalenodontoides*, its unique combination of characters fully support it as a new genus and species.

Some morphological features of the new traversodontid, mostly linked to dentition, resemble those observed in *E. riograndensis* and *E. argentinus* (Bonaparte, 1962; Abdala et al., 2002). The spatulated and procumbent incisors, as well as the lower postcanines, are practically identical to those from *E. riograndensis* (Abdala et al., 2002; Liparini et al., 2013). The new taxon also shares with *Exaeretodon* the lack of an internarial bar, the divergent zygomatic arches, the well projected posteriorly angular process of dentary and a tall coronoid process covering the last postcanine (Bonaparte, 1962; Abdala et al., 2002; Liparini et al., 2013). One prootic crest is present in the holotype of *Siriusgnathus niemeyerorum*, whereas two crests are represented in *E. riograndensis* (Abdala et al., 2002).

On the other hand, *Siriusgnathus niemeyerorum* differs from *Exaeretodon* in several anatomic features (Fig. 11): 1) the length of both temporal and rostral region is almost equivalent, whereas in *Exaeretodon* the rostrum is longer (Fig. 11A–B); 2) the postorbital bar and consequently the orbit of the new taxon, are more anteriorly placed, in relation to the ventral margin of the subtemporal fenestra, than in *Exaeretodon* and consequently, the orbit is hidden on the ventral view of the skull, differing from the condition of *Exaeretodon* (Fig. 11A–D); 3) the protuberances formed by the overlapping of the postorbital on the prefrontal, as well as the interorbital depressions are both less pronounced than in and *E. riograndensis* (Fig. 11A–B); 4) the descending process of the jugal is incipient, whereas well developed protuberances are present in *Exaeretodon* (Fig. 11A–B, G-H); 5) the ventral portion of the posteriormost region of the jugal, as exposed laterally, is dorsoventrally narrow and tapering posteriorly, distinct from *Exaeretodon*, in which this structure is quadrangular at its posterior end (Fig. 11G–H); 6) the anterior tip of the zygomatic process of the squamosal does not reach the posterior level of the postorbital bar, as occurs in *Exaeretodon* (see Bonaparte, 1962; Abdala et al., 2002, Fig. 11G–H); 7) the contact of the zygomatic process of the squamosal with the jugal is almost flat and smooth, whereas in *E. riograndensis,* this contact forms a conspicuous longitudinal crest (Fig. 11G–H); 8) associated to the previous trait, in *E. riograndensis*, the zygomatic portion of the squamosal bears a longitudinal sulcus, interrupted by a pronounced dorsoventral crest at the middle region of this portion, this crest is comparatively tenuous in *S. niemeyerorum* (Fig. 11G–H); 9) the posterior portion of the zygoma, at the posteriormost border of the zygomatic process of squamosal, is posteriorly projected in *Exaeretodon* (Fig. 11G–H); 10) in dorsal view, the lambdoidal crest is less convex and the union between this crest and the zygoma is less deep than in *Exaeretodon* (Fig. 11A–B); 11) the basicranium is short as in *Exaeretodon*, however it is not as broad transversally (Bonaparte, 1962; Abdala et al., 2002, Fig. 11C–D); (12) there are two upper and two/three lower incisors in *S. niemeyerorum*, whereas in *Exaeretodon* there are three upper and three lower incisors (Abdala et al., 2002; Bonaparte, 1962, Fig. 11C–D). It is important to note that Ray (2015) interpreted that *Exaeretodon statisticae* Chatterjee, 1982 from India (considered as *Exaeretodon* sp. by Liu and Abdala, 2014) has two lower incisors, contrary to the original description of Chatterjee (1982), in which three lower incisors were mentioned; 13) in *S. niemeyerorum*, there is less ontogenetic variation in the number of postcanines (See Table S5), as all the specimens have eight upper postcanines (plus one in eruption), whereas in *Exaeretodon* there is a significant tendency to reduce the number of upper postcanines through ontogeny (see Abdala et al., 2002). Comparing adults of the three taxa, the number of upper postcanines of *S. niemeyerorum* (CAPPA/UFSM 0032, basal skull length (BL) 220.4 mm, eight PC is more similar to that observed in *E. argentinus* (MCZ 111-64A, BL 219, seven PC) than *E. riograndensis* (MCP 1522 PV, BL 223, five-six PC) (Abdala et al., 2002, Fig. 11C–D); 14) the first upper postcanine of *S. niemeyerorum* is triangular, whereas in *E. riograndensis* it is rectangular (Abdala et al., 2002, Fig. 11C–D); 15) the mesial accessory labial cusp in *S. niemeyerorum* is less mesially displaced than in *E. riograndensis* and because of this, the shouldering is less pronounced (Fig. 11E–F); 16) the distal accessory labial cusp is more lingually positioned in *E. riograndensis* than in *S. niemeyerorum* (Fig. 11E–F).

Siriusgnathus niemeyerorum and *Scalenodontoides* share a short and broad rostrum, although in *Scalenodontoides* it is much broader (see Battail, 2005). However, the interorbital width is narrow in the new taxon whereas the temporal region is more elongated (compare with Gow and Hancox, 1993; Battail, 2005). Furthermore, the nuchal table is a remarkable autapomorphy represented in one specimen of *Scalenodontoides* (considered as a sexual dimorphism by Battail (2005). Also, the upper postcanines of *Scalenodontoides* have similar morphology, in which the shouldering is less pronounced than in *S. niemeyerorum.*

Siriusgnathus niemeyerorum shares with other gomphodontosuchines (e.g., *Gomphodontosuchus brasiliensis* von Huene, 1928 and *Protuberum cabralense* Reichel et al., 2009) the short and broad rostrum (see Reichel et al., 2009; Liu and Abdala, 2014). *Menadon* presents a tall and robust rostrum, as well as an internarial bar (Kammerer et al., 2008; Melo et al., 2015), differing from *S. niemeyerorum*. The zygomatic process of the jugal is absent in *Menadon*, but well developed in *Protuberum* (Kammerer et al., 2008; Reichel et al., 2009; Melo et al., 2015). Those taxa also diverge from *S. niemeyerorum* in both tooth morphology and number of teeth. *Gomphodontosuchus* has four upper and three lower incisors, the first upper postcanine is triangular in occlusal view, becoming quadrangular towards the distal end of the row (Liu and Abdala, 2014). *Menadon* has four upper and three lower incisors, and the upper postcanines are quadrangular (Kammerer et al., 2008; Melo et al., 2015). *Protuberum* has three upper incisors, and the upper

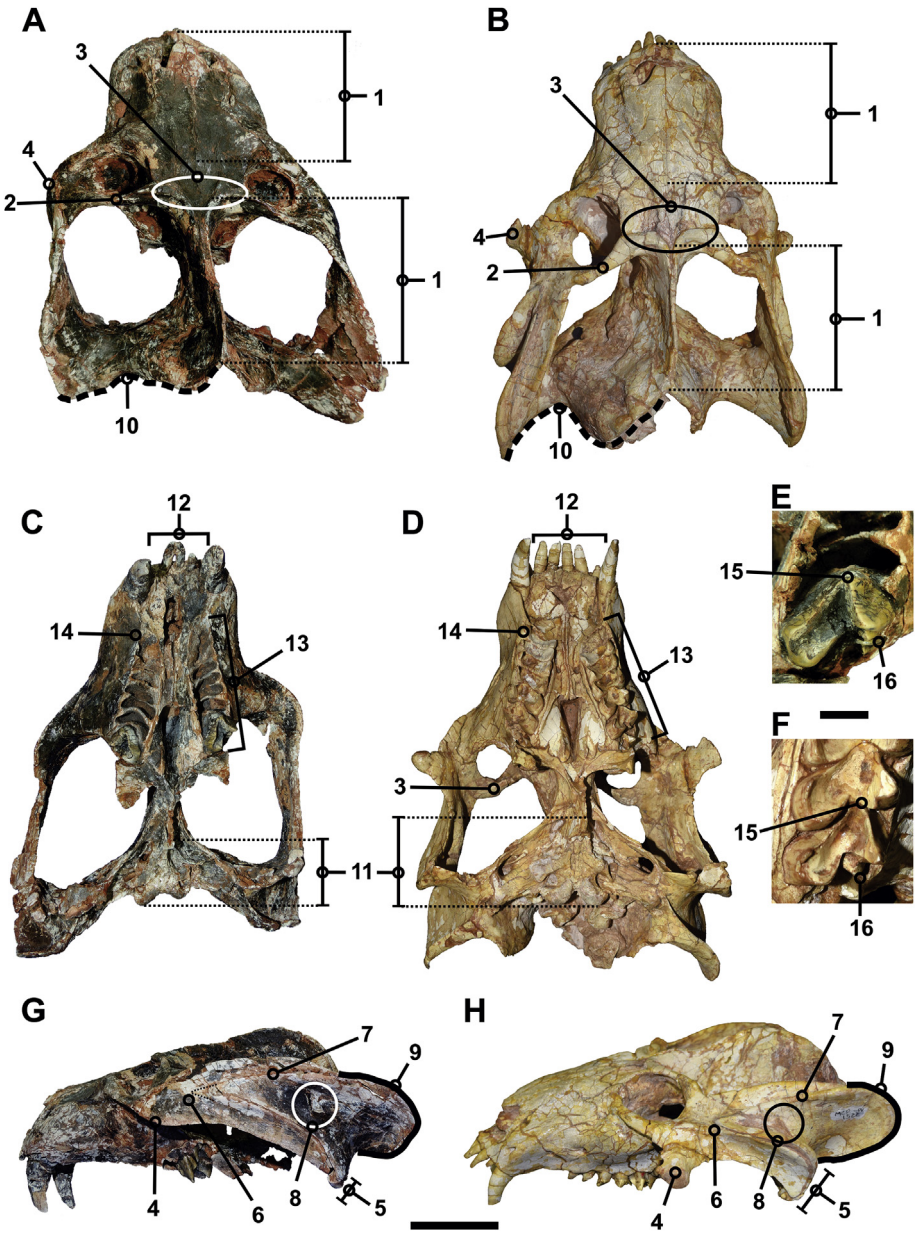

Fig. 11. Comparisons between the holotype of *Siriusgnathus niemeyerorum* gen. et sp. nov. (CAPPA/UFSM 0032) and the holotype of *Exaeretodon riograndensis* (MCP 1522 PV). Dorsal view of **A**, CAPPA/UFSM 0032 and **B**, *E. riograndensis*; ventral view of **C**, CAPPA/UFSM 0032 and **D**, *E. riograndensis*; Upper postcanines teeth of **E**, CAPPA/UFSM 0032 and **F**, *E. riograndensis*; left lateral view of **G**, CAPPA/UFSM 0032 and **H**, *E. riograndensis*. The numeration follows the text (section 6.11). The specimens are in scale. Scale bar: 50 mm (A-D, G-H) and 10 mm (E–F).

postcanines have two main cusps with no shouldering (Reichel et al., 2009). The presence of two upper and two/three lower incisors in *S. niemeyerorum* is unique in Traversodontidae, although two lower incisors are present in *E. statisticae*, according to Ray (2015). *Mandagomphodon hirschsoni* Crompton, 1972 has two lower, but three upper incisors (Hopson, 2013).

7. Systematic paleontology of the remaining specimens

7.1. Non-traversodontids cynodonts

Probainognathia Hopson, 1990
Probainognathia indet.

7.1.1. Material

CAPPA/UFSM 0099, partial right humerus.

7.1.2. Anatomical description

The preserved length of the partial humerus is 100 mm (Fig. 12A–E). The humerus is somewhat mediolaterally compressed, and the distal extremity is almost flat, probably because of a dorsoventral compression. The humeral head is dorsally projected and continuous with the lesser tuberosity (Fig. 12A, E). The most proximal part of the greater tuberosity is not preserved. The deltopectoral crest is broad and well developed, abruptly inflected ventrally, and extending until almost half of the humeral shaft, constituting a deep bicipital groove (Fig. 12C–E). The distal extremity is broken at the level of the entepicondylar foramen (Fig. 12B, D). The ectepicondylar foramen is absent. The ectepicondylar crest is broad. Only a rounded humeral capitulum is preserved (Fig. 12A–B).

7.1.3. Taxonomic remarks

The general morphology of the humerus resembles that from

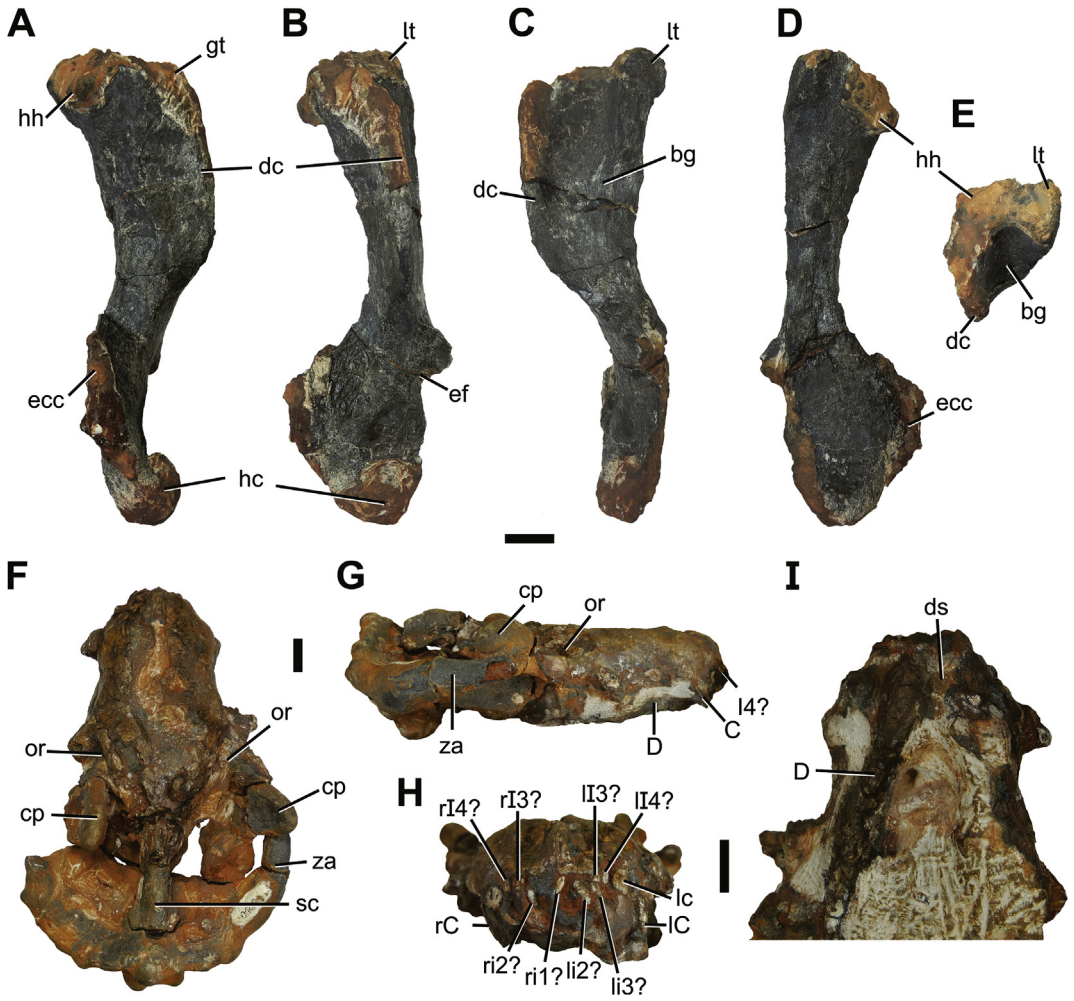

Fig. 12. Probainognathia from the Niemeyer site. CAPPA/UFSM 0099, right humerus in **A-E**, lateral, anterior, medial, posterior, and proximal views. CAPPA/UFSM 0100, skull and mandible in **F**, dorsal; **G**, right lateral; **H**, anterior view; **I**, ventral views. Abbreviations: **bg**, bicipital groove; **C**, upper canine; **cp**, coronoid process; **D,** dentary; **dc**, deltopectoral crest; **ds**, dentary symphysis; **ecc**, ectepicondylar crest; **ef**, entepicondylar foramen; **gt**, greater tuberosity; **hc**, humeral capitulum; **hh**, humeral head; **I**, upper incisor; **lC**, left upper canine; **lc**, left lower canine; **lI**, left upper incisor; **li**, left lower incisor; **lt**, lesser tuberosity; **or**, orbital region; **rC**, right upper canine; **rI**, right upper incisor; **ri**, right lower incisor; **sc**, sagittal crest; **za**, zygomatic arch. Scale bar: 10 mm.

Trucidocynodon riograndensis Oliveira et al., 2010. Although it is smaller than *T. riograndensis*, in which the humeral length is 136.5 mm, both share the presence of a deep bicipital groove, deltopectoral crest abruptly inflected ventrally, large ectepicondylar crest, and absence of the ectepicondylar foramen (Oliveira et al., 2010).

Prozostrodontia Liu and Olsen, 2010

7.1.4. Material

CAPPA/UFSM 0100, skull and lower jaw.

7.1.5. Anatomical description

CAPPA/UFSM 0100 has a basal skull length of 120 mm (Fig. 12F–I). The specimen lacks postorbital bars (Fig. 12F). The rostrum, in dorsal view, presents a slight medial constriction close to its midpoint and the anteriormost region is triangular. The internarial bar is preserved. Both rostral and temporal region are similar in length (Fig. 12F). The zygomatic arches are slender (Fig. 12G). The horizontal ramus of the dentary is low, showing unfused symphysis (Fig. 12G, I). Upper and lower canines are small. There are two upper and two lower small and conical exposed incisors, but the exact number is unknown because they are still covered by matrix (Fig. 12H).

7.1.6. Taxonomic remarks

The absence of the postorbital bar and an unfused dentary symphysis are synapomorphies of Prozostrodontia, (Liu and Olsen, 2010). This clade includes *Prozostrodon brasiliensis* Barberena et al., 1987, *Therioherpeton cargnini* Bonaparte and Barberena, 1975, tritylodontids, trithelodontids, brasilodontids and mammaliaforms (Liu and Olsen, 2010). Among prozostrodontians, CAPPA/UFSM 0100 shows more affinities with *Prozostrodon* regarding the triangular shape of the orbits, the dorsal region of the skull posterior to the orbit, and the rostral region with a slight constriction at the middle point and sharp on its anterior tip (see Bonaparte and Barberena, 2001). However, it is much larger than *Prozostrodon*. Nonetheless, the specimen is still covered by a hard matrix, so it needs further preparation in order to achieve a less inclusive taxonomical assessment.

7.2. Archosauromorphs

Diapsida Osborn, 1903
Archosauromorpha von Huene, 1946
Archosauromorpha indet.

7.2.1. Material

CAPPA/UFSM 0133, vertebral centrum.

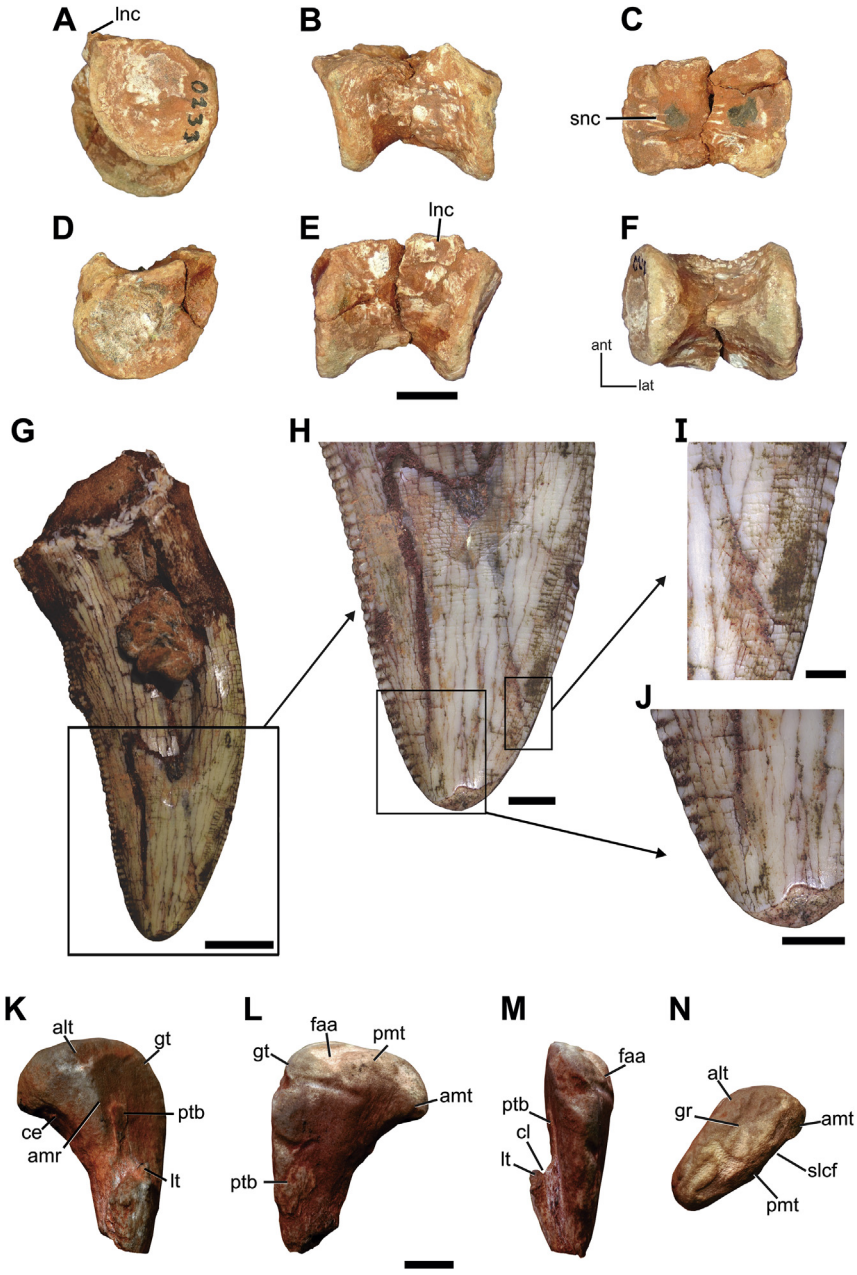

Fig. 13. Archosauromorpha from the Niemeyer site. CAPPA/UFSM 0133, vertebral centrum in **A-F**, anterior, left lateral, dorsal, posterior, right lateral, and ventral views. CAPPA/UFSM 0132, **G**, isolated tooth; **H**, apical portion; **I**, mesial carena; **J**, distal carena. CAPPA/UFSM 0157, proximal portion of left femur in **K-N**, anterior, posterior, medial and proximal views. Abbreviations: **alt**, anterolateral tuber; **amr**, anteromedial ridge; **amt**, anteromedial tuber; **ant**, anterior; **ce**, concave emargination; **cl**, cleft; **faa**, *facies articularis antitrochanterica*; **gr**, groove; **gt**, greater trochanter; **lat**, lateral; **lnc**, lateral portion of the neural canal; **lt**, lesser trochanter; **pmt**, posteromedial tuber; **ptb**, protuberance; **slcf**, sulcus for *ligamentum captis femoris*; **snc**, sulcus for the neural canal. Scale bar: 10 mm (A-F, K-N), 5 mm (G) and 1 mm (H–J).

7.2.2. Anatomical description

The specimen consists of an isolated centrum with about 32 mm in length (Fig. 13A–F). It is longer than taller (maximum dorsoventral height is 22.5 mm), spool-shaped, transversely constricted at its mid-point, and amphicoelous (Fig. 13B and E). There is no parapophysis in any of the lateral surfaces, indicating that it corresponds to a mid to posterior dorsal or caudal vertebra. Also, the lateral surface also lacks any pneumatic openings or pleurocoels. Indeed, such a surface is smooth (Fig. 13B and E). The anterior articular surface is 19.4 mm in height and 21.3 mm in width (Fig. 13A), whereas the posterior is 17.6 mm in height and 24 mm in width (Fig. 13D). The dorsal surface of the element bears a longitudinal sulcus that corresponds to the floor of the neural canal (Fig. 13C). The anterior aperture of the sulcus is approximately 0.74 cm in width, but posteriorly it becomes wider, with 10 mm at the posterior aperture. The bone portion that bounds the sulcus laterally forms the lateroventral portion of the neural canal. This lateral portion of the dorsal surface, where the neural arch would attach, is very rough, indicating that both portions were disarticulated, but not broken (Fig. 13C). Therefore, it is inferred that the centrum was not yet co-ossified with the neural arch. The ventral bone surface is smooth, lacking any keel. In lateral view, this surface is concave, as both articular facets are more developed ventrally than the midpoint of the centrum (Fig. 13F).

7.2.3. Taxonomic remarks

The general morphology of CAPPA/UFSM 0133 (e.g., spool-shaped, transversely constricted at the mid-point, and amphicoelous) consists with the general archosauromorph pattern. Ventral keels are usually present in cervical and anterior dorsal vertebrae. Therefore CAPPA/UFSM 0133 is putatively a vertebral centrum of a posteriormost dorsal vertebra.

7.3. Archosauriforms

Archosauriformes Gauthier, 1986

7.3.1. Material

CAPPA/UFSM 0132, an isolated tooth.

7.3.2. Anatomical description

The specimen is strongly labiolingually compressed and measures 35 mm in height (Fig. 13G–J). It is broken at the root level. Its crown is distally recurved with no sign of constriction at its base. It is ziphodont, bearing conspicuous serrations, on both medial and distal carinae. The serrations on the mesial carina start at the mid-height of the crown and extend until the apex, whereas the distal serrations extend along the entire length (Fig. 13G–H). The serrations are composed of tiny subrectangular denticles perpendicularly oriented to the axis of the carinae, with 9–10 denticles per 50 mm (Fig. 13I–J).

7.3.3. Taxonomic remarks

The labiolingual compression of CAPPA/UFSM 0132 is probably exaggerated by taphonomic deformation. The general ziphodont morphology of CAPPA/UFSM 0132 is typical of carnivorous archosauriforms (Nesbitt, 2011).

7.4. Archosaurs

Archosauria Cope, 1869
cf. Dinosauromorpha Benton, 1985

7.4.1. Material

CAPPA/UFSM 0157, proximal portion of a left femur.

7.4.2. Anatomical description

The specimen has 47.7 mm of preserved length (Fig. 13K–N). The proximal surface is 33 mm in width, rough, and bears a sulcus, which is interpreted as the transverse groove (Fig. 13N). There is a slight expansion on the anterolateral surface that contacts a ventral descendant ridge. Such expansion corresponds to the anterolateral tuber, which results in a convex, rather than straight, anterior margin in dorsal view (Fig. 13A and N). Two additional tubers are located in the opposite margin. The first one is the anteromedial tuber, which contributes to the medial expansion of the femoral head (Fig. 13L and N). The other is the posteromedial tuber, located close to the midpoint of the posterior margin of the proximal portion. Such as the anteromedial tuber, this one is also quite reduced (Fig. 13L and N). This arrangement results in a shallow sulcus for the *ligamentum capitis femoris* (Fig. 13N). The region correspondent to the *facies articularis antitrochanterica* is ventral to the greater trochanter (Fig. 13L–M). Therefore, the anterolateral portion of the proximal surface is higher than the posterolateral one.

The femoral head becomes enlarged medially and is separated from the shaft by a marked ventral concavity. The specimen lacks a proximal condylar fold. In dorsal view, the medial articular surface of the head is rounded. The lateral portion of the head comprises the greater trochanter, which is also rounded (Fig. 13K–L). The anterolateral surface of the dorsal portion of the bone is smooth. Indeed, the specimen lacks any structure related to the dorsolateral trochanter on this surface. The posterolateral portion of the dorsal part of the femur bears a 10 mm long protuberance (Fig. 13L).

The posterolateral margin of the femur CAPPA/UFSM 0157 slightly expands posteriorly along its dorsoventral length. A conspicuously enlarged ridge occurs on the anterior surface of the bone, probably corresponding to the lesser trochanter (Fig. 13K and M). It is 20 mm in length and 13 mm in width. The proximal tip of that structure tapers to a point, being separated from the shaft by a marked cleft (Fig. 13M). This putative lesser trochanter expands medially forming an unusual medial flange. Dorsal to this structure, there is an eight mm long bone protuberance (Fig. 13M). There is no trochanteric shelf associated with the distal portion of the lesser trochanter.

7.4.3. Taxonomic remarks

Despite its fragmentary condition, the specimen bears a set of traits that could enable its inclusion in a less inclusive archosaurian clade. For instance, the femoral head expands significantly and separates ventrally from the shaft by a concave emargination, a feature that, among archosaurs, is only reported in dinosaurs (Sereno and Arcucci, 1994). In contrast, there are no early dinosaurs without an expansion of the dorsolateral trochanter at the anterior surface of the proximal portion of the femur. However, the presence of a well-developed lesser trochanter reinforces a possible dinosauromorph affinity. Also, the enlarged cleft between the proximal tip of the trochanter and the femoral shaft is a feature present in some silesaurids, theropods, and ornithischians, among dinosauromorphs (Langer and Ferigolo, 2013). On the other hand, the ventrally descended *facies articularis antitrochanterica* does not occur in silesaurids (Nesbitt, 2011). The posterolateral portion of the dorsal part of the femur bears a 10 mm long protuberance (Fig. 13L). Griffin and Nesbitt (2016) recognized a scar in a similar position of the protuberance in the posterolateral portion of the dorsal part of CAPPA/UFSM 0157 in some femora of the silesaurid *Asilisaurus kongwe* Nesbitt et al., 2010. Those authors recognized it as the posterior portion of the dorsolateral trochanter. Also, the early sauropodomorph *Buriolestes schultzi* Cabreira et al., 2016 has a scar in the femur that seems homologous to this protuberance (Cabreira et al., 2016). Some dinosauriforms (e.g., *Asilisaurus kongwe*, *Buriolestes schultzi*, Cabreira et al., 2016) share a scar or protuberance in a similar position to the protuberance dorsal to the lesser trochanter of CAPPA/UFSM 0157. A greater trochanter with rounded shape is unusual in early dinosauriforms but is present in *Marasuchus lilloensis* Romer, 1972 (Sereno and Arcucci, 1994). In contrast, a rounded shape is the general trait reported to lagerpetids. The combination of features of CAPPA/UFSM 0157 suggests dinosauromorph affinities.

8. Final remarks

A new Triassic fossiliferous assemblage is reported from Southern Brazil. The abundance of collected fossils includes several specimens ascribed to the new traversodontid *Siriusgnathus niemeyerorum*, probainognathians, a putative dinosauromorph, and indeterminate archosauromorphs. The high frequency of traversodontid cynodonts is particularly notable. However, at this point, no index fossils have been found at the Niemeyer Site precluding a secure assignation of this fauna to any known AZ of the Brazilian Triassic. Nonetheless, other sites pertaining to the Agudo structural block, which also encompass this new site (Da-Rosa and Faccini, 2005; Da-Rosa, 2015), show a biostratigraphic correlation to the late Carnian *Hyperodapedon* AZ (e.g., Janner site, see Langer et al., 2007; Müller et al., 2015; Pretto et al., 2015; Langer et al., 2018, Fig. 1C) and the Norian *Riograndia* AZ (i.e., *Sacisaurus* site, see Ferigolo and Langer, 2007; Ribeiro et al., 2011; Langer and Ferigolo, 2013; Langer et al., 2018, Fig. 1C).

The lithology of the Niemeyer site is consistent with that found in the Candelária Sequence *sensu* Horn et al. (2014). Given that no traversodontids are recorded on the upper levels of this unit, this site might also be included in the lower levels of the sequence, of putative Carnian age. In order to more accurately verify such age assumption, absolute dating is necessary for all structural blocks of the Santa Maria Supersequence.

Acknowledgments

We are thankful to the Niemeyer family for kindly allowing the paleontological prospection and fieldwork at their property. We are grateful to the editor Francisco Vega and the reviewers Fernando Abdala and Tomaz P. Melo for comments that greatly improved this manuscript; the students of Universidade Federal de Santa Maria (UFSM) and especially to Lúcio Roberto da Silva (Universidade Luterana do Brasil - ULBRA) for their helpful assistance during the

collection of the specimens here described. We thank Agustín Martinelli, Ana Maria Ribeiro, Marina Bento Soares and Téo Veiga de Oliveira for comments that significantly improved the early versions of this manuscript; Valnir de Paula and medical clinic Dix (Diagnóstico por Imagem do Hospital de Caridade, Santa Maria, Rio Grande do Sul) for kindly allow access to their CT-Scan. This work was supported by the Coordenação de Aperfeiçoamento de Pessoal de Nível Superior to the scholarship to AEBP, Fundação de Amparo à Pesquisa do Estado do Rio Grande do Sul (FAPERGS 17/2551-0000816-2) to LK, and Conselho Nacional de Desenvolvimento Científico e Tecnológico (CNPq, 306352/2016-8) to SDS. We also thank the Willi Henning Society, for the gratuity of TNT software.

Appendix A. Supplementary data

Supplementary data related to this article can be found at https://doi.org/10.1016/j.jsames.2018.08.016.

References

Abdala, F., Barberena, M.C., Dornelles, J.E., 2002. A new species of the traversodontid cynodont *Exaeretodon* from the Santa Maria formation (Middle/Late triassic) of southern Brazil. J. Vertebr. Paleontol. 22 (2), 313–325. https://doi.org/10.1671/0272-4634(2002)022[0313:ANSOTT]2.0.CO;2.

Abdala, F., Martinelli, A.G., Soares, M.B., Fuente, M. de la, Ribeiro, A.M., 2009. South American Middle Triassic continental faunas with amniotes: biostratigraphy and correlation. Palaeontol. Afr. 44, 83–87.

Abdala, F., Ribeiro, A.M., 2003. A new traversodontid cynodont from the Santa Maria Formation (Ladinian-Carnian) of southern Brazil, with a phylogenetic analysis of Gondwanan traversodontids. Zool. J. Linn. Soc. 139 (4), 529–545. https://doi.org/10.1111/j.1096-3642.2003.00096.x.

Abdala, F., Ribeiro, A.M., 2010. Distribution and diversity patterns of triassic cynodonts (therapsida, Cynodontia) in gondwana. Palaeogeogr. Palaeoclimatol. Palaeoecol. 286, 202–217. https://doi.org/10.1016/j.palaeo.2010.01.01.

Abdala, F., Ribeiro, A.M., Schultz, C.L., 2001. A rich cynodont fauna of Santa Cruz do Sul, Santa Maria formation, (Middle-Late triassic), southern Brazil. Neues Jahrbuch Geol. Palaontol. Monatsh. (11), 669–687 2001.

Abdala, F., Sá-Teixeira, A.M., 2004. A traversodontid cynodont of african affinity in the south american triassic. Palaeontol. Afr. 40, 11–22.

Badgley, C., 1986. Counting individuals in mammalian fossil assemblages from fluvial environments. Palaios 1 (3), 328–338. https://doi.org/10.2307/3514695.

Barberena, M.C., Bonaparte, J.F., Sá-Teixeira, A.M., 1987. *Thrinaxodon brasiliensis* sp. Nov., a primeira ocorrência de cinodontes galessaurus para o Triássico do Rio Grande do Sul. In: X Congresso Brasileiro de Paleontologia, Anais, pp. 67–76.

Battail, B., 2005. Late triassic traversodontids (synapsida: Cynodontia) in southern Africa. Palaeontol. Afr. 41, 67–80.

Behrensmeyer, A.K., 1975. The taphonomy and paleoecology of plio-pleistocene vertebrate assemblages of lake rudolf, Kenya. Bull. Mus. Comp. Zool. 146, 473–578.

Behrensmeyer, A.K., 1978. Taphonomic and ecologic information from bone weathering. Paleobiology 4 (2), 150–162. https://doi.org/10.1017/S0094837300005820.

Behrensmeyer, A.K., 1982. Time resolution in fluvial vertebrate assemblages. Paleobiology 8 (3), 211–227. https://doi.org/10.1017/S0094837300006941.

Behrensmeyer, A.K., 1991. Terrestrial vertebrate accumulations. In: Allinson, P.A., Briggs, D.E.G. (Eds.), Taphonomy: Releasing the Data Locked in the Fossil Record. Plenum, New York, pp. 291–335.

Benton, M.J., 1985. Classification and phylogeny of the diapsid reptiles. Zool. J. Linn. Soc. 84, 97–164. https://doi.org/10.1111/j.1096-3642.1985.tb01796.x.

Bonaparte, J.F., 1962. Descripción del cráneo y mandíbula de *Exaeretodon frenguellii*, Cabrera y su comparación con Diademodontidae, Tritylodontidae y los cinodontes sudamericanos. Publicaciones del Mus. Munic. Cienc. Nat. Misc. y Tradicionales de Mar del Plata 1, 137–202.

Bonaparte, J.F., 1966. Una nueva "fauna" triásica de Argentina (Therapsida: Cynodontia Dicynodontia) consideraciones filogenéticas y paleobiogeográfica. Ameghiniana 4 (8), 243–296.

Bonaparte, J.F., 1969. Dos nuevas "faunas" de reptiles triásicos de Argentina. In: Gondwana Stratigraphy, I.U.G.S. Coloquio Mar del Plata, pp. 283–302 1967.

Bonaparte, J.F., 1971. Los tetrapodos del sector superior de la Formacion Los Colorados, La Rioja, Argentina. Opera Lilloana 22, 1–183.

Bonaparte, J.F., Barberena, M.C., 1975. A possible mammalian ancestor from the Middle Triassic of Brazil (Therapsida-Cynodontia). J. Paleontol. 49 (5), 931–936.

Bonaparte, J.F., Barberena, M.C., 2001. On two advanced carnivorous cynodonts from the Late Triassic of southern of Brazil. Bull. Mus. Comp. Zool. 156 (1), 59–80.

Bonaparte, J.F., Martinelli, A.G., Schultz, C.L., 2005. New information on the sister-group of mammals: *brasilodon* and *brasilitherium* (Cynodontia, Probainognathia) from the later triassic of southern Brazil. Rev. Bras. Palaontol. 8 (1), 25–46.

Bonaparte, J.F., Martinelli, A.G., Schultz, C.L., Rubert, R., 2003. The sister group of mammals: small cynodonts from the Late Triassic of Southern Brazil. Rev. Bras. Palaontol. 5, 5–27.

Bonaparte, J.F., Schultz, C.L., Soares, M.B., Martinelli, A.G., 2010. La fauna local de Faxinal do Soturno, Triásico Tardío de Rio Grande do Sul, Brasil. Rev. Bras. Palaontol. 13 (3), 233–246. https://doi.org/10.4072/rbp.2010.3.07.

Bonaparte, J.F., Soares, M.B., Martinelli, A.G., 2013. Discoveries in the Late Triassic of Brazil improve knowledge on the origin of mammals. Hist. Nat. (Corr.) 2 (2), 5–30.

Brink, A.S., 1963. Two cynodonts from the ntawere formation in the Luangwa valley of northern rhodesia. Palaeontol. Afr. 8, 77–96.

Broom, B., 1905. On the use of the term Anomodontia. Records of the Albany Museum 1 (4), 266–269.

Cabreira, S.F., Kellner, A.W.A., Dias-da-Silva, S., Roberto-da-Silva, L., Bronzati, M., Marsola, J.C.A., Müller, R.T., Bittencourt, J.S., Batista, B.J., Raugust, T., Carrilho, R., Brodt, A., Langer, M.C., 2016. A unique Late Triassic dinosauromorph assemblage reveals dinosaur ancestral anatomy and diet. Curr. Biol. 26, 3090–3095. https://doi.org/10.1016/j.cub.2016.09.040.

Cabreira, S.F., Schultz, C.L., Bittencourt, J.S., Soares, M.B., Roberto-da-Silva, L., Langer, M.C., 2011. New stem-sauropodomorph (dinosauria, saurischia) from the triassic of Brazil. Naturwissenschaften 98, 1035–1040. https://doi.org/10.1007/s00114-011-0858-0.

Cabrera, A., 1943. El primer hallazgo de terápsidos en la Argentina, vol. 8. Notas del Museo de La Plata, pp. 317–331.

Chatterjee, S., 1982. A new cynodont reptile from the Triassic of India. J. Paleontol. 56 (1), 203–214.

Cope, E.D., 1869. Synopsis of the extinct batrachia, reptilia, and aves of north America. Part 1. Trans. Am. Phil. Soc. 14, 1–252.

Crompton, A.W., 1955. On some Triassic cynodonts from Tanganyika. Proc. Zool. Soc. Lond. 125, 617–669. https://doi.org/10.1111/j.1096-3642.1955.tb00620.x.

Crompton, A.W., 1972. Postcanine occlusion in cynodonts and tritylodontids. Bull. Br. Mus. (Nat. Hist.) Geol. 21, 29–71.

Crompton, A.W., Ellenberger, F., 1957. On a new cynodont from the Molteno beds and the origin of the tritylodontids. Ann. S. Afr. Mus. 44, 1–13.

Da-Rosa, A.A.S., 2015. Geological context of the dinosauriform-bearing outcrops from the Triassic of Southern Brazil. J. S. Am. Earth Sci. 61, 108–119. https://doi.org/10.1016/j.jsames.2014.10.008.

Da-Rosa, A.A.S., Faccini, U.F., 2005. Delimitação de blocos estruturais de diferentes escalas em sequências mesozoicas do Estado do Rio Grande do Sul: implicações bioestratigráficas. Gaea 1 (1), 16–23.

Dodson, P., 1971. Sedimentology and taphonomy of the oldman formation (campanian), dinosaur provincial park, alberta (Canada). Palaeogeogr. Palaeoclimatol. Palaeoecol. 10 (1), 21–74. https://doi.org/10.1016/0031-0182(71)90044-7.

Ezcurra, M.D., Fiorelli, L.E., Martinelli, A.G., Rocher, S., Baczko, M.B. von, Ezpeleta, M., Taborda, J.R.A., Hechenleitner, E.M., Trotteyn, M.J., Desojo, J.B., 2017. Deep faunistic turnovers preceded the rise of dinosaurs in southwestern Pangaea. Nat. Ecol. Evol. 1, 1477–1483. https://doi.org/10.1038/s41559-017-0305-5.

Fedorov, A.R., Beichel, J., Kalpathy-Cramer, M.S., Finet, J.-C., Fillion-Robin, S., Pujol, C., Bauer, D., Jennings, F., Fennessy, M., Sonka, J., Buatti, S., Aylward, J.V., Miller, J.V., Pieper, S., Kikinis, R., 2012. 3D Slicer as an image computing platform for the quantitative imaging network. Magn. Reson. Imag. 30 (9), 1323–1341. https://doi.org/10.1016/j.mri.2012.05.001.

Ferigolo, J., Langer, M.C., 2007. A late Triassic dinosauriform from south Brazil and the origin of the ornithischian predentary bone. Hist. Biol. 19 (1), 23–33. https://doi.org/10.1080/08912960600845767.

Flynn, J.J., Parrish, J.M., Rakotosamimanana, B., Ranivoharimanana, L., Simpson, W.F., Wyss, A.R., 2000. New traversodontid (synapsida, eucynodontia) from the triassic of Madagascar. J. Vertebr. Paleontol. 20 (3), 422–427. https://doi.org/10.1671/0272-4634(2000)020[0422:NTSEFT]2.0.CO;2.

Gauthier, J.A., 1986. Saurischian monophyly and the origin of birds. Memoir. Calif. Acad. Sci. 8, 1–55.

Goloboff, P.A., Farris, J.S., Nixon, K.C., 2008. TNT, a free program for phylogenetic analysis. Cladistics 24, 774–786. https://doi.org/10.1111/j.1096-0031.2008.00217.x.

Gow, C.E., Hancox, P.J., 1993. First complete skull of the late triassic *Scalenodontoides* (reptilia Cynodontia) from southern Africa. In: In: Lucas, S.G., Morales, M. (Eds.), The Nonmarine Triassic. New Mexico Museum of Natural History & Science Bulletin, vol. 3. pp. 161–168.

Griffin, C.T., Nesbitt, S.J., 2016. The femoral ontogeny and long bone histology of the Middle Triassic (?late Anisian) dinosauriform *Asilisaurus kongwe* and implications for the growth of early dinosaurs. J. Vertebr. Paleontol. 36 (3), e1111224. https://doi.org/10.1080/02724634.2016.1111224.

Hopson, J.A., 1990. Cladistic analysis of therapsid relationships. J. Vertebr. Paleontol. 10 (3), 28A.

Hopson, J.A., 2013. The traversodontid cynodont *Mandagomphodon hirschsoni* from the middle triassic of the ruhuhu valley, Tanzania. In: Kammerer, C.F., Angielczyk, K.D., Fröbisch, J. (Eds.), Early Evolutionary History of the Synapsida. Springer, Dordrecht, pp. 233–253.

Horn, B.L.D., Melo, T.M., Schultz, C.L., Philipp, R.P., Kloss, H.P., Goldberg, K., 2014. A new third-order sequence stratigraphic framework applied to the Triassic of the Paraná Basin, Rio Grande do Sul, Brazil, based on structural, stratigraphic and paleontological data. J. S. Am. Earth Sci. 55, 123–132. https://doi.org/10.1016/j.jsames.2014.07.007.

von Huene, F., 1928. Ein Cynodontier aus der Trias Brasiliens. Centralblatt für Mineralogie. Geol. Paläontol. Abt. B 251–270 1928.

von Huene, F., 1936. 2. Cynodontia. 93–159. Die fossilen Reptilien des sudamerikanischen Gondwanalandes. Ergebnisse der Sauriergrabungen in Sudbrasilien 1928–29. Franz F. Heine, Tubingen.

von Huene, F., 1946. Die grossen Stämme der Tetrapoden in den geologischen Zeiten. Biol. Zentralblatt 65, 268–275.

Huxley, T.H., 1859. Postscript to Murchinson, R. I.. On the sandstones of Morayshire (Elgin, &c.) containing reptilian remains; and their relations to the Old Red Sandstone

of that country. Q. J. Geol. Soc. Lond. 15, 138–152.
Kammerer, C.F., Flynn, J.J., Ranivoharimanana, L., Wyss, R.R., 2008. New material of *Menadon besairiei* (Cynodontia, Traversodontidae) from the triassic of Madagascar. J. Vertebr. Paleontol. 28 (2), 445–462. https://doi.org/10.1671/0272-4634(2008)28[445:NMOMBC]2.0.CO;2.
Kemp, T.S., 1982. Mammal-like Reptiles and the Origin of Mammals. Academic Press, London, pp. 1–363.
Kent, D.V., Malnis, P.M., Colombi, C.E., Alcober, O.A., Martínez, R.N., 2014. Age constraints on the dispersal of dinosaurs in the late triassic from magnetochronology of the los Colorados Formation (Argentina). Proc. Natl. Acad. Sci. Unit. States Am. 111 (22), 7958–7963. https://doi.org/10.1073/pnas.1402369111.
Kirkland, J., Bader, K., 2010. Insect trace fossils associated with *protoceratops* carcasses in the djadokhta formation (upper cretaceous), Mongolia. In: Ryan, M.J., Chinnery-Allgeier, B.J., Eberth, D.A. (Eds.), New Perspectives on Horned Dinosaurs: the Royal Tyrell Museum Ceratopsian Symposium. Indiana University Press, Bloomington, pp. 509–519.
Langer, M.C., Abdala, F., Richter, M., Benton, M.J., 1999. A sauropodomorph dinosaur from the upper triassic (carnian) of southern Brazil. Comptes Rendus de l'Académie des Sciences, Paris, Sciences de la Terre et des Planètes 329, 511–551.
Langer, M.C., Ferigolo, J., 2013. The late triassic dinosauromorph *Sacisaurus agudoensis* (caturrita formation; Rio Grande do Sul, Brazil): anatomy and affinities. Geol. Soc.London, Special Publ. 379, 353–392. https://doi.org/10.1144/SP379.16.
Langer, M.C., Ramezani, J., Da-Rosa, A.A.S., 2018. U-Pb age constraints on dinosaur rise from south Brazil. Gondwana Res. 57, 133–140. https://doi.org/10.1016/j.gr .2018.01.005.
Langer, M.C., Ribeiro, A.M., Schultz, C.L., Ferigolo, J., 2007. The continental tetrapod bearing Triassic of south Brazil. Bull. N. M.Mus. Nat. Hist. Sci. 41, 201–218.
Liparini, A., Oliveira, T.V., Pretto, F.A., Soares, M.B., Schultz, C.L., 2013. The lower jaw and dentition of the traversodontid *Exaeretodon riograndensis* Abdala, Barberena and dornelles, from the brazilian triassic (Santa Maria 2 sequence, *Hyperodapedon* assemblage zone). Alcheringa 37 (3), 331–337. https://doi.org/10.1080/03115518.2013.752607.
Liu, J., Abdala, F., 2014. Phylogeny and taxonomy of the Traversodontidae. In: Kammerer, C.F., Angielczyk, K.D., Fröbisch, J. (Eds.), Early Evolutionary History of the Synapsida. Springer, Dordrecht, pp. 255–279.
Liu, J., Olsen, P., 2010. The phylogenetic relationships of eucynodontia (amniota: synapsida). J. Mamm. Evol. 17 (3), 151–176. https://doi.org/10.1007/s10914-010-9136-8. doi: 10.1007/s10914-010-9136-8.
Marsicano, C.A., Irmis, R.B., Mancuso, A.C., Mundile, R., Chemale, F., 2016. The precise temporal calibration of dinosaur origins. Proc. Natl. Acad. Sci. Unit. States Am. 113 (3), 509–513. https://doi.org/10.1073/pnas.1512541112.
Martinelli, A.G., Kammerer, C.F., Melo, T.P., Paes Neto, V.D., Ribeiro, A.M., Da-Rosa, A.A.S., Schultz, C.L., Soares, M.B., 2017. The african cynodont *Aleodon* (Cynodontia, Probainognathia) in the triassic of southern Brazil and its biostratigraphic significance. PLoS One 12 (6), e0177948. https://doi.org/10.1371/journal.pone.0177948.
Martinelli, A.G., Soares, M.B., Schwanke, C., 2016. Two new cynodonts (therapsida) from the middle-early late triassic of Brazil and comments on south american probainognathians. PLoS One 11 (10), 1–43. https://doi.org/10.1371/journal.pone.0162945.
Martínez, R.N., Apaldetti, C., Alcober, O.A., Colombi, C.E., Sereno, P.C., Fernandez, E., Malnis, P.S., Correa, G.A., Abelin, D., 2013. Vertebrate succession in the Ischigualasto Formation. J. Vertebr. Paleontol. 32 (6), 10–30. https://doi.org/10.1080/02724634.2013.818546.
Martinez, R.N., Sereno, P.C., Alcober, O.A., Colombi, C.E., Renne, P.R., Montañez, I.P., Currie, B.S., 2011. A basal dinosaur from the dawn of the dinosaur era in southwestern pangaea. Science 331 (6014), 206–210. https://doi.org/10.1126/science.1198467.
Melo, T.P., Abdala, F., Soares, M.B., 2015. The malagasy cynodont *Menadon besairiei* (Cynodontia; Traversodontidae) in the middle–upper triassic of Brazil. J. Vertebr. Paleontol. 35 (6), e1002562. https://doi.org/10.1080/02724634.2014.1002562.
Melo, T.P., Martinelli, A.G., Soares, M.B., 2017. A new gomphodont cynodont (Traversodontidae) from the middle-late triassic Dinodontosaurus assemblage zone of the Santa Maria supersequence, Brazil. Palaeontology 60 (4), 571–582. https://doi.org/10.1111/pala.12302.
Müller, R.T., Araújo-Júnior, H.I., Aires, A.S.S., Roberto-da-Silva, L., Dias-da-Silva, S., 2015. Biogenic control on the origin of a vertebrate monotypic accumulation from the Late Triassic of southern Brazil. Geobios 48 (4), 331–340. https://doi.org/10.1016/j.geobios.2015.05.001.
Müller, R.T., Langer, M.C., Dias-da-Silva, S., 2017. Biostratigraphic significance of a new early sauropodomorph specimen from the Upper Triassic of southern Brazil. Hist. Biol. 29 (2), 187–202. https://doi.org/10.1080/08912963.2016.1144749.
Nesbitt, S.J., 2011. The early evolution of archosaurs: relationships and the origin of major clades. Bull. Am. Mus. Nat. Hist. 352, 1–292.
Nesbitt, S.J., Sidor, C.A., Irmis, R.B., Angielczyk, K.D.R., Smith, M.H., Tsuji, L.A., 2010. Ecologically distinct dinosaurian sister group shows early diversification of Ornithodira. Nature 464, 95–98. https://doi.org/10.1038/nature08718.
Oliveira, T.V., Schultz, C.L., Soares, M.B., 2007. O esqueleto pós-craniano de *Exaeretodon riograndensis* Abdala et al. (Cynodontia, Traversodontidae), Triássico do Brasil. Rev. Bras. Palaontol. 10 (2), 79–94.
Oliveira, T.V., Soares, M.B., Schultz, C.L., 2010. *Trucidocynodon riograndensis* gen. nov. et sp. nov. (Eucynodontia), a new cynodont from the Brazilian Upper Triassic (Santa Maria Formation). Zootaxa 2382, 1–71.
Osborn, H.F., 1903. On the primary division of the Reptilia into two sub-classes, Synapsida and Diapsida. Science 17 (424), 275–276.
Ottone, E.G., Monti, M., Marsicano, C.A., de la Fuente, M.S., Naipauer, M., Armstrong, R., Mancuso, A.C., 2014. A new Late Triassic age for the Puesto Viejo Group (San Rafael depocenter, Argentina): SHRIMP U–Pb zircon dating and biostratigraphic correlations across southern Gondwana. J. S. Am. Earth Sci. 56, 186–199. https://doi.org/10.1016/j.jsames.2014.08.008.
Owen, R., 1861. Palaeontology, or a Systematic Summary of Extinct Animals and Their Geological Relations. Adam and Charles Black, Edinburgh, pp. 1–463.
Paes Neto, V.D., Parkinson, A.H., Pretto, F.A., Soares, M.B., Schwanke, C., Schultz, C.L., Kellner, A.W., 2016. Oldest evidence of osteophagic behavior by insects from the Triassic of Brazil. Palaeogeogr. Palaeoclimatol. Palaeoecol. 453, 30–41. https://doi.org/10.1016/j.palaeo.2016.03.026.
Parrington, F.R., 1946. On the cranial anatomy of cynodonts. Proc. Zool. Soc. Lond. 116, 181–197. https://doi.org/10.1111/j.1096-3642.1946.tb00116.x.
Philipp, R.P., Closs, H., Schultz, C.L., Basei, M., Horn, B.L.D., Soares, M.B., 2013. Proveniência por U-Pb LA-ICP-MS em zircão detrítico e idade de deposição da Formação Santa Maria, Triássico da Bacia do Paraná, RS: evidências da estruturação do Arco do Rio Grande. In: VIII Symposium International on Tectonics and XIV Simpósio Nacional de Estudos Tectónicos, Anais, pp. 154–157.
Pirrone, C.A., Buatois, L.A., Bromley, R.G., 2014. Ichnotaxobases for bioerosion trace fossils in bones. J. Paleontol. 88 (1), 195–203. https://doi.org/10.1666/11-058.
Pretto, F.A., Langer, M.C., Schultz, C.L., 2015. New dinosaur remains from the late triassic of southern Brazil (Candelária sequence, *Hyperodapedon* assemblage zone). Alcheringa 39 (2), 264–273. https://doi.org/10.1080/03115518.2015.994114.
Ray, S., 2015. A new late triassic traversodontid cynodont (therapsida, eucynodontia) from India. J. Vertebr. Paleontol. 35 (3), e930472. https://doi.org/10.1080/02724634.2014.930472.
Reichel, M., Schultz, C.L., Soares, M.B., 2009. A new traversodontid cynodont (therapsida, eucynodontia) from the middle triassic Santa Maria formation of Rio Grande do Sul, Brazil. Palaeontology 52, 229–250. https://doi.org/10.1111/j.1475-4983.2008.00824.x.
Ribeiro, A.M., Abdala, F., Bertoni, R.S., 2011. Traversodontid cynodonts (Therapsida-Eucynodontia) from two upper Triassic localities of the Paraná Basin, southern Brazil. Ameghiniana 48 (4) R111.
Rogers, R.R., Arcucci, A.B., Abdala, F., Sereno, P.C., Forster, C.A., May, C.L., 2001. Paleoenvironment and taphonomy of the Chañares Formation tetrapod assemblage (middle triassic), northwestern Argentina: spectacular preservation in volcanogenic concretions. Palaios 16, 461–481. https://doi.org/10.1669/0883-1351(2001)016<0461:PATOTC>2.0.CO,2.
Romer, A.S., 1943. Recent mounts of fossil reptiles and amphibians in the Museum of Comparative Zoology. Bull. Mus. Comp. Zool. 92, 331–338.
Romer, A.S., 1967. The Chañares (Argentina) triassic reptile fauna. Iii. Two new gomphodonts, *Massetognathus pascuali* and *M. teruggii*. Breviora 264, 1–25.
Romer, A.S., 1972. The Chañares (Argentina) Triassic reptile fauna. XV. Further remains of the thecodonts *Lagerpeton* and *Lagosuchus*. Breviora 394, 1–7.
Schultz, C.L., Scherer, C.M.S., Barberena, M.C., 2000. Biostratigraphy of southern brazilian middle-upper triassic. Rev. Bras. Geociencias 30, 491–494.
Schultz, C.L., Langer, M.C., Montefeltro, F.C., 2016. A new rhynchosaur from south Brazil (Santa Maria Formation) and rhynchosaur diversity patterns across the Middle-Late Triassic boundary. Paläontol. Z. 90 (3), 593–609. https://doi.org/10.1007/s12542-016-0307-7.
Seeley, H.G., 1894. Researches on the structure, organization, and classification of the fossil Reptilia. - Part IX. Section 1. On the Therosuchia. Philos. Trans. R. Soc. London, Ser. A B 185, 987–1018. https://doi.org/10.1080/00222939408677718.
Sereno, P.C., Arcucci, A.B., 1994. Dinosaurian precursors from the Middle Triassic of Argentina: *Marasuchus lilloensis*, gen. nov. J. Vertebr. Paleontol. 14 (1), 53–73. https://doi.org/10.1080/02724634.1994.10011538.
Smith, R.M.H., Sidor, C.A., Angielczyk, K.D., Nesbitt, S.J., Tabor, N.J., 2018. Taphonomy and paleoenvironments of middle triassic bone accumulations in the lifua member of the Manda beds, songea group (ruhuhu basin), Tanzania. J. Vertebr. Paleontol. 37 (6), 65–79. https://doi.org/10.1080/02724634.2017.1415915.
Soares, M.B., Schultz, C.L., Horn, B.L.D., 2011. New information on *Riograndia guaibensis* Bonaparte, Ferigolo and Ribeiro, 2001 (eucynodontia, tritheledontidae) from the late triassic of southern Brazil: anatomical and biostratigraphic implications. An Acad. Bras Ciências 83 (1), 329–354. https://doi.org/10.1590/S0001-37652011000100021.
Sues, H.-D., Hopson, J.A., Shubin, N.H., 1992. Affinities of ?*Scalenodontoides plemmyridon* Hopson, 1984 (synapsida: Cynodontia) from the upper triassic of nova scotia. J. Vertebr. Paleontol. 12 (2), 168–171. https://doi.org/10.1080/02724634.1992.10011447.
Vallon, L.H., Rindsberg, A.K., Bromley, R.G., 2016. An updated classification of animal behaviour preserved in substrates. Geodin. Acta 28 (1–2), 5–20. https://doi.org/10.1080/09853111.2015.1065306.
Voorhies, M.R., 1969. Taphonomy and population dynamics of an early pliocene vertebrate fauna, knox country, Nebraska. Contrib. Geol. Spec. Pap. 8, 1–69. https://doi.org/10.2113/gsrocky.8.special_paper_1.1.
Xing, L., Parkinson, A.H., Ran, H., Pirrone, C.A., Roberts, E.M., Zhang, J., Burns, M.E., Wang, T., Choiniere, J., 2016. The earliest fossil evidence of bone boring by terrestrial invertebrates, examples from China and South Africa. Hist. Biol. 28 (8), 1108–1117. https://doi.org/10.1080/08912963.2015.1111884.
Xing, L., Roberts, E.M., Harris, J.D., Gingras, M.K., Ran, H., Zhang, J., Xu, X., Burns, M.E., Dong, Z., 2013. Novel insect traces on a dinosaur skeleton from the lower jurassic lufeng formation of China. Palaeogeogr. Palaeoclimatol. Palaeoecol. 388, 58–68. https://doi.org/10.1016/j.palaeo.2013.07.028.
Zerfass, H., Lavina, E.L., Schultz, C.L., Garcia, A.J.V., Faccini, U.F., Chemale Jr., F., 2003. Sequence stratigraphy of continental Triassic strata of Southernmost Brazil: a contribution to Southwestern Gondwana palaeogeography and paleoclimate. Sediment. Geol. 161, 85–105. https://doi.org/10.1016/S0037-0738(02)00397-4.

Supplementary Material

In this file, the following sections are included:

1. Table with the list of published species of the four Assemblage Zones (AZ) of Middle-Late Triassic of Southern Brazil;

2. Modifications in the data matrix of Liu and Abdala (2014) after modifications of Melo et al. (2015, 2017);

3. Additional figure, showing the general view of the sectors of Niemeyer site;

4. Table with specimens collected in Niemeyer site;

5. Table of measurements (in mm) of the specimens of *Siriusgnathus niemeyerorum* gen. et sp. nov.

Table S1. List of published species of the four Assemblage Zones (AZ) of Middle-Late Triassic of Southern Brazil

***Dinodontosaurus* AZ** Ladinian- early Carnian	**Cynodontia Owen, 1861** *Luangwa sudamericana* Abdala and Sa-Teixeira, 2004 *Massetognathus ochagaviae* Barberena, 1981 *Massetognathus pascuali* Romer, 1967 *Protuberum cabralensis* Reichel, Schultz and Soares, 2009 *Scalenodon ribeiroae* Melo, Martinelli and Soares, 2017 *Traversodon stahleckeri* von Huene, 1936 *Aleodon cromptoni* Martinelli, Kammerer, Melo, Paes-Neto, Ribeiro, Da-Rosa, Schultz and Soares, 2017 *Chiniquodon theotonicus* von Huene, 1936 *Bonacynodon schultzi* Martinelli, Soares and Schwanke, 2016 *Candelariodon barberenai* Oliveira, Schultz, Soares and Rodrigues, 2011 *Protheriodon estudianti* Bonaparte, Soares and Schultz, 2006 **Dicynodontia Owen, 1859** *Dinodontosaurus pedroanum* Tupi-Caldas 1936 *Stahleckeria potens* von Huene, 1935 **Archosauromorpha von Huene, 1946** *Brasinorhynchus mariantensis* Schultz, Langer and Montefeltro, 2016 *Archeopelta arborensis* Desojo, Ezcurra and Schultz, 2011 *Procerosuchus celer* von Huene, 1942 *Spondylosoma absconditum* von Huene, 1942 *Barberenasuchus brasiliensis* Mattar, 1987 *Chanaresuchus bonapartei* Romer, 1971 *Pagosvenator candelariensis* Lacerda, França and Schultz, 2018 *Prestosuchus chiniquensis* von Huene, 1942 *Decuriasuchus quartacolonia* França, Ferigolo and Langer, 2011 **Owenettidae Broom, 1939** *Candelaria barbouri* Price, 1947

***Santacruzodon* AZ** Early Carnian	**Cynodontia** *Massetognathus* sp. Romer, 1967 *Menadon besairiei* Flynn, Parrish, Rakotosamimanana, Ranivoharimanana, Simpson and Wyss, 2000 *Santacruzodon hopsoni* Abdala and Ribeiro, 2003 *Chiniquodon* sp. von Huene, 1936 *Santacruzgnathus abdalai* Martinelli, Soares and Schwanke, 2016 Dicynodontia indet. **Archosauromorpha** *Chanaresuchus bonapartei* Romer, 1971 *Dagasuchus santacruzensis* Lacerda, Schultz and Bertoni-Machado, 2015
***Hyperodapedon* AZ** Late Carnian	**Cynodontia** *Exaeretodon riograndensis* Abdala, Barberena and Dornelles, 2002 *Gomphodontosuchus brasiliensis* von Huene, 1929 *Therioherpeton cargnini* Bonaparte and Barberena, 1975 *Prozostrodon brasiliensis* Bonaparte and Barberena, 2001 *Charruodon tetracuspidatus* Abdala and Ribeiro, 2000 *Trucidocynodon riograndensis* Oliveira, Soares and Schultz, 2010 *Alemoatherium huebneri* Martinelli, Eltink, Da-Rosa and Langer, 2017 **Archosauromorpha** *Hyperodapedon mariensis* Tupi-Caldas, 1933 *Hyperodapedon huenei* Langer and Schultz, 2000 *Hyperodapedon sanjuanensis* Sill, 1970 *Teyumbaita sulcognathus* Azevedo and Schultz, 1987 *Proterochampsa nodosa* Barberena, 1982 *Rauisuchus tiradentis* von Huene, 1942 *Hoplitosuchus raui* von Huene, 1942 *Cerritosaurus binsfeldi* Price, 1946 *Rhadinosuchus gracilis* von Huene, 1942 *Aetobarbakinoides brasiliensis* Desojo, Ezcurra and Kischlat, 2012 *Aetosauroides scagliai* Casamiquela, 1960 *Polesinesuchus aurelioi* Roberto-da-Silva, Desojo, Cabreira, Aires, Müller, Pacheco and Dias-da-Silva, 2014

***Hyperodapedon* AZ** Late Carnian	*Ixalerpeton polesinensis* Cabreira, Kellner, Dias-da-Silva, Roberto-da-Silva, Bronzati, Marsola, Müller, Bittencourt, Batista, Raugust, Carrilho, Brodt and Langer, 2016 *Buriolestes schultzi* Cabreira, Kellner, Dias-da-Silva, Roberto-da-Silva, Bronzati, Marsola, Müller, Bittencourt, Batista, Raugust, Carrilho, Brodt and Langer, 2016 *Bagualosaurus agudoensis* Pretto, Langer and Schultz, 2018 *Pampadromaeus barberenai* Cabreira, Schultz, Bittencourt, Soares, Fortier, Roberto-da-Silva and Langer, 2011 *Saturnalia tupiniquim* Langer, Abdala, Richter and Benton , 1999 *Staurikosaurus pricei* Colbert, 1970 **Temnospondyli von Zittel, 1887** *Compsocerops* sp. Sengupta, 1995
***Riograndia* AZ** Norian	**Cynodontia** *Riograndia guaibensis* Bonaparte, Ferigolo and Ribeiro, 2001 *Brasilodon quadrangularis* Bonaparte, Martinelli, Schultz and Rubert, 2003 *Brasilitherium riograndensis* Bonaparte, Martinelli, Schultz and Rubert, 2003 *Irajatherium hernandezi* Martinelli, Bonaparte Schultz and Rubert, 2005 *Minicynodon maieri* Bonaparte, Schultz, Soares and Martinelli, 2010 *Botucaraitherium belarminoi* Soares, Martinelli and Oliveira, 2014 **Dicynodontia** *Jachaleria candelariensis* Araujo and Gonzaga, 1980 **Archosauromorpha** *Faxinalipterus minima* Bonaparte, Schultz and Soares, 2010 *Guaibasaurus candelariensis* Bonaparte, Ferigolo and Ribeiro, 1999 *Unaysaurus tolentinoi* Leal, Azevedo, Kellner and Da-Rosa, 2004 *Sacisaurus agudoensis* Ferigolo and Langer, 2007 **Procolophonidae Lydekker, 1889** *Soturnia caliodon* Cisneros and Schultz, 2003 **Lepidosauria Haeckel, 1866** *Cargninia enigmatica* Bonaparte, Schultz, Soares and Martinelli, 2010 *Clevosaurus riograndensis* Bonaparte and Sues, 2006

S2. Modifications in the data matrix of Liu and Abdala (2014) after modifications of Melo et al. (2015, 2017)

a) Changes in character-states of *Exaeretodon riograndensis*

Character 33. Coronoid process of the mandible: covers the last postcanine (0), does not cover (1).

State (?) is change to state (0). (Based in CAPPA/UFSM 0030, Müller et al., 2015)

Character 50. Number of cusps in the transverse crest of the upper postcanines: two (0), three or more (1). State (?) is change to state (-). (Based in CAPPA/UFSM 0030, Müller et al., 2015)

Character 77. The trochanter major position relative to the femoral head: distal (0), close, major part in same height. State (?) is change to state (1) (Based in CAPPA/UFSM 0033)

b) Changes in character-states of *Arctotraversodon*

Character 64. Size of the anterior cusps in the lower postcanines: labial lower than lingual (0), labial higher than lingual (1). State (2) is change to state (?) (Based in Hopson, 1984). State 2 is a typing error.

c) Codification for *Siriusgnathus niemeyerorum* gen. et sp. nov.

0?0?1111121101????10110021111122010?111101131012l??00?111121021111?????????
?

Figure S3. Additional figure

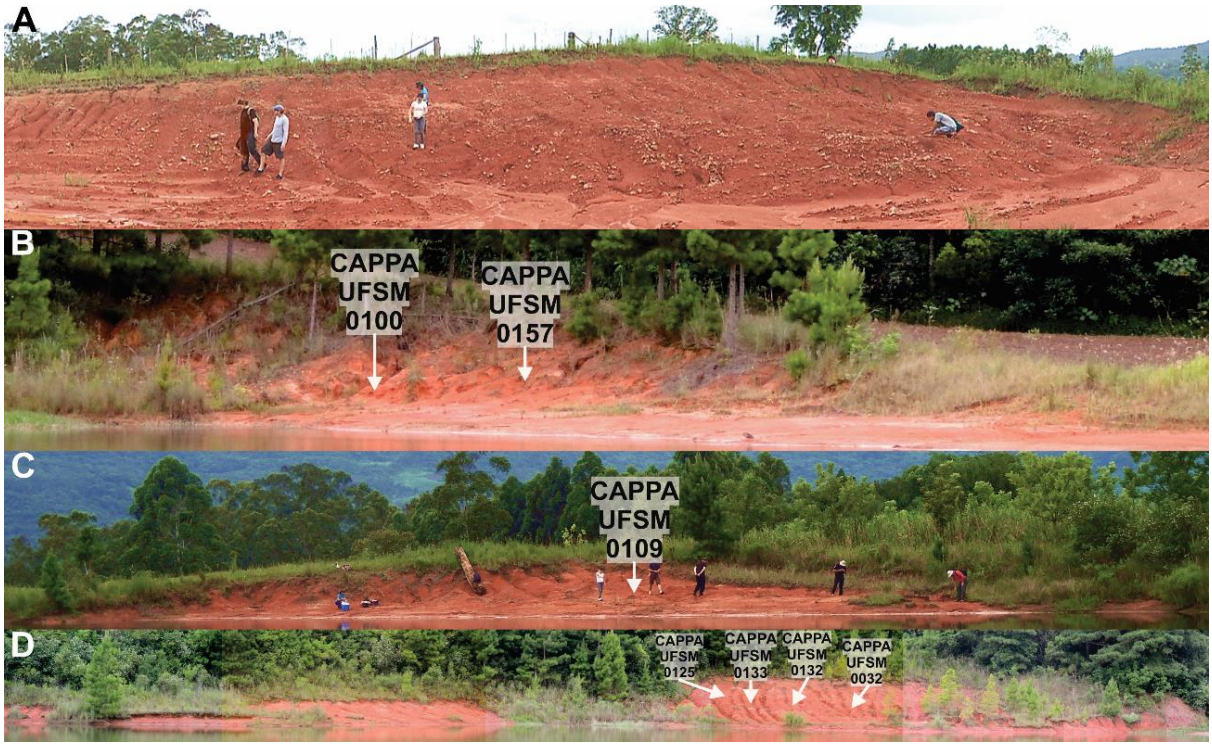

General view of the sectors of Niemeyer site indicating collection points of most complete specimens. **A**, sector 1; **B**, sector 2; **C** sector 3; **D**, sector 4.

Table S4. Specimens collected in Niemeyer site

Specimen: fossils recovered isolated at the outcrop; sample: employed to an agglomerated of fossils found at a same area; W/No: without number; n/a: data not avaliable.

Number	Taxonomy	Brief description	Sector
CAPPA/UFSM 0032	Traversodontidae	Skull with associated lower jaw	4
CAPPA/UFSM 0054	Traversodontidae	Right mandibular ramus	n/a
CAPPA/UFSM 0055	Traversodontidae	Left mandibular ramus	n/a
CAPPA/UFSM 0056	Traversodontidae	Right mandibular ramus	n/a
CAPPA/UFSM 0057	Traversodontidae	Right mandibular ramus	n/a
CAPPA/UFSM 0058	Traversodontidae	Lower jaw	n/a
CAPPA/UFSM 0059	Traversodontidae	Lower jaw	n/a
CAPPA/UFSM 0060	Traversodontidae	Right mandibular ramus	n/a
CAPPA/UFSM 0061	Traversodontidae	Lower jaw	n/a
CAPPA/UFSM 0062	Traversodontidae	Left mandibular ramus	n/a
CAPPA/UFSM 0063	Traversodontidae	Right mandibular ramus	n/a
CAPPA/UFSM 0064	Traversodontidae	Fragment of left maxilla	n/a
CAPPA/UFSM 0065	Traversodontidae	Lower jaw	n/a
CAPPA/UFSM 0066	Traversodontidae	Right mandibular ramus	n/a
CAPPA/UFSM 0067	Traversodontidae	Fragment of right maxilla	n/a
CAPPA/UFSM 0068	Traversodontidae	Left mandibular ramus	n/a
CAPPA/UFSM 0069	Traversodontidae	Right mandibular ramus	n/a
CAPPA/UFSM 0070	Traversodontidae	Lower jaw	n/a
CAPPA/UFSM 0071	Traversodontidae	Lower jaw	n/a
CAPPA/UFSM 0072	Traversodontidae	Right mandibular ramus	n/a
CAPPA/UFSM 0073	Traversodontidae	Left mandibular ramus	n/a
CAPPA/UFSM 0074	Traversodontidae	Posterior cranial portion	n/a
CAPPA/UFSM 0075	Traversodontidae	Right mandibular ramus	n/a
CAPPA/UFSM 0076	Traversodontidae	Left humerus	n/a
CAPPA/UFSM 0077	Traversodontidae	Right humerus	n/a
CAPPA/UFSM 0078	Traversodontidae	Right humerus	n/a
CAPPA/UFSM 0079	Traversodontidae	Right tibia	n/a
CAPPA/UFSM 0080	Traversodontidae	Left tibia	n/a
CAPPA/UFSM 0081	Traversodontidae	Right ulna	n/a
CAPPA/UFSM 0082	Cynodontia	Vertebra	n/a
CAPPA/UFSM 0083	Cynodontia	Vertebra	n/a
CAPPA/UFSM 0084	Cynodontia	Vertebra	n/a
CAPPA/UFSM 0085	Cynodontia	Vertebra	n/a
CAPPA/UFSM 0086	Cynodontia	Vertebra	n/a
CAPPA/UFSM 0087	Traversodontidae	Right mandibular ramus	n/a
CAPPA/UFSM 0088	Traversodontidae	Left mandibular ramus	n/a

CAPPA/UFSM 0089	Traversodontidae	Right mandibular ramus	n/a
CAPPA/UFSM 0090	Traversodontidae	Lower jaw	n/a
CAPPA/UFSM 0091	Traversodontidae	Lower jaw	n/a
CAPPA/UFSM 0092	Traversodontidae	Coracoid	n/a
CAPPA/UFSM 0093	Traversodontidae	Right mandibular ramus	n/a
CAPPA/UFSM 0094	Traversodontidae	Fragment of left maxilla	n/a
CAPPA/UFSM 0095	Traversodontidae	Left femur	n/a
CAPPA/UFSM 0096	Traversodontidae	Left femur	n/a
CAPPA/UFSM 0098	Traversodontidae	Left humerus	n/a
CAPPA/UFSM 0099	Probainognathia	Right humerus	n/a
CAPPA/UFSM 0100	Probainognathia	Skull with articulated lower jaw	2
CAPPA/UFSM 0101	Cynodontia	Fragment of right ilium	n/a
CAPPA/UFSM 0102	Traversodontidae	Right femur	n/a
CAPPA/UFSM 0103	Traversodontidae	Posterior cranial portion	n/a
CAPPA/UFSM 0104	Traversodontidae	Posterior cranial portion	n/a
CAPPA/UFSM 0105	Traversodontidae	Posterior cranial portion	n/a
CAPPA/UFSM 0106	Traversodontidae	Left humerus	n/a
CAPPA/UFSM 0107	Cynodontia	Right femur	n/a
CAPPA/UFSM 0108	Cynodontia	Six Phalanges	n/a
CAPPA/UFSM 0109	Traversodontidae	Skull with lower jaw articulated and associated postcranium	3
CAPPA/UFSM 0124	Traversodontidae	Skull	n/a
CAPPA/UFSM 0125	Traversodontidae	Skull with associated lower jaw	4
CAPPA/UFSM 0126	Traversodontidae	Left mandibular ramus	4
CAPPA/UFSM 0127	Traversodontidae	Left mandibular ramus	4
CAPPA/UFSM 0128	Traversodontidae	Left mandibular ramus	4
CAPPA/UFSM 0132	Archosauromorpha	Isolated tooth	4
CAPPA/UFSM 0133	Archosauromorpha	Vertebra	4
CAPPA/UFSM 0157	Archosauromorpha	Left femur	2
CAPPA/UFSM 0188	Cynodontia	Fragment of left ilium	n/a
CAPPA/UFSM 0190	Traversodontidae	Lower jaw	n/a
CAPPA/UFSM 0191	Traversodontidae	Skull	3
CAPPA/UFSM 0192	Traversodontidae	Skull with articulated lower jaw	3
CAPPA/UFSM 0193	Traversodontidae	Fragment of right maxilla	n/a
CAPPA/UFSM 0194	Traversodontidae	Right mandibular ramus	n/a
Sample 02	Traversodontidae	Right mandibular ramus	3
Sample 03	Traversodontidae	Fragment of left maxilla	3
Sample 03	Traversodontidae	Fragment of right maxilla	3
Sample 04	Traversodontidae	Vertebra	3
Sample 04	Traversodontidae	Vertebra	3
Sample 05	Traversodontidae	Left scapula	3
Sample F01	Cynodontia	Fragment of rib	3
Sample F01	Cynodontia	Fragment of rib	3

Sample F01	Cynodontia	Fragment of rib	3
Sample F01	Cynodontia	Fragment of rib	3
Sample F01	Traversodontidae	Left femur	3
Sample F01	Traversodontidae	Skull with associated lower jaw	3
Sample F02	Cynodontia	Fragment of rib	3
Sample F02	Cynodontia	Fragment of rib	3
Sample F02	Cynodontia	Fragment of rib	3
Sample F02	Cynodontia	Fragment of rib	3
Sample F02	Cynodontia	Fragment of rib	3
Sample F02	Cynodontia	Fragment of rib	3
Sample F02	Cynodontia	Fragment of rib	3
Sample F02	Cynodontia	Fragment of rib	3
Sample F02	Cynodontia	Fragment of rib	3
Sample F02	Cynodontia	Fragment of rib	3
Sample F02	Traversodontidae	Left mandibular ramus	3
Sample F02	Traversodontidae	Left mandibular ramus	3
Sample F03	Traversodontidae	Left mandibular ramus	3
Sample F03	Traversodontidae	Posterior cranial portion	3
Sample F03	Traversodontidae	Posterior cranial portion	3
Sample F03	Traversodontidae	Right femur	3
Sample F03	Traversodontidae	Right mandibular ramus	3
Sample F04	Cynodontia	Fragment of rib	3
Sample F04	Traversodontidae	Isolated tooth	3
Sample F04	Traversodontidae	Left femur	3
Sample F04	Traversodontidae	Posterior cranial portion	3
Sample F07	Traversodontidae	Right humerus	3
Sample F08	Traversodontidae	Isolated tooth	3
Sample F08	Traversodontidae	Isolated tooth	3
Sample F08	Traversodontidae	Isolated tooth	3
Sample F08	Traversodontidae	Right mandibular ramus	3
Sample F09	Traversodontidae	Fragment of left maxilla	3
Sample F09	Traversodontidae	Fragment of right maxilla	3
Sample F09	Traversodontidae	Posterior cranial portion	3
Sample F10	Traversodontidae	Right ulna	3
Sample F11	Cynodontia	Fragment of rib	3
Sample F13	Traversodontidae	Left ulna	3
Sample F15	Traversodontidae	Isolated tooth	3
Sample F19	Traversodontidae	Isolated tooth	3
Sample F21	Indet.	Humerus	3
Sample F23	Cynodontia	Fragment of rib	4
Sample F23	Cynodontia	Fragment of rib	4
Sample F23	Cynodontia	Fragment of rib	4
Sample F23	Cynodontia	Fragment of rib	4

Sample F23	Cynodontia	Fragment of rib	4
Sample F23	Traversodontidae	Isolated tooth	4
Sample F23	Traversodontidae	Isolated tooth	4
Sample F23	Traversodontidae	Posterior cranial portion	4
Sample F23	Traversodontidae	Posterior cranial portion	4
Sample F23	Cynodontia	Vertebra	4
Sample F25	Cynodontia	Fragment of rib	4
Sample F26	Traversodontidae	Left femur	4
Sample F27	Traversodontidae	Isolated tooth	4
Sample F27	Traversodontidae	Isolated tooth	4
Sample F27	Traversodontidae	Right femur	4
Sample F27	Cynodontia	Vertebra	4
Sample F28	Traversodontidae	Right mandibular ramus	4
Sample F29	Traversodontidae	Isolated tooth	4
Sample F29	Traversodontidae	Isolated tooth	4
Sample F29	Traversodontidae	Isolated tooth	4
Sample F29	Traversodontidae	Isolated tooth	4
Sample F29	Traversodontidae	Isolated tooth	4
Sample F29	Traversodontidae	Isolated tooth	4
Sample F29	Traversodontidae	Isolated tooth	4
Sample F29	Traversodontidae	Isolated tooth	4
Sample F30	Cynodontia	Fragment of rib	4
Sample F30	Traversodontidae	Isolated tooth	4
Sample W/No	Traversodontidae	Isolated tooth	n/a
Sample W/No	Traversodontidae	Left humerus	n/a
Sample W/No	Traversodontidae	Right femur	n/a
Sample W/No	Traversodontidae	Right ulna	n/a
Specimen W/No	Cynodontia	Fragment of rib	n/a
Specimen W/No	Cynodontia	Fragment of rib	n/a
Specimen W/No	Cynodontia	Fragment of rib	n/a
Specimen W/No	Cynodontia	Fragment of rib	n/a
Specimen W/No	Cynodontia	Fragment of rib	n/a
Specimen W/No	Cynodontia	Fragment of rib	n/a
Specimen W/No	Cynodontia	Fragment of rib	n/a
Specimen W/No	Cynodontia	Fragment of rib	n/a
Specimen W/No	Cynodontia	Fragment of rib	n/a
Specimen W/No	Cynodontia	Fragment of rib	n/a
Specimen W/No	Cynodontia	Fragment of rib	n/a
Specimen W/No	Cynodontia	Fragment of rib	n/a
Specimen W/No	Cynodontia	Fragment of rib	n/a
Specimen W/No	Traversodontidae	Isolated tooth	n/a
Specimen W/No	Traversodontidae	Isolated tooth	n/a
Specimen W/No	Traversodontidae	Isolated tooth	n/a
Specimen W/No	Traversodontidae	Isolated tooth	n/a

Specimen W/No	Traversodontidae	Isolated tooth	n/a
Specimen W/No	Traversodontidae	Isolated tooth	n/a
Specimen W/No	Traversodontidae	Isolated tooth	n/a
Specimen W/No	Traversodontidae	Isolated tooth	n/a
Specimen W/No	Traversodontidae	Isolated tooth	n/a
Specimen W/No	Traversodontidae	Isolated tooth	n/a
Specimen W/No	Traversodontidae	Isolated tooth	n/a
Specimen W/No	Traversodontidae	Isolated tooth	n/a
Specimen W/No	Traversodontidae	Isolated tooth	n/a
Specimen W/No	Traversodontidae	Isolated tooth	n/a
Specimen W/No	Traversodontidae	Isolated tooth	n/a
Specimen W/No	Traversodontidae	Isolated tooth	n/a
Specimen W/No	Traversodontidae	Isolated tooth	n/a
Specimen W/No	Traversodontidae	Isolated tooth	n/a
Specimen W/No	Traversodontidae	Isolated tooth	n/a
Specimen W/No	Traversodontidae	Isolated tooth	n/a
Specimen W/No	Cynodontia	Vertebra	n/a
Specimen W/No	Cynodontia	Vertebra	n/a
Specimen W/No	Cynodontia	Vertebra	n/a
Specimen W/No	Cynodontia	Vertebra	n/a

Table S5. Measurements (in mm) of the specimens of *Siriusgnathus niemeyerorum* gen. et sp. nov.

	CAPPA/UFSM			
	0109	**0032**	**0125**	**0124**
Basal length of the skull	255.0*	220.4#	176.6	125.0*
Rostrum length	-	78.8#	44,8	46.5
Palate length	-	96.5	72.0	52.0*
Upper postcanine tooth row length	-	80.3	69.3	50.9
Total temporal region length	104.5	80.8#	67.8	40.0*
Maximum skull width	250.4	207.7#	122.4	-
Maximum height of the zygomatic arch	87.2	66.5	60.8	-
Orbital length	34.0	28.8	35.0	22.8*
Interorbital distance	57.8*	52.2	34.7	31.0*
Basicranial length	44.8	41.7	31.0	-
Height of the occipital plate	81.4	87.6	60.4	-
Occipital plate width	144.1	108.8	72.0	-
Dentary height	146.0*	141.0	110.0*	-
Dentary length;	185.0*	192.0*	155.0*	-
Lower postcanine row length	106.0*	100.5	77.8	-

* Estimated because of incompleteness.
# Estimated because of taphonomic deformation.

References

Hopson, J.A., 1984. Late Triassic traversodont cynodonts from Nova Scotia and southern Africa. Palaeontologia Africana, 25, 181–201.

Liu, J., Abdala, F., 2014. Phylogeny and Taxonomy of the Traversodontidae. In: Kammerer, C.F., Angielczyk, K.D., Fröbisch, J. (Eds.), Early Evolutionary History of the Synapsida, Springer, Dordrecht, 255-279.

Melo, T.P., Abdala, F., Soares, M.B., 2015. The Malagasy cynodont *Menadon besairiei* (Cynodontia; Traversodontidae) in the Middle–Upper Triassic of Brazil. Journal of Vertebrate Paleontology, 35(6), e1002562. doi: 10.1080/02724634.2014.1002562

Melo, T.P., Martinelli, A.G., Soares, M.B., 2017. A new gomphodont cynodont (Traversodontidae) from the Middle-Late Triassic Dinodontosaurus Assemblage Zone of the Santa Maria Supersequence, Brazil. Palaeontology, 60(4), 571–582. doi: 10.1111/pala.12302

Müller, R.T., Araújo-Júnior, H.I., Aires, A.S.S., Roberto-da-Silva, L., Dias-da-Silva, S., 2015a. Biogenic control on the origin of a vertebrate monotypic accumulation from the Late Triassic of southern Brazil. Geobios, 48(4), 331-340. doi: 10.1016/j.geobios.2015.05.001

Supplementary Material 6

PDF file of the 3D model of the holotype (CAPPA/UFSM 0032) of *Siriusgnathus niemeyerorum*. https://doi.org/10.1016/j.jsames.2018.08.016.

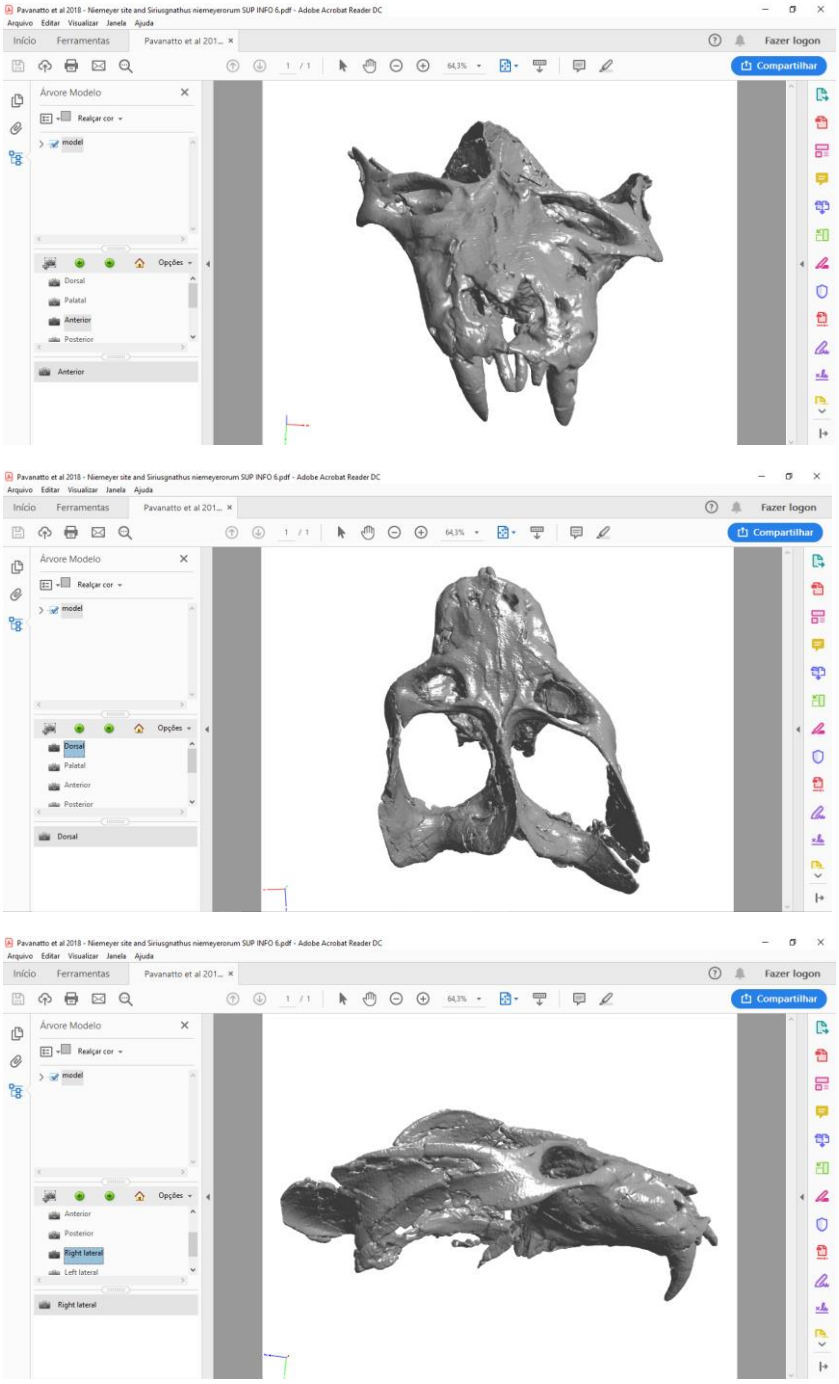

4 ARTIGO 2

O Artigo 2 intitulado: "*Virtual reconstruction of cranial endocasts of traversodontid cynodonts (Eucynodontia: Gomphodontia) from the Upper Triassic of southern Brazil*", está aceito para publicação pelo periódico *Journal of Morphology* e está formatado de acordo com as normas do mesmo.

Journal of Morphology

Decision Letter (JMOR-19-0075.R1)

From: starck@jmorph.com

To: anepavanatto@hotmail.com, leonardokerber@gmail.com, paleosp@gmail.com

CC:

Subject: Journal of Morphology - Decision on Manuscript ID JMOR-19-0075.R1

Body: 10-Jun-2019

Dear Miss Pavanatto,

I am pleased to inform you that your revised manuscript entitled, Virtual reconstruction of cranial endocasts of traversodontid cynodonts (Eucynodontia: Gomphodontia) from the Upper Triassic of southern Brazil, has now been accepted for publication in the Journal of Morphology.

Your manuscript will now be sent to the publisher. You will receive page proofs from the production department due course.

Your article cannot be published until the publisher has received the appropriate signed license agreement. Within the next few weeks the corresponding author will receive an email from Wiley's Author Services system which will ask them to log in and will present them with the appropriate license for completion.

Please feel free to contact Ms. Strauss at jmorph@wiley.com if you have any questions about the publication process.

Thank you for submitting your work to the Journal of Morphology. I look forward to seeing more of your work in the future.

Sincerely,

Prof. Matthias Starck
Editor-in-Chief, Journal of Morphology
starck@jmorph.com

P. S. Bring your research to life by creating a video abstract for your article! Wiley partners with Research Square to offer a service of professionally produced video abstracts. Learn more about video abstracts at www.wileyauthors.com/videoabstracts and purchase one for your article at https://www.researchsquare.com/wiley/ or through your Author Services Dashboard. If you have any questions, please direct them to videoabstracts@wiley.com.

Date Sent: 10-Jun-2019

Virtual reconstruction of cranial endocasts of traversodontid cynodonts (Eucynodontia: Gomphodontia) from the Upper Triassic of southern Brazil

Virtual brain endocasts of traversodontid cynodonts

Ane Elise Branco Pavanatto[1], Leonardo Kerber[1,2], Sérgio Dias-da-Silva[1,2]

[1] Programa de Pós-Graduação em Biodiversidade Animal, Centro de Ciências Naturais e Exatas, Universidade Federal de Santa Maria, Santa Maria, Brazil

[2] Centro de Apoio à Pesquisa Paleontológica da Quarta Colônia, Centro de Ciências Naturais e Exatas, Universidade Federal de Santa Maria, São João do Polêsine, Brazil

Abstract

The brain endocasts of the Late Triassic (Carnian) traversodontids (Eucynodontia: Gomphodontia) *Siriusgnathus niemeyerorum* and *Exaeretodon riograndensis* from southern Brazil are described for the first time based on virtual models generated using computed tomography scan data. Their skull anatomy resembles that of other non-mammaliaform cynodonts, showing an endocranial cavity that is not fully ossified. A 'V-shaped' orbitosphenoid, neither fully developed nor ossified is present in *E. riograndensis*. The nasal cavity is confluent with the encephalic cavity. Thus, the anterior limit of the olfactory bulbs is not definite. The brain endocast is elongated, being narrow anteriorly and wide posteriorly, with the maximum width at the parafloccular cast. The olfactory bulbs do not present a clear division between their counterparts, due to the absence of a longitudinal sulcus. A longitudinal sulcus in the forebrain delimiting the cerebral hemispheres, the pineal tube, and the parietal foramen are absent in both taxa. The large and well developed unossified zone is partially separated from the remaining endocast by a notch formed by the supraoccipital. The encephalization quotients, as well as the endocranial volume/body mass relationships of *S. niemeyerorum* and *E. riograndensis* are within the range expected for non-mammaliaform Therapsida.

Keywords: *Exaeretodon*; *Siriusgnathus*; Cynognathia; Endocranial morphology; CT-Scan

1. INTRODUCTION

The study of brain endocasts of non-mammaliaform cynodonts is a unique opportunity to investigate both morphological and evolutionary changes in the endocranial anatomy linked to the emergence of the mammaliaform brain, which is remarkably large in comparison to other synapsids. This is derived from an increase in encephalization and the origin and growth of the cerebral neocortex, one of the most striking traits and biologically significant features of mammals (Kemp, 2009). A well-developed encephalon is correlated with more elaborate motor control and improved sensory systems (Kielan-Jaworowska, Cifelli, & Luo, 2004; Rowe, Macrini, & Luo, 2011). The enlargement of the mammalian brain could be correlated with the improvement of both auditory and olfactory senses related to the occupation of nocturnal niches by early mammals (Jerison, 1973). Another hypothesis correlates brain enlargement with the increase in metabolic rate and development of endothermy (Allman, 1990; Kemp, 2006; Quiroga, 1980b). In comparison, the brain of non-mammaliaform cynodonts is conspicuously narrow; the olfactory bulbs are poorly developed, without a clear division; and the braincase is not fully ossified (Hopson, 1979; Kielan-Jaworowska et al., 2004; Rowe et al., 2011).

Traversodontidae is a clade of herbivorous/omnivorous non-mammaliaform gomphodont cynodonts from the Middle–Late Triassic, characterized by the presence of labiolingually expanded upper postcanine teeth with a deep occlusal basin (Abdala & Gaetano, 2018; Kammerer, Flynn, Ranivoharimanana, & Wyss, 2008; Liu & Abdala, 2014). The oldest records of traversodontids are from the Anisian of Africa (Brink, 1963; Crompton, 1955) and South America (Bonaparte, 1966b, 1969; but see Ottone et al., 2014, for other interpretations of the age of the Argentinean Puesto Viejo fauna, traditionally considered Anisian). The clade reached a cosmopolitan distribution during the Ladinian to Carnian, becoming the most diverse

clade of Triassic non-mammaliaform cynodonts (Abdala & Ribeiro, 2010; Liu & Abdala, 2014).

Middle-Upper Triassic beds from southern Brazil record abundance of traversodontids in the majority of the known Assemblage Zones (AZ): *Luangwa sudamericana*, *Massetognathus ochagaviae*, *Protuberum cabralense*, *Traversodon stahleckeri*, and *Scalenodon ribeiroae* from the *Dinodontosaurus* AZ (Pinheiros-Chiniquá Sequence, Santa Maria Supersequence, Ladinian-lower Carnian; Horn et al., 2014; Liu & Abdala, 2014; Melo, Martinelli, & Soares, 2017); *Menadon besairiei*, *Santacruzodon hopsoni*, and *Massetognathus ochagaviae* from the *Santacruzodon* AZ (Santa Cruz Sequence, Santa Maria Supersequence, lower Carnian; Horn et al., 2014; Liu & Abdala, 2014; Melo, Abdala, & Soares, 2015; Philipp et al., 2013; Schmitt, Martinelli, Melo, & Soares, 2019); and *Gomphodontosuchus brasiliensis* and *Exaeretodon riograndensis* from the *Hyperodapedon* AZ (Candelária Sequence, Santa Maria Supersequence, upper Carnian; Horn et al., 2014; Liu & Abdala, 2014). Recently, *Siriusgnathus niemeyerorum* was described based on specimens found in a single outcrop, which it's the AZ of which is still uncertain (Pavanatto et al., 2018).

The external morphology of the skull of several traversodontid cynodonts is well known, with detailed descriptions published over the last few years (e.g., Kammerer et al., 2008; Kammerer, Flynn, Ranivoharimanana, & Wyss, 2012; Melo et al., 2017, 2015). In comparison, their endocranial morphology has received less attention. Bonaparte (1966a) introduced the first skull endocast description of a traversodontid cynodont – *Exaeretodon argentinus* – based on natural endocasts. The same contribution also described the nasal cavities and presented some considerations about the inner ear. Quiroga (1979a) described the endocranial morphology of *Massetognathus* sp., based upon a natural endocast, and some quantitative data (i.e., endocast volume, body mass, and encephalization quotient estimation). In another contribution, Quiroga (1979b) also described the morphology of the inner ear of the same specimen, and a year later,

Quiroga (1980a) briefly described the endocast of *Andescynodon mendozensis* and *Massetognathus pascuali* and performed a quantitative analysis, also based on natural endocasts. Recently, Crompton, Musinsky, Rougier, Bhullar, & Miyamae (2018), presented and discussed some aspects of the endocranial cavity of *Massetognathus pascuali*, based on computed tomography (CT)-scan data.

In the last few years, several studies have been carried out, improving the knowledge of the endocranial morphology of several non-mammaliaform therapsids through digital reconstruction of the endocast as follows: the biarmosuchian *Lemurosaurus* (Benoit, Fernandez, Manger, & Rubidge, 2017); the dinocephalian *Moschops* (Benoit, Manger, Norton, Fernandez, & Rubidge, 2017); the dicynodonts *Pristerodon* (Laaß, 2015), *Diictodon* (Laaß, Schillinger, & Kaestner, 2017), *Kawingasaurus* (Laaß & Kaestner, 2017), and *Niassodon* (Castanhinha et al., 2013); the gorgonopsian *Cynariops* (Bendel, Kammerer, Kardjilov, Fernandez, & Fröbisch, 2018); the early non-mammaliaform cynodont *Galesaurus* (Pusch, Kammerer, & Fröbisch, 2019), and the prozostrodontid non-mammaliaform cynodonts *Riograndia* (Rodrigues et al., 2018) and *Brasilodon* (Rodrigues, Ruf, & Schultz, 2014).

Here, we present the first virtual reconstructions of the brain endocast of two traversodontids from the Brazilian Upper Triassic, *Siriusgnathus niemeyerorum* and *Exaeretodon riograndensis*.

2. MATERIAL AND METHODS

2.1 Specimens

For this study, we selected the best-preserved traversodontid specimens from Brazilian Upper Triassic housed at the Centro de Apoio à Pesquisa Paleontológica da Quarta Colônia – Universidade Federal de Santa Maria (CAPPA/UFSM).

CAPPA/UFSM 0032, the holotype of *Siriusgnathus niemeyerorum*, comes from the Niemeyer site, Agudo, Rio Grande do Sul (Upper Triassic, Candelária Sequence of Santa Maria Supersequence; Pavanatto et al., 2018). It comprises an almost complete and well-preserved skull with a basal skull length of 220.4 mm. Taphonomic compression slightly distorts this specimen. In ventral view, the posterior border of the premaxilla is broken, and the specimen presents several fractures over its entire length, mainly in the zygomatic arches and lateral wall of the braincase (Figure 1a,b).

CAPPA/UFSM 0030 and CAPPA/UFSM 0227, both assigned to *Exaeretodon riograndensis*, were collected at the Janner site, Agudo, Rio Grande do Sul (*Hyperodapedon* Assemblage Zone, Upper Triassic, Candelária Sequence of the Santa Maria Supersequence; Horn et al., 2014). CAPPA/UFSM 0030 (Figure 1c, d) comprises a skull in which the premaxilla is missing, with a basal skull length of 224.9 mm. The ventral surface is partially covered by concretion, mainly in the basicranial region. The lateral wall of the braincase presents several fractures. The ventral border of the left pterygoparoccipital foramen is broken. Internally, the specimen has a massive infilling of concretion, occupying a large portion of the endocranial space (Figure 2d-f).

CAPPA/UFSM 0227 is a complete and quite well-preserved skull with the lower jaw in occlusion, with a basal skull length of 168.2 mm. Despite its good preservation, CAPPA/UFSM

0227 also presents fractures in the rostral region. A portion of the premaxilla and the anteriormost part of the nasals (bordering the nasal opening) are missing. At the middle point of the right zygomatic arch there is a dorsoventral fracture. The cranial process of the right squamosal is also fractured, and part of its middle region is lost. On the lateral wall of the braincase, the anterior portion of the right prootic is missing. In the left side, there is also a missing area in the proximal region, hampering the segmentation of this part of the endocranial cavity. In ventral view, the pterygoid is broken at the left side, close to the parasphenoid. In the basicranium, both the *fenestra ovalis* and jugular foramen are filled with concretion, and the edges of the right jugular foramen are badly preserved (Figure 1e,f).

- Insert Figure 1 around here

2.2 X-ray computed tomography and 3D-modeling of the brain endocast

The holotype of *Siriusgnathus niemeyerorum* (CAPPA/UFSM 0032) and two specimens of *Exaeretodon riograndensis* (CAPPA/UFSM 0030 and 0227) were scanned in a medical clinic, using a Philips Brilliance 16-Slice CT Scanner and a Philips Brilliance 64-Slice CT Scanner (Table 1). The raw scan data were exported from the scanner computer in DICOM format. The software 3D Slicer 4.8 (Fedorov et al., 2012) was employed to segment the endocranial cavity of the specimens and generate 3D models. The slices were analyzed individually, and the endocranial cavity was manually filled. As there is no evident anterior limit of the olfactory bulbs, a flat cut was used to delimitate the anterior end of the endocast (see Balanoff et al., 2016). The ventral limit of the anteriormost region of the endocast was estimated based on the dorsal limit of the interorbital vacuity. For CAPPA/UFSM 0030 and 0227, the ventral limit of the anterior region of the endocast was delimited based on the presence

of an ossified orbitosphenoid, not preserved in CAPPA/UFSM 0032. The software Geomagic Studio was used to increase the quality of the endocasts by removing imperfections generated during the segmentation. After these procedures, the resulting files (.STL) were imported to Design Spark Mechanical 2.0, colored, and exported to PDF format.

- Insert Table 1 around here

2.3 Body mass estimation and encephalization quotients

The quantifier tools of 3D Slicer 4.8 provided the volume and dimensions of the endocasts. In addition, in order to test the accuracy of these data, we also prototyped the 3D models with a 3D printer and checked the measurements. We considered the volume of the whole endocast, without the volume of the cavum epiptericum, and including and excluding the olfactory bulbs, following Benoit, Fernandez, et al., (2017) and Benoit, Manger, et al., (2017), because olfactory bulbs are not usually fully ossified in non-mammaliaform therapsids and, consequently, the precise volume of this region is uncertain. Comparison of endocranial volumes from this study with previously published ones employed the encephalization quotient (EQ) as a way of comparing the endocranial volume between taxa with different body masses (Hurlburt, Ridgely, & Witmer, 2013; Jerison, 1973; Manger, 2006). The EQ is defined as the ratio between the endocranial volume (EV) of a given animal (a fossil taxon) and the expected endocranial volume for an animal with similar body mass (BM) (Jerison, 1973). Following Benoit, Manger, et al., (2017), we used three versions of the equation to calculate the EQ, as follows:

The Jerison EQ, frequently used in previous studies (Jerison, 1973).

$EQ_1 = EV \div (0.12 \times BM^{2/3})$.

The Manger EQ, derived from the Eisenberg (1981) EQ, but considered mathematically more accurate, as it includes a larger amount of taxa to calculate the regression equation, and those taxa considered as outliers (such as cetaceans and primates) are excluded (Manger, 2006).

$$EQ_2 = EV \div (0.0535 \times BM^{0.7294})$$

The EQ of Hurlburt et al. (2013), adapted to compare endocast volumes with smaller values. This EQ usually provides higher values, in comparison to the abovementioned EQ equations, because of the taxa used in the calculation of its regression equation, the data sample being composed of extant non-avian reptiles and birds (Hurlburt et al., 2013).

$$EQ_3 = EV \div (0.0155 \times BM^{0.553})$$

Estimation of body mass in extinct taxa can be problematic, mostly because the frequent incompleteness of specimens. Accordingly, we used three different equations to calculate body mass, based on skull length (SL).

Quiroga (1980b, 1984) developed an equation in order to obtain body mass estimation from skull length, based on data from cynodonts and other therapsids.

$$BMa = 2.7 \times (SL \div 10)^3$$

Hu, Meng, Wang, & Li (2005) used an equation for body mass estimation derived from Van Valkenburgh (1990), for which the data sample is composed of extant mammals.

$$BMb = 10^{(3.13 \times \log(SL) - 5.59)} \times 1000$$

Castanhinha et al. (2013) estimated the body mass based upon an indirect estimation of femoral length from skull length. Their equation is derived from the equation of Campione & Evans (2012), which is calculated using the estimated femoral length. Sookias, Butler, & Benson (2012) demonstrated a strong correlation between the skull and femoral lengths in synapsids.

$$BMc = 10^{(2.9307 \times (\log(0.6908 \times (SL) + 4.3337)) - 2.1677)}$$

In order to calculate the EQs, we employed the average of the three body mass equations. To standardize these data, for comparison purposes, we accessed published values of skull lengths and endocast volumes for other therapsids and recalculated body masses and EQs. When the skull length was not available, we considered body mass estimates from previous studies in the literature (e.g. *Thrinaxodon*, Rowe et al., 2011 and *Diademodon*, Jerison, 1973). For those small cynodonts (i.e., *Riograndia* and *Brasilodon*), mammaliaforms and mammals, we also employed body mass values from the literature (see Supporting Information Table S1).

3. RESULTS

3.1 Description of the endocranial cavity and brain endocast of *S. niemeyerorum* and *E. riograndensis*

Encephalic cavity

The brain endocast is dorsally encapsulated anteriorly by the frontals, and the parietals form the dorsal roof of the midbrain. The nasal cavity and the brain cavity are confluent, without a clear separation between them, differing from mammals, which possess an ossified cribriform plate (Novacek, 1993) (Figure 2c,f,i). Thus, the anterior limit of the olfactory bulbs is not clear in the reconstruction. Anteroventrally, the forebrain and bulbs were possibly delimited by the orbitosphenoid. This bone is present in specimens of *E. riograndensis* analyzed here (CAPPA/UFSM 0030 and 0227) (Figure 2), but is neither fully developed nor fully ossified and does not form either a complete lateral wall or a floor to the anterior region of the braincase (Figure 2g). In CAPPA/UFSM 0030, the orbitosphenoid is better preserved, and it is V-shaped in cross-section, with a prominent ventral keel, but it is not clear if both orbitosphenoids are

fused (Figure 2d,e). On the other hand, the analyzed specimen of *S. niemeyerorum* (CAPPA/UFSM 0032) does not show any evidence of orbitosphenoid bones (Figure 2a). In all specimens, the orbital vacuity is large, without clear evidence of an interorbital septum. *S. niemeyerorum* (CAPPA/UFSM 0032) possesses a ridge, probably formed by the palatine bone at the floor of the interorbital vacuity (Figure 2a).

The posterior ventral limit (posterior to the interorbital vacuity) mainly comprises the parasphenoid, the basisphenoid, and the basioccipital (which is fused with the basisphenoid in all specimens). The prootic forms the floor of the cavum epiptericum. The lateral wall (posterior to the interorbital vacuity) is composed dorsally by the parietal, anteroventrally by the epipterygoid, and posteroventrally by the prootic. The area of the unossified zone is enclosed dorsolaterally by the parietals, posteriorly by the interparietal, and posteroventrally by the supraoccipital. In *E. riograndensis* (CAPPA/UFSM 0227), the supraoccipital forms a notch ventrally, which partially separates the unossified zone from the remaining endocast (Figure 2i). In CAPPA/UFSM 0032, this notch is apparently formed by the supraoccipital, but it is much less developed in comparison (Figure 2c). In *E. riograndensis* (CAPPA/UFSM 0030), this feature could not be observed because of the poor preservation of the specimen (Figure 2f). CAPPA/UFSM 0227 (*E. riograndensis*) shows a longitudinal groove on the ventral surface of the parietals that extends approximately from the posterior limit of the interorbital vacuity up to the unossified zone (Figure 2h).

- Insert Figure 2 around here

Endocast morphology

General aspects

The brain endocast of both *S. niemeyerorum* and *E. riograndensis* are anteroposteriorly elongated, anteriorly narrow, and posteriorly wide. The maximum width/length ratio is ~0.32 in CAPPA/UFSM 0032 (*S. niemeyerorum*) and CAPPA/UFSM 0030 (*E. riograndensis*), and ~0.39 in CAPPA/UFSM 0227 (*E. riograndensis*). The endocast increases gradually in size, posterior to the level of the orbital vacuity, reaching its maximum width at the level of the paraflocculars cast (Table 2). The endocast widens posterior to the interorbital vacuity, reaching its maximum height in the hindbrain region. In lateral view, the endocast is thinner anteriorly, with the region of the olfactory bulbs poorly differentiated from the rest of the cavity.

Olfactory bulbs and the olfactory tracts

In *S. niemeyerorum* (CAPPA/UFSM 0227) and *E. riograndensis* (CAPPA/UFSM 0030, 0032), as previously mentioned, both the anterior limit and the precise shape of the olfactory bulbs are not clear, because of the absence of full ossification in this region, mainly in the ventral portion, where a fully ossified anterior floor is absent. A dorsal longitudinal sulcus is also absent. Consequently, the olfactory bulbs cannot be differentiated from each other (Figure 3). Likewise, the boundary between the olfactory bulbs and the olfactory tract is not clear (Figure 3). In *E. riograndensis* (CAPPA/UFSM 0030 and 0227), the olfactory bulbs and tracts are more robust in comparison to *S. niemeyerorum* (CAPPA/UFSM 0032) (Figure 3a,c,d). Also, in *E. riograndensis* (CAPPA/UFSM 0030 and 0227), there is a slight constriction, after the presumed region of the olfactory bulbs, which may indicate the boundary between the olfactory bulbs and the tract with the forebrain (Figure 3c,e).

Forebrain

The forebrain in elongated and slightly narrower than the region of the olfactory bulbs in all specimens (Figure 3a,c,e). As for the olfactory bulbs and the olfactory tracts, the forebrain is more robust in *E. riograndensis* (CAPPA/UFSM 0030 and 0227) than in *S. niemeyerorum* (CAPPA/UFSM 0032). None of the specimens exhibit the longitudinal sulcus in the forebrain that would allow delimitation of the cerebral hemispheres (Figure 3a,c,e). The pineal tube and the parietal foramen are also absent in all specimens (Figures 2c,f,i, 3 and 4).

- Insert Table 2 around here

Midbrain

The midbrain comprises an unossified zone dorsally and the hypophyseal cast ventrally (Figure 3). Besides the unossified zone, there is no evidence of other structures, such as the anterior and posterior *colliculi*, on the dorsal surface in any of the specimens. The unossified zone is large and well developed in both species. In the specimen CAPPA/UFSM 0030 (*E. riograndensis*), the posterior limit of the unossified zone is not definite because the matrix inside the endocranial cavity has a similar density to the bone (Figure 2f). However, the unossified zone of CAPPA/UFSM 0030 is more developed in width and height than in CAPPA/UFSM 0032 (*S. niemeyerorum*) and 0227 (*E. riograndensis*) (Figure 4). In *S. niemeyerorum* (CAPPA/UFSM 0032), the unossified zone is placed more anteriorly, near to the forebrain (Figure 4a,b), than in *E. riograndensis* (CAPPA/UFSM 0030 and 0227), in which the unossified zone is more posteriorly placed, close to the level of the paraflocular cast (Figure 4c-f). The hypophyseal cast is well delimited and developed in *S. niemeyerorum* (CAPPA/UFSM 0032) (Figure 3b), whereas in the specimens assigned to *E. riograndensis* (CAPPA/UFSM 0030 and 0227) it is poorly developed, almost indistinguishable from the

midbrain body. However, this aspect might be related to the bad preservation of the specimens (Figure 3d,f).

Hindbrain

The boundary between the midbrain and the hindbrain is not clear. However, the anterior limit of the hindbrain is probably close to the level of the unossified zone, because in this region the endocast becomes more enlarged, in comparison to the anteriormost region (Kielan-Jaworowska et al., 2004). The dorsal surface of the cerebellum, in all specimens, is slightly convex, without any structure that could indicate the presence of a division between the cerebellar hemispheres (Figure 3a,c,e).

- Insert Figure 3 around here

In all specimens, the region of the parafloccular cast represents the area of the maximum width of the endocast. The parafloccular cast in *S. niemeyerorum* (CAPPA/UFSM 0032) and 0227 (*E. riograndensis*) is barely distinguishable from the hindbrain body (Figure 4a,b,e,f), whereas in CAPPA/UFSM 0030 (*E. riograndensis*), the parafloccular cast is more prominent and laterally projected, in comparison (Figure 4c,d).

The medulla oblongata is rounded in *E. riograndensis* (CAPPA/UFSM 0030, 0227) (Figure 3c-f), and more anteroposteriorly elongated in CAPPA/UFSM 0030 than in CAPPA/UFSM 0227. In *S. niemeyerorum* (CAPPA/UFSM 0032), the medulla oblongata has a rounded outline, being observable ventrally (Figure 3b), as in *Massetognathus* (Quiroga, 1979a). The jugular foramen and the *fenestra ovalis* are well marked and not confluent in *S. niemeyerorum* (CAPPA/UFSM 0032), the jugular foramen being slightly more developed than the *fenestra ovalis* (Figure 3b). In the analyzed specimens of *E. riograndensis*, it was not

possible to observe these structures, since this region of the basicranium is badly preserved. Neither the inner ear nor other vascular canals could be observed.

- Insert Figure 4 around here

3.2. Body mass estimation and encephalization quotients

We estimated the body mass and calculated the EQs following previous protocols (Benoit, Fernandez, et al., 2017). The highest values of body mass estimation were provided by BMb (Hu et al., 2005), and the lowest by BMc (Castanhinha et al., 2013), as previously observed by Benoit, Fernandez, et al. (2017). In *S. niemeyerorum* (CAPPA/UFSM 0032) there is a range of about 33% (BMb 55,495 g; BMc 18,385g), and in *E. riograndensis* of 33% in CAPPA/UFSM 0030 (BMb 59,119g; BMc 19,475g) and 36% in CAPPA/UFSM 0227 (BMb 23,805g; BMc 8,535g) between the highest and lowest values (see Supporting Information Table S1). The EQ values, using the total volume of the endocast, are very similar between *S. niemeyerorum* (CAPPA/UFSM 0032; EQ1 0.26 ± 0.08; EQ2 0.28 ± 0.10; EQ3 6.10 ± 1.63) and *E. riograndensis* (CAPPA/UFSM 0030; EQ1 0.25 ± 0.08; EQ2 0.27 ± 0.10; EQ3 6.00 ± 1.61). When excluding the olfactory bulbs, there is a more conspicuous variation between them (Supporting Information Table S1). In CAPPA/UFSM 0227 the EQs values, using the total volume of the endocast, were EQ1 0.20 ± 0.06; EQ2 0.23 ± 0.08; and EQ3 4.37 ± 1.07. The EQ values of *S. niemeyerorum* (CAPPA/UFSM 0032) and *E. riograndensis* (CAPPA/UFSM 0030, 0227) are within the variation expected for non-mammaliaform cynodonts. However, the EQs of these specimens appear to be higher than previous estimates for traversodontids (Figure 5).

4. DISCUSSION

Morphology and comparisons

As expected, the general endocast morphology of *Siriusgnathus niemeyerorum* (CAPPA/UFSM 0227) and *Exaeretodon riograndensis* (CAPPA/UFSM 0030 and 0227) is closer to that observed in 'reptilian' endocasts than in mammaliaforms and mammals. The poorly ossified orbitosphenoid and a large interorbital vacuity are also observed in *Massetognathus pascuali*, *Exaeretodon argentinus*, and *Chiniquodon*, although in the latter taxon, the orbitosphenoid is ossified (Benoit, Jasinoski, Fernandez, & Abdala, 2017; Crompton, Owerkowicz, Bhullar, & Musinsky, 2017; Kemp, 2009). According to Benoit, Jasinoski, et al. (2017), in the traversodontids *Massetognathus* and *Exaeretodon*, as in other analyzed Gomphodontia, the orbitosphenoid is a fragile cancellous bone. Thus, preservation of the orbitosphenoid is unlikely during the fossilization process. This characteristic might explain its absence in *S. niemeyerorum*. The absence of an interorbital septum makes the interorbital vacuity large and widely open (Benoit, Jasinoski, et al., 2017; Kielan-Jaworowska et al., 2004). The presence of both the orbitosphenoid *in situ* in *E. riograndensis* and a ridge in the floor of the interorbital cavity of *S. niemeyerorum* suggests the presence of a cartilaginous interorbital septum supporting the orbitosphenoid (Benoit, Jasinoski, et al., 2017). In the analyzed specimens, there is no longitudinal sulcus dividing the olfactory bulbs, which could be related to the preservation of the specimens, because this structure was documented in the traversodontid *Massetognathus* sp. (Quiroga, 1979a).

The elongated and tubular endocast becomes enlarged in the hindbrain, with poorly defined olfactory bulbs, undifferentiated cerebral hemispheres, and a cerebellum, resembling the condition described for other cynodonts such as *Thrinaxodon* and *Galesaurus*, the

gomphodont *Trirachodon*, the traversodontids *Massetognathus* and *E. argentinus*, and the basal probainognathian cf. *Probelesodon* (Bonaparte, 1966a; Hopson, 1979; Kielan-Jaworowska et al., 2004; Pusch et al., 2019; Quiroga, 1979a, 1980a). These characteristics are considered plesiomorphic in comparison to mammals (Kielan-Jaworowska et al., 2004). In contrast, in *Probainognathus*, *Riograndia*, and *Brasilodon* the olfactory bulbs are more differentiated; the cerebral hemispheres have a clear division between them; and there is an increase in the olfactory bulbs and the cerebral hemispheres, mainly in *Riograndia* and *Brasilodon* (Rodrigues et al., 2018, 2014). However, they still lack a cribriform plate, separating the endocast from the nasal cavity, and a full ossification of the anterior floor of the braincase (Quiroga, 1980b; Rodrigues et al., 2018, 2014). Usually, the midbrain is not visible on the dorsal surface of endocasts from cynodonts, probably because an anterior expansion of the cerebellum or a posterior expansion of the telencephalon overlaps this region, which also might be covered by the meninges and blood sinuses or by a combination of these structures (Edinger, 1964; Macrini, Muizon, Cifelli, & Rowe, 2007; Rodrigues et al., 2018, 2014). A possible exception is *Probainognathus*, which would preserve a partial exposition of the midbrain because of the presence of the anterior *colliculus* (Quiroga, 1980b). However, Kielan-Jaworowska (1986) interpreted this structure as the cast of the transverse sinus.

The unossified zone is quite developed in Late Triassic traversodontids (CAPPA/UFSM 0030, 0032 and 0227). Several hypotheses about which structure would fill the unossified zone have been raised: the vermis of the cerebellum (Kielan-Jaworowska et al., 2004); blood sinuses, such as the sagittal superior sinus (Macrini, 2006; Quiroga, 1979; Rowe, Carlson, & Bottorff, 1995); the pineal gland (Kemp, 2009); or a cartilaginous area in the supraoccipital (Olson, 1944). Recently, the hypothesis of blood sinuses was reinforced: based on a well-preserved skull of *Diictodon feliceps* (Anomodontia), Laaß et al. (2017) recognized impressions of blood vessels in the unossified zone, interpreted as the junction of the superior sagittal sinus and the

transverse sinuses, housed by the terminal chamber of the anterior segment of the medial head. The supraoccipital notch, which partially separates the unossified zone from the remaining endocast, present in *S. niemeyerorum* (CAPPA/UFSM 0032) and *E. riograndensis* (CAPPA/UFSM 0227), is similar to that described in the anomodont *Diictodon feliceps* (Laaß et al., 2017). The shape and location of the unossified zone in *S. niemeyerorum* (CAPPA/UFSM 0032) is similar to that observed in *Galesaurus*, *E. argentinus*, and cf. *Probelesodon* (Bonaparte, 1966a; Pusch et al., 2019; Quiroga, 1979a), whereas in *E. riograndensis* (CAPPA/UFSM 0030 and 0227) it is more posteriorly positioned, similar to that observed in *Massetognathus* (Quiroga, 1979a). The longitudinal groove apparently connected with the unossified zone in *E. riograndensis* (CAPPA/UFSM 0227) could be the impression of a blood vessel, similar to that observed in *Diictodon feliceps* (Laaß et al., 2017). A prominent parafloccular cast, as observed to *E. riograndensis* (CAPPA/UFSM 0030), is also observed in *Massetognathus*, *E. argentinus*, cf. *Probelesodon*, and *Probainognathus* (Bonaparte, 1966a; Quiroga, 1979a, 1980b). *Galesaurus* also has a prominent parafloccular cast, but it is much larger and more laterally protruding than in any other therapsid with a known endocast, which suggests a full occupation of the hindbrain at this point in the encephalic cavity (Pusch et al., 2019). According to Kielan-Jaworowska et al. (2004), the presence of prominent *paraflocculi* is a derived character for cynodonts, in comparison to other therapsids, in which the *paraflocculi* are poorly developed. Rodrigues et al. (2014) pointed out that the presence of prominent *paraflocculi* is a plesiomorphic condition in eucynodonts, as observed in *Thrinaxodon* (Kielan-Jaworowska et al., 2004; Rowe, 1996) and *Nythosaurus* (= *Thrinaxodon*, Hopson, 1979). However, Hopson (1979) pointed out that the presence/absence of parafloccular fossae can be related to the grade of contact between the brain and brain cavity, as observed in dicynodonts. In small taxa, such as *Kawingasaurus*, in which there is a close contact between the brain and brain cavity, the parafloccular fossae are well developed; on the other hand, in

large taxa the parafloccular fossae are absent (e.g. *Kannemeyeria*) or vestigial (e.g. *Lystrosaurus*)(Angielczyk & Kurkin, 2003; Laaß & Kaestner, 2017). Assuming that the unossified zone is filled by blood sinuses, there is no other structure that could indicate the presence of the vermis of the cerebellum in the specimens here analyzed. On the other hand, the prozostrodontians *Riograndia* and *Brasilodon* exhibit a slight bulging structure on the dorsal surface of the cerebellum, which could correspond to the vermis of the cerebellum (Rodrigues et al., 2018, 2014).

The most remarkable difference among the specimens herein analyzed concerns the dimensions, and consequently volume, of the region of the olfactory bulbs and forebrain. These structures in *S. niemeyerorum* (CAPPA/UFSM 0032) are much more slender and thin in comparison to *E. riograndensis* (CAPPA/UFSM 0030 and 0227). Indeed, the dimensions of the forebrain of *S. niemeyerorum* resemble those observed in *Exaeretodon* sp., although the olfactory bulbs in the latter taxon are more enlarged (Bonaparte, 1966a). There is a difference of about 36% between the volume of the olfactory bulbs of *S. niemeyerorum* (CAPPA/UFSM 0032) in relation to *E. riograndensis* (CAPPA/UFSM 0030), whereas there is little difference between the total volume of the endocast (see Supporting Information Table S1) of those specimens.

Regarding the specimens of *E. riograndensis* (CAPPA/UFSM 0030 and 0227), there is no notable ontogenetic difference between them, and despite the size difference, both may consist of mature individuals. The observed differences include a more developed unossified zone, and the medulla oblongata being, more elongated in CAPPA/UFSM 0030 (larger specimen) than in CAPPA/UFSM 0227. It is important to mention that the endocasts of both specimens of *E. riograndensis* are morphologically more similar to each other than to *S. niemeyerorum*.

Presence/absence of the parietal foramen and pineal tube in traversodontids

Both the parietal foramen and the pineal tube are absent in the specimens here analyzed. Except for the Probainognathia, in which the parietal foramen is consistently absent, there is variation in the presence/absence of this structure among non-mammaliaform cynodonts. The parietal foramen and the pineal tube are present in basal epicynodonts such as *Procynosuchus*, *Thrinaxodon*, *Platycraniellus*, and *Galesaurus* (Abdala, 2007; Benoit, Abdala, Brandt, & Manger, 2015; Liu & Olsen, 2010; Pusch et al., 2019). In the Eucynodontia, the parietal foramen, and probably the whole pineal complex, disappeared in some lineages (Benoit, Abdala, Manger, & Rubidge, 2016; Rodrigues et al., 2014). However, several eucynodont taxa still possess the parietal foramen, such as the cynognathians *Cynognathus* and *Diademodon*, and the trirachodontids *Langbergia* and *Cricodon* (Liu & Olsen, 2010; Sidor & Hopson, 2017). The presence of a parietal foramen is variable in adult individuals of the basal non-mammaliaform cynodont *Cynosaurus* and the trirachodontid *Trirachodon* (Abdala, Neveling, & Welman, 2006; Benoit et al., 2015, 2016). In the trirachodontids *Beishanodon* and *Sinognathus*, the parietal foramen is absent (Gao, Fox, Zhou, & Li, 2010; Liu & Abdala, 2014).

Within the Traversodontidae, the presence of the parietal foramen is also variable (Figure 6), as it is present in *Scalenodon, Luangwa, Traversodon*, and *Protuberum* (Liu & Abdala, 2014), but absent in *Andescynodon*, *Pascualgnathus*, *Massetognathus* (adult specimens; see below), *Boreogomphodon*, *Dadadon*, *Menadon*, *Scalenodontoides*, *Exaeretodon*, and *Siriusgnathus* (Liu & Abdala, 2014; Melo et al., 2015; Pavanatto et al., 2018). In the remaining traversodontids, presence or absence of the parietal foramen is uncertain (Liu & Abdala, 2014).

There is also an ontogenetic variation in the presence/absence of the parietal foramen in some traversodontids. In *Massetognathus pascuali*, the parietal foramen is present in

individuals considered immature (i.e., small–medium skull sizes), but there is a gradual decrease in size until the complete obliteration of the foramen in adult individuals (large-sized skulls; Abdala & Giannini, 2000). There is, however, the possibility that the pineal tube remains and only the parietal foramen closes. According to Benoit et al. (2016), in juvenile specimens of *Dadadon* the parietal foramen is also present, while it is absent in adult individuals. Concerning the traversodontids herein analyzed, in *E. riograndensis* the parietal foramen, as well as the pineal tube, are both absent in the small specimen (CAPPA/UFSM 0227) and the large one (CAPPA/UFSM 0030). Additional CT scanning is required to investigate the presence/absence of the pineal tube through ontogeny in non-mammaliaform cynodonts and its paleobiological implications.

- Insert Figure 6 around here

The parietal foramen housed the "third eye" (pineal eye), which composes, together with other structures (i.e., the pineal gland), the pineal complex in extant reptiles and controls body functions such as ~~like~~, regulation of body temperature and circadian rhythms (Benoit et al., 2015; Eakin, 1973; Quay, 1979; Ralph, Firth, Gern, & Owens, 1979). The absence of the parietal foramen in eucynodonts might be related to the stability of the environmental temperatures, which would cause loss of functionality in the pineal eye, as observed in extant reptiles from equatorial latitudes (Benoit et al., 2015; Gundy, Ralph, & Wurst, 1975; Ralph et al., 1979). However, Benoit et al. (2015) hypothesized that the loss of the parietal foramen, and consequently, the pineal eye, in *Cynosaurus* occurred because this structure became dispensable to the animal, which lived in a region with seasonality, in the highest latitudes. In this case, the absence of the pineal eye could be related to an improvement in the metabolic rate, consequently allowing better control of body temperature; or the acquisition of specialized cells in the lateral

eyes, which could replace or compensate for the absence of the pineal eye (Benoit et al., 2015). Nonetheless, the loss of the parietal foramen in the Traversodontidae seems to have occurred independently, since the presence/absence of this structure is variable in the phylogeny (Figure 6). Considering the stratigraphic distribution of the Brazilian fossil record of traversodontids, the parietal foramen is present in most taxa spanning from the Ladinian to early Carnian (i.e., *Luangwa sudamericana*, *Traversodon*, and *Protuberum*; with the exception of *Massetognathus*); and absent in early-late Carnian taxa (i.e, *Menadon*; *S. niemeyerorum*, and *E. riograndensis*). Furthermore, according to Benoit et al. (2016), there is a parallel trend occurring in both lineages of the Eucynodontia to the loss of the parietal foramen toward the Late Triassic.

Encephalization quotients

The EQs and endocranial volume/body mass relationships of the specimens are in the expected range for non-mammaliaform Therapsida (Figures 5 and 7). *S. niemeyerorum* (CAPPA/UFSM 0032) and *E. riograndensis* (CAPPA/UFSM 0030 and 0227) show a higher encephalization degree than in other traversodontids (Figure 5). However, taking into account the EQ value variation because of the different body mass estimations, these specimens are within the variation expected for non-mammaliaform cynodonts (see Supporting Information Table S1). Due to these high values, on a plot of the relationship between body mass and endocast volume (Figure 7), *S. niemeyerorum* (CAPPA/UFSM 0032) and *E. riograndensis* (CAPPA/UFSM 0030 and 0227) diverge from other traversodontids, except for *Exaeretodon* sp. (point 25) and *Diademodon* (point 16), and are closely distributed to the dicynodont *Pristerodon* (point 6; Figure 7).

The EQ values of the studied taxa are more similar to those observed for *Diademodon*, *Thrinaxodon*, and non-cynodontian therapsids (Benoit, Fernandez, et al., 2017; Benoit, Manger, et al., 2017; Jerison, 1973; Rowe et al., 2011). This difference draws more attention when we compare our results with *Exaeretodon* sp., which has a longer skull length, but a lower endocast volume when compared to the Brazilian specimens (Quiroga, 1980b; Supporting Information Table S1). This is particularly noteworthy when taking into account that these taxa are phylogenetically close (Liu & Abdala, 2014; Pavanatto et al., 2018). Such divergence might be explained by differences in the techniques employed to obtain the endocast volumes. The endocast volumes of other traversodontids (i.e., *Andescynodon*, *Massetognathus*, *Exaeretodon* sp.) were obtained via natural endocasts, whereas the specimens here presented had their endocast volumes assessed via CT-scanning and manual segmentation, which could generate the observed divergence in results (Holloway, 2018).

- Insert Figure 7 around here

5. CONCLUSIONS

In this contribution we presented, for the first time, the reconstruction and description of virtual brain endocasts of *Siriusgnathus niemeyerorum* and *Exaeretodon riograndensis*. The general morphology of S. *niemeyerorum* and *E. riograndensis* – i.e., not fully ossified endocranial cavity and the tubular, elongated, and poorly differentiated endocast – is similar to that observed in other therapsids and considered the plesiomorphic condition for Therapsida.

The endocranial volume and EQ values are within the expected values for non-mammaliaform cynodonts. The fact that these values are slightly higher than in other traversodontid cynodonts may be related to differences in technique used to calculate the

volume (CT-scanning) in this study compared to previous studies on traversodontids (natural endocasts; Quiroga, 1979, 1980a).

The orbitosphenoid is incompletely ossified in both specimens of *E. riograndensis*. It is absent in the analyzed specimen of *S. niemeyerorum*, which could be related to the degree of ossification or preservation of this bone. The unossified zone in S. *niemeyerorum* and *E. riograndensis* (CAPPA/UFSM 0227) is partially separated from the remaining endocast by a notch formed by the supraoccipital. The parietal foramen and pineal tube are absent in both S. *niemeyerorum* and *E. riograndensis*. The presence/absence of the parietal foramen is variable within the Traversodontidae, and apparently, the loss of the parietal foramen seems to have occurred independently. However, new information based on CT-scans is necessary to fully assess the absence of the pineal tube in those taxa in which the parietal foramen is absent. Nonetheless, this study improves knowledge about the internal anatomy of the traversodontid skull.

Acknowledgments

We thank Centro de Apoio à Pesquisa Paleontológica da Quarta Colônia (CAPPA/ UFSM) for the infrastructure provided and the access to the fossils housed there; Valnir de Paula and the medical clinic DIX – Diagnóstico por Imagem do Hospital de Caridade for the allowance to access of the CT-Scan. We also thank to the reviewers, Julien Benoit and the anonymous reviewer, for the comments that greatly improved this manuscript. This study is supported by Coordenação de Aperfeiçoamento de Pessoal de Nível Superior – Brasil (CAPES) – Finance Code 001 (AEBP); Fundação de Amparo à Pesquisa do Estado do Rio Grande do Sul (FAPERGS 17/2551-0000816-2) and Conselho Nacional de Desenvolvimento Científico e Tecnológico (CNPq 422568/2018-0) (LK); (306352/2016-8) (SDS).

Conflict of Interest: The authors declare no conflict of interest.

6. REFERENCES

Abdala, F., & Gaetano, L. C. (2018). The Late Triassic Record of Cynodonts: Time of Innovations in the Mammalian Lineage. In L. H. Tanner (Ed.), *The Late Triassic World* (pp. 407–445). Springer US. https://doi.org/10.1007/978-3-319-68009-5_11

Abdala, F., Neveling, J., & Welman, J. (2006). A new trirachodontid cynodont from the lower levels of the Burgersdorp Formation (Lower Triassic) of the Beaufort Group, South Africa and the cladistic relationships of Gondwanan gomphodonts. *Zoological Journal of the Linnean Society*, *147*(3), 383–413. https://doi.org/10.1111/j.1096-3642.2006.00224.x

Abdala, Fernando. (2007). Redescription of *Platycraniellus elegans* (Therapsida, Cynodontia) from the lower Triassic of South Africa, and the cladistic relationships of Eutheriodonts. *Palaeontology*, *50*(3), 591–618. https://doi.org/10.1111/j.1475-4983.2007.00646.x

Abdala, Fernando, & Giannini, N. P. (2000). Gomphodont Cynodonts of the Chañares Formation : the Analysis of an Ontogenetic Sequence. *Journal of Vertebrate Paleontology*, *20*(3), 501–506. https://doi.org/10.1671/0272-4634(2000)020[0501:GCOTCA]2.0.CO;2

Abdala, Fernando, & Ribeiro, A. M. (2010). Distribution and diversity patterns of Triassic cynodonts (Therapsida, Cynodontia) in Gondwana. *Palaeogeography, Palaeoclimatology, Palaeoecology*, *286*, 202–217. https://doi.org/10.1016/j.palaeo.2010.01.011

Allman, J. (1990). The origin of the neocortex. *The Neurosciences*, *2*, 257–262.

Angielczyk, K. D., & Kurkin, A. A. (2003). Phylogenetic analysis of Russian Permian dicynodonts (Therapsida: Anomodontia): Implications for Permian biostratigraphy and Pangaean biogeography. *Zoological Journal of the Linnean Society*, *139*(2), 157–212. https://doi.org/10.1046/j.1096-3642.2003.00081.x

Balanoff, A. M., Bever, G. S., Colbert, M. W., Clarke, J. A., Field, D. J., Gignac, P. M., … Witmer, L. M. (2016). Best practices for digitally constructing endocranial casts: examples from birds and their dinosaurian relatives. *Journal of Anatomy*, *229*(2), 173–190.

https://doi.org/10.1111/joa.12378

Bendel, E.-M., Kammerer, C. F., Kardjilov, N., Fernandez, V., & Fröbisch, J. (2018). Cranial anatomy of the gorgonopsian *Cynariops robustus* based on CT- reconstruction. *PLoS ONE*, *13*(11), e0207367. https://doi.org/10.1371/journal.pone.0207367

Benoit, J., Abdala, F., Brandt, M. J. Van Den, & Manger, P. R. (2015). Physiological implications of the abnormal absence of the parietal foramen in a late Permian cynodont (Therapsida). *The Science of Nature*, *102*(69), 1–4. https://doi.org/10.1007/s00114-015-1321-4

Benoit, J., Abdala, F., Manger, P. R., & Rubidge, B. S. (2016). The sixth sense in mammalians forerunners: Variability of the parietal foramen and the evolution of the pineal eye in South African Permo-Triassic eutheriodont therapsids. *Acta Palaeontologica Polonica*, *61*(4), 777–789. https://doi.org/10.4202/app.00219.2015

Benoit, J., Fernandez, V., Manger, P. R., & Rubidge, B. S. (2017). Endocranial Casts of Pre-Mammalian Therapsids Reveal an Unexpected Neurological Diversity at the Deep Evolutionary Root of Mammals. *Brain, Behavior and Evolution*, *90*(4), 311–333. https://doi.org/10.1159/000481525

Benoit, J., Jasinoski, S. C., Fernandez, V., & Abdala, F. (2017). The mystery of a missing bone: revealing the orbitosphenoid in basal Epicynodontia (Cynodontia, Therapsida) through computed tomography. *The Science of Nature*, *104*(66), 1–10. https://doi.org/10.1007/s00114-017-1487-z

Benoit, J., Manger, P. R., Norton, L., Fernandez, V., & Rubidge, B. S. (2017). Synchrotron scanning reveals the palaeoneurology of the head-butting *Moschops capensis* (Therapsida, Dinocephalia). *PeerJ*, *5*(e3496), 1–27. https://doi.org/10.7717/peerj.3496

Bonaparte, J. F. (1966a). Sobre las cavidades cerebral, nasal y otras estructuras del cráneo de *Exaeretodon*. *Acta Geológica Lilloana*, *8*, 5–29.

Bonaparte, J. F. (1966b). Una nueva “fauna” triásica de Argentina (Therapsida: Cynodontia Dicynodontia) Consideraciones filogenéticas y paleobiogeográficas. *Ameghiniana*, *4*(8), 243–296.

Bonaparte, J. F. (1969). Dos nuevas ‘“faunas”’ de reptiles triásicos de Argentina. In *Gondwana Stratigraphy, I.U.G.S* (pp. 283–302).

Brink, A. S. (1963). Two cynodonts from the Ntawere Formation in the Luangwa Valley of northern Rhodesia. *Palaeontologia Africana*, *8*, 77–96.

Campione, N. E., & Evans, D. C. (2012). A universal scaling relationship between body mass and proximal limb bone dimensions in quadrupedal terrestrial tetrapods. *BMC Biology*, *10*(60), 1–21. https://doi.org/10.1186/1741-7007-10-60

Castanhinha, R., Araújo, R., Júnior, C. L., Angielczyk, K. D., Martins, G. G., Martins, R. M. S., … Wilde, F. (2013). Bringing Dicynodonts Back to Life : Paleobiology and Anatomy of a New Emydopoid Genus from the Upper Permian of Mozambique. *PLoS ONE*, *8*(12), e80974. https://doi.org/10.1371/journal.pone.0080974

Crompton, A. W. (1955). On some Triassic cynodonts from Tanganyika. *Proceedings of the Zoological Society of London*, *125*(3–4), 617–669. https://doi.org/10.1111/j.1096-3642.1955.tb00620.x

Crompton, A. W., Musinsky, C., Rougier, G. W., Bhullar, B. A. S., & Miyamae, J. A. (2018). Origin of the Lateral Wall of the Mammalian Skull: Fossils, Monotremes and Therians Revisited. *Journal of Mammalian Evolution*, *25*(3), 301–313. https://doi.org/10.1007/s10914-017-9388-7

Crompton, A. W., Owerkowicz, T., Bhullar, B. A. S., & Musinsky, C. (2017). Structure of the nasal region of non-mammalian cynodonts and mammaliaforms: Speculations on the evolution of mammalian endothermy. *Journal of Vertebrate Paleontology*, *37*(1). https://doi.org/10.1080/02724634.2017.1269116

Eakin, R. M. (1973). *The third eye*. Berkeley: University of California Press.

Edinger, T. (1964). Midbrain exposure and overlap in Mammals. *American Zoologist, 4*, 5–19.

Eisenberg, J. F. (1981). *The Mammalian Radiations: An Analysis of Trends in Evolution, Adaptation, and Behavior*. Chicago: University Chicago Press.

Fedorov, A., Beichel, R., Kalphaty-Cramer, J., Finet, J., Fillion-Robbin, J.-C., Pujol, S., … Kikinis, R. (2012). 3D Slicer as an Image Computing Platform for the Quantitative Imaging Network. *Magnetic Resonance Imaging*, *30*(9), 1323–1341. https://doi.org/10.1016/j.mri.2012.05.001.

Gao, K.-Q., Fox, R. C., Zhou, C.-F., & Li, D.-Q. (2010). A New Nonmammalian Eucynodont (Synapsida: Therapsida) from the Triassic of Northern Gansu Province, China, and its Biostratigraphic and Biogeographic Implications. *American Museum Novitates*, *3685*, 1–25. https://doi.org/10.1206/649.1

Gundy, G. C., Ralph, C. L., & Wurst, G. Z. (1975). Parietal Eyes in Lizards: Zoogeographical Correlates. *Science*, *190*(4215), 671–673. https://doi.org/10.1126/science.1237930

Holloway, R. L. (2018). On the Making of Endocasts: The New and the Old in Paleoneurology. In E. Bruner, N. Ogihana, & H. Tanabe (Eds.), *Digital Endocasts* (pp. 1–8). Tokyo: Springer. https://doi.org/10.1007/978-4-431-56582-6_1

Hopson, J. A. (1979). Paleoneurology. In C. Gans, G. R. Northcutt, & P. Ulinski (Eds.), *Biology of the Reptilia*. New York: Academic Press.

Horn, B. L. D., Melo, T. M., Schultz, C. L., Philipp, R. P., Kloss, H. P., & Goldberg, K. (2014). A new third-order sequence stratigraphic framework applied to the Triassic of the Paraná Basin, Rio Grande do Sul, Brazil, based on structural, stratigraphic and paleontological data. *Journal of South American Earth Sciences, 55*, 123–132. https://doi.org/10.1016/j.jsames.2014.07.007

Hu, Y., Meng, J., Wang, Y., & Li, C. (2005). Large Mesozoic mammals fed on young dinosaurs.

Nature, *433*, 149–152. https://doi.org/10.1038/nature03102

Hurlburt, G. R., Ridgely, R. C., & Witmer, L. M. (2013). Relative size of brain and cerebrum in tyrannosaurid dinosaurs: an analysis using brain-endocast quantitative relationships in extant alligators. In J. M. Parrish, R. E. Molnar, P. J. Currie, & E. B. Koppelhus (Eds.), *Tyrannosaurid paleobiology* (pp. 135–154). Bloomington: Indiana University Press.

Jerison, H. J. (1973). *Evolution of the brain and intelligence*. New York: Academic Press.

Kammerer, C. F., Flynn, J. J., Ranivoharimanana, L., & Wyss, A. R. (2008). New material of *Menadon besairiei* (Cynodontia: Traversodontidae) from the Triassic of Madagascar. *Journal of Vertebrate Paleontology*, *28*(2), 445–462. https://doi.org/10.1671/0272-4634(2008)28[445:nmombc]2.0.co;2

Kammerer, C. F., Flynn, J. J., Ranivoharimanana, L., & Wyss, A. R. (2012). Ontogeny in the Malagasy Traversodontid *Dadadon isaloi* and a Reconsideration of its Phylogenetic Relationships. *Fieldiana: Life and Earth Sciences*, *5*, 112–125. https://doi.org/10.3158/2158-5520-5.1.112

Kemp, T. S. (2006). The origin of mammalian endothermy: A paradigm for the evolution of complex biological structure. *Zoological Journal of the Linnean Society*, *147*(4), 473–488. https://doi.org/10.1111/j.1096-3642.2006.00226.x

Kemp, T. S. (2009). The endocranial cavity of a nonmammalian eucynodont, *Chiniquodon theotenicus*, and its implications for the origin of the mammalian brain. *Journal of Vertebrate Paleontology*, *29*(4), 1188–1198. https://doi.org/10.1671/039.029.0430

Kielan-Jaworowska, Z. (1986). Brain evolution in Mesozoic mammals. In K. M. Flanagan & J. A. Lillegraven (Eds.), *Vertebrates, Phylogeny, and Philosophy* (pp. 21–34). University of Wyoming. https://doi.org/10.2113/gsrocky.24.special_paper_3.21

Kielan-Jaworowska, Z., Cifelli, R. L., & Luo, Z.-X. (2004). *Mammals from the Age of Dinosaurs - Origins, Evolution and Structure*. New York: Columbia University Press.

Laaß, M. (2015). Virtual Reconstruction and Description of the Cranial Endocast of *Pristerodon mackayi* (Therapsida, Anomodontia). *Journal of Morphology*, *276*(6), 1089–1099. https://doi.org/10.1002/jmor.20397

Laaß, M., & Kaestner, A. (2017). Evidence for convergent evolution of a neocortex-like structure in a late Permian therapsid. *Journal of Morphology*, *278*(8), 1033–1057. https://doi.org/10.1002/jmor.20712

Laaß, M., Schillinger, B., & Kaestner, A. (2017). What Did the "Unossified Zone" of the Non-Mammalian Therapsid Braincase House ? *Journal of Morphology*, *278*(8), 1020–1032. https://doi.org/10.1002/jmor.20583

Liu, J., & Abdala, F. (2014). Phylogeny and Taxonomy of the Traversodontidae. In C. F. Kammerer, K. D. Angielczyk, & J. Fröbisch (Eds.), *Early Evolutionary History of the Synapsida (Vertebrate Paleobiology and Paleoanthropology Series)* (pp. 289–304). Dordrecht: Springer. https://doi.org/10.1007/978-94-007-6841-3

Liu, J., & Olsen, P. (2010). The phylogenetic relationships of Eucynodontia (Amniota: Synapsida). *Journal of Mammalian Evolution*, *17*(3), 151–176. https://doi.org/10.1007/s10914-010-9136-8

Macrini, Thomas E, Muizon, C. De, Cifelli, R. L., & Rowe, T. (2007). Digital cranial endocast of *Pucadelphys andinus*, a Paleocene metatherian. *Journal of Vertebrate Paleontology*, *27*(1), 99–107. https://doi.org/10.1671/0272-4634(2007)27[99:DCEOPA]2.0.CO;2

Macrini, Thomas Edward. (2006). *The Evolution of Endocranial Space in Mammals and Non-mammalian Cynodonts*. The University of Texas at Austin.

Manger, P. R. (2006). An examination of cetacean brain structure with a novel hypothesis correlating thermogenesis to the evolution of a big brain. *Biological Reviews*, *81*, 293–338. https://doi.org/10.1017/S1464793106007019

Melo, Tomaz P., Martinelli, A. G., & Soares, M. B. (2017). A new gomphodont cynodont

(Traversodontidae) from the Middle–Late Triassic Dinodontosaurus Assemblage Zone of the Santa Maria Supersequence, Brazil. *Palaeontology*, *60*(4), 571–582. https://doi.org/10.1111/pala.12302

Melo, Tomaz Panceri, Abdala, F., & Soares, M. B. (2015). The Malagasy cynodont *Menadon besairiei* (Cynodontia; Traversodontidae) in the Middle-Upper Triassic of Brazil. *Journal of Vertebrate Paleontology*, *35*(6), e1002562. https://doi.org/10.1080/02724634.2014.1002562

Novacek, M. J. (1993). Patterns of diversity in the mammalian skull. In J. Hanken & B. K. Hall (Eds.), *The Skull* (Vol. 2, pp. 438–545). Chicago: The University of Chicago Press.

Olson, E. C. (1944). Origin of the mammals based upon cranial morphology of their therapsid suborders. *GSA, Special Paper*, *55*, 1–136.

Ottone, E. G., Monti, M., Marsicano, C. A., de la Fuente, M. S., Naipauer, M., Armstrong, R., & Mancuso, A. C. (2014). A new Late Triassic age for the Puesto Viejo Group (San Rafael depocenter, Argentina): SHRIMP U-Pb zircon dating and biostratigraphic correlations across southern Gondwana. *Journal of South American Earth Sciences*, *56*, 186–199. https://doi.org/10.1016/j.jsames.2014.08.008

Pavanatto, A. E. B., Pretto, F. A., Kerber, L., Müller, R. T., Da-Rosa, Á. A. S., & Dias-da-Silva, S. (2018). A new Upper Triassic cynodont-bearing fossiliferous site from southern Brazil, with taphonomic remarks and description of a new traversodontid taxon. *Journal of South American Earth Sciences*, *88*, 179–196. https://doi.org/10.1016/j.jsames.2018.08.016

Philipp, R. P., Closs, H., Schultz, C. L., Basei, M., Horn, B. L. D., & Soares, M. B. (2013). Proveniência por U-Pb LA-ICP-MS em zircão detrítico e idade de deposição da Formação Santa Maria, Triássico da Bacia do Paraná, RS: evidências da estruturação do Arco do Rio Grande. In *Anais do VIII Symposium International on Tectonics & XIV Simpósio Nacional de Estudos Tectônicos* (pp. 154–157). Cuiabá, Mato Grosso.

Pusch, L., Kammerer, C. F., & Fröbisch, J. (2019). Cranial anatomy of the early cynodont *Galesaurus planiceps* and the origin of mammalian endocranial characters. *Journal of Anatomy*. https://doi.org/10.1111/joa.12958

Quay, W. B. (1979). The parietal eye-pineal complex. In C. Gans, R. G. Northcutt, & P. Ulinski (Eds.), *Biology of the Reptilia* (Volume 9, pp. 245–406). New York: Academic Press.

Quiroga, J. C. (1979a). The brain of two mammal-like reptiles (Cynodontia-Therapsida). *Journal Für Hirnforschung*, *20*, 351–359.

Quiroga, J. C. (1979b). The inner ear of two cynodonts (Reptilia-Therapsida) and some comments on the evolution of the inner ear from Pelycosaurs to Mammals. *Gegenbaurs Morphologisches Jahrbuch*, *125*(2), 178–190.

Quiroga, J. C. (1980a). Further studies on cynodont endocasts (Reptilia-Therapsida). *Zeitschrift Für Mikroskopisch-Anatomische Forschung*, *94*(4), 580–592.

Quiroga, J. C. (1980b). The brain of the mammal-like reptile *Probainognathus jenseni* (Therapsida, Cynodontia). A correlative paleo-neoneurological approach to the neocartex at retile-mammal transition. *Journal Für Hirnforschungnal F*, *21*, 299–336.

Quiroga, J. C. (1984). The endocranial cast of the advanced mammal-like reptile *Therioherpeton cargnini* (Therapsida-Cynodontia) form the Middle Triassic of Brazil. *Journal Für Hirnforschung*, *25*(3), 285–290.

Ralph, C. L., Firth, B. T., Gern, W. A., & Owens, D. W. (1979). The Pineal Complex and Thermoregulation. *Biological Reviews*, *54*, 41–72.

Rodrigues, P. G., Martinelli, A. G., Schultz, C. L., Corfe, I. J., Gill, P. G., Soares, M. B., & Rayfield, E. J. (2018). Digital cranial endocast of *Riograndia guaibensis* (Late Triassic, Brazil) sheds light on the evolution of the brain in non-mammalian cynodonts. *Historical Biology*, 1–18. https://doi.org/10.1080/08912963.2018.1427742

Rodrigues, P. G., Ruf, I., & Schultz, C. L. (2014). Study of a digital cranial endocast of the non-

mammaliaform cynodont *Brasilitherium riograndensis* (Later Triassic, Brazil) and its relevance to the evolution of the mammalian brain. *Paläontologische Zeitschrift*, *88*(3), 329–352. https://doi.org/10.1007/s12542-013-0200-6

Rowe, T. (1996). Coevolution of the Mammalian Middle Ear and Neocortex. *Science*, *273*(5275), 651–654. https://doi.org/10.1126/science.273.5275.651

Rowe, T. B., Carlson, W. D., & Bottorff, W. W. (1995). *Thrinaxodon, Digital Atlas of the Skull*. Austin: University of Texas Press

Rowe, T. B., Macrini, T. E., & Luo, Z.-X. (2011). Fossil Evidence on Origin of the Mammalian Brain. *Science*, *332*, 955–957. https://doi.org/10.1126/science.1203117

Schmitt, M. R., Martinelli, A. G., Melo, T. P., & Soares, M. B. (2019). On the occurrence of the traversodontid *Massetognathus ochagaviae* (Synapsida, Cynodontia) in the early late Triassic *Santacruzodon* Assemblage Zone (Santa Maria Supersequence, southern Brazil): Taxonomic and biostratigraphic implications. *Journal of South American Earth Sciences*. https://doi.org/10.1016/j.jsames.2019.04.011

Sidor, C. A., & Hopson, J. A. (2017). Cricodon metabolus (Cynodontia: Gomphodontia) from the Triassic Ntawere Formation of northeastern Zambia: patterns of tooth replacement and a systematic review of the Trirachodontidae. *Journal of Vertebrate Paleontology*, *37*(6), 39–64. https://doi.org/10.1080/02724634.2017.1410485

Sookias, R. B., Butler, R. J., & Benson, R. B. J. (2012). Rise of dinosaurs reveals major body-size transitions are driven by passive processes of trait evolution. *Proceedings of the Royal Society B: Biological Sciences*, *279*, 2180–2187. https://doi.org/10.1098/rspb.2011.2441

Van Valkenburgh, B. (1990). Skeleton and dental predictors of body mass in carnivores. In J. Damuth & B. J. MacFadden (Eds.), *Body size in mammalian paleobiology: Estimation and biological implication* (pp. 181–205). Cambridge: Cambridge University Press.

Figure captions:

Figure 1 – Photography (top) and virtual reconstructions of the skulls (bottom) of *Siriusgnathus niemeyerorum* (CAPPA/UFSM 0032) and *Exaeretodon riograndensis* (CAPPA/UFSM 0030 and 0227). CAPPA/UFSM 0032 in dorsal (**A**) and lateral (**B**) views. CAPPA/UFSM 0030 in dorsal (**C**) lateral (**D**) views. CAPPA/UFSM 0227 in dorsal (**E**) and lateral (**F**) views. Scale: 50 mm.

Figure 2 – Tomographic slices through the endocranial cavity of late Triassic traversodontids from southern Brazil. The 3D-model of the skulls show the position of the slices. **A-C**, *Siriusgnathus niemeyerorum* (CAPPA/UFSM 0032). **D-I**, *Exaeretodon riograndensis*: CAPPA/UFSM 0030, **D-F**; CAPPA/UFSM 0227, **G-I**. **Abbreviations**: **Bs**, Basisphenoid; **bv**, blood vessel; **ce**, cavum epiptericum; **F**, Frontal; **f**, hard matrix filling; **FB**, forebrain; **fm**, foramen magnum; **hf**, hypophyseal fossa; **iv**, interorbital vacuity; **k**, ventral keel; **MB**, midbrain; **nc**, nasal cavity; **ob+ot**, olfactory bulbs and olfactory tracts; **Os**, Orbitosphenoid; **Pa**, Parietal; **Pos**, Postorbital; **Pt**, Pterygoid; **r**, ridge; **So**, Supraoccipital; **uz**, unossified zone. The arrow indicates the notch of the supraoccipital. Scale: 20 mm.

Figure 3 – Digital endocast of late Triassic Traversodontidae from southern Brazil**. A-B**, *Siriusgnathus niemeyerorum* (CAPPA/UFSM 0032) in dorsal **(A**) and ventral (**B**) views. **C-E,** *Exaeretodon riograndensis*: CAPPA/UFSM 0030 in dorsal (**C**) and ventral (**D**) views; and CAPPA/UFSM 0227 in dorsal (**E**) and ventral (**F**) views. **Abbreviations**: **ce**, cavum epiptericum; **FB**, forebrain; **fm**, foramen magnum; **fo**, *fenestra ovalis*; **HB**, hindbrain; **hyp**, hypophyseal cast; **jf**, jugular foramen; **MB**, midbrain; **mo**, medulla oblongata; **ob+ot**, olfactory bulbs and olfactory tracts; **pfl**, parafloccular cast; **uz**, unossified zone. Scale: 50 mm.

Figure 4 – Digital endocast of late Triassic Traversodontidae from southern Brazil. **A-B**, *Siriusgnathus niemeyerorum* (CAPPA/UFSM 0032) in right (**A)** lateral and left lateral (**B**) views. **C-E**, *Exaeretodon riograndensis*: CAPPA/UFSM 0030 in right lateral (**C**) and left lateral (**D**) views; and CAPPA/UFSM 0227 in right lateral (**E**) and left lateral (**F**) views. **Abbreviations**: **ce**, cavum epiptericum; **FB**, forebrain; **fm**, foramen magnum; **fo**, *fenestra ovalis*; **HB**, hindbrain; **hyp**, hypophyseal cast; **jf**, jugular foramen; **MB**, midbrain; **mo**, medulla oblongata; **ob+ot**, olfactory bulbs and olfactory tracts; **pfl**, parafloccular cast; **uz**, unossified zone. Scale: 50 mm.

Figure 5 – The encephalization quotients (EQs) of Therapsida and phylogenetic relationships. Data set in Table S1. **Abbreviations**: **EQ1**, Jerison's EQ; **EQ2**, Manger's EQ; **EQ3**, Hurlburt et al.'s EQ; **[1]** NMQR 1702 (Benoit, Fernandez, et al., 2017); **[2]** BP/1/816 (Benoit, Fernandez, et al., 2017); **[3]** Endocast volume without the pineal tube (Benoit, Manger, et al., 2017); **[4]** UCMP 40466 (Macrini, 2006); **[5]** Rowe et al. (2011); **[6]** UCMP 42446 (Macrini, 2006); **[7]** Jerison (1973); **[8]** PVL 3899 (Quiroga, 1980a); **[9]** PVL 3894 (Quiroga, 1980a); **[10]** PVL 4016 (Quiroga, 1979; 1980b); **[11]** PVL 3905 (Quiroga, 1980a); **[12]** PVL 4168 (Quiroga, 1980a); **[13]** BP/1/4245 (Benoit, Fernandez, et al., 2017); **[14]** Quiroga (1980b); **[15]** BP/1/4778 (Benoit, Fernandez, et al., 2017); **[16]** BP/1/5088 (Benoit, Fernandez, et al., 2017). Drawing sources: *Thrinaxodon* and *Morganucodon* – Kielan-Jaworowska et al. (2004); *Massetognathus* – Quiroga (1979); *Probainognathus* – Quiroga (1980b); *Riograndia* – Rodrigues et al. (2018).

Figure 6 – The presence/absence of the parietal foramen/pineal tube in some non-mammaliaform cynodonts. **Bolt**: parietal foramen absent. **+** Parietal foramen present; **?** Presence/absence of the parietal foramen uncertain. The arrow indicates the pineal tube. Grey: Cynognathia; Purple: Trirachodontidae; Blue: Traversodontidae. Phylogenetical relationships

based on Pavanatto et al. (2018). Drawing sources: *Galesaurus* – Pusch et al. (2019); *Thrinaxodon* – Kielan-Jaworowska et al. (2004); *Trirachodon* – Hopson (1979); *Massetognathus* – Quiroga (1979).

Figure 7 – Comparative chart between the relative endocast volume of the *Siriusgnathus niemeyerorum* (point 26, double underline) and *Exaeretodon riograndensis* specimens (27 and 28, simple underline) and the other cynodonts (red cross), non-cynodonts therapsids (black circles), mammaliaforms (green squares), and mammals (blue triangles). The black arrows point the traversodontids cynodonts. The specimens' numbers and the data set follow Supporting Information Table S1.

Figure 1

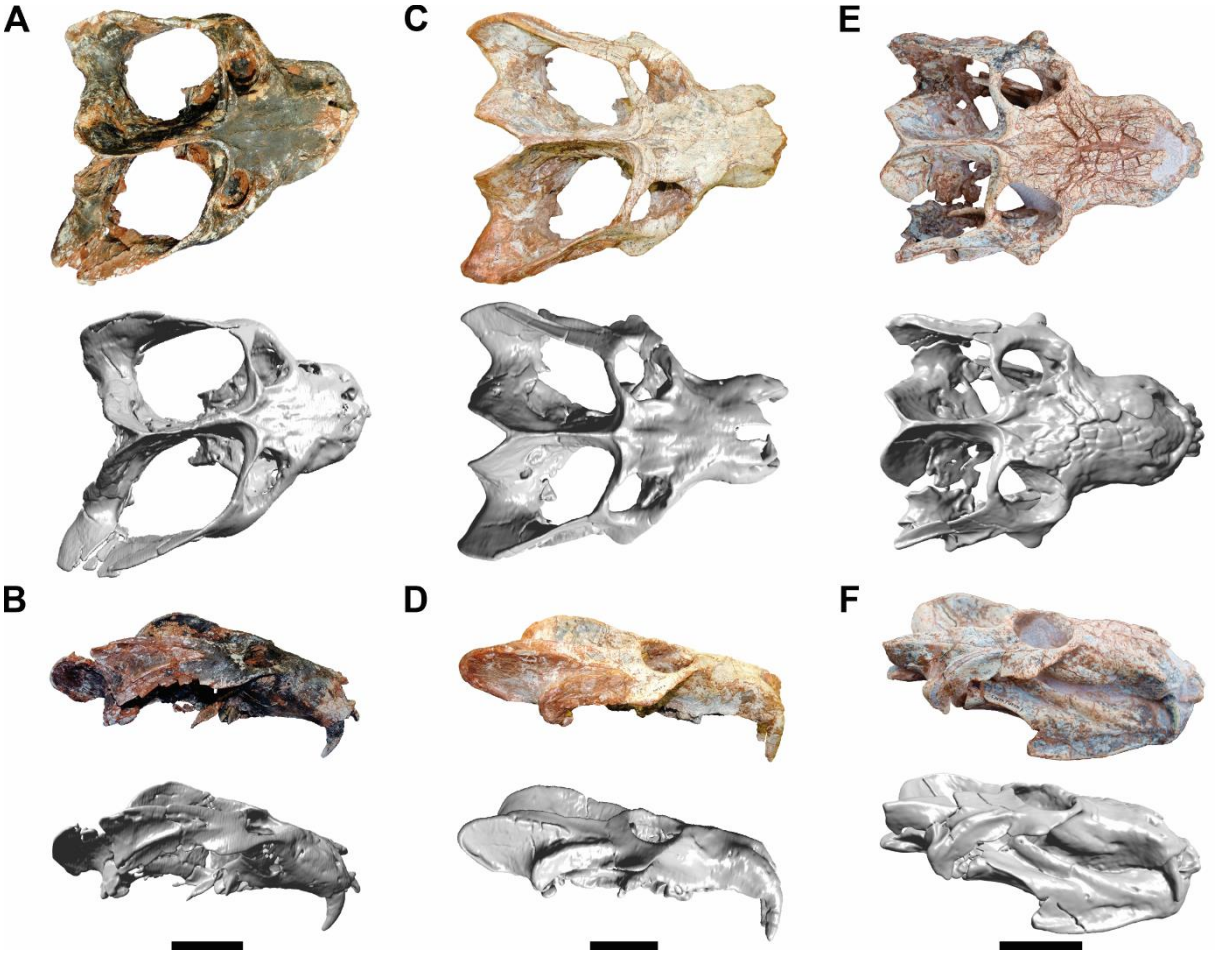

Figure 2

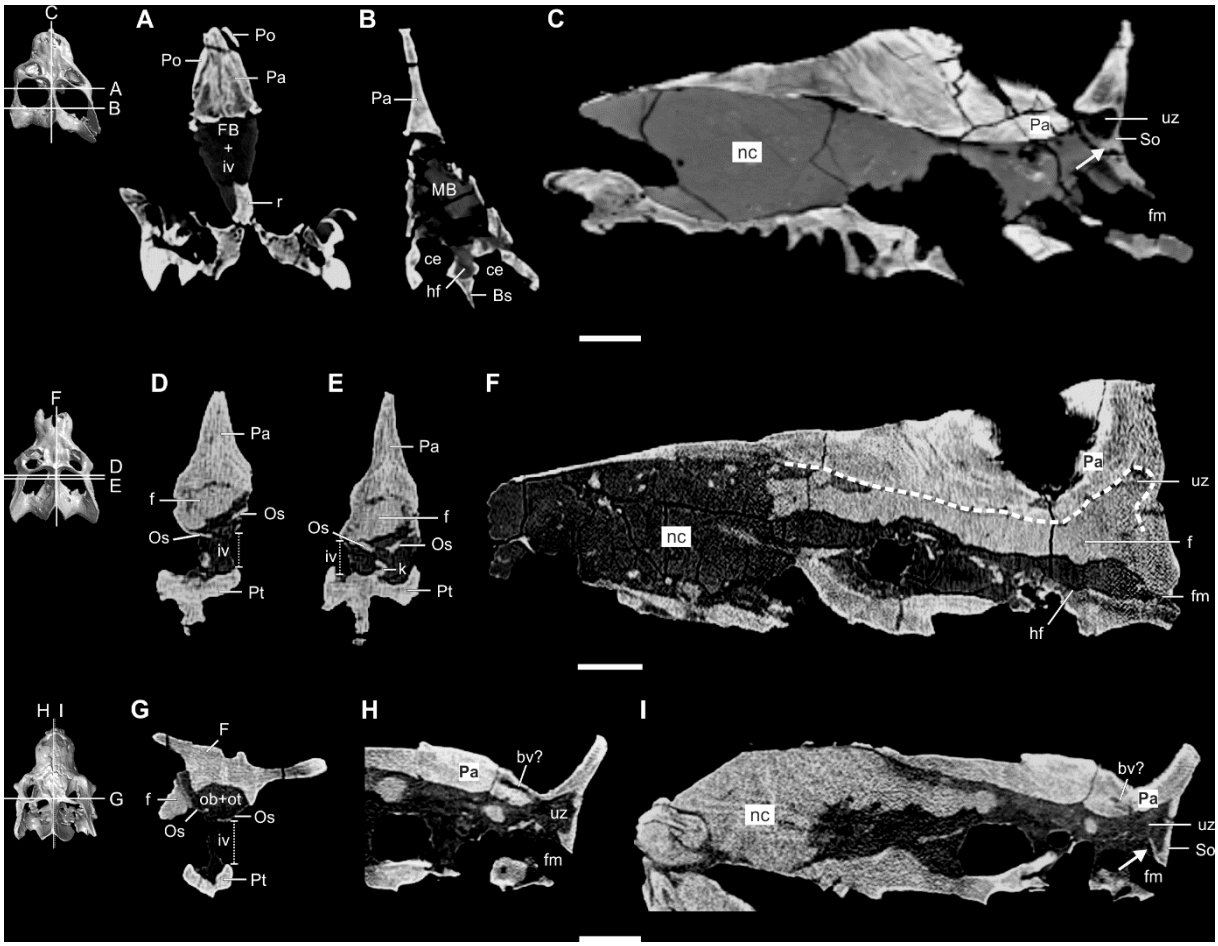
C
A
B
A
Po
Po
Pa
FB
+
iv
r
B
Pa
MB
ce
ce
hf
Bs
C
nc
Pa
uz
So
fm
F
D
E
D
Pa
f
Os
Os
iv
Pt
E
Pa
f
Os
Os
iv
k
Pt
F
nc
Pa
uz
f
fm
hf
H I
G
G
F
f
ob+ot
Os
Os
iv
Pt
H
Pa
bv?
uz
fm
I
nc
bv?
Pa
uz
So
fm

Figure 3

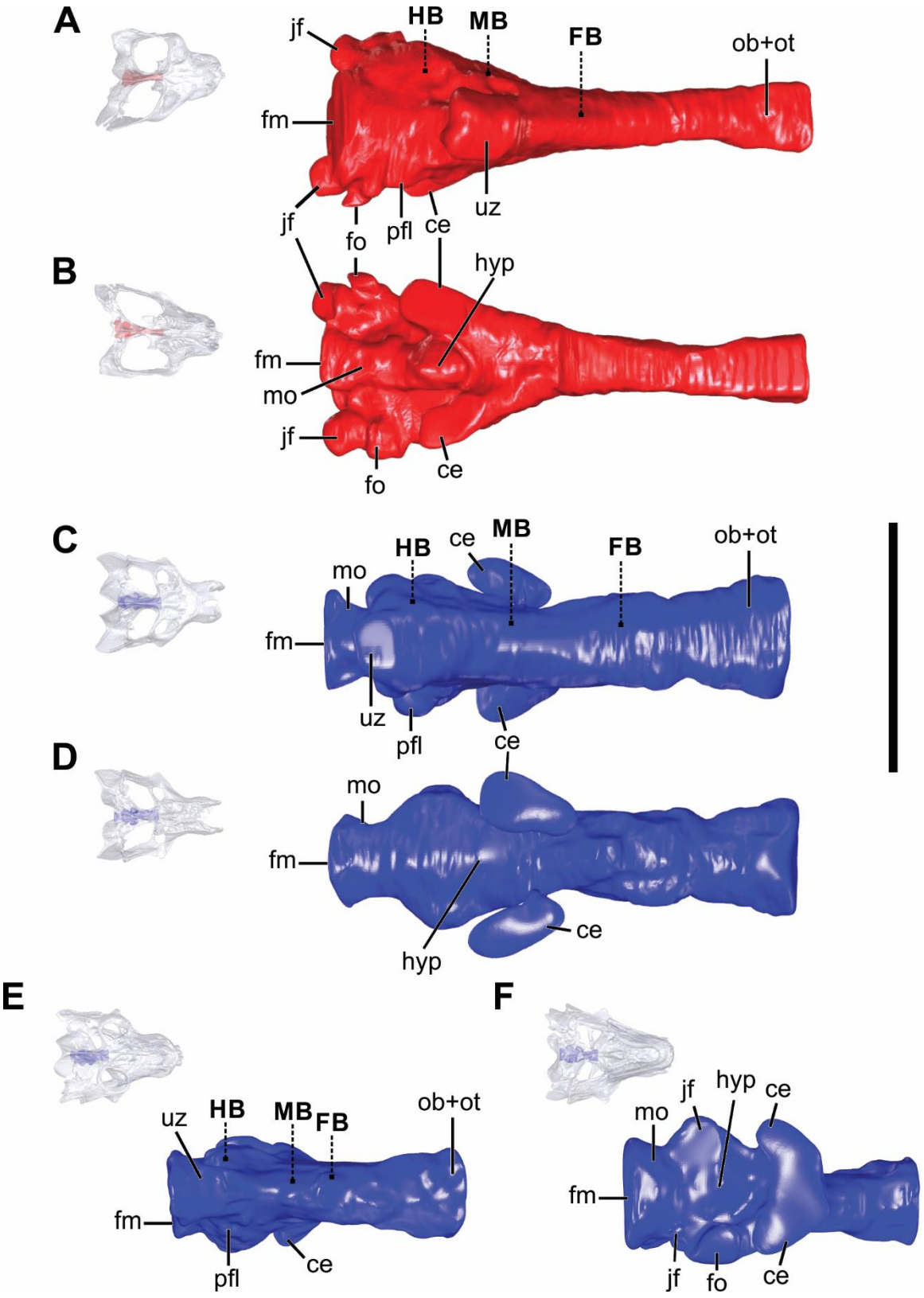
A
jf
HB
MB
FB
ob+ot
fm
jf
fo
pfl
ce
uz
B
hyp
fm
mo
jf
fo
ce
C
HB
ce
MB
FB
ob+ot
mo
fm
uz
pfl
ce
D
mo
fm
hyp
ce
E
uz
HB
MB
FB
ob+ot
fm
pfl
ce
F
jf
hyp
ce
mo
fm
jf
fo
ce

Figure 4

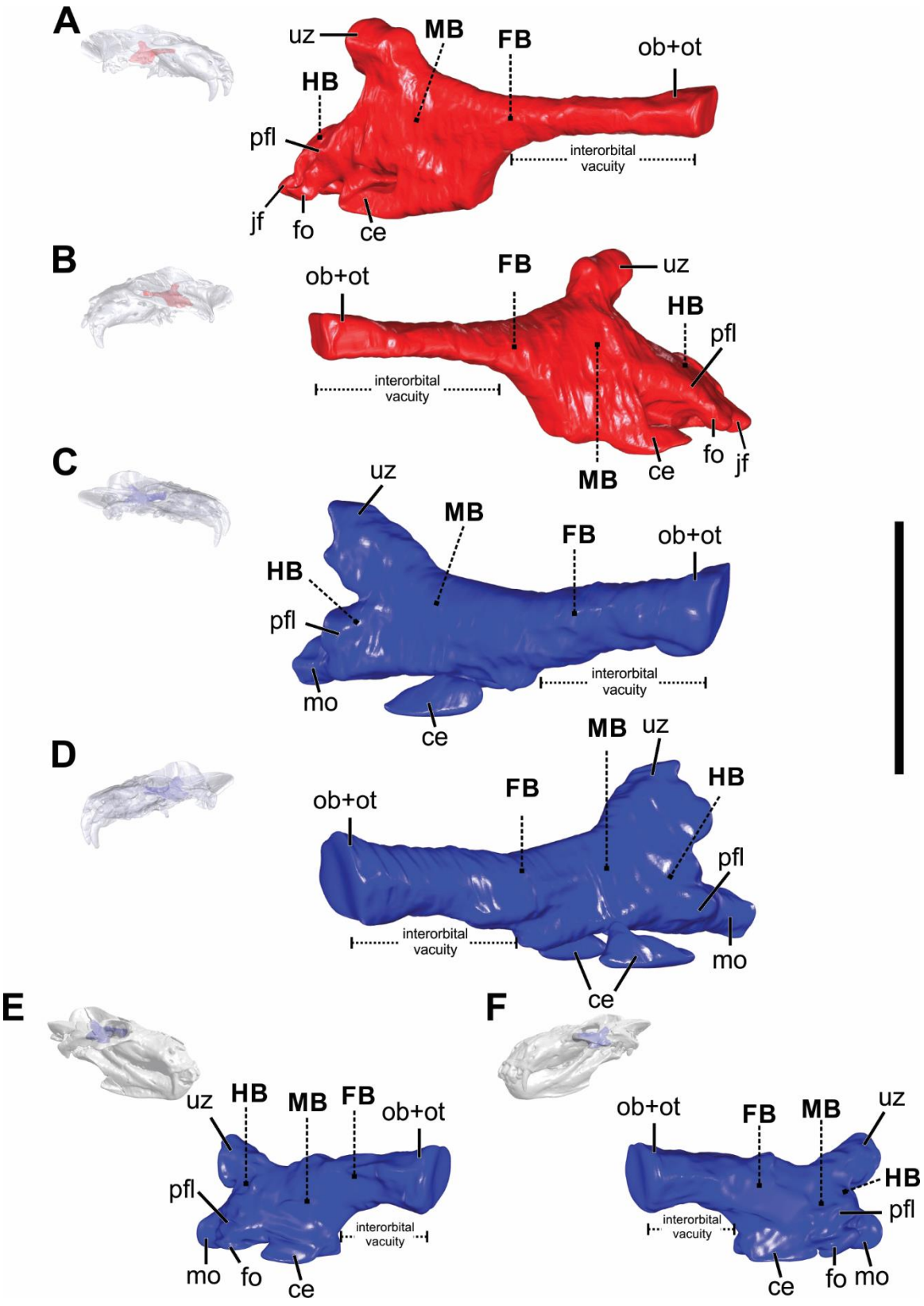
A
uz
MB
FB
ob+ot
HB
pfl
interorbital vacuity
jf
fo
ce
B
ob+ot
FB
uz
HB
pfl
interorbital vacuity
fo
jf
MB
ce
C
uz
MB
FB
ob+ot
HB
pfl
interorbital vacuity
mo
ce
D
MB
uz
HB
ob+ot
FB
pfl
interorbital vacuity
mo
ce
E
uz
HB
MB
FB
ob+ot
pfl
interorbital vacuity
mo
fo
ce
F
ob+ot
FB
MB
uz
HB
pfl
interorbital vacuity
ce
fo
mo

Figure 5


EQ1 and EQ2
EQ3
EQ1
EQ2
EQ3
Lemurosaurus¹
Lemurosaurus²
Moschops
Moschops³
Struticocephalus
Pristerodon
Lystrosaurus
Kawingasaurus
Niassodon
Aelurosaurus
Aloposaurus
Tetracynodon
Microgomphodon
Thrinaxodon⁴
Thrinaxodon⁵
Diademodon⁶
Diademodon⁷
Trirachodon
Andescynodon⁸
Andescynodon⁹
Massetognathus sp.¹⁰
Massetognathus¹¹
Massetognathus¹²
Massetognathus¹³
Exaeretodon sp.¹⁴
CAPPA/UFSM 0030
CAPPA/UFSM 0227
CAPPA/UFSM 0032
cf. Probelesodon
Probelesodon sp.
Probainognathus
Therioherpeton
Riograndia
Trirhyodon¹⁵
Trirhyodon¹⁶
Brasilodon
Morganucodon
Hadrocodium
Obourodon
Tachyglossus
Triconodon sp.
Ptilodus
Chulsanbaatar
Kryptobaatar
Vincelestes
Didelphis
Kennalestes
Asioryctes
Zambadalestes
Dasypus
Mammalia
Mammaliaformes
Probainognathia
Eucynodontia
Cynodontia
Theriodontia
Therapsida
Traversodontidae
Cynognathia
Gorgonopsia
Therocephalia
Dicynodontia
Dinocephalia
Biarmosuchia

Figure 6

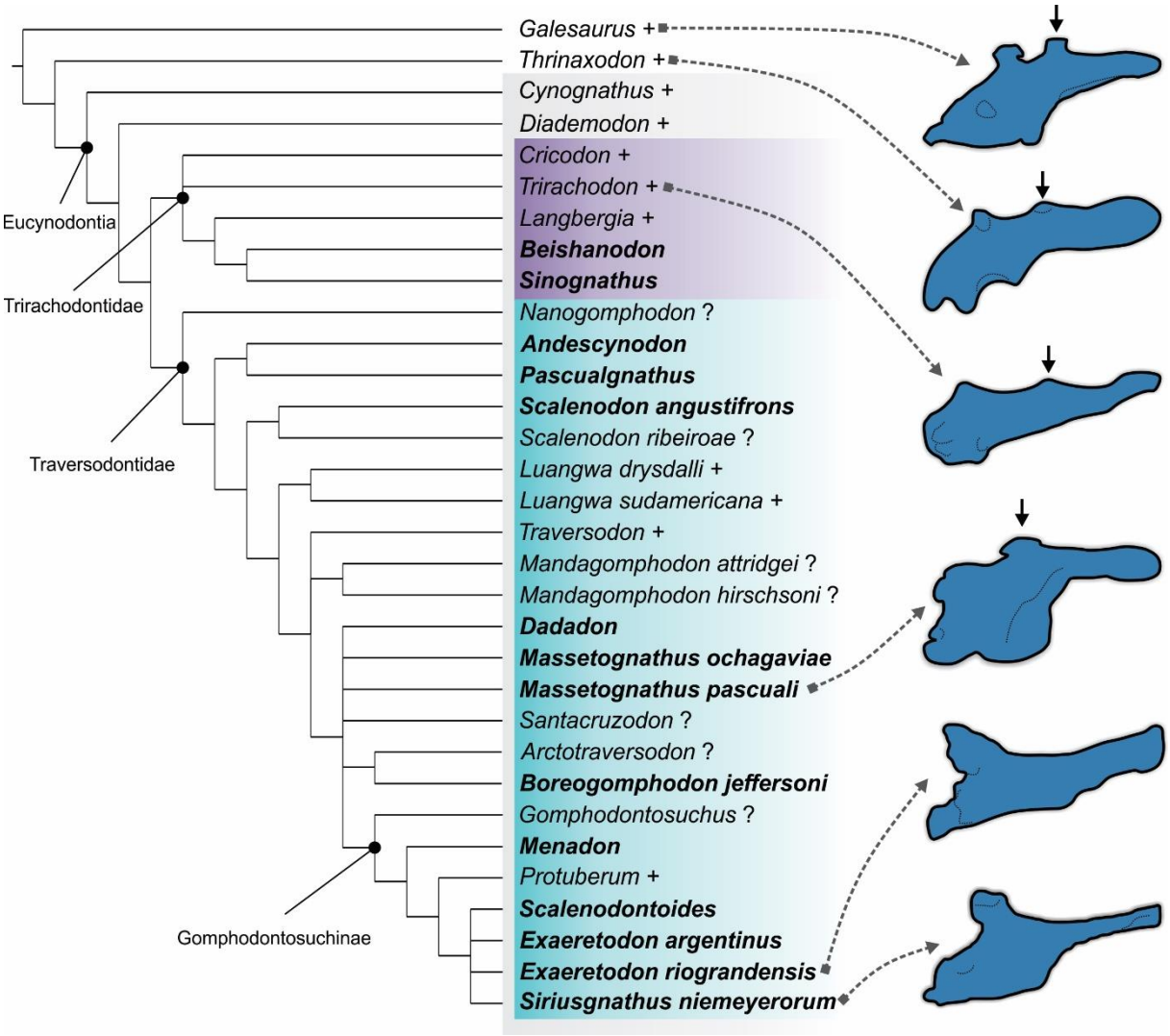
Galesaurus +
Thrinaxodon +
Cynognathus +
Diademodon +
Cricodon +
Trirachodon +
Langbergia +
Beishanodon
Sinognathus
Nanogomphodon ?
Andescynodon
Pascualgnathus
Scalenodon angustifrons
Scalenodon ribeiroae ?
Luangwa drysdalli +
Luangwa sudamericana +
Traversodon +
Mandagomphodon attridgei ?
Mandagomphodon hirschsoni ?
Dadadon
Massetognathus ochagaviae
Massetognathus pascuali
Santacruzodon ?
Arctotraversodon ?
Boreogomphodon jeffersoni
Gomphodontosuchus ?
Menadon
Protuberum +
Scalenodontoides
Exaeretodon argentinus
Exaeretodon riograndensis
Siriusgnathus niemeyerorum
Eucynodontia
Trirachodontidae
Traversodontidae
Gomphodontosuchinae

Figure 7

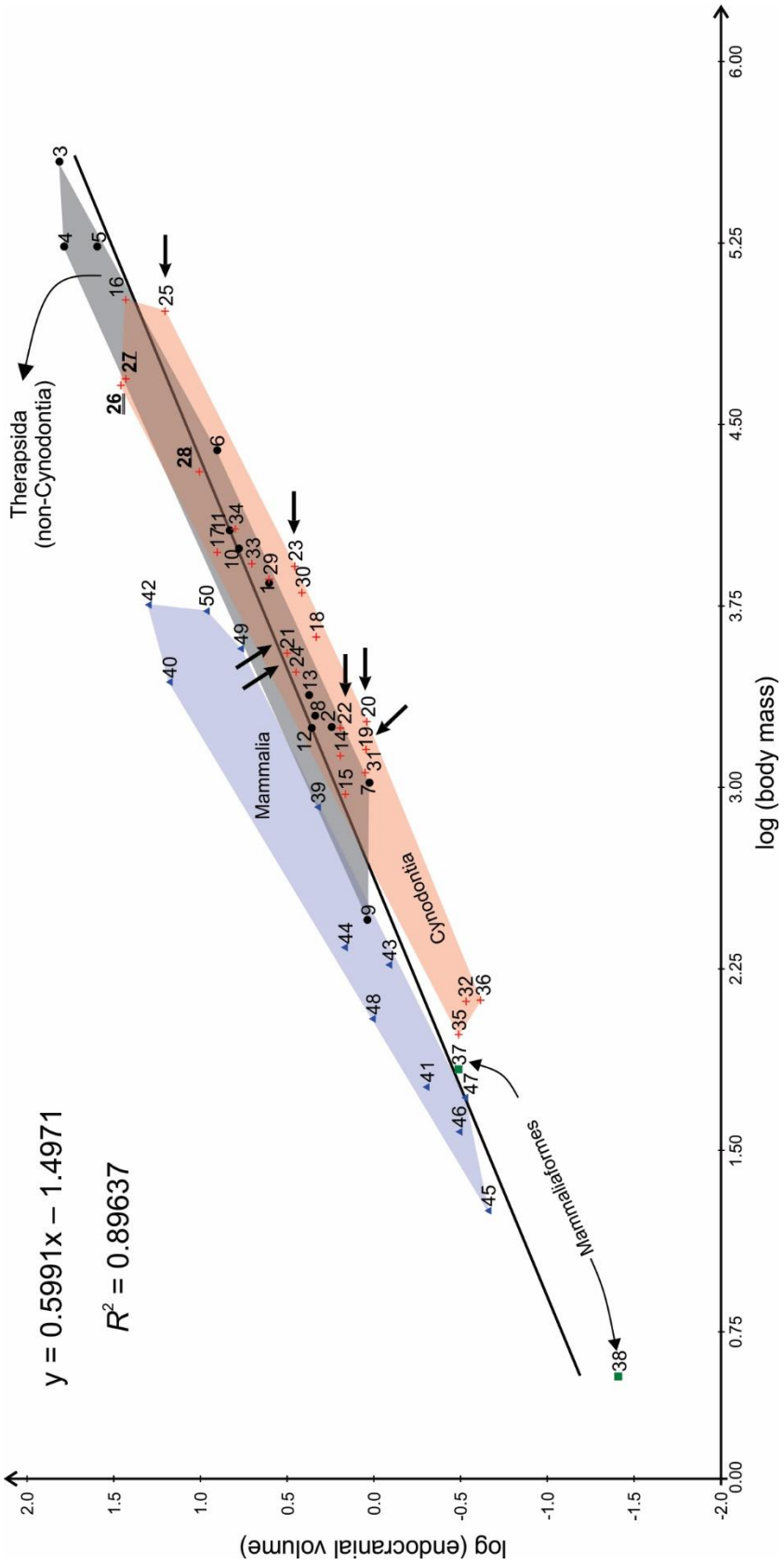
y = 0.5991x – 1.4971
R^2 = 0.89637
Therapsida
(non-Cynodontia)
Mammalia
Cynodontia
Mammaliaformes
log (endocranial volume)
log (body mass)
2.0
1.5
1.0
0.5
0.0
-0.5
-1.0
-1.5
0.00
0.75
1.50
2.25
3.00
3.75
4.50
5.25
6.00

Supporting Information

Table S1 - Estimation of the encephalization quotients and body mass. Data set of the Figures 5 and 7.

	Taxon		Specimen	SL	EVt	EV	OB	Source
1	*Lemurosaurus*	Biarmosuchia	NMQR 1702	118.53	—	**4.02**	—	Benoit, Fernandez, et al. (2017)
2	*Lemurosaurus*	Biarmosuchia	BP/1/816	75.2	—	**1.75**	—	Benoit, Fernandez, et al. (2017)
3	*Moschops*	Dinocephalia	AM 4950	340.19	—	**61.12**	—	Benoit, Manger, et al. (2017)
4	*Moschops*	Dinocephalia	AM 4950	—	—	**39.35**†	—	Benoit, Manger, et al. (2017)
5	*Strutiocephalus*	Dinocephalia	—	442.97	**65**	—	—	Boonstra (1968)
6	*Pristerodon*	Dicynodontia	MB.R. 985	78	**2.18**	—	—	Laaß (2015)
7	*Lystrosaurus*	Dicynodontia	—	180	—	**8**	—	Jerison (1973)
8	*Kawingasaurus*	Dicynodontia	GPIT/RE/9272	40.5	**1.09**	—	—	Laaß & Kaestner (2017)
9	*Niassodon*	Dicynodontia	ML 1620	63	**1.06**	—	—	Castanhinha et al. (2013)
10	*Aelurosaurus*	Gorgonopsia	BP/1/216	132.17	—	**6**	—	Benoit, Fernandez, et al. (2017)
11	*Aloposaurus* sp.	Gorgonopsia	GPIT/RE/7124	140	—	**6.77**	—	Araújo, Fernandez, Polcyn, Fröbisch, & Martins (2017)
12	*Tetracynodon*	Therocephalia	UCMP 42869	75	—	**2.28**‡	—	Sigurdsen, Huttenlocker, Modesto, Rowe, & Damiani (2012)
13	*Microgomphodon*	Therocephalia	SAM-PK-10160	83.2	—	**2.36**	—	Benoit, Fernandez, et al. (2017)
14	*Thrinaxodon*	Cynodontia	UCMP 40466	68.64	**1.56**	—	—	Macrini (2006)
15	*Thrinaxodon*	Cynodontia	—	—	**1.46**	—	—	Rowe et al. (2011)
16	*Diademodon*	Cynodontia	UCMP 42446	288	**26.97**	—	—	Macrini (2006)
17	*Diademodon*	Cynodontia	—	—	—	**8**	—	Jerison (1973)
18	*Trirachodon*	Cynodontia	—	100	—	**2.15**‡	—	Hopson (1979)
19	*Andescynodon*	Cynodontia	PVL 3899	70	1.2	**1.11**	0.09	Quiroga (1980a)
20	*Andescynodon*	Cynodontia	PVL 3894	76.5	—	**1.1**	—	Quiroga (1980a)
21	*Massetognathus* sp.	Cynodontia	PVL 4016	95	3.33	**3.163**	0.167	Quiroga (1979a; 1980b)
22	*M. pascuali*	Cynodontia	PVL 3905	75	1.66	**1.56**	0.1	Quiroga (1980a)
23	*M. pascuali*	Cynodontia	PVL 4168	125	3.15	**2.86**	0.29	Quiroga (1980a)
24	*M. pascuali*	Cynodontia	BP/1/4245	89.5	—	**2.81**	—	Benoit, Fernandez, et al. (2017)
25	*Exaeretodon* sp.	Cynodontia	—	278	19.91	**15.98**	3.93	Quiroga (1980b)
26	***Siriusgnathus***	**Cynodontia**	**CAPPA/UFSM 0032**	220.4	30.43	**28.80**	1.63	**This study**
27	***E. riograndensis***	**Cynodontia**	**CAPPA/UFSM 0030**	224.9	30.96	**26.43**	4.53	**This study**
28	***E. riograndensis***	**Cynodontia**	**CAPPA/UFSM 0227**	168.18	13.83	**11.47**	2.36	**This study**
29	cf. *Probelesodon*	Cynodontia	PVL 4015	120	4.33	**4.015**	0.315	Quiroga (1979a; 1980b)
30	*Probelesodon* sp.	Cynodontia	PVL 4167	115	3.1	**2.6**	0.48	Quiroga (1980a)
31	*Probainognathus*	Cynodontia	PVL 4169	65	1.2	**1.123**	0.077	Quiroga (1980b)
32	*Therioherpeton*	Cynodontia	MVP 05.22.04	31	0.36	**0.294**	0.065	Quiroga (1984)
33	*Riograndia*	Cynodontia	UFRGS-PV-596-T	35.08	0.404	**0.32**	0.079	Rodrigues et al. (2018)
34	*Tritylodon*	Cynodontia	BP/1/4778	126	—	**5.06**	—	Benoit, Fernandez, et al. (2017)
35	*Tritylodon*	Cynodontia	BP/1/5088	140.65	—	**6.30**	—	Benoit, Fernandez, et al. (2017)
36	*Brasilodon*	Cynodontia	UFRGS-PV-1043-T	38.03	0.378	**0.243**	0.136	Rodrigues et al. (2014)
37	*Morganucodon*	Mammaliaform	IVPP 8685	—	**0.325**	—	—	Rowe et al. (2011)
38	*Hadrocoidium*	Mammaliaform	IVPP 8275	12	0.045	**0.039**	0.006	Macrini (2006)
39	*Obdurodon*	Mammalia	QM F20568	134.4	15.443	**15.150**	0.293	Macrini, Rowe, & Archer (2006)
40	*Tachyglossus*	Mammalia	AMNH 154457	99	**20.013**	—	—	Macrini (2006)
41	*Triconodon* sp.	Mammalia	—	—	**0.820**	—	—	Quiroga (1980b)
42	*Ptilodus* sp.	Mammalia	—	—	**1.480**	—	—	Krause & Kielan-Jaworowska (1993)
43	*Chulsanbaatar*	Mammalia	—	—	**0.220**	—	—	Kielan-Jaworowska (1983)
44	*Kryptobaatar*	Mammalia	PSS-MAE 101	26	0.343	**0.323**	0.020	Macrini (2006)
45	*Vincelestes*	Mammalia	MACN-N 04	63	2.371	**2.115**	0.256	Macrini, Rougier, & Rowe (2007)
46	*Didelphis*	Mammalia	TMM M-2517	—	6.608	**5.879**	0.729	Macrini, Muizon, Cifelli, & Rowe (2007)
47	*Kennalestes*	Mammalia	ZPAL MgM-I/2; I/3	—	**0.299**	—	—	Kielan-Jaworowska (1984)
48	*Asioryctes*	Mammalia	ZPAL MgM-I/56	3	**0.500**	—	—	Kielan-Jaworowska (1984)
49	*Zalambdalestes*	Mammalia	ZPAL MgM-I/14 - 16	—	**1.02**	—	—	Kielan-Jaworowska (1984)
50	*Dasypus*	Mammalia	TMM M-7417	86.8	10.546	**9.254**	1.292	Macrini (2006)

(Continued on next page)

Table S1 (continued)

	BMa	BMb	BMc	ABM¶	EQ1 EVt	EQ2 EVt	EQ3 EVt	EQ1 EV	EQ2 EV	EQ3 EV
1	4496	7963	3198	5219	—	—	—	0,12 ± 0,03	0,15 ± 0,04	2,28 ± 0,49
2	1148	1917	916	1327	—	—	—	0,13 ± 0,03	0,17 ± 0,04	2,12 ± 0,36
3	106299	215918	63748	128655	—	—	—	0,22 ± 0,08	0,21 ± 0,09	5,89 ± 1,77
4	—	—	—	128655	—	—	—	0,14	0,14	3,79
5	234686	493346	136495	288176	0,14 ± 0,05*	0,13 ± 0,06	4,01 ± 1,28	—	—	—
6	1281	2149	1012	1481	0,15 ± 0,03	0,20 ± 0,05	2,48 ± 0,44	—	—	—
7	15746	29444	10342	18511	—	—	—	0,10 ± 0,03	0,12 ± 0,04	2,25 ± 0,57
8	179	276	180	212	0,26 ± 0,03	0,41 ± 0,06	3,64 ± 0,40	—	—	—
9	675	1101	570	782	0,11 ± 0,02	0,15 ± 0,03	1,72 ± 0,26	—	—	—
10	6234	11198	4334	7255	—	—	—	0,14 ± 0,04	0,17 ± 0,05	2,84 ± 0,64
11	7409	13409	5093	8637	—	—	—	0,14 ± 0,05	0,17 ± 0,05	2,91 ± 0,67
12	1139	1901	910	1317	—	—	—	0,17 ± 0,03	0,23 ± 0,05	2,77 ± 0,47
13	1555	2630	1206	1797	—	—	—	0,14 ± 0,03	0,19 ± 0,04	2,41 ± 0,44
14	873	1440	717	1010	0,14 ± 0,03	0,19 ± 0,04	2,19 ± 0,36	—	—	—
15	—	—	—	*700*	0,16	0,23	2,52	—	—	—
16	64497	128203	39506	77402	0,13 ± 0,05	0,14 ± 0,05	3,44 ± 0,99	—	—	—
17	—	—	—	*7000*	—	—	—	0,19	0,23	3,86
18	2700	4677	1997	3125	—	—	—	0,09 ± 0,02	0,11 ± 0,03	1,62 ± 0,32
19	926	1532	755	1071	0,10 ± 0,02	0,14 ± 0,03	1,63 ± 0,27	0,09 ± 0,02	0,13 ± 0,03	1,51 ± 0,25
20	1209	2022	960	1397	—	—	—	0,08 ± 0,02	0,10 ± 0,02	1,29 ± 0,22
21	2315	3984	1734	2677	0,15 ± 0,04	0,20 ± 0,05	2,73 ± 0,53	0,14 ± 0,03	0,19 ± 0,05	2,60 ± 0,50
22	1139	1901	910	1317	0,12 ± 0,02	0,16 ± 0,04	2,02 ± 0,35	0,11 ± 0,02	0,15 ± 0,04	1,90 ± 0,36
23	5273	9404	3709	6129	0,08 ± 0,03	0,10 ± 0,03	1,64 ± 0,36	0,08 ± 0,02	0,09 ± 0,03	1,48 ± 0,33
24	1936	3305	1472	2238	—	—	—	0,14 ± 0,03	0,19 ± 0,05	2,55 ± 0,48
25	58009	114778	35699	69496	0,11 ± 0,04	0,11 ± 0,04	2,70 ± 0,77	0,08 ± 0,03	0,09 ± 0,03	2,17 ± 0,62
26	28907	55495	18385	34262	0,20 ± 0,06	0,23 ± 0,08	4,37 ± 1,07	0,17 ± 0,05	0,19 ± 0,06	3,62 ± 0,89
27	30714	59119	19475	36436	0,26 ± 0,08	0,28 ± 0,10	6,10 ± 1,63	0,24 ± 0,08	0,27 ± 0,10	5,77 ± 1,54
28	12844	23805	8535	15061	0,25 ± 0,08	0,27 ± 0,10	6,00 ± 1,61	0,21 ± 0,07	0,23 ± 0,08	5,12 ± 1,38
29	4666	8276	3310	5417	0,12 ± 0,03	0,15 ± 0,04	2,41 ± 0,52	0,11 ± 0,03	0,14 ± 0,04	2,23 ± 0,48
30	4106	7244	2940	4764	0,10 ± 0,02	0,12 ± 0,03	1,85 ± 0,39	0,08 ± 0,02	0,10 ± 0,03	1,55 ± 0,33
31	741	1215	619	858	0,12 ± 0,02	0,16 ± 0,03	1,85 ± 0,29	0,11 ± 0,02	0,15 ± 0,03	1,73 ± 0,27
32	80	120	93	98	0,15 ± 0,02	0,24 ± 0,03	1,84 ± 0,17	0,12 ± 0,01	0,19 ± 0,02	1,51 ± 0,14
33	—	—	—	*71.15*	0.20	0.34	2.47	0,16	0,27	1,98

34	5401	9642	3792	6278	—	—	—	0,13 ± 0,03	0,16 ± 0,05	2,59 ± 0,57
35	7512	13604	5159	8759	—	—	—	0,13 ± 0,04	0,16 ± 0,05	2,68 ± 0,62
36	—	—	—	*98.6*	0.15	0.25	1.93	0,12 ± 0,03	0,15 ± 0,04	2,28 ± 0,49
37	—	—	—	*51*	0.20	0.35	2.38	—	—	—
38	—	—	—	*2.75*§	0.19	0.40	1.66	0.17	0.35	1.44
39	—	—	—	*2038*	0.84	1.11	14.74	0.83	1.09	14.46
40	—	—	—	*4250*	0.67	0.84	12.72	—	—	—
41	—	—	—	*138*	0.26	0.42	3.47	—	—	—
42	—	—	—	*163*	0.43	0.67	5.71	—	—	—
43	—	—	—	*13.3*	0.33	0.62	3.39	—	—	—
44	—	—	—	*28.18*	0.32	0.56	3.49	0.30	0.53	3.29
45	—	—	—	*619*	0.28	0.41	4.37	0.25	0.36	3.90
46	—	—	—	*2800*	0.29	0.38	5.29	0.26	0.34	4.71
47	—	—	—	*39*	0.22	0.39	2.54	—	—	—
48	—	—	—	*43.2*	0.35	0.60	4.02	—	—	—
49	—	—	—	*82.69*	0.46	0.76	5.73	—	—	—
50	—	—	—	*4000*	0.37	0.46	6.93	0.32	0.41	6.08

Notes: **SL** - Basal skull length (in mm); **EVt** - Endocast volume total (with the olfactory bulb), in g or cm^3; **EV** - Endocast volume without the olfactory bulb (in g or cm^3); **OB** - Olfactory bulbs volume (in g or cm^3); **BM** - Body mass (in g); **BMa** – Quiroga (1980); **BMb** - Hu et al. (2005); **BMc** - Castanhinha et al. (2013); **ABM** - Average body mass; **EQ** - Encephalization quotient; **EQ1** – Jerison (1973); **EQ2** – Manger (2006); **EQ3** – Hurlburt et al. (2013). † EV without the pineal tube; ‡ EV from Benoit, Fernandez, et al. (2017), using graphic double integration; **§** Body mass from Luo, Crompton, & Sun (2001). ¶ The body mass values in italic were taken from the literature. * Variation of the EQ value according to the BM variation. The EVs in bold were the values used in the chart of Figure 7. Data modified from Benoit, Fernandez, et al. (2017); Benoit, Manger, et al. (2017); Laaß (2015); Laaß & Kaestner (2017).

5 DISCUSSÃO

5.1 BIOESTRATIGRAFIA DO SÍTIO NIEMEYER

Os resultados obtidos nessa tese trazem novas informações sobre cinodontes da família Traversodontidae, assim como a apresentação de uma nova localidade fossilífera para o Triássico do sul do Brasil. A nova localidade, nomeada Sítio Niemeyer, apresenta uma fauna distinta daquelas encontradas nas quatro Zonas de Associação (ZAs) da Supersequência Santa Maria classificadas pelos seus conteúdos faunísticos, presentes no Meso- e Neotriássico do sul do Brasil. Como nenhum fóssil representativo das quatro ZAs foi encontrado no Sítio Niemeyer até o momento, não foi possível atribuí-lo a uma das ZAs conhecidas, contudo a sua litologia é consistente com a da Sequência Candelária (HORN et al., 2014).

O conteúdo fossilífero do Sítio Niemeyer chama atenção devido à grande acumulação de fósseis de cinodontes traversodontídeos, possivelmente pertencentes ao mesmo táxon, que representa uma nova unidade taxonômica, nomeada de *Siriusgnathus niemeyerorum*, o qual apresenta proximidade morfológica e filogenética com *Exaeretodon riograndensis*. A ZA de *Santacruzodon*, Sequência Santa Cruz, também apresenta um predomínio de registros de traversodontídeos, sendo representados por *Santacruzodon hopsoni*, *Menadon besairiei* e *Massetognathus ochagaviae* (ABDALA et al., 2009; ABDALA; RIBEIRO, 2010; MELO; ABDALA; SOARES, 2015; SCHMITT et al., 2019). O Sítio Niemeyer está inserido no bloco estrutural Agudo, onde são encontrados afloramentos que apresentam correlação bioestratigráfica com a ZA de *Hyperodapedon* e de *Riograndia*, ambas da Sequência Candelária (DA-ROSA, 2015; DA-ROSA; FACCINI, 2005; HORN et al., 2014). Para a ZA de *Hyperodapedon* (Final do Carniano, Nível Inferior da Sequência Candelária) temos o Sítio Janner, localizado nas cercanias do Município de Agudo (HORN et al., 2014; LANGER et al., 2007; LANGER; RAMEZANI; DA-ROSA, 2018; MÜLLER et al., 2015a; PRETTO; SCHULTZ; LANGER, 2015); os sítios ASSERMA e Concórdia, na área urbana do Município de Agudo, preliminarmente atribuídos a ZA de *Hyperodapedon* devido a presença de formas semelhantes a *Exaeretodon*. Para ZA de *Riograndia* (Noriano, Nível Superior da Sequência Candelária), o local da coleta do holótipo de *Sacisaurus agudoensis*, na área urbana do Município de Agudo (FERIGOLO; LANGER, 2007; LANGER; FERIGOLO, 2013; LANGER; RAMEZANI; DA-ROSA, 2018; RIBEIRO; ABDALA; BERTONI, 2011). Além dessas localidades, também está inserido no bloco Agudo o Sítio Wachholz localizado na área rural do Município de Agudo, início do Noriano (Nível Superior da Sequência Candelária),

onde foram coletados dinossauros sauropodomorfos (MÜLLER et al., 2015b; MÜLLER; LANGER; DIAS-DA-SILVA, 2017, 2018). O conteúdo faunístico do Sítio Niemeyer e da ZA de *Hyperodapedon* apresentam semelhanças dignas de nota e assim relevantes para sua possível conexão com essa ZA, como a presença de um traversodontídeo de grande porte, a possível presença compartilhada de *Trucidocynodon* Oliveira; Soares; Schultz, 2010, uma vez que um úmero proveniente do Sítio Niemeyer apresenta características que lembram o úmero do referido táxon, como canal bicipital profundo, crista deltopeitoral fortemente voltada ventralmente, crista ectepicondilar grande e forâmen ectepicondilar ausente. Além da presença de um possível Dinosauromorpha Benton, 1985. Contudo a ausência de registros de *Hyperodapedon* no Sítio Niemeyer, ou de outros taxa da ZA de *Hyperodapedon*, impossibilita uma atribuição segura deste sítio com essa ZA. Como, a princípio, não há registros de traversodontídeos nos níveis superiores do Sequência Candelária (e.g., ZA de *Riograndia*), é mais provável que o Sítio Niemeyer esteja inserido nos níveis inferiores da Sequência Candelária. Contudo, como mencionado anteriormente (subitem 1.4), Ribeiro; Abdala; Bertoni (2011) reportam a presença de registros fragmentários de Traversodontidae (cf. *Exaeretodon*) para a ZA de *Riograndia*, o que levanta duas hipóteses:

1. *Exaeretodon* poderia ter sobrevivido até a ZA de *Riograndia*, com um registro mais longevo do que o observado até então;

2. *Exaeretodon* poderia ter sobrevivido até o contato entre as ZAs de *Hyperodapedon* e *Riograndia*. Sendo primeiramente preservado no topo da ZA de *Hyperodapedon*, posteriormente retrabalhado e finalmente redepositado na ZA de *Riograndia*.

No entanto, com a descrição de *Siriusgnathus*, levando em consideração a semelhença na morfologia, principalmente em relação à dentição, entre *Siriusgnathus* e *E. riograndensis*, e a ausência de uma ZA definida para o primeiro táxon, levanta uma terceira hipótese alternativa:

3. Os espécimens de Traversodontidae da ZA de *Riograndia*, podem ser *Siriusgnathus*, em vez de *Exaeretodon*, sendo os seus registros mais recentes do que o teorizado previamente.

No entanto, novas informações precisam ser levantadas para a corroborar ou não alguma dessas hipóteses.

5.2 PALEONEUROLOGIA EM TRAVERSODONTIDAE

O novo táxon descrito, *S. niemeyerorum*, proveniente do Sitio Niemeyer, teve além de sua morfologia externa, a morfologia interna da cavidade cerebral também foi descrita, juntamente com a de *E. riograndensis*. De formal geral, a morfologia do endocrânio de ambas as espécies é mais próxima do padrão "reptiliano" do que do observado em mamaliaformes e mamíferos, já que apresentam bulbos olfatórios, hemisférios cerebrais e cerebelo ainda pouco diferenciados, como é o caso observado em outros cinodontes como *Thrinaxodon*, *Galesaurus*, *Trirachodon*, *Massetognathus*, *Exaeretodon argentinus* e cf. *Probelesodon* (BONAPARTE, 1966b; HOPSON, 1979; KIELAN-JAWOROWSKA; CIFELLI; LUO, 2004; PUSCH; KAMMERER; FRÖBISCH, 2019; QUIROGA, 1979a, 1980a). Por outro lado, nos probainognátios *Probainognathus*, *Riograndia* e *Brasilitherium*, os bulbos olfatórios e hemisférios cerebrais são mais diferenciados e apresentam um grande aumento no volume, principalmente em *Riograndia* e *Brasilitherium* (QUIROGA, 1980b; RODRIGUES et al., 2018; RODRIGUES; RUF; SCHULTZ, 2014).

Uma estrutura que chama a atenção no molde endocraniano de *S. niemeyerorum* e *E. riograndensis* é a zona não ossificada. Está estrutura é bem deselvolvida e diferenciada do resto do molde endocraniano em ambos os taxa. Qual estrutural cerebral preencheria a zona não ossificado bem sendo debatida ao longo dos anos e várias hipóteses foram levantadas:

1. O *vermis* do cerebelo (KIELAN-JAWOROWSKA; CIFELLI; LUO, 2004);

2. Seios venosos, como o seio sagital superior (MACRINI, 2006; QUIROGA, 1979a; ROWE; CARLSON; BOTTORFF, 1995);

3. A glândula pineal (KEMP, 2009);

4. Área cartilaginosa no osso supraoccipital (OLSON, 1944).

A hipótese dos seios venosos vem ganhando força, recentemente Laass; Schillinger; Kaestner (2017), com base em um crânio bem preservado do dicinodonte *Diictodon feliceps* Owen, 1876, encontraram impressões de vasos sanguíneos na zona não ossificada, sendo interpretados como a junção do seio sagital superior e do seio transverso. Em um dos espécimens de *E. riograndensis* analisados (CAPPA/UFSM 0227; ver artigo 2, Seção 4 – Figura 2H), apresenda uma possível impressão de um vaso sanguíneo, aparentemente conectado com a zona não ossificada, de forma similar ao observado em *D. feliceps*. Outra semelhança compartilhada entre *S. niemeyerorum* e *E. riograndensis* com *D. feliceps* é a presença de um entalhe formado pelo supraoccipital, que separa de parcialmente a zona não ossificada do resto do molde endocraniano (LAASS; SCHILLINGER; KAESTNER, 2017).

E. riograndensis (CAPPA/UFSM 0030) apresenta o molde dos *paraflocculus* proeminentes, como observado em *Galesaurus*, *Massetognathus*, *E. riograndensis*, cf. *Probelesodon* e *Probainognathus* (BONAPARTE, 1966b; PUSCH; KAMMERER; FRÖBISCH, 2019; QUIROGA, 1979a, 1980b). Em *S. niemeyerorum* o molde dos *paraflocculus* são poucos distinguíveis do restante do molde endocraniano. A presença de *paraflocculus* proeminentes foi considerada como uma característica derivada dentro de Cynodontia por Kielan-Jaworowska; Cifelli; Luo (2004), em comparação com os demais Therapsida, que apresentam *paraflocculus* pouco desenvolvidos. Por outro lado, Hopson (1979) argumenta que a presença/ausência de *paraflocculus* pode estar relacionado com o grau de contato entre o cérebro e a cavidade cerebral, como exemplificado pelos dicinodontes: em taxa de pequeno tamanho (e.g., *Kawingasaurus* Cox, 1972), onde há um contado mais próximo entre o cérebro e a cavidade cerebral, os *paraflocculus* apresentam-se bem desenvolvidos (LAASS; KAESTNER, 2017). Já em taxa de grande tamanho, onde haveria um maior espaço entre o cérebro e a cavidade cerebral, os *paraflocculus* estão ausentes (e.g. *Kannemeyeria*) ou são vestigiais (e.g. *Lystrosaurus* Cope, 1870) (ANGIELCZYK; KURKIN, 2003; LAASS; KAESTNER, 2017).

Em *S. niemeyerorum* e *E. riograndensis* o foramen parietal, bem como tubo pineal estão ausentes. Dentro de Traversodontidae há uma grande variação na presença/ausência dessas estruturas. Mais especificamente em relação aos traversodontídeos do Triássico sul-brasileiro, o foramen parietal está presente nos taxa do Ladiniano-Eocarniano: *Luangwa sudamericana*, *Traversodon* e *Protuberum* (LIU; ABDALA, 2014). Nos taxa do Eo-Neocarniano, *Menadon*, *S. niemeyerorum* e *E. riograndensis*, o foramen pineal está ausente. Contudo, há também uma variação ontogenética na presença/ausência do foramen parietal em Traversodondidae. Em *Massetognathus pascuali*, o parietal foramen está presente em espécimens considerados imaturos, mas vai gradualmente sendo reduzido em tamanho até a completa obliteração do foramen em espécimens considerados adultos (ABDALA; GIANNINI, 2000). Contudo, possivelmente apenas o foramen parietal é perdido, permanecendo o tubo pineal. Em Massetognathus ochagaviae, o foramen parietal é considerado ausente, mas o tubo pineal está presente (HOFFMANN, 2018; LIU; ABDALA, 2014). Em Dadadon, também há variação ontogenética, estando o foramen parietal presente em espécimens juvenis e ausente em indivíduos adultos (BENOIT et al., 2016).

6 CONCLUSÕES

Na presente tese um novo táxon da família Traversodontidae, *Siriusgnathus niemeyerorum* foi apresentado e descrito, o qual é morfológica e filogeneticamente relacionado a *Exaeretodon riograndensis*. O novo táxon procede de uma nova localidade fossilífera, nomeada Sítio Niemeyer também aqui apresentada. O conteúdo fossilífero do Sítio Niemeyer possui afinidades com a fauna da ZA de *Hyperodapedon*. Contudo, como nenhum fóssil guia foi encontrado até o momento, não foi possível atribuir com segurança esta nova localidade a nenhuma das ZA conhecidas. Foi atribuída uma idade Carniana para o Sítio Niemeyer, devido a sua litologia condizente com a da Sequência Candelária e devido a provável ausência de registros de cinodontes traversodontídeos nos níveis superiores e recentes da sequência (i.e., ZA de *Riograndia*).

A anatomia crânio-dental *S. niemeyerorum* foi descrita em detalhes, assim como a anatomia da sua cavidade cerebral, bem como a cavidade cerebral de *E. riograndensis*. Apesar de não possuir nenhuma autapomorfia clara, *S. niemeyerorum* apresenta uma combinação de características crânio-dentais única. A cavidade cerebral de ambos os taxa não é completamente ossificada e o endocrânio é alongado, com as estruturas cerebrais pouco diferenciadas, como observado para outros cinodontes não-mamaliaformes. Contudo em *E. riograndensis* foi possível observar a presença do orbitoesfenoide, *S. niemeyerorum* apresenta a fossa hipofiseal bem desenvolvida e em ambos a zona não ossificada é grande e bem desenvolvida.

Sendo assim, este trabalho amplia o conhecimento sobre a família Traversodontidae, com a apresentação do novo táxon e agrega novas informações sobre o endocrânio de cinodontes não-mamaliaformes, ainda pouco estudado.

7 REFERÊNCIAS BIBLIOGRÁFICAS

ABDALA, F. Redescription of *Platycraniellus elegans* (Therapsida, Cynodontia) from the lower Triassic of South Africa, and the cladistic relationships of Eutheriodonts. **Palaeontology**, v. 50, n. 3, p. 591–618, 2007.

ABDALA, F. et al. A non-mammaliaform cynodont from the Upper Triassic of South Africa: a therapsid Lazarus taxon? **Palaeontologia Africana**, v. 42, p. 17–23, 2007.

ABDALA, F. et al. South American Middle Triassic continental faunas with amniotes: biostratigraphy and correlation. **Palaeontologia Africana**, v. 44, p. 83–87, 2009.

ABDALA, F.; BARBERENA, M. C.; DORNELLES, J. A new species of the traversodontid cynodont *Exaeretodon* from the Santa Maria Formation (Middle/Late Triassic) of Southern Brazil. **Journal of Vertebrate Paleontology**, v. 22, n. 2, p. 313–325, 2002.

ABDALA, F.; GIANNINI, N. P. Gomphodont Cynodonts of the Chañares Formation : the Analysis of an Ontogenetic Sequence. **Journal of Vertebrate Paleontology**, v. 20, n. 3, p. 501–506, 2000.

ABDALA, F.; NEVELING, J.; WELMAN, J. A new trirachodontid cynodont from the lower levels of the Burgersdorp Formation (Lower Triassic) of the Beaufort Group, South Africa and the cladistic relationships of Gondwanan gomphodonts. **Zoological Journal of the Linnean Society**, v. 147, n. 3, p. 383–413, 2006.

ABDALA, F.; RIBEIRO, A. M. A new traversodontid cynodont from the Santa Maria Formation (Ladinian-Carnian) of southern Brazil , with a phylogenetic analysis of Gondwanan traversodontids. **Zoological Journal of the Linnean Society**, v. 139, p. 529–545, 2003.

ABDALA, F.; RIBEIRO, A. M. Distribution and diversity patterns of Triassic cynodonts (Therapsida, Cynodontia) in Gondwana. **Palaeogeography, Palaeoclimatology, Palaeoecology**, v. 286, p. 202–217, 2010.

ABDALA, F.; RIBEIRO, A. M.; SCHULTZ, C. L. A rich cynodont fauna of Santa Cruz do Sul, Santa Maria Formation (Middle-Late Triassic), southern Brazil. **Neues Jahrbuch für Geologie und Paläontologie - Monatshefte**, v. 2001, n. 11, p. 669–687, 2001.

ABDALA, F.; SA-TEIXEIRA, A. M. A traversodontid cynodont of African affinity in the South American Triassic. **Palaeontologia Africana**, v. 40, p. 11–22, 2004.

ALLMAN, J. The origin of the neocortex. **The Neurosciences**, v. 2, p. 257–262, 1990.

ANGIELCZYK, K. D.; KURKIN, A. A. Phylogenetic analysis of Russian Permian dicynodonts (Therapsida: Anomodontia): Implications for Permian biostratigraphy and Pangaean biogeography. **Zoological Journal of the Linnean Society**, v. 139, n. 2, p. 157–212, 2003.

ARAÚJO, R. et al. Aspects of gorgonopsian paleobiology and evolution: insights from the basicranium, occiput, osseous labyrinth , vasculature, and neuroanatomy. **PeerJ**, v. 5, n. e3119, p. 1–45, 2017.

BARBERENA, M. Novos Materiais de *Traversodon stahleckeri* da Formação Santa Maria (Triássico do Rio Grande do Sul). **Pesquisas em Geociências**, v. 14, n. 14, p. 149–162, 1981a.

BARBERENA, M. Uma Nova Espécie de *Massetognathus* (*Massetognathus ochagaviae*, sp.nov.). **Pesquisas em Geociências**, v. 14, n. 14, p. 181–195, 1981b.

BENDEL, E.-M. et al. Cranial anatomy of the gorgonopsian *Cynariops robustus* based on CT-reconstruction. **PLoS ONE**, v. 13, n. 11, p. e0207367, 2018.

BENOIT, J. et al. The sixth sense in mammalians forerunners: Variability of the parietal foramen and the evolution of the pineal eye in South African Permo-Triassic eutheriodont therapsids. **Acta Palaeontologica Polonica**, v. 61, n. 4, p. 777–789, 2016.

BENOIT, J. et al. Endocranial Casts of Pre-Mammalian Therapsids Reveal an Unexpected Neurological Diversity at the Deep Evolutionary Root of Mammals. **Brain, Behavior and Evolution**, v. 90, n. 4, p. 311–333, 2017a.

BENOIT, J. et al. Synchrotron scanning reveals the palaeoneurology of the head-butting *Moschops capensis* (Therapsida , Dinocephalia). **PeerJ**, v. 5, n. e3496, p. 1–27, 2017b.

BENOIT, J. et al. The bony labyrinth of late Permian Biarmosuchia: palaeobiology and diversity in non-mammalian Therapsida. **Palaeontologica Africana**, v. 52, p. 58–77, 2017c.

BENOIT, J.; MANGER, P. R.; RUBIDGE, B. S. Palaeoneurological clues to the evolution of defining mammalian soft tissue traits. **Scientific Reports**, v. 6, n. 25604, p. 1–10, 2016.

BENTON, M. J. No gap in the Middle Permian record of terrestrial vertebrates. **Geology**, v. 40, n. 4, p. 339–342, 2012.

BONAPARTE, J. F. Descripción del cráneo y mandíbula de *Exaeretodon frenguellii*, Cabrera. **Publicaciones del Museo Municipal de Ciencias Naturales y Tradicional de Mar del Plata**, v. 1, p. 137–202, 1962.

BONAPARTE, J. F. Una nueva "fauna" triásica de Argentina (Therapsida: Cynodontia Dicynodontia) Consideraciones filogenéticas y paleobiogeográficas. **Ameghiniana**, v. 4, n. 8, p. 243–296, 1966a.

BONAPARTE, J. F. Sobre las cavidades cerebral, nasal y otras estructuras del cráneo de *Exaeretodon*. **Acta Geológica Lilloana**, v. 8, p. 5–29, 1966b.

BONAPARTE, J. F. Dos nuevas "faunas" de reptiles triásicos de Argentina. Gondwana Stratigraphy, I.U.G.S. In: IUGS SYMPOSIUM - GONDWANA STRATIGRAPHY, 1., 1967, Buenos Aires/AR. **Anais**… Buenos Aires/AR, 1969, p. 283-306.

BONAPARTE, J. F. et al. The sister group of Mammals: Small cynodonts from the Late Triassic of Southern Brazil. **Revista Brasileira de Paleontologia**, v. 5, p. 5–27, 2003.

BONAPARTE, J. F. et al. La fauna local de Faxinal do Soturno, Triásico Tardío de Rio Grande do Sul, Brasil. **Revista Brasileira de Paleontologia**, v. 13, n. 3, p. 233–246, 2010.

BONAPARTE, J. F.; FERIGOLO, J.; RIBEIRO, A. M. A primitive Late Triassic “ictidosaur” from Rio Grande do Sul, Brazil. **Palaeontology**, v. 44, n. 4, p. 623–635, 2001.

BONAPARTE, J. F.; MARTINELLI, A. G.; SCHULTZ, C. L. On the sister group of mammals: *Brasilodon* and *Brasilitherium* (Cynodontia, Probainognathia) from the Late Triassic of Southern Brazil. **Revista Brasileira de Paleontologia**, v. 8, n. 1, p. 25–46, 2005.

BONAPARTE, J. F.; SOARES, M. B.; MARTINELLI, A. G. Discoveries in the Late Triassic of Brazil Improve Knowledge on the Origin of Mammals. **Historia Natural**, v. 2, n. 2, p. 5–30, 2013.

BOONSTRA, L. D. The braincase, basicranial axis and mediam septum in the Dinocephalia. **Annals of The South African Museum**, v. 50, p. 195–273, 1968.

BOTHA-BRINK, J.; MODESTO, S. P. A mixed-age classed “pelycosaur” aggregation from South Africa: Earliest evidence of parental care in amniotes? **Proceedings of the Royal Society B: Biological Sciences**, v. 274, n. 1627, p. 2829–2834, 2007.

BOTHA, J.; ABDALA, F.; SMITH, R. The oldest cynodont: New clues on the origin and early diversification of the Cynodontia. **Zoological Journal of the Linnean Society**, v. 149, n. 3, p. 477–492, 2007.

BRINK, A. S. Two cynodonts from the Ntawere Formation in the Luangwa Valley of northern Rhodesia. **Palaeontologia Africana**, v. 8, p. 77–96, 1963.

CABREIRA, S. F. et al. New stem-sauropodomorph (Dinosauria, Saurischia) from the Triassic of Brazil. **Naturwissenschaften**, v. 98, n. 12, p. 1035–1040, 2011.

CABREIRA, S. F. et al. A Unique Late Triassic Dinosauromorph Assemblage Reveals Dinosaur Ancestral Anatomy and Diet. **Current Biology**, v. 26, n. 22, p. 3090–3095, 2016.

CASTANHINHA, R. et al. Bringing Dicynodonts Back to Life : Paleobiology and Anatomy of a New Emydopoid Genus from the Upper Permian of Mozambique. **PLoS ONE**, v. 8, n. 12, p. e80974, 2013.

CHATTERJEE, S. A New Cynodont Reptile from the Triassic of India. **Journal of Paleontology**, v. 56, n. 1, p. 203–214, 1982.

CROMPTON, A. W. On some Triassic cynodonts from Tanganyika. **Proceedings of the Zoological Society of London**, v. 125, n. 3–4, p. 617–669, 1955.

CROMPTON, A. W. Postcanine Occlusion in Cynodonts and Tritylodontids. **Bulletin of the British Museum (Natural History)**, v. 21, n. 2, p. 27–71, 1972.

CROMPTON, A. W.; ELLENBERGER, F. On a new cynodont from the Molteno beds and the origin of the Tritylodontids. **Annals of the South African Museum**, v. 44, p. 1–14, 1957.

DA-ROSA, Á. A. S. Geological context of the dinosauriform-bearing outcrops from the Triassic of Southern Brazil. **Journal of South American Earth Sciences**, v. 61, p. 108–119,

2015.
DA-ROSA, Á. A. S.; FACCINI, U. F. Delimitação de blocos estruturais de diferentes escalas em seqüências mezosóicas do Estado do Rio Grande do Sul: implicações bioestratigraficas. **Gaea-Journal of Geoscience**, v. 1, n. 1, p. 16–23, 2005.

DAY, M. O. et al. When and how did the terrestrial mid-Permian mass extinction occur? Evidence from the tetrapod record of the Karoo Basin, South Africa. **Proceedings of the Royal Society B: Biological Sciences**, v. 282, n. 1811, p. 20150834, 2015.

EDINGER, T. Midbrain exposure and overlap in Mammals. **American Zoologist**, v. 4, p. 5–19, 1964.

EZCURRA, M. et al. Deep faunistic turnovers preceded the rise of dinosaurs in southwestern Pangaea. **Nature Ecology & Evolution**, v. 1, p. 1477–1483, 2017.

FERIGOLO, J.; LANGER, M. C. A Late Triassic dinosauriform from south Brazil and the origin of the ornithischian predentary bone. **Historical Biology**, v. 19, n. 1, p. 23–33, 2007.

FLYNN, J. J. et al. New Traversodontids (Synapsida: Eucynodontia) from the Triassic of Madagascar. **Journal of Vertebrate Paleontology**, v. 20, n. 3, p. 422–427, 2000.

GAO, K.-Q. et al. A New Nonmammalian Eucynodont (Synapsida: Therapsida) from the Triassic of Northern Gansu Province, China, and its Biostratigraphic and Biogeographic Implications. **American Museum Novitates**, v. 3685, p. 1–25, 2010.

GUIGNARD, M. L.; MARTINELLI, A. G.; SOARES, M. B. The postcranial anatomy of *Brasilodon quadrangularis* and the acquisition of mammaliaform traits among non-mammaliaform cynodonts. **PLoS ONE**, v. 14, n. 5, p. e0216672, 2019.

HOFFMANN, C. A. **Aspectos da anatomia cerebral de cinodontes não-mammaliaformes e suas implicações na evolução do cérebro dos mamíferos**. 2018. 75p. Dissertação (Mestrado em Zoologia)-Pontifícia Universidade Católica do Rio Grande do Sul, Porto Alegre, 2018.

HOPSON, J. A. The Origin and Adaptive Radiation of Mammal-Like Reptiles and Nontherian Mammals. **Annals of the New York Academy of Sciences**, v. 167, n. 1, p. 199–216, 1969.

HOPSON, J. A. Paleoneurology. In: GANS, C.; NORTHCUTT, G. R.; ULINSKI, P. (Eds.). **Biology of the Reptilia**. New York: Academic Press, 1979. cap 2, p. 39-146.

HOPSON, J. A. Synapsid evolution and the radiation of non-eutherian mammals. **Short Courses in Paleontology**, v. 7, p. 190–219, 1994.

HOPSON, J. A.; KITCHING, J. W. A probainognathian cynodont from South Africa and the phylogeny of nonmammalian cynodonts. **Bulletin of the Museum of Comparative Zoology**, v. 156, n. 1, p. 5–35, 2001.

HOPSON, J. A.; SUES, H.-D. A traversodont cynodont from the Middle Triassic (Ladinian) of Baden-Württemberg (Germany). **Paläontologische Zeitschrift**, v. 80, n. 2, p. 124–129, 2006.

HORN, B. L. D. et al. A new third-order sequence stratigraphic framework applied to the Triassic of the Paraná Basin, Rio Grande do Sul, Brazil, based on structural, stratigraphic and paleontological data. **Journal of South American Earth Sciences**, v. 55, p. 123–132, 2014.

HU, Y. et al. Large Mesozoic mammals fed on young dinosaurs. **Nature**, v. 433, p. 149–152, 2005.

HURLBURT, G. R.; RIDGELY, R. C.; WITMER, L. M. Relative size of brain and cerebrum in tyrannosaurid dinosaurs: an analysis using brain-endocast quantitative relationships in extant alligators. In: PARRISH, J. M. et al. (Eds.). **Tyrannosaurid paleobiology**. Bloomington: Indiana University Press, 2013. cap. 6, p. 135–154.

JERISON, H. J. **Evolution of the brain and intelligence**. New York: Academic Press, 1973. 482 p.

KAMMERER, C. F. et al. New material of *Menadon besairiei* (Cynodontia: Traversodontidae) from the Triassic of Madagascar. **Journal of Vertebrate Paleontology**, v. 28, n. 2, p. 445–462, 2008.

KAMMERER, C. F. Systematics of the Anteosauria (Therapsida: Dinocephalia). **Journal of Systematic Palaeontology**, v. 9, n. 2, p. 261–304, 2011.

KAMMERER, C. F. et al. Ontogeny in the Malagasy Traversodontid *Dadadon isaloi* and a Reconsideration of its Phylogenetic Relationships. **Fieldiana: Life and Earth Sciences**, v. 5, p. 112–125, 2012.

KAMMERER, C. F. Theriodontia: Introduction. In: KAMMERER, C. F.; ANGIELCZYK, K. D.; FRÖBISCH, J. (Eds.). **Early Evolutionary History of the Synapsida, Vertebrate Paleobiology and Paleoanthropology**. Dordrecht: Springer, 2014. p. 165–169.

KAMMERER, C. F. A new taxon of cynodont from the *Tropidostoma* Assemblage Zone (upper Permian) of South Africa, and the early evolution of Cynodontia. **Papers in Palaeontology**, v. 2, n. 3, p. 387–397, 2016.

KEMP, T. S. The primitive cynodont *Procynosuchus*: Functional anatomy of the skull and relationships. **Philosophical Transactions of the Royal Society of London**, v. 285, n. 1005, p. 73–122, 1979.

KEMP, T. S. **Mammal-like reptiles and the origin of mammals**. London: Academic Press, 1982. 363 p.

KEMP, T. S. **The Origin and Evolution of Mammals**. Oxford: Oxford University Press, 2005. 331 p.

KEMP, T. S. The origin of mammalian endothermy: A paradigm for the evolution of complex biological structure. **Zoological Journal of the Linnean Society**, v. 147, n. 4, p. 473–488, 2006.

KEMP, T. S. The endocranial cavity of a nonmammalian eucynodont, *Chiniquodon theotenicus*, and its implications for the origin of the mammalian brain. **Journal of Vertebrate Paleontology**, v. 29, n. 4, p. 1188–1198, 2009.

KEMP, T. S. The Origin and Radiation of Therapsids. In: CHINSAMY-TURAN, A. (Ed.). . **Forerunners of Mammals**. Bloomington: Indiana University Press, 2012. p. 330.

KENT, D. V. et al. Age constraints on the dispersal of dinosaurs in the Late Triassic from magnetochronology of the Los Colorados Formation (Argentina). **Proceedings of the National Academy of Sciences of the United States of America**, v. 111, n. 22, p. 7958–7963, 2014.

KIELAN-JAWOROWSKA, Z. Multituberculate endocranial casts. **Palaeoverlebrala**, v. 13, n. 1–2, p. 1–12, 1983.

KIELAN-JAWOROWSKA, Z. Evolution of the Therian Mammals in the Late Cretaceous of Asia. Part VI. Endocranial casts of Eutherian Mammals. **Palaeontologia Polonica**, v. 46, p. 157–171, 1984.

KIELAN-JAWOROWSKA, Z. Brain evolution in Mesozoic mammals. **Rocky Mountain Geology**, v. 24, n. special_paper_3, p. 21–34, 1986.

KIELAN-JAWOROWSKA, Z.; CIFELLI, R. L.; LUO, Z.-X. **Mammals from the Age of Dinosaurs - Origins, Evolution and Structure**. New York: Columbia University Press, 2004. 630 p.

KRAUSE, D. W.; KIELAN-JAWOROWSKA, Z. The endocranial cast and encephalization quotient of *Ptilodus* (Multituberculata, Mammalia). **Palaeovertebrata**, v. 22, n. 2–3, p. 99–112, 1993.

LAASS, M. Virtual Reconstruction and Description of the Cranial Endocast of *Pristerodon mackayi* (Therapsida, Anomodontia). **Journal of Morphology**, v. 276, n. 6, p. 1089–1099, 2015.

LAASS, M.; KAESTNER, A. Evidence for convergent evolution of a neocortex-like structure in a late Permian therapsid. **Journal of Morphology**, v. 278, n. 8, p. 1033–1057, 2017.

LAASS, M.; SCHILLINGER, B.; KAESTNER, A. What Did the “Unossified Zone” of the Non-Mammalian Therapsid Braincase House? **Journal of Morphology**, v. 278, n. 8, p. 1020–1032, 2017.

LANGER, M. C. et al. A sauropodomorph dinosaur from the Upper Triassic (Carnian) of southern Brazil. **Comptes Rendus de l’Académie des Sciences - Series IIA - Earth and Planetary Science**, v. 329, n. 7, p. 511–517, 1999.

LANGER, M. C. et al. The Continental Tetrapod-Bearing Triassic of South Brazil. **New Mexico Museum of Natural History and Science Bulletin**, v. 41, p. 201–218, 2007.

LANGER, M. C.; FERIGOLO, J. The Late Triassic dinosauromorph *Sacisaurus agudoensis* (Caturrita Formation; Rio Grande do Sul, Brazil): anatomy and affinities. **Geological Society,**

London, Special Publications, v. 379, p. 353–392, 2013.
LANGER, M. C.; RAMEZANI, J.; DA-ROSA, Á. A. S. U-Pb age constraints on dinosaur rise from south Brazil. **Gondwana Research**, v. 57, p. 133–140, 2018.

LANGSTON, W. J. *Oedaleops campi* (Reptilia: Pelycosauria) New Genus and Species from the Lower Permian of New Mexico , and the Family Eothyrididae. **Bulletin of the Texas Memorial Museum**, n. 9, p. 1–47, 1965.

LIU, J. The taxonomy of the traversodontid cynodonts *Exaeretodon* and *Ischignathus*. **Revista Brasileira de Paleontologia**, v. 10, n. 2, p. 133–136, 2007.

LIU, J.; ABDALA, F. Phylogeny and Taxonomy of the Traversodontidae. In: KAMMERER, C. F.; ANGIELCZYK, K. D.; FRÖBISCH, J. (Eds.). **Early Evolutionary History of the Synapsida (Vertebrate Paleobiology and Paleoanthropology Series)**. Dordrecht: Springer, 2014. p. 289–304.

LIU, J.; OLSEN, P. The phylogenetic relationships of Eucynodontia (Amniota: Synapsida). **Journal of Mammalian Evolution**, v. 17, n. 3, p. 151–176, 2010.

LIU, J.; POWELL, J. Osteology of *Andescynodon* (Cynodontia: Traversodontidae) from the Middle Triassic of Argentina. **American Museum Novitates**, v. 37, n. 3674, p. 1–19, 2009.

LIU, J.; SOARES, M. B.; REICHEL, M. *Massetognathus* (Cynodontia, Traversodontidae) from the Santa Maria Formation of Brazil. **Revista Brasileira de Paleontologia**, v. 11, n. 1, p. 27–36, 2008.

LUO, Z.-X. Transformation and diversification in early mammal evolution. **Nature**, v. 450, n. 7172, p. 1011–1019, 2007.

LUO, Z. X.; CROMPTON, A. W.; SUN, A. L. A new mammaliaform from the early Jurassic and evolution of mammalian characteristics. **Science**, v. 292, n. 5521, p. 1535–1540, 2001.

MACRINI, T. E. **The Evolution of Endocranial Space in Mammals and Non-mammalian Cynodonts**. 2006. 277p. Tese (Doutorado)- The University of Texas at Austin, Austin, EUA, 2006.

MACRINI, T. E. et al. Digital cranial endocast of *Pucadelphys andinus*, a Paleocene metatherian. **Journal of Vertebrate Paleontology**, v. 27, n. 1, p. 99–107, 2007.

MACRINI, T. E.; ROUGIER, G. W.; ROWE, T. Description of a Cranial Endocast From the Fossil Mammal *Vincelestes neuquenianus* (Theriiformes) and Its Relevance to the Evolution of Endocranial Characters in Therians. **The Anatomical Record**, v. 290, p. 875–892, 2007.

MACRINI, T. E.; ROWE, T.; ARCHER, M. Description of a Cranial Endocast From a Fossil Platypus , *Obdurodon dicksoni* (Monotremata, Ornithorhynchidae), and the Relevance of Endocranial Characters to Monotreme Monophyly. **Journal of Morphology**, v. 267, p. 1000–1015, 2006.

MANGER, P. R. An examination of cetacean brain structure with a novel hypothesis correlating thermogenesis to the evolution of a big brain. **Biological Reviews**, v. 81, p. 293–338, 2006.

MARSICANO, C. A. et al. The precise temporal calibration of dinosaur origins. **Proceedings of the National Academy of Sciences of the United States of America**, v. 113, n. 3, p. 509–513, 2016.

MARTINELLI, A. G. et al. A new tritheledontid (Therapsida, Eucynodontia) from the Late Triassic of Rio Grande do Sul (Brazil) and its phylogenetic relationships among carnivorous non-mammalian eucynodonts. **Ameghiniana**, v. 42, n. 1, p. 191–208, 2005.

MARTINELLI, A. G. On the postcanine dentition of *Pascualgnathus polanskii* Bonaparte (Cynodontia, Traversodontidae) from the Middle Triassic of Argentina. **Geobios**, v. 43, n. 6, p. 629–638, 2010.

MARTINELLI, A. G. et al. The African cynodont *Aleodon* (Cynodontia, Probainognathia) in the Triassic of southern Brazil and its biostratigraphic significance. **PLoS ONE**, v. 12, n. 6, p. e0177948, 2017.

MARTINELLI, A. G.; FUENTE, M. D. LA; ABDALA, F. *Diademodon tetragonus* Seeley, 1894 (Therapsida: Cynodontia) in the Triassic of South America and its biostratigraphic implications. **Journal of Vertebrate Paleontology**, v. 29, n. 3, p. 852–862, 2009.

MARTINELLI, A. G.; SOARES, M. B.; SCHWANKE, C. Two new cynodonts (Therapsida) from the Middle-Early Late Triassic of Brazil and comments on South American probainognathians. **PLoS ONE**, v. 11, n. 10, p. e0162945, 2016.

MARTINEZ, R. N. et al. A Basal Dinosaur from the Dawn of the Dinosaur Era in Southwestern Pangaea. **Science**, v. 206, n. 2011, p. 206–210, 2011.

MARTÍNEZ, R. N. et al. Vertebrate Succession in the Ischigualasto Formation. **Journal of Vertebrate Paleontology**, v. 32, n. S1, p. 10–30, 2012.

MATSUOKA, H.; KUSUHASHI, N.; CORFE, I. J. A new Early Cretaceous tritylodontid (Synapsida, Cynodontia, Mammaliamorpha) from the Kuwajima Formation (Tetori Group) of central Japan. **Journal of Vertebrate Paleontology**, v. 36, n. 4, p. e1112289, 2016.

MELO, T. P.; ABDALA, F.; SOARES, M. B. The Malagasy cynodont *Menadon besairiei* (Cynodontia; Traversodontidae) in the Middle-Upper Triassic of Brazil. **Journal of Vertebrate Paleontology**, v. 35, n. 6, p. e1002562, 2015.

MELO, T. P.; MARTINELLI, A. G.; SOARES, M. B. A new gomphodont cynodont (Traversodontidae) from the Middle–Late Triassic Dinodontosaurus Assemblage Zone of the Santa Maria Supersequence, Brazil. **Palaeontology**, v. 60, n. 4, p. 571–582, 2017.

MODESTO, S. P. The skull of the herbivorous synapsid *Edaphosaurus boanerges* from the Lower Permian of Texas. **Palaeontology**, v. 38, n. 1, p. 213–239, 1995.

MODESTO, S. P. et al. The last "pelycosaur": A varanopid synapsid from the *Pristerognathus* Assemblage Zone, Middle Permian of South Africa. **Naturwissenschaften**, v. 98, n. 12, p. 1027–1034, 2011.

MÜLLER, R. T. et al. Biogenic control on the origin of a vertebrate monotypic accumulation from the Late Triassic of southern Brazil. **Geobios**, v. 48, n. 4, p. 331–340, 2015a.

MÜLLER, R. T. et al. Wachholz, a new exquisite dinosaur-bearing fossiliferous site from the Upper Triassic of southern Brazil. **Journal of South American Earth Sciences**, v. 61, p. 120–128, 2015b.

MÜLLER, R. T.; LANGER, M. C.; DIAS-DA-SILVA, S. Biostratigraphic significance of a new early sauropodomorph specimen from the Upper Triassic of southern Brazil. **Historical Biology**, v. 29, n. 2, p. 187–202, 2017.

MÜLLER, R. T.; LANGER, M. C.; DIAS-DA-SILVA, S. An exceptionally preserved association of complete dinosaur skeletons reveals the oldest long-necked sauropodomorphs. **Biology Letters**, v. 14, n. 11, p. 20180633, 2018.

OLSON, E. C. Origin of the mammals based upon cranial morphology of their therapsid suborders. **GSA, Special Paper**, v. 55, p. 1–136, 1944.

OTTONE, E. G. et al. A new Late Triassic age for the Puesto Viejo Group (San Rafael depocenter, Argentina): SHRIMP U-Pb zircon dating and biostratigraphic correlations across southern Gondwana. **Journal of South American Earth Sciences**, v. 56, p. 186–199, 2014.

PAVANATTO, A. E. B. et al. A new Upper Triassic cynodont-bearing fossiliferous site from southern Brazil, with taphonomic remarks and description of a new traversodontid taxon. **Journal of South American Earth Sciences**, v. 88, p. 179–196, 2018.

PHILIPP, R. P. et al. **Proveniência por U-Pb LA-ICP-MS em zircão detrítico e idade de deposição da Formação Santa Maria, Triássico da Bacia do Paraná, RS: evidências da estruturação do Arco do Rio Grande**. In: SYMPOSIUM INTERNATIONAL ON TECTONICS, 8. & SIMPÓSIO NACIONAL DE ESTUDOS TECTÔNICOS, 14., 2013, Cuiabá/MT. **Anais**... Cuiabá/MT, 2013. p. 154-157.

PHILIPP, R. P. et al. Middle Triassic SW Gondwana paleogeography and sedimentary dispersal revealed by integration of stratigraphy and U-Pb zircon analysis: The Santa Cruz Sequence, Paraná Basin, Brazil. **Journal of South American Earth Sciences**, v. 88, p. 216–237, 2018.

PRETTO, F. A.; LANGER, M. C.; SCHULTZ, C. L. A new dinosaur (Saurischia: Sauropodomorpha) from the Late Triassic of Brazil provides insights on the evolution of sauropodomorph body plan. **Zoological Journal of the Linnean Society**, v. 185, n. 2, p. 388–416, 2018.

PRETTO, F. A.; SCHULTZ, C. L.; LANGER, M. C. New dinosaur remains from the Late Triassic of southern Brazil (Candelária Sequence, *Hyperodapedon* Assemblage Zone). **Alcheringa**, v. 39, n. 2, p. 264–273, 2015.

PUSCH, L.; KAMMERER, C. F.; FRÖBISCH, J. Cranial anatomy of the early cynodont *Galesaurus planiceps* and the origin of mammalian endocranial characters. **Journal of Anatomy**, 2019.

QUIROGA, J. C. The brain of two mammal-like reptiles (Cynodontia-Therapsida). **Journal für Hirnforschung**, v. 20, p. 351–359, 1979a.

QUIROGA, J. C. The inner ear of two cynodonts (Reptilia-Therapsida) and some comments on the evolution of the inner ear from Pelycosaurs to Mammals. **Gegenbaurs morphologisches Jahrbuch**, v. 125, n. 2, p. 178–190, 1979b.

QUIROGA, J. C. Further studies on cynodont endocasts (Reptilia-Therapsida). **Zeitschrift für mikroskopisch-anatomische Forschung**, v. 94, n. 4, p. 580–592, 1980a.

QUIROGA, J. C. The brain of the mammal-like reptile *Probainognathus jenseni* (Therapsida, Cynodontia). A correlative paleo-neoneurological approach to the neocartex at retile-mammal transition. **Journal für Hirnforschungnal f**, v. 21, p. 299–336, 1980b.

QUIROGA, J. C. The endocranial cast of the advanced mammal-like reptile *Therioherpeton cargnini* (Therapsida-Cynodontia) form the Middle Triassic of Brazil. **Journal für Hirnforschung**, v. 25, n. 3, p. 285–290, 1984.

RANIVOHARIMANANA, L. et al. New material of *Dadadon isaloi* (Cynodontia,Traversodontidae) from the Triassic of Madagascar. **Journal of Vertebrate Paleontology**, v. 31, n. 6, p. 1292–1302, 2011.

RAY, S. A new Late Triassic traversodontid cynodont (Therapsida, Eucynodontia) from India. **Journal of Vertebrate Paleontology**, v. 35, n. 3, p. 37–41, 2015.

REICHEL, M.; SCHULTZ, C. L.; SOARES, M. B. A new traversodontid cynodont (therapsida, eucynodontia) from the middle triassic Santa Maria formation of Rio Grande Do Sul, Brazil. **Palaeontology**, v. 52, n. 1, p. 229–250, 2009.

REISZ, R. R. "Pelycosaur"-Grade Synapsids: Introduction. In: KAMMERER, C. F.; ANGIELCZYK, K. D.; FRÖBISCH, J. (Eds.). **Early Evolutionary History of the Synapsida, Vertebrate Paleobiology and Paleoanthropology**. Dordrecht: Springer, 2014. p. 3–5.

REISZ, R. R.; GODFREY, S. J.; SCOTT, D. *Eothyris* and *Oedaleops*: Do these Early Permian synapsids from Texas and New Mexico form a clade? **Journal of Vertebrate Paleontology**, v. 29, n. 1, p. 39–47, 2009.

RIBEIRO, A. M.; ABDALA, F.; BERTONI, R. S. Traversodontids cynodonts (Therapsida - Eucynodontia) from two Upper Triassic localities of the Paraná Basin, Southern Brazil. Ameghiniana. In: CONGRESO LATINOAMERICANO DE PALEONTOLOGÍA DE VERTEBRADOS, 4., 2011, San Juan/AR. **Ameghiniana, v. 48, n. 4 - Suplemento 2011– Resúmenes**. Buenos Aires/AR, 2011. p. R111.

RODRIGUES, P. G. et al. Digital cranial endocast of *Riograndia guaibensis* (Late Triassic, Brazil) sheds light on the evolution of the brain in non-mammalian cynodonts. **Historical Biology**, p. 1–18, 2018.

RODRIGUES, P. G.; RUF, I.; SCHULTZ, C. L. Study of a digital cranial endocast of the non-mammaliaform cynodont *Brasilitherium riograndensis* (Later Triassic, Brazil) and its relevance to the evolution of the mammalian brain. **Paläontologische Zeitschrift**, v. 88, n. 3, p. 329–352, 2014.

ROGERS, R. R. et al. The Ischigualasto Tetrapod Assemblage (Late Triassic, Argentina) and $^{40}Ar/^{39}Ar$ Dating of Dinosaur Origins. **Science**, v. 260, n. 5109, p. 794–797, 1993.

ROMER, A. S.; PRICE, L. I. Review of the Pelycosauria. **Geological Society of America Special Papers**, v. 28, p. 1–538, 1940.

ROWE, T. B.; CARLSON, W. D.; BOTTORFF, W. W. ***Thrinaxodon,* Digital Atlas of the Skull**. Austin: University of Texas Press, 1995.

ROWE, T. B.; MACRINI, T. E.; LUO, Z.-X. Fossil Evidence on Origin of the Mammalian Brain. **Science**, v. 332, p. 955–957, 2011.

RUBIDGE, B. S.; SIDOR, C. A. Evolutionary patterns among Permo-Triassic Therapsids. **Annual Review of Ecology and Systematics**, v. 32, p. 449–480, 2001.

RUBIDGE, B. S.; SIDOR, C. A. On the Cranial Morphology of the Basal Therapsids *Burnetia* and *Proburnetia* (Therapsida: Burnetiidae). **Journal of Vertebrate Paleontology**, v. 22, n. 2, p. 257–267, 2002.

RUTA, M. et al. The radiation of cynodonts and the ground plan of mammalian morphological diversity. **Proceedings of the Royal Society B: Biological Sciences**, v. 280, n. 1769, p. 1–10, 2013.

SCHMITT, M. R. et al. On the occurrence of the traversodontid *Massetognathus ochagaviae* (Synapsida, Cynodontia) in the early late Triassic *Santacruzodon* Assemblage Zone (Santa Maria Supersequence, southern Brazil): Taxonomic and biostratigraphic implications. **Journal of South American Earth Sciences**, 2019.

SCHULTZ, C. L.; LANGER, M. C.; MONTEFELTRO, F. C. A new rhynchosaur from south Brazil (Santa Maria Formation) and rhynchosaur diversity patterns across the Middle-Late Triassic boundary. **Paläontologische Zeitschrift**, v. 90, n. 3, p. 593–609, 2016.

SCHULTZ, C. L.; SCHERER, C. M. DOS S.; BARBERENA, M. C. Bioestratigraphy of Southern Brazilian Middle-Upper Triassic. **Revista Brasileira de Geociências**, v. 30, n. 3, p. 495–498, 2000.

SIDOR, C. A. et al. **A new species of traversodont cynodont with tritylodont-like features and possible arboreal adaptations from the Upper Ntawere Formation, Northeastern Zambia**. In: SOCIETY OF VERTEBRATE PALEONTOLOGY ANNUAL MEETING, 76., 2016, Salt Lake City/EUA. **Journal of Vertebrate Paleontology (Supplement Abstract)**. Salt Lake City/EUA, 2016. p. 224.

SIDOR, C. A.; HOPSON, J. A. *Cricodon metabolus* (Cynodontia: Gomphodontia) from the Triassic Ntawere Formation of northeastern Zambia: patterns of tooth replacement and a systematic review of the Trirachodontidae. **Journal of Vertebrate Paleontology**, v. 37, n. 6, p. 39–64, 2017.

SIGOGNEAU-RUSSEL, D. Theriodontia I. In: WELLNHOFER, P. (Ed.). **Encyclopedia of Paleoherpetology**. Stuttgart, New York: Gustav Fisher Verlag, 1989. v. Part 17B/Ip. 127.

SIGURDSEN, T. et al. Reassessment of the morphology and paleobiology of the therocephalian *Tetracynodon darti* (Therapsida), and the phylogenetic relationships of Baurioidea. **Journal of Vertebrate Paleontology**, v. 32, n. 5, p. 1113–1134, 2012.

SIMPSON, G. G. Mesozoic Mammalia. IX. The brain of Jurassic mammals. **American Journal of Science**, v. 14, n. 82, p. 259–268, 1927.

SOARES, M. B.; SCHULTZ, C. L.; HORN, B. L. D. New information on *Riograndia guaibensis* Bonaparte, Ferigolo & Ribeiro, 2001 (Eucynodontia, Tritheledontidae) from the Late Triassic of southern Brazil: Anatomical and biostratigraphic implications. **Anais da Academia Brasileira de Ciencias**, v. 83, n. 1, p. 329–354, 2011.

SUES, H.-D. The relationships of the Tritylodontidae (Synapsida). **Zoological Journal of the Linnean Society**, v. 85, n. 3, p. 205–217, 1985.

SUES, H.-D.; REISZ, R. R. Origins and early evolution of herbivory in tetrapods. **Trends in Ecology and Evolution**, v. 13, n. 4, p. 141–145, 1998.

WATSON, D. M. S. XL.— The skull of *Diademodon*, with notes on those of some other Cynodonts. **Annals and Magazine of Natural History: Series 8**, v. 8, n. 45, p. 293–330, 1911.

WATSON, D. M. S. XXV.— Further notes on the skull, brain, and organs of special sense of *Diademodon*. **Annals and Magazine of Natural History: Series 8**, v. 12, n. 68, p. 217–228, 1913.

ZERFASS, H. et al. Sequence stratigraphy of continental Triassic strata of Southernmost Brazil: a contribution to Southwestern Gondwana palaeogeography and palaeoclimate. **Sedimentary Geology**, v. 161, n. 1–2, p. 85–105, 2003.